NEW STILBENOIDS ISOLATED FROM FUNGUS-CHALLENGED PEANUT SEEDS AND THEIR BIOACTIVITY EVALUATION

LIU ZHONGWEI

NATIONAL UNIVERSITY OF SINGAPORE

2013

NEW STILBENOIDS ISOLATED FROM FUNGUS-CHALLENGED PEANUT SEEDS AND THEIR BIOACTIVITY EVALUATION

LIU ZHONGWEI

B.Agr.China Agricultural University

M.Agr.China Agricultural University

A THESIS SUBMITTED

FOR THE DEGREE OF DOCTOR OF PHILOSOPHY

DEPARTMENT OF CHEMISTRY

NATIONAL UNIVERSITY OF SINGAPORE

2013

Declaration Page

I hereby declare that this thesis is my original work and it has been written by me in its entirety, under the supervision of Associate Professor Huang Dejian, (in the laboratory S13-level 5), Chemistry Department, National University of Singapore, between Jan 2009 and Jan 2013.

I have duly acknowledged all the sources of information which have been used in the thesis.

This thesis has also not been submitted for any degree in any university previously.

The content of the thesis has been partly published in:

1) Liu, Z.W., Wu, J.E., Huang, D.J., 2013. New arahypins isolated from fungal-challenged peanut seeds and their glucose uptake-stimulatory activity in 3T3-L1 adipocytes. Phytochem. Lett. 6, 123-127.
2) Liu, Z.W., Wu, J.E., Huang, D.J., 2013. New stilbenoids isolated from fungus-challenged black skin peanut seeds and their adipogenesis inhibitory activity in 3T3-L1 cells. J. Agric. Food Chem. 61, 4155-4161.
3) Liu, Z.W., Yan, Y., Wang, S.H., Ong, W.Y., Huang, D.J., 2013. Assaying myeloperoxidase inhibitors and hypochlorous acid scavengers in HL60 cell line using quantum dots as the luminescent probe. Am. J. Biomed. Sci. 5, 140-153.
4) Yan, Y., Wang, S.H., Liu, Z.W., Wang, H.Y., Huang, D.J., 2010. The CdSe-ZnS Quantum Dots for selective and sensitive detection and quantification of hypochlorite. Anal. Chem. 82, 9775-9978.

Liu Zhongwei	Liu Zhongwei	July 23 2013
Name	Signature	Date

Acknowledgements

First and foremost, I wish to express my utmost gratitude to my supervisor Prof. Huang Dejian for his insightful advice, valuable guidance, and consistent encouragement given throughout my PhD candidature. I feel honored to have him as my supervisor and benefit greatly from his profound knowledge in food chemistry, strict requirements for experiment design, and inspiring discussions on my research project. Without his strong support, I cannot complete my research project and PhD thesis. I am also deeply grateful for his great help in my access to various research resources and technique assistance from other labs and academic staffs.

Next, I would like to express my special thanks to Dr. Wu Ji'en for his crucial help in the acquisition of 2D NMR spectra, structure elucidations, and data presentation in manuscripts. Besides, his rich research experience in natural product chemistry had significantly optimized my experiment plan and greatly accelerated my research progress. Without his critical technique assistance, my research project after qualification examination may be another scene. Here, I also want to express my sincere gratitude to Dr. Wang Suhua who have helped my research project with his high quality quantum dots. It is my great fortune to know these two warm-hearted staffs with rich research experiences in their respective areas.

I am much indebted to Prof. Ong Wei Yi Who allowed me to learn the cell culture and basic molecular biology techniques in his lab. His helpful and friendly students leave me a very deep impression as well. My thanks also go out to Prof. Tan Kwon Huat for

his generosity in providing cell strains and resourceful suggestions on my research projects. In addition, I give my sincere appreciation to Ms Lee Chooi Lan, Ms Jiang Xiao hui, Ms Lew Huey Lee, and my lab colleagues Dr. Quek Yi Ling, Mr. Wu Ziyun, Ms Chen wei, Ms Yan Yan et al. for their kind help and advice throughout my research projects. I am also really grateful to NUS for research scholarship and funding which finance me and my research project.

Last but not least, I would like to express my family style thanks to my parents who have always supports me materially and spiritually throughout these years. Their love and understanding is my greatest motivation to complete this thesis.

Liu Zhongwei

March 1st 2013

Table of Contents

Summary

The objective of this study was to isolate and characterize new and/or known peanut stilbenoids and to evaluate their biological activities. Four new prenylated stilbene dimers (arahypin-8, arahypin-9, arahypin-11, arahypin-12) of novel construction patterns and two new stilbene derivatives arahypin-10 and MIP were isolated for the first time from wounded India peanut seeds and Chinese black skin peanut seeds challenged by a *Rhizopus oligoporus* strain, a food grade starter culture for soybean fermentation in Southeast Asia. The structures of the six new stilbene compounds were elucidated on the basis of HRESIMS, UV, 1D and 2D NMR spectroscopy and the plausible mechanisms of their formations were also proposed. The antioxidant, anti-diabetic, anti-obesity and anticancer effects of six new peanut stilbenoids together with three known peanut stilbenoids (arachidin-1, arachidin-3, and SB-1) and resveratrol were tested and compared in different cell based assays. In the antioxidant assay, arachidin-1 displayed the highest inhibitory effect on the highly reactive oxidative species (hROS) generated by myeloperoxidase (MPO) in HL60 differentiated cells, compared with resveratrol which was shown to be a potent MPO inhibitor in another assay using quantum dots (QDs) fabricated for specific detection of HClO. In the glucose uptake assay, arahypin-8, arahypin-9, and arahypin-10 exhibited insulin sensitizing activity by significantly increasing glucose uptake in differentiated 3T3-L1 adipocytes. In the adipogenesis inhibition assay, arachidin-1 was found to suppress the differentiation of 3T3-L1 preadipocytes most effectively among the 10 stilbenes tested while arahypin-11 and arahypin-12 exhibited a significant cytotoxicity in 3T3-L1 preadipocytes in the MTT assay. The results of our

study indicate that the fungus-stressed peanut seeds may become a new potential source of natural pharmaceuticals.

List of Tables

List of Figures

List of Abbreviations

Abbreviation	Description
ABAH	4-aminobenzoic acid hydrazide
AMPK	AMP-activated protein kinase
APF	3 ´-(*p*-aminophenyl) fluorescein
CBR	cannabinoid receptor
DCFH-DA	2,7-dichlorofluorescin diacetate
DEX	dexamethasone
GLUT4	glucose transporter 4
HClO	hypochlorous acid
hROS	highly reactive oxidative species
H_2O_2	hydrogen peroxide
HPF	hydroxyphenyl fluorescein
IBMX	3-isobutyl-1-methyl-xanthine
IPD	trans-3'-isopentadienyl-3, 5, 4'-trihydroxystilbene
KRPB	Krebs-Ringers phosphate buffer
LPS	lipopolysaccharide
MCP	*Momordica charantia* peroxidase
MIP	3,5,3'-trihydroxy-4'-methoxy-5'-isopentenylstilbene
MPO	myeloperoxidase
MTT	Thiazolyl blue tetrazolium bromide
2-NBDG	2-(*N*-(7-nitrobenz-2-oxa-1,3-diazol-4-yl)amino)-2-deoxyglucose

NO	nitric oxide
$^{\cdot}OH$	hydroxyl radical
$ONOO^{-}$	peroxynitrite
$^{1}O_2$	singlet oxygen
PPARs	peroxisome proliferator-activated receptors
PMA	phorbol 12-myristate 13-acetate
QDs	quantum dots
RNHCl	chloramines
R.oligoporus	*Rhizopus oligoporus*
Rosi	rosiglitazone
SS	stilbene synthase
TNB	5-thio-2-nitrobenzoic acid

Chapter 1

Introduction

Stilbenoids, as a class of plant polyphenols, have attracted considerable research attention for their intricate structures and diverse bioactivities. Trans-resveratrol is by far the most extensively investigated and reported stilbene which is widely distributed in human diet and various plant sources including peanuts, cranberries, and grapes. Resveratrol and its derivatives have drawn significant interest for pharmaceutical research and development due to their potential in therapeutic or preventive applications. The study on oligomeric stilbenes has also become a hot topic recently as their diverse skeletons, complex configurations and different degrees of oligomerization are shown to engender interesting bioactivities to be explored.

Along with grapes and their derivatives, peanuts (*Arachis hypogaea*) and peanut butter are considered as major dietary sources of stilbenes (Cassidy et al., 2000) which are often found in plants that are not routinely consumed for food or in the edible tissue. Use of phytochemicals present in crop plants or foodstuff may carry a low risk of intoxication or biological toxicity. Stilbenes found in peanuts are involved in defense mechanisms against physical injuries and microbial infection (Lopes et al., 2011). The peanut tissues (leaves, callus, stems, roots, and seeds) produced stilbene phytoalexins during normal cultivation when peanut plants are inevitably challenged by surrounding microflora and environmental stresses. Compared with uninjured plants, stilbene production is more efficient in injured plant tissues such as germinated seeds or stems of *Arachis hypogaea* which are challenged by natural flora including

various fungi (Keen et al., 1976; Aguamah et al., 1981). Peanut seeds, as agricultural materials readily available in a large amount, show a great potential of being a bioreactor to produce stilbene compounds to accommodate the need of research and market use.

The potential medical importance and health benefits of stilbenoids from peanuts have been reported by several researchers recently (Chang et al., 2006; Lopes et al., 2011; Kwon et al., 2012; Minakawa et al., 2012). Despite significant progress in peanut phytochemistry research, few new stilbene compounds, especially new stilbene oligomers, were isolated from peanut seeds (Sobolev et al., 2009; Sobolev et al., 2010). Further exploration of the potential bioactivities of peanut stilbenoids is of considerable interest since emerging evidences suggest that natural stilbenes may become novel sources of lead compounds to be developed as antioxidants, anti-inflammatory, anti-obesity and anti-diabetic agents (Shen et al., 2009).

Hence, this thesis work aims to investigate the ability of peanut seeds to produce novel stilbenoids and to further explore the biological potential of the isolated peanut stilbenoids. In chapter 3, a new fluorescent assay using Quantum Dots (QDs) was established for comparing the hypochlorite (HClO) elimination efficiency of resveratrol with that of other myeloperoxidase (MPO) inhibitors and HClO scavengers. In chapter 4 and 5, a new processing method has been developed for eliciting stilbenoid production in fungus-challenged peanut seeds, from which six

novel stilbenoids and three known stilbenoids were isolated. In chapter 6, the MPO inhibition efficiency, anti-diabetic, anti-obesity, and cytotoxic effects of the nine isolated peanut stilbenoids plus resveratrol were evaluated and compared in different cell based microplate assays.

Chapter 2

Literature Review

2.1 Structures, sources, and bioavailability of natural stilbenes

2.1.1 Structural classifications of natural stilbenes

From a phytochemistry viewpoint, natural stilbenes, as a group of phenolic compounds derived from the general phenylpropanoid pathway, include basic stilbenes, bibenzyls, or dihydrostilbenes, bis(bibenzyls), phenanthrenes, 9,10-dihydrophenanthrenes, and related compounds (Figure 2.1) (Riviere et al.,2012). This study will focus on (*E*)-stilbenes, a group of non-flavonoid polyphenolic compounds, which are structurally characterized by the presence of 1,2 diphenylethylene nucleus in the *trans* olefinic configuration.

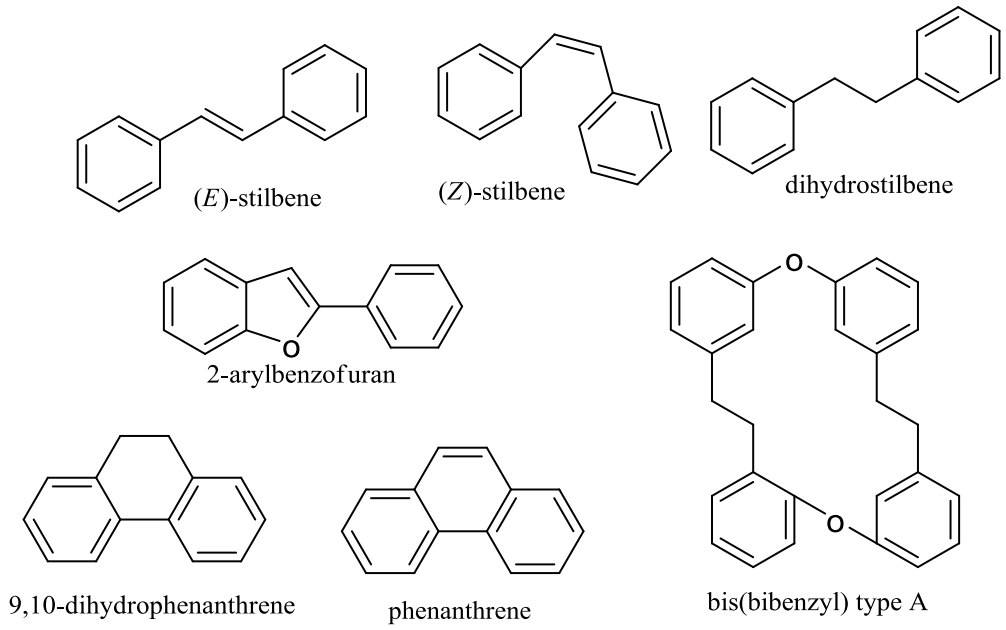

Figure 2.1 General skeletons of common stilbenoids (Adapted from Riviere et al.,2012. Nat. Prod. Rep. 29, 1317-1333.)

Resveratrol (3,5,4'-trihydroxy-*trans*-stilbene) is the most famous representative of this class of stilbenes and initially attracted attention for its cardioprotective effect in red wine. It became a 'star compound' due to its preventive potential for cancer, cardiovascular disease, ischemic injuries, etc. Many comprehensive reviews regarding resveratrol's chemical and biological aspects have appeared (Bradamante et al., 2004; Baur and Sinclair, 2006; Athar et al., 2007). The vast majority of naturally occurring monomeric stilbenes bear hydroxyl or methoxyl substituent groups on their aromatic rings. The monomeric stilbenes can also exist in the forms of stilbene aglycones and stilbene glycosides, or stilbenes substituted by isopentenyl units which can cyclize to form new rings (Shen et al., 2009). The stilbenes containing hydroxyl groups on the aromatic rings are also termed as stilbenoids. The structural diversity of stilbenes leads to a wide range of biological and pharmacological activities including anti-inflammatory, anti-tumoral, anti-atherogenic, anti-viral, and most recently, neuroprotective effects (Riviere et al., 2012).

2.1.2 Plant sources of natural stilbenes

Stilbenes bearing one 1,2-diphenylethylene nucleus in the molecules occur within a rather limited but heterogeneous group of plant families because the key botanical enzyme involved in stilbene biosynthesis, stilbene synthase (SS), is not ubiquitously present in all plant species (Chong et al., 2009). However, the occurrence of stilbenes in plants is rather widespread, being found in taxonomically distant species within the Embryophyta phylum (land plants), from less complex species like liverworts to the

more advanced angiosperms (Riviere et al., 2012). Monomeric stilbenes can be found in the species of twenty three families, of which eight have also produced new oligomeric stilbenes, namely the Cyperaceace, Dipterocarpaceae, Gnetaceae, Iridaceae, Leguminosae, Moraceae, Orchidaceae and Polygonaceae which are also known for their high stilbene contents (Shen et al., 2009). Among these families, the Leguminosae is the richest source of new monomeric stilbenes while Dipterocarpaceae contains the largest number of new oligomeric stilbenes.

2.1.3 Bioavailability of natural stilbenes

Trans-resveratrol is by far the most extensively investigated and reported stilbene for *in vivo* studies, as compared to its analogs, like its *cis* counterpart, pinosylvin (trans-3,5-dihydroxystilbene) and piceatannol (trans-3,5, 3′,4′-tetrahydroxystilbene). Pharmacokinetic studies show that circulating resveratrol in the plasma is extensively metabolized in human body and the oral bioavailability of resveratrol is extremely low (Wenzel and Somoza, 2005), being restricted by limited absorption, limited chemical stability and degradation by intestinal microflora and intestinal enzymes (Day et al., 1998). In a human bioavailability study, when ^{4}C-resveratrol doses of 25 mg were orally administered to six healthy volunteers, the peak resveratrol and metabolite plasma concentration was 491 ng/mL or equivalent to 2 μM after an hour, followed by a second peak of 1.3 μM and plasma concentrations decreased exponentially thereafter (Walle et al., 2004). Animal *in vivo* models have also been frequently used to investigate the bioavailability of resveratrol and most studies

indicated that the oral bioavailability of resveratrol is very low for the poor absorption and rapid and extensive metabolism leading to formation of various metabolites such as resveratrol glucuronides and resveratrol sulfates (Wenzel and Somoza, 2005; Neves et al., 2012). Concentrations of resveratrol detected in tissues or at the cellular sites of actions do not appear to be sufficiently adequate to exert bioactivity *in vivo*. Nevertheless, the physiological benefits of resveratrol including anti-inflammatory, antioxidant, anti-diabetic and cardiovascular protective effects of resveratrol have been demonstrated by recent human clinical trials (Ghanim et al., 2011; Brasnyo et al., 2011; Kennedy et al., 2010). Therefore, the therapeutic and preventive potential of resveratrol would be significantly strengthened if the limitations related to its bioavailability can be overcome. Researchers are currently exploring alternative methods for enhancing resveratrol bioavailability, including: 1) co-administration with metabolic inhibitors in order to extend its presence *in vivo*, 2) discovery of new resveratrol analogs endowed with better bioavailability, and 3) development of nanotechnology delivery systems. As for the first approach, some researchers have evaluated the possibility of improving the pharmacokinetic parameters of resveratrol by partially inhibiting its glucuronidation with specific inhibitors (Hoshino et al., 2010). The second strategy also attracts increasing interest, which focuses on evaluation of new naturally-occurring and/or synthetic analogs of resveratrol endowed with the same structural backbone and some chemical modifications resulting in better bioavailability (Cai et al., 2011; Szekeres et al., 2011). Since conventional formulations alone are probably inadequate to resolve the problem of the

physiochemical and pharmacokinetic limitations governing resveratrol bioavailability, novel delivery systems using nano- and micro-formulations for resveratrol encapsulations including liposomes, polymeric nanoparticles, solid lipid nanoparticles, lipospheres, cyclodextrins, polymeric microsphere, yeast cell carriers, and calcium or zinc pectinate beads have been developed to protect and stabilize resveratrol and enhance its bioavailability *in vivo* (Amri et al., 2012).

2.2 Bioactivities of natural stilbenoids

2.2.1 The antioxidant and anti-inflammatory bioactivities of stilbenoids

Oxidative stress plays an important role in the appearance and development of inflammatory diseases including cancers, atherosclerosis and other cardiovascular pathologies (Chapple, 1997; Reuter et al., 2010). Resveratrol, the most reported stilbene, is linked to the famous "French paradox" phenomenon which associates a diet rich in saturated fatty fats and a moderate consumption of red wine with a low incidence of coronary heart disease in southern France (Sun et al., 2002). One of the proposed mechanisms involved in the beneficial effect of red wine on cardiovascular diseases is the capacity of resveratrol and some other stilbene derivatives in red wine to scavenge reactive oxidative species (ROS) in vascular endothelium (Das & Das, 2010). Among the ROS contributing to oxidative tissue damages, hypochlorous acid (HClO) generated by myeloperoxidase (MPO) has received notable interest recently because of the compelling evidence for the role of HClO and MPO in the initiation and propagation of various inflammatory diseases, most prominently (cardio)vascular

diseases (Pattison & Davies, 2006). MPO is a heme enzyme that is abundantly expressed in neutrophils and to a lesser extent in monocytes and certain types of macrophages (Klebanoff et al., 1999), which participates in innate immune defense against microorganism invasions through formation of diffusible ROS. Under pathological conditions, persistent activation of the MPO-H_2O_2-Cl^- system at inappropriate locations or times within the body can lead to tissue damage. Depending on the local milieu, the MPO-H_2O_2 system is capable of generating a wide range of ROS including HClO, chloramines, hydroxyl radicals ($^{\cdot}OH$), singlet oxygen ($^1O_2$), and ozone (O_3). (Figure 2.2) (van der Veen et al., 2009). Among MPO-derived oxidants, HClO is the product of the unique property of MPO to catalyze the 2-electron peroxidation of Cl^- in the presence of H_2O_2. HClO is a membrane-permeant potent oxidant and able to initiate modification reactions targeting lipids, DNA and (lipo) proteins, including halogenations, nitration and oxidative cross-linking (Malle et al., 2007). The fact that circulating levels of MPO have been shown to predict risks for major adverse cardiac events and that levels of HClO–derived chlorinated compounds are specific biomarkers for disease progression, has attracted considerable interest in the development of therapeutically useful HClO scavengers and MPO inhibitors.

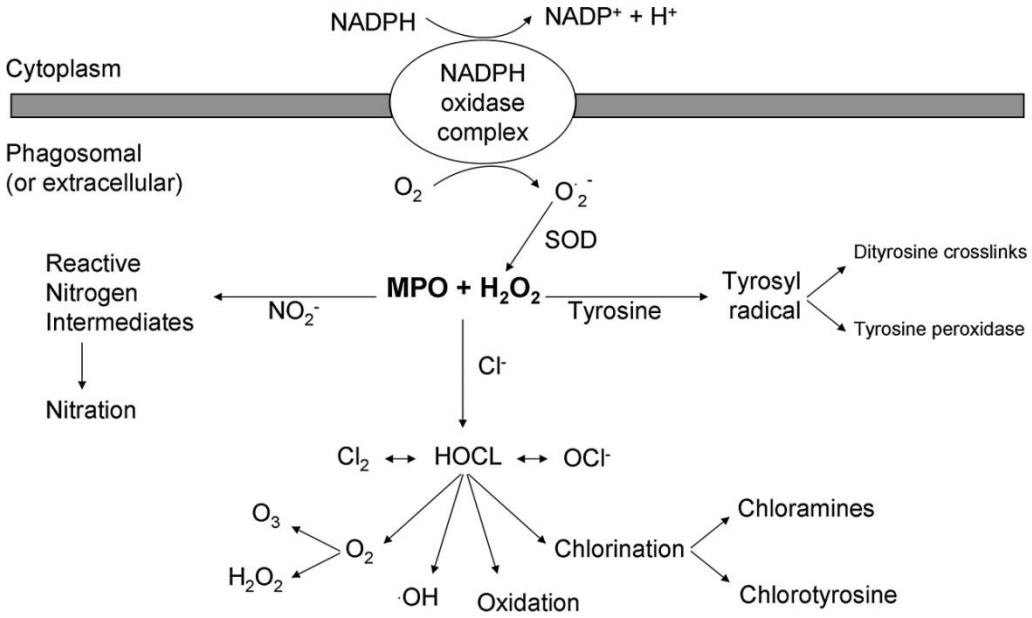

Figure 2.2 Schematic representation of the MPO–H_2O_2 system and its products (van der Veen et al., 2009. Antioxid. Redox Signal 11, 2899-2937.)

Cavallaro et al. (2003) reported that resveratrol dose-dependently inhibited generation of HClO in human neutrophils and Kohnen et al. (2007) later demonstrated that resveratrol inhibit the peroxidation and chlorination activity of MPO by a direct interaction with enzyme. Besides resveratrol, there are few reports on HClO scavenging and MPO inhibitory activities of other stilbene derivatives. Piceatannol (3,5,3′,4′-tetrahydroxy-trans-stilbene) was shown to significantly reduce colonic MPO activity in Piceatannol-treated mice compared to vehicle-treated mice (Kim et al., 2008b). *In vitro* research also revealed that pterostilbene, a structural analogue of resveratrol found in blue berries and grapes, dose dependently decreased superoxide generation and MPO release in stimulated human neutrophils (Macickova et al, 2012). Therefore, extensive and systematic research work should be carried out for finding out more stilbenoids as potential MPO inhibitors.

2.2.2 Assays for MPO inhibitors and HClO scavengers

Both colorimetric and fluorescent assays are routinely used for the evaluation of the HClO scavengers and MPO inhibitors. The most commonly used method for screening of HClO scavengers was developed based on inhibition of the oxidation of 5-thio-2-nitrobenzoic acid (TNB). Yellow TNB can be oxidized by HClO to colorless 5,5-dithiobis (2-ntirobenzoic acid) (DTNB), which is an extremely sensitive colorimetric assay and has a lower detection limit of 5 μM for HClO (Weiss et al., 1982). TNB can also oxidized by HClO chlorinated products such as taurine chloramine (tauNHCl) that is used for MPO inhibition assay (Thomas et al., 1986). For fluorescent assays, the most reported probe for measurement of MPO chlorination activity is 3′-(*p*-aminophenyl) fluorescein (APF), which is selectively cleaved by HClO to yield fluorescein (Setsukinai et al., 2003). A great advantage of using fluorescent probes for HClO detection lies in their mix-and-read convenience to allow high-throughput screening for specific HClO scavengers and MPO inhibitors. Till now, all the HClO scavenger and MPO inhibitor assays are carried out in solutions and cell lysates, none of which is compatible with real-time detection of HClO generated by the living cells.

Although a variety of compounds were identified as efficient HClO scavengers through the different established assays, the information on potent MPO inhibiting compounds in the literature is sparse. A previous study revealed that MPO inhibitors

could prevent HClO induced oxidative damage more effectively than HClO scavengers at micromolar concentrations (Jerlich et al., 2000). However, there is still no report on comparison of the effectiveness of HClO scavengers and MPO inhibitors in eliminating HClO generated by living cells. Therefore, it is meaningful to develop a cell-based assay using a selective and sensitive HClO probe which can directly compare the HClO eliminating effect of resveratrol, the most reported natural MPO inhibitor, with other known efficient MPO inhibitors and HClO scavengers. The result of the assay would also provide important support for exploring the potential of stilbenoids as novel antioxidants and anti-inflammatory agents that protect against tissue damage caused by MPO derived oxidants.

2.2.3 ROS sensing by QDs as the fluorescent probes

Quantum dots (QDs), also called colloidal semiconductor nanocrystals, possess outstanding optical properties including high quantum yields, broad absorption spectra, narrow and symmetric size-tunable emission, and strong resistance to photobleaching, which make them advantageous over traditional organic fluorophores for biosensing and bioimaging applications (Li et al., 2013). Typical QDs are core-shell (e.g., CdSe core with a ZnS shell) or core-only structures functionalized with different coatings, displaying inherent fluorescent properties that can be altered by particle size, make-up (e.g., CsTe, CsSe, CdSe, CdTe) and surface modifications

(Li et al., 2013). QDs with multiple shells were suitable for experiments with living cells exposed for longer time periods (hours and even days) without significant cellular toxicity (Winnik et al., 2013). Since Chan et al. (1998) reported the use of QDs in the detection of biological targets in 1998, a series of QD-based fluorescent biosensors have been well developed for cellular and *in vivo* targeting and imaging. However, there are few reports on the application of QDs to the detection of ROS generated in biological system. For example, negatively-capped CdSe/ZnS QDs conjugated to oxidized Cytochrome c was developed as an selective senor for supoeroxide ($O_2^{\cdot -}$) which readily reduced the oxidized Cytochrome c and lead to enhanced fluorescence of QDs in a dose dependent manner (Li et al., 2011). Furthermore, this probe was demonstrated to be able to detect $O_2^{\cdot -}$ changes in HeLa cells stimulated with PMA ans showed lower cellular toxicity compared to traditional ROS dyes. Altering quenching of Tris (N-(dithiocarboxy)sarcosine)iron(III) linked QDs has been applied to nitric oxide (NO) sensing in our group's previous study as well, where NO binding to the iron complex restores the fluorescence of the QDs specifically (Wang et al., 2009). It was also demonstrated that HOCl in its neutral form is especially potent in quenching and degrading polymer-encapsulated (poly(acrylic acid) graft dodecylamine) QDs in comparison with other ROS such as peroxynitrite ($ONOO^-$), $O_2^{\cdot -}$, and $^{\cdot}OH$ (Mancini et al., 2008). The author also pointed out the potential of QDs applied to HClO sensing in phagocytic cells (e.g., neutrophils and monocytes) and macrophages which are known to generate HClO at concentrations over 20 μM and accumulate QDs in vivo.

2.2.4 The anti-diabetic bioactivity of stilbenoids

Resveratrol has been reported to act as an anti-diabetic agent *in vivo* and *in vitro* (Harikumar et al., 2008). Different mechanisms have been proposed to explain the anti-diabetic action of this stilbene, one of which is modulation of SIRT1 leading to increased whole-body glucose homeostasis and insulin sensitivity in diabetic rats (Milne et al., 2007). It is also reported that in L6 rat skeletal muscle cells, resveratrol stimulated glucose ([^{3}H] 2-deoxy-D-glucose) uptake (201±8.90% of control, $p<0.001$) through a mechanism that involves sirtuins and AMP-activated protein kinase (AMPK) and possibly stimulation of glucose transporter 4 (GLUT4) intrinsic activity (Breen et al., 2008). The study of Chen et al. (2007) showed that insulin secretion of pancreatic beta cells was increased in the presence of resveratrol which inhibits K_{ATP} and K_V channel in beta cells. A recent study demonstrated that piceatannol, a hydroxylated derivative of resveratrol, could promote glucose uptake through GLUT4 translocation to plasma membrane in L6 myocytes and decrease blood glucose levels in type 2 diabetic model mice (Minakawa et al., 2012). The anti-diabetic effects of more complex stilbene derivatives also attracted intense interest for their intricate structures and different anti-diabetic mechanisms. Based on a bioassay-guided fractionation against α-glucosidase, two stilbene dimers 13-hydroxykompasinol A and scirpusin C isolated from seeds of *Syarus romanzoffiana* were found to possess potent inhibitory activity against α-glucosidase type IV from *Bacillus stearothermophilus*, with IC_{50} values of 6.5 and 4.9 μM, respectively (positive control: acarbose, IC_{50}:40 nM) (Lam et al., 2008). Monomeric stilbenes are able to form a C2-O-C8 linkage by a coupling

between the C2 hydroxyl and C8 to produce an arylbenzofuran moiety (Figure 2.3) and some of stilbene derivatives containing this structure exhibited anti-diabetic effects *in vivo* and *in vitro*. For example, moracin M isolated from the root bark of *Morus alba* L.(Moraceae) suppressed the blood glucose levels in alloxan-induced diabetic mice (Zhang et al., 2009). The prenyl-substituted arylbenzofurans 2′-*O*-Demethylbidwillol B and addisofurans A and B isolated from *Erythrina addisoniae* are inhibitors of the type II diabetes target protein tyrosine phosphatase 1B, with IC_{50} values of 13.6-15.7 μM (Na et al., 2007). It is supposed that the linear prenyl group is responsible for these compounds' inhibitory activity which is decreased by the cyclization of the prenyl group.

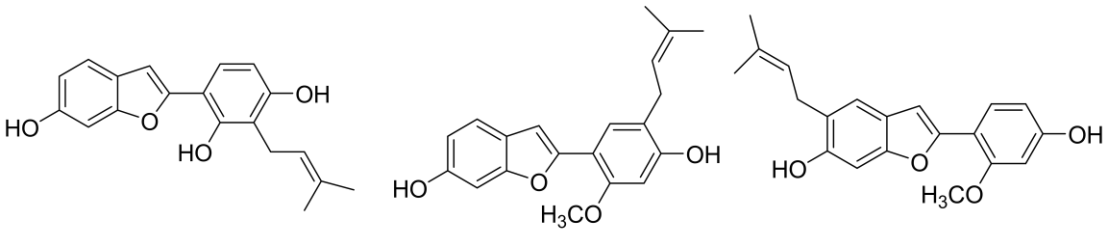

2′-*O*-Demethylbidwillol B addisofurans A addisofurans B

Figure 2.3 Monomeric stilbenes containing arylbenzofuran moiety

Although there are plentiful reports on the anti-diabetic effects of stilbenes from various plant sources, few natural stilbenes have been tested for their insulin sensitizing activity which has become a research focus in the treatment of insulin resistance of type 2 diabetic patients. Resveratrol was shown to reduce blood glucose levels in diabetic rats and stimulate glucose uptake *in vitro*. However, a recent study by Floyd et al. (2008) revealed that resveratrol inhibited insulin-dependent changes in

glucose uptake and suppressed insulin sensitivity in 3T3-L1 adipocytes. Till now, reports on natural stilbenes acting as insulin sensitizers are still rarely seen (Hung et al., 2012). Therefore, finding out novel stilbene derivatives with effective insulin enhancing activity remains as a potential area to explore.

2.2.5 The anti-obesity bioactivity of stilbenoids

Obesity has become a worldwide public health concern and imposes significant risks on metabolic disorders including type 2 diabetes, hypertension, and coronary heart disease. Inhibition of adipocyte differentiation has been one of anti-obesity strategies since obesity is caused by both hypertrophy and hyperplasia of adipocytes. The entire adipogenic process could be mimicked *in vitro* by the 3T3-L1 adipocyte differentiation consisting of the preadipocyte proliferation and their differentiation into mature adipocytes. In the study of Kim et al.(2008c), the effects of 18 stilbene compounds including resveratrol on 3T3-L1 adipocyte differentiation were tested and six compounds exhibited anti-adipogenic effects: stilbestrol, 3,5,4'-trimethoxystilbene, resveratrol, ampelopsin A, vitisin B, and vitisin A with IC_{50} ranging from 5 μM to 38.4 μM. Another recent study showed that resveratrol hydroxylated analog piceatannol could also inhibit 3T3-L1 adipocyte differentiation through inhibition of mitotic clonal expansion and insulin receptor activity in the early phase of differentiation (Kwon et al., 2012). Except the above mentioned stilbenoids, scarce information is currently available regarding the adipogenesis inhibition activity of

other natural stilbenes (Vermaak et al., 2011).

2.3 Stilbenoids isolated from peanuts and their bioactivities

2.3.1 Stilbenoids isolated from peanuts

Stilbenoids are a common structural motif of phytoalexins found in peanuts (*Arachis hypogeal*, Leguminosae). These stilbene phytoalexins are produced by peanuts as defensive reactions to physical injuries and microbial contamination (Lopes et al., 2011). The synthesis of stilbenes in peanuts starts from the conversion of phenylalanine to trans-cinnamic acid which subsequently hydroxylates to form *p*-coumaric acid serving as the precursor in the production of resveratrol and other stilbene derivatives (Figure 2.4).

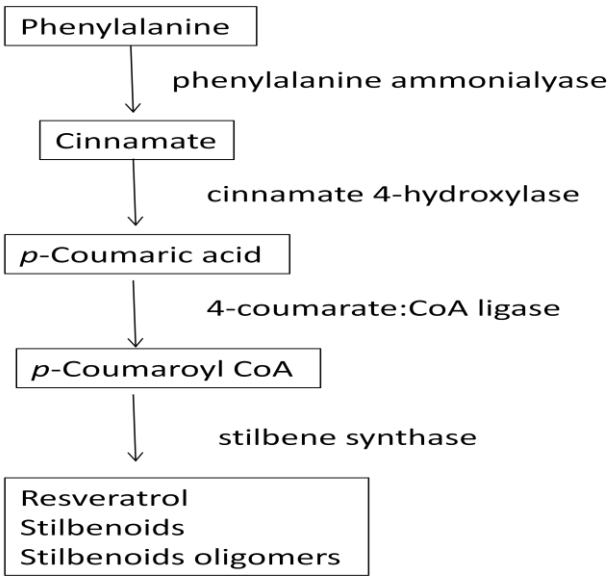

Figure 2.4 Proposed biosynthetic pathway of stilbenoids in peanuts catalyzed by series enzymes (Adapted from Wu et al., 2011. J. Agric. Food Chem. 59, 5993-6003.)

Although stilbenes in minor amounts can be found in uninfected and uninjured peanuts, their synthesis is mainly associated with resistance to some common peanut diseases, in particular to fungal contamination. The stilbene production in peanuts is also elicited by injuries, insect damage, UV irradiation and other exogenous stimuli (Sobolev et al., 2007; Kim et al., 2008a). Stilbenoids of diverse structures have been isolated from different organs of peanuts such as leaves, callus, roots, stems, and seeds (Sobolev et al., 1995; Tokusoglu et al., 2005; Sanders et al., 2000; Chen et al., 2002; Cooksey et al., 1988; Ku et al., 2005; Sobolev et al., 2008; Keen et al., 1976; Ingham et al., 1976; Medina-Bolivar et al., 2007). The reported ones include *trans*-resveratrol (3,5,4′-trihydroxy-*trans*-stilbene), piceid, IPD (*trans*-3′-isop e-ntadienyl-3,5,4′-trihydroxystilbene), piceatannol, arachidin-1 (*trans*-4-(3-methyl-1-butenyl)-3,5,3′4′-tetrahydroxystilben), arachidin-2, arachidin-3 (*trans*-4-(3-methyl-1-butenyl)-3,5,4′-trihydroxystilbene), *cis*-3,5,4′-trihydroxy-4-isopentenylstilbene and *cis*-isomer of resveratrol (Figure 2.5).

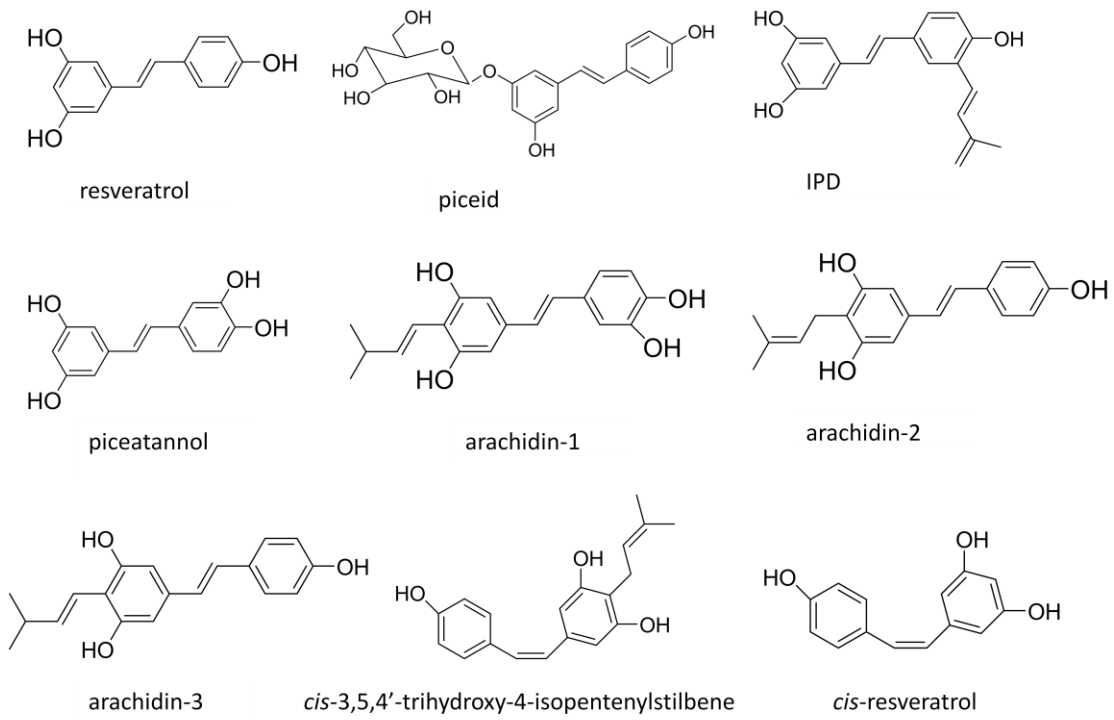

Figure 2.5 Structures of stilbenoids found in peanut tissue /organs

Prenylation plays an important role in the diversification of peanut stilbenoids which bear isopentenyl, isopentyl, or isopentadienyl moieties. Most of new peanut prenylated stilbenoids were isolated from peanut seeds challenged by fungal strains. Some new stilbene derivatives have been isolated from fungi-stressed peanut seeds, including trans-SB-1, chiricanine A (*trans*-4′-deoxyarachidin-2), arahypin-1(*trans*-4′-deoxyarachidin-3), arahypin-2(*trans*-3′-(2′′,3′′-dihydroxy-3′′-methylbutyl) resveratrol, arahypin-3(*trans*-4-(2′′,3′′-dihydroxy-3′′-methylbutyl) resveratrol, arahypin-4(*trans*-4-(2′′,3′′-dihydroxy-3′′-methylbutyl)-4′-deoxyresveratrol, and arahypin-5 (Figure 2.6).

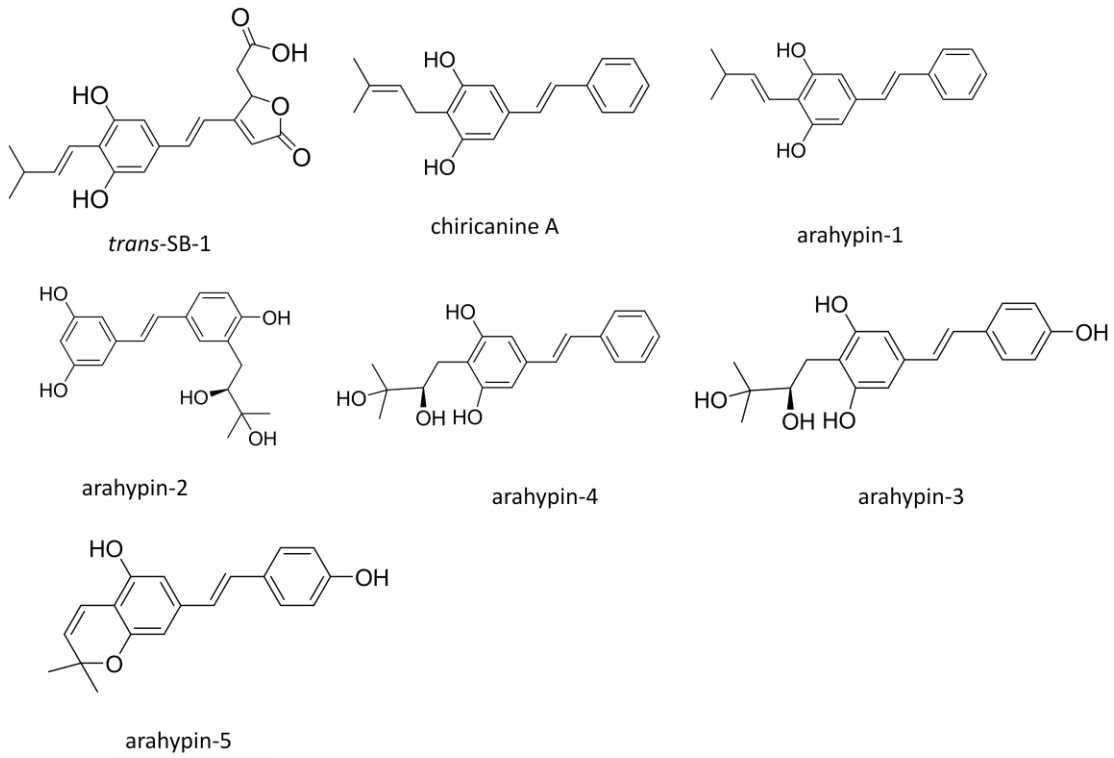

Figure 2.6 Structures of stilbenoids found in fungus-challenged peanut seeds

Till now, only *Aspergillus* species has been used to challenge a few types of peanut seeds to produce new stilbene phytoalexins (Sobolev et al., 2008; Sobolev et al., 2009; Sobolev et al., 2010). The pathways of formation of stilbenoids in peanut seeds suggest that peanut seeds be capable of producing stilbenoids of novel structures. In addition, peanut seeds are readily available in a large amount, indicating the potential of the plant materials as new sources of bioactive stilbenoids.

2.3.2 Bioactivities of peanut stilbenoids

Peanut stilbenoids are strictly in the *trans* olefinic configuration and the olefinic

double bond in the stilbene skeleton is an important determinant of bioactivity (Aggarwal et al., 2004). Prenylation provides peanut stilbenoids greater lipophilicity, which allows the molecules to readily penetrate through cell membranes. The increased lipophilicity often correlates positively with higher bioactivity and bioavailability within groups of compounds of similar structure (Schultz et al., 1997). A most recent study revealed that the peanut stilbenoids arachidin-1 and arachidin-3 exhibited a higher binding affinity for cannabinoid receptor (CBR) compared to their non-prenylated parent compounds piceatannol and resveratrol, which indicates the potential of slower metabolism and enhanced bioavailability of arachidin-1 and arachidin-3 *in vivo* (Brents et al., 2012). In addition, the number and positions of hydroxyl groups in peanut stilbenoids were also found to be crucial factors in regulating biological activities of these compounds (Pont et al., 1990; Schultz et al., 1991; Schultz et al.,1992; Matsuoka et al., 2002; Lappano et al., 2009). For example, due to resonance effects, the stilbenoids with a 4′-hydroxy group exhibited higher cytogenetic and estrogenic activities than those having 3′- and 5′-hydroxy groups (Aggarwal et al., 2004).

Although the bioactivities of resveratrol have been extensively explored, the biological potency of prenylated peanut stilbenoids were reported by only a few studies (Chang et al., 2006; Djoko et al., 2007; Abbott et al., 2010; Huang et al., 2010). Anticancer properties of arachidin-1, arachidin-3, IPD, and resveratrol isolated from germinating peanut kernels were investigated (Huang et al., 2010). Among the four

compounds tested, arachidin-1 exhibited the highest efficacy in inducing mitochondrion-mediated apoptosis of HL60 cells with an approximately 4-fold lower EC_{50} than resveratrol. Arachidin-1 demonstrated its efficacy as an anticancer agent by inducing caspase-independent death of cancer cells with mutations in key apoptotic genes. The antioxidant and anti-inflammatory activities of some peanut stilbenoids were also characterized (Chang et al., 2006; Djoko et al., 2007). Arachidin-1, piceatannol, and resveratrol showed effective inhibitory effect on lipopolysaccharide (LPS)-induced nitric oxide (NO) production in RAW 264.7 macrophages; piceatannol presents highest inhibitory potency on LPS-induced prostaglandin E_2/NO production, C/EBPδ gene expression, and nuclear fator-κB activation (Djoko et al., 2007). In another study by the same research group, arachidin-1 displayed the significantly higher antioxidant potency compared with stilbenes arachidin-3, IPD, and resveratrol isolated from peanut kernels (Chang et al., 2006). Usually all the tested peanut stilbenoids perform anti-inflammatory and antioxidant activities but with different potencies, which could be attributed to 4′-hydroxyl group as the most important determinant of bioactivities (Chang et al., 2006). An 3′-hydroxyl group also plays an important role in the more potent antioxidant, anti-inflammatory and anti-cancer bioactivities of arachidin-1 and piceatannol compared with other peanut stilbenoids (Lopes et al., 2011). Besides the bioassays performed in mammalian cells, Sobolev et al. (2011) evaluated the antifungal effect of peanut stilbenoids against plant pathogenic fungi and the toxicity of the compounds to mosquito larvae and adults. The study revealed a diverse range of biological activities displayed by individual

stilbenoids with close structural similarities. Although considerable research progress has been made in exploring therapeutic or preventive potential of natural stilbenes, there are no reports on the anti-diabetic and anti-obesity activities of peanut prenylated stilbenoids.

2.4 Stilbene oligomers and their bioactivities

Natural stilbenes, structurally characterized by the presence of 1,2-diphenylethylene backbone, can be divided into two categories, monomeric and oligomeric stilbenes. Oligomeric stilbenes, with diverse skeletons, complex configurations and different degrees of oligomerization, are produced by coupling between homogeneous or heterogeneous monomeric stilbenes. They can be classified into four major groups of 29 construction patterns on the basis of the number of connective bonds (C-C or C-O-C) and linkage points between two monomeric stilbene units (Shen et al., 2009): a) two monomeric stilbene units connected by one C-C or C-O-C bond with two linkage points; b) two monomeric units connected by two C-C or C-O-C bonds with four linkage points, usually forming a ring; c) two monomeric units connected by three C-C or C-O-C bonds with six linkage points, leading to the formation of two rings; d) two monomeric units linked by four C-C or C-O-C bonds with eight linkage points, this pattern is rare and only two compounds belong to this group. Due to the copyright reason, the figures of the 29 construction patterns of stilbene oligomers are not shown and can be found in the article of Shen et al. (2009).

Stilbene dimers and oligomers isolated so far typically connect through the stilbene olefinic and aromatic carbon and the phenolic groups. According to various possible monomeric units, stilbene oligomers can also be classified into seven categories, resveratrol oligomers, isorhapontigenin oligomers, piceatannol oligomers, oxyresveratrol oligomers, resveratrol and oxyresveratrol oligomers, and miscellaneous oligomers .

As for peanut stilbene oligomers, only two stilbene dimers arahypin-6 and arahypin-7 (Figure 2.7) were isolated from fungus-challenged peanut seeds (Sobolev et al., 2010). Based on the two connective bonds and four linkage points, arahypin-6 and arahypin-7 are constructed using one of 29 known patterns. However, the monomeric units of these two dimers arachidin-1 and arachidin-3 are prenylated stilbenes which have not been reported before in the literature on stilbene oligomers.

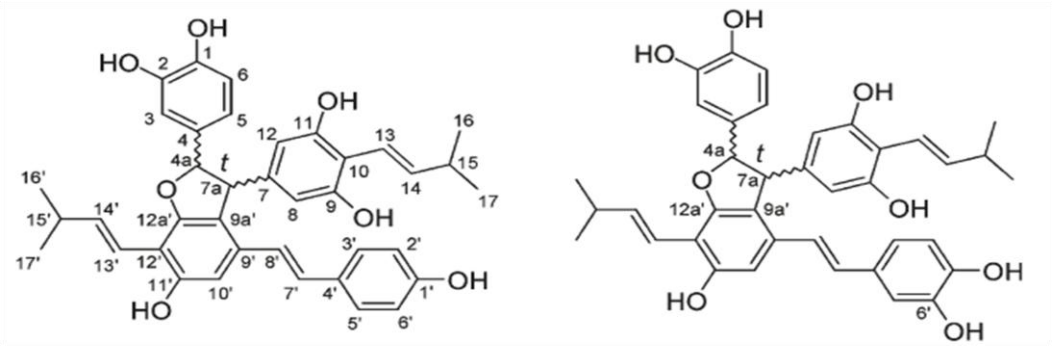

Figure 2.7 Structures of arahypin-6 and arahypin-7. (Sobolev et al., 2010. J. Agric. Food Chem. 58, 875–881.)

Oligomeric stilbenes have shown diverse bioactivities including antioxidant, cytotoxic, anti-inflammatory, anti-diabetic, and anti-obesity properties (Shen et al., 2009). Some of them exhibited more potent activities than their corresponding monomeric units. For example, Vaticanol C is a resveratrol tetramer isolated from *Vatica rassak* and showed cytotoxicity against a panel of human cancer lines including HL60 cells with a 4-7 fold higher potency than resveratrol (Ito et al., 2003). In another study, the anti-adipogenic effect of a resveratrol tetramer vitisin A abundant in the stembark of *Vitis* was evaluated together with 17 other stilbenes including resveratrol. Among the 18 stilbenes tested (Kim et al. 2008c), vitisin A was the most effective in inhibiting 3T3-L1 adipocyte differentiation with an IC_{50} of 5.0 μM. The study of Wan et al. (2011) also revealed that piceatannol dimers showed a higher α–glucosidase inhibitory activity than piceatannol. Although there are a few reports on the anti-diabetic and anti-obesity activities of stilbene oligomers (Shen et al., 2009), the various construction patterns displaying a wide range of bioactivities indicate that stilbene oligomers are rich sources of lead compounds in search for novel anti-diabetic and anti-obesity agents. Since flavonoid oligomers larger than trimers are difficult to be absorbed in the small intestine (D'Archivio et al., 2007; Halliwell et al., 2000), finding out bioactive polyphenol dimers or trimers may be more practical for the prospective *in vivo* applications.

Chapter 3 Fluorescent assay using Quantum Dots for screening of MPO inhibitors and HClO scavengers

3.1 Introduction

Quantum Dots (QDs), as a new type of semiconductor material, have superior luminescence properties and can be molecularly engineered as chemosensors through grafting, on the QD surface, a layer of organic molecules responsive to analytes by switching the luminescence on/off. The long-term photostability and brightness of QDs also make them become ideal candidates for live organisms targeting and imaging. QDs have been applied to quick detection of both scavengers and generators of ROS such as hydroxyl radical ($^{\cdot}OH$) and H_2O_2 (Jiang & Ju, 2007; Hay et al., 2007). There were also reports on QDs used for sensing nitric oxide (NO) and singlet oxygen ($^1O_2$) (Wang et al., 2009; Zhang et al., 2006).

A previous study (Mancini et al., 2008) reported the oxidative quenching of QD fluorescence by HClO. Based on the same fluorescence quenching mechanism, Yan et al. (2010) synthesized a new type of inert polymer encapsulated QDs (QDs-poly-CO_2^-) for monitoring HClO in tape water and MPO activity. The QDs-poly-CO_2^- showed good selectivity for HClO over other biologically important ROS including H_2O_2, peroxynitrite ($ONOO^-$), superoxide ($O_2^{\cdot -}$), and $^{\cdot}OH$, which suggests a potential of the QDs to be applied to a cell based fluorescent imaging and microplate assay. Since it is

important to correlate the results of *in vitro* assays with i*n vivo* effects, development of a cell based method is necessary for the direct examination of HClO scavengers and MPO inhibitors under physiological conditions.

Due to the non-diffusive property of QDs, in this study HL60 cells were differentiated into macrophage and neutrophil phenotypes for intracellular and extracellular HClO detection, respectively. The intracellular HClO detection was achieved through fluorescent imaging while the extracellular HClO detection depended on microplate reading applied to screening effective HClO scavengers and MPO inhibitors. The performances of microplate assays using QDs, 2,7-dichlorofluorescin diacetate (DCFH-DA), and APF were also compared in terms of selectivity for HClO. More importantly, resveratrol together with other known efficient MPO inhibitors and HClO scavengers would be tested in the QDs based microplate assay, the result of which would provide the rationale for further investigating the MPO inhibitory efficiency of peanut stilbenoids.

3.2 Materials and methods

3.2.1 Chemicals and materials

All materials for cell culture were from GIBCO (Grand Island, NY, USA). Sodium hypochlorite solution (NaClO, available chlorine 10-13%), phorbol 12-myristate 13-acetate (PMA, 99%), 2,7-dichlorofluorescin diacetate (DCFH-DA, 97%), thiourea (99%), resveratrol (99%), 4-aminobenzoic acid hydrazide (ABAH, 95%), sodium

azide (NaN_3, 99%), L-ascorbic acid (99%), methionine (99%), taurine (99%) and glutathione (GSH, 98%) were purchased from Sigma Chemical Co. (St. Louis, MO, USA). H_2O_2 (30%) was from Merck (KGaA, Darmstadt, Germany). 3´-(*p*-aminophenyl) fluorescein (APF) (5mM solution in DMF) was purchased from Cell Technology, Inc. The chemicals were dissolved in different solvents as stock solutions: DCFH-DA (10 mM), ABAH (100 mM) in DMSO; PMA (1 mg/ml),and resveratrol (100 mM) in ethanol; thiourea (500 mM), taurine (200 mM), methionine (10 mM), GSH (200 mM), L-ascorbic acid (200 mM) and NaN_3 (1 M) in distilled water. The stock solutions of GSH and L-ascorbic acid were freshly prepared each day. Krebs-Ringers phosphate buffer (KRPB; 114 mM NaCl, 4.6 mM KCl, 2.4 mM $MgSO_4$, 1.0 mM $CaCl_2$, 15 mM NaH_2PO_4, 15 mM Na_2HPO_4, pH 7.4) was used for dilution of the above stock solutions for the subsequent analyses. Hydrophilic QD by polymer encapsulation (QDs-Poly-CO_2^-) was prepared as described in the study of Yan et al. (2010). All other chemicals were of analytical grade.

3.2.2 Cell Culture

HL60 cells were purchased from the American Type Culture Collection (ATCC, Manassas, VA, USA) and grown in IMDM medium supplemented with 10% fetal bovine serum, 100 U/ml penicillin, and 100 μg/ml streptomycin at 37 ℃ in a 5% CO_2 humidified environment. The passage number of the cells used in the assay was between 10-30.

3.2.3 Confocal microscopy imaging

The cell suspension (10^6/mL) was seeded on a chambered coverglass (Lab-Tek chambered#1.0 Borosilicate Coverglass System) with the medium containing phorbol 12-myristate 13-acetate (PMA, 50 ng/mL, Sigma) to induce the differentiation to macrophage-like cells. After 48 h, the medium was discarded and the new medium with QDs-poly-CO_2^- (1.5 μM) was added for overnight incubation. Then the excessive QDs were removed by washing three times (30 min for each time) with Krebs Ringer Phosphate buffer (KRPB). The intracellular localization of QDs in single cells were investigated by a sequential z-step scanning using confocal microscopy (Olympus IX 81, Fluoview FV1000) equipped with a 100× oil lens. QDs were excited with a 405 nm Ar laser and the fluorescent images were collected using filters sets more than 560 nm. Images were processed in IMARIS 3.0 (BITPLANE AG) software.

3.2.4 Effect of HClO on the intracellular QDs

After verification of the intracellular QDs, the cells were treated with HClO (a final concentration of 200 μM) diluted in KRPB for 30 min at room temperature. Central sections of single cells were chosen as the fixed site for monitoring fluorescence changes of QDs. The images were recorded with the same optical parameters of confocal microscopy at a time interval of 15 min.

3.2.5 Fluorescent microplate assay

To differentiate HL60 cells into a neutrophil-like phenotype, 60 mM DMSO was added to the cell growth medium, in which the cells were cultured for 7 days. On day 7, differentiated HL60 cells were centrifuged at 800 g for 5 min and resuspended in KRPB. Viable cells were counted on a hemocytometer using trypan blue exclusion.

100 μL of the cell suspension in KRPB (1×10^6/ml) were added to each cell of the 96-well plate (Greiner, black wells flat bottom). The cells were incubated with 100 μL of the test chemicals of different concentrations for 1h. Thereafter 20 μL of QDs (5 nM) and 20 μL of PMA (2 μg/mL) or H_2O_2 (200 μM) were added sequentially. The microplate was shaken gently every 5 minutes to ensure that the cells and QDs were kept in suspension. After incubation for 30 min, the fluorescence was measured on a microplate reader (Tecan, Infinite M200) in the top reading mode with an excitation wavelength at 400 nm and emission at 595 nm. For the DCFH-DA or APF assay, 20 μL of DCFH-DA (100 μM) or APF (100 μM) was added in replacement of QDs and fluorescence was measured with an excitation wavelength at 485 nm and emission at 530 nm.

3.2.6 Data analysis

The ability of test chemicals to scavenge or inhibit the generation of HClO was measured by PMA or H_2O_2 treated controls in the presence or absence of the test

chemicals. The inhibition rates of fluorescence quenching per well was calculated using the formula $[(F_t-F_p)/(F_c-F_p)]*100]$, where F_c = fluorescence without the test chemical and PMA or H_2O_2, F_t = fluorescence with the test chemical and PMA or H_2O_2 and, F_p = fluorescence with PMA or H_2O_2. The same formula was also used in the DCFH-DA and APF microplate assay to calculate the inhibition rates of fluorescence increase per well.

3.3 Results and Discussions

3.3.1 Effective cellular uptake of QDs-poly-CO_2^-

The PMA differentiated HL60 cells were chosen because they bear mature macrophage characteristics including the ability to phagocytize large particles such as latex beads or yeast cells (Rovera et al., 1979; Ackerma et al., 1989). In addition, the differentiation induced cell adherence to surfaces, which allowed the washing step to be used for removing the excessive QDs. The Z-stack gallery image (Figure 3.1A) clearly shows that the macrophage-like cells could effectively phagocytize the QDs-poly-CO_2^- which was suspended inside the cells. A 3D image (Figure 3.1 B) was also given to demonstrate the depth distribution of QDs-poly-CO_2^- inside the cell.

3.3.2 Quenching effect of HClO on QDs-poly-CO_2^-

Figure 3.1 (upper panel) shows the quenching effect of HClO on the intracellular QDs-poly-CO_2^-. It can be seen that the fluorescence of QDs-poly-CO_2^- was completely quenched after treatment with NaClO (200 μM) for 30 min. In contrast, no apparent quenching effect was observed during the same incubation time without HClO treatment (lower panel). The results indicate that the QDs-poly-CO_2^- can be used for the detection of intracellular HClO and one potential application of the QDs-poly-CO_2^- is to find out those effective intracellular HClO scavengers.

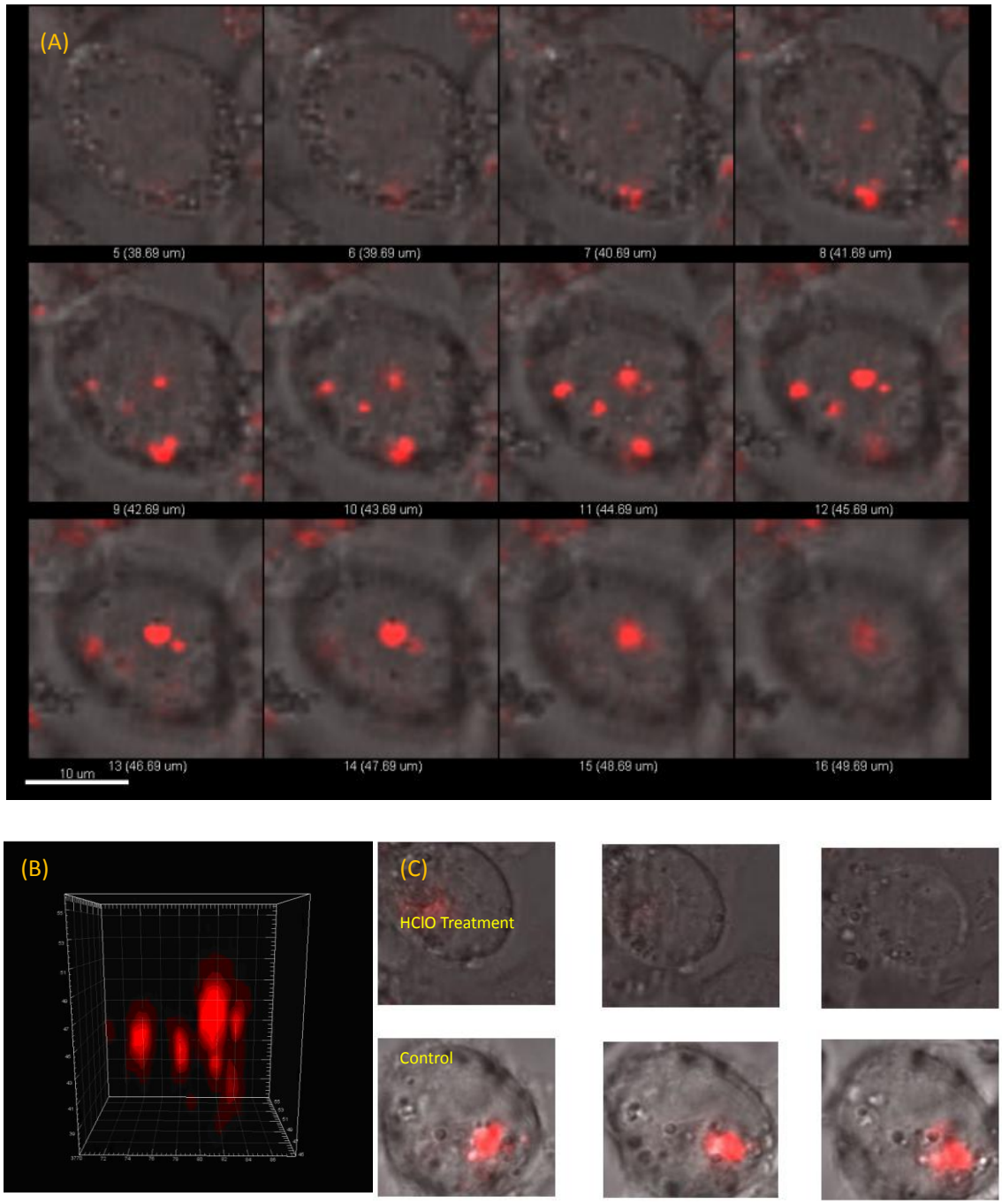

Figure 3.1 Fluorescent imaging of QDs-poly-CO_2^- in HL60 cells A) Z-stack gallery images of intracellular QDs-poly-CO_2^-. The confocal z stacks were acquired with 1-μm spacing, showing QDs-poly-CO_2^- distribution at various depths within the cell. B) 3D image of intracellular QDs-poly-CO_2^- created by assembling the z stack images from successive focal planes with 1-μm spacing. C) Quenching effect of HClO on the intracellular QDs-poly-CO_2^- (from right to left: 0, 15 and 30min). (Yan et al., 2010. Anal. Chem. 82, 9775-9978.)

Although there were biological imaging studies to detect HClO in living cells (Chen et al., 2010; Lin et al., 2009; Chen et al., 2008; Shi et al., 2010; Yang et al., 2009), the chemosensors used in these studies were organic fluorescent probes. Compared with the QDs, the organic dyes have good cell permeability and can easily enter the cells in a diffusible way. On the other hand, the poor dye properties such as photobleaching and autoxidation limit their applications to cell imaging, especially under confocal microscopy where long-time exposures of samples to the intensive laser illumination are often required. Therefore, the better performance of QDs to overcome these limitations provides an alternative choice for intracellular imaging. Although QDs for sensing HClO in biological samples were reported previously (Mancini et al., 2008), they were not applied to live cell imaging before.

3.3.3 Quenching effect of PMA stimulated cells on QDs-poly-CO_2^-

The fluorescence quenching of QDs by PMA-stimulated neutrophil-like cells is shown in Figure 3.2. Resveratrol (160 μM) was used as a MPO inhibitor (Cavallaro et al., 2003; Kohnen et al., 2007) and reduced the amount of QD fluorescence quenching. Cell suspension of higher densities caused a more significant fluorescence quenching because of more HClO generation. Resveratrol was found to have a maximum inhibition rate at a cell density of 1×10^6/ml which was adopted in this study to achieve a good sensitivity. To rule out the possibility of interaction between QDs and PMA, the QD fluorescence in KRPB without cells was investigated (Figure 3.3).

The results show that PMA has no influence on QD fluorescence quenching.

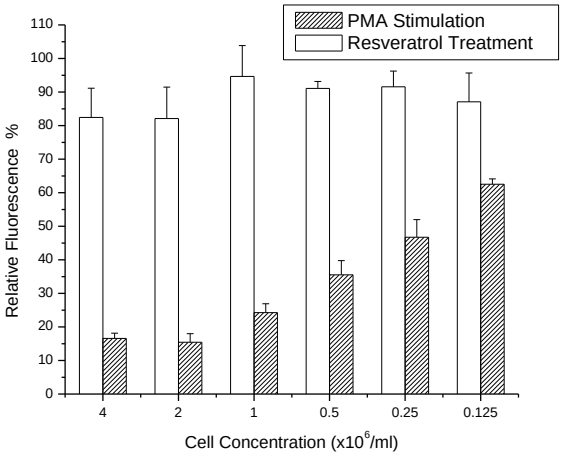

Figure 3.2 Quenching of QD fluorescence by different concentrations of neutrophil-like HL60 cells after PMA stimulation. When incubated with the same concentration of QDs and PMA for 30 min, the neutrophil-like cells caused fluorescence quenching in a cell concentration-dependent manner. Pre-incubation with resveratrol (160 μM) for 1 h could inhibit the QD fluorescence quenching induced by PMA stimulation at all the cell concentrations. The relative fluorescence was calculated as the ratio of QD fluorescence values between the measured wells to the control well without PMA and resveratrol treatment. The error bars represent the standard deviations of four replicate wells (n = 4)

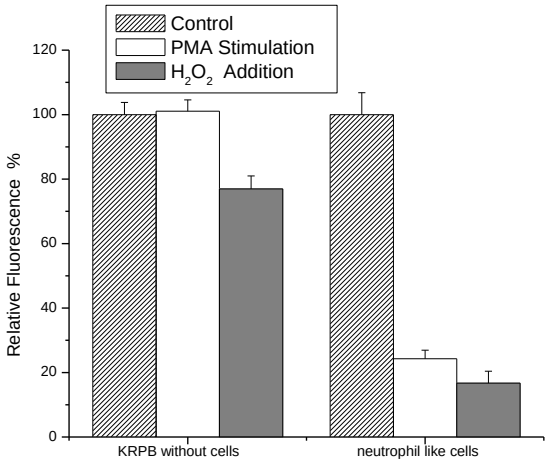

Figure 3.3 The influence of PMA and H_2O_2 on the QD fluorescence quenching. The PMA or H_2O_2 was incubated with neutrophil-like cells for 30 min after the addition of QDs. The QD fluorescence in KRPB or cell suspensions (1×10^6/mL) without PMA and H_2O_2 treatment was taken as 100% of relative fluorescence. The error bars represent the standard deviations of four replicate wells (n = 4)

3.3.4 QD microplate assay for HClO scavengers and MPO inhibitors

The effects of MPO inhibitors and HClO scavengers on QD fluorescence quenching inhibition are shown in Figure 3.4. For MPO inhibitors (Figure 3.4 A), the percentage of fluorescence quenching inhibition is correlated with the concentration in the range from 20 μM to 320 μM. A similar dose-response relationship was found for HClO scavengers in the concentration range from 40 μM to 10 mM (Figure 3.4 B). The potency of MPO inhibitors tested, compared by the inhibition rate at 40 μM and 320 μM, showed the following order: reveratrol > ABAH > sodium azide (Table 3.1). The inhibition rates of HClO scavengers showed the order:

thiourea ≈ methionine > GSH > taurine ≈ L-ascorbic acid. Although both MPO inhibitors and HClO scavengers dose dependently inhibited the fluorescence quenching of QDs, the concentration response relationship of MPO inhibitors is more obvious than that of HClO scavengers. For example, the inhibition rate of sodium azide at 40 μM is much lower than methionine and thiourea at the same concentration. However, at 320 μM the inhibition rate of sodium azide is significantly higher than those of methioine and thiourea. These results have important implications for the difference between MPO inhibitors and HClO scavengers in terms of their HClO-removing mechanisms and performances to limit HClO-mediated oxidative damage.

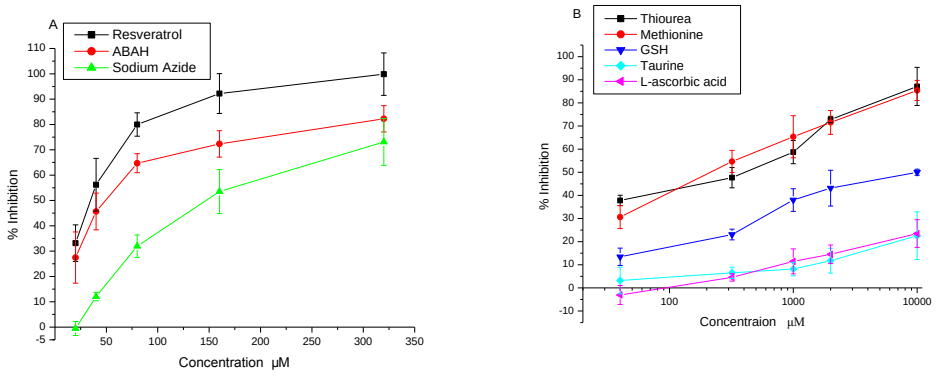

Figure 3.4 The dose relationship of QD fluorescence quenching inhibition by MPO inhibitors (A) and HClO scavengers (B). The MPO inhibitors and HClO scavengers were incubated with the neutrophil-like cells for 1 h before the addition of QDs and PMA. The concentration range was from 20 μM to 320 μM (20, 40, 80, 160 and 320 μM) for MPO inhibitors and from 40 μM to 10 mM (40 μM, 320 μM, 1mM, 2 mM, 10 mM) for HClO scavengers. The error bars represent the inter-day variations of three independent assays (n = 3) in which the mean of data was from 4 replicated wells (n = 4).

Table 3.1 Comparison of the potency of MPO inhibitors and HClO scavengers in inhibiting the QD fluorescence quenching induced by PMA stimulation

Compounds	Inhibition (%) (mean ± S.D.) at 40 μM	Inter-day variation (%) (R.S.D., n=3)	Intra-day variation (%) (R.S.D., ,n=4)	Inhibition (%) (mean ± S.D.) at 320 μM	Inter-day variation (%) (R.S.D., n=3)	Intra-day variation (%) (R.S.D., ,n=4)
MPO inhibitors						
Resveratrol	56.21 ± 10.40	18.50	2.66	99.86 ± 8.37	8.38	3.50
ABAH	45.24 ± 7.25	16.03	6.47	82.24 ± 5.20	6.32	6.07
Sodium Azide	12.50 ± 1.68	13.44	7.14	73.10 ± 9.26	12.67	7.23
HClO scavengers						
Thiourea	37.80 ± 2.26	5.98	17.11	47.66 ± 4.39	9.21	15.81
Methionine	30.65 ± 4.98	16.25	11.74	54.65 ± 4.80	8.78	7.46
GSH	13.45 ± 3.76	27.96	20.20	23.08 ± 2.32	9.95	13.75
Taurine	-	-	-	6.53 ± 2.43	37.21	44.08
L-ascorbic Acid	-	-	-	4.55 ± 1.62	35.60	41.14

-, No inhibition effect.

Since MPO is expressed in the neutrophil-like HL60 cells, H_2O_2 was added to the cells to generate HClO through the MPO–H_2O_2–Cl^-system. Although H_2O_2 could quench the fluorescence of QDs (Figure 3.3) in the cell-free condition, this effect was not significant when compared to fluorescence quenching in the presence of the cells. The potency of MPO inhibitors, compared by the inhibition rates at 20 μM and 320 μM, showed the order: resveratrol > ABAH > sodium azide (Table 3.2). For HClO scavengers, the observed order is as follows: thiourea ≈ methionine > GSH >

L-ascorbic acid > taurine. The cell permeable MPO inhibitors resveratrol and ABAH showed a significantly higher efficiency of quenching inhibition compared with all the HClO scavengers, which is consistent with the results from the PMA stimulated cells.

Table 3.2 Comparison of the potency of MPO inhibitors and HClO scavengers in inhibiting the QD fluorescence quenching induced by H_2O_2 addition

Compounds	Inhibition (%) (mean ± S.D.) at 20 μM	Inter-day variation (%) (R.S.D., n=3)	Intra-day variation (%) (R.S.D., ,n=4)	Inhibition (%) (mean ± S.D.) at 320 μM	Inter-day variation (%) (R.S.D., ,n=3)	Intra-day variation (%) (R.S.D., ,n=4)
MPO inhibitors						
Resveratrol	60.52±7.03	11.62	4.68	86.97±4.17	4.79	2.61
ABAH	52.72±7.03	13.33	8.23	85.20±0.65	0.76	2.79
Sodium Azide	-	-	-	65.73±0.57	0.87	3.69
HClO scavengers						
Thiourea	40.30±5.09	12.63	3.35	41.55±2.16	5.20	6.80
Methionine	20.17±7.33	36.34	5.97	46.96±9.70	20.66	3.37
GSH	11.10±5.81	52.34	12.12	21.80±7.50	34.40	18.70
L-ascorbic Acid	-	-	-	2.46±0.90	36.59	30
Taurine	-	-	-	-	-	-

-, No inhibition effect.

PMA and H_2O_2 were used to induce HClO generation by HL60 neutrophil-like cells. Unlike the neutrophils isolated from whole blood, the commercially available HL60 cells are not limited by availability of blood samples, and hence more suitable for the

large-scale screening assay. Compared with other adherent cell types, non-adherent neutrophil-like cells used in the microplate assay also have the advantages including no need for pre-seeding and reduced variability of the assay due to the variable cell numbers. Most importantly, myeloid derived HL60 cells overexpress MPO and could be induced to produce a much higher level of HClO than other cell lines.

Both MPO inhibitors and HClO scavengers tested in PMA and H_2O_2 based assays could inhibit the QDs fluorescence quenching but MPO inhibitors showed a more obvious concentration response relationship than HClO scavengers. This could be explained by different HClO removal mechanisms. HClO scavengers could not block the generation of HClO and produced a reduction of QD fluorescence quenching through a competitive mechanism. Therefore, a significantly higher concentration of HClO scavengers was required to reach an inhibition rate over 70% when compared with MPO inhibitors. Jerlich et al. (2000) also reported that higher concentrations of HClO scavengers than MPO inhibitors were required for the prevention of low density lipoprotein oxidation by the MPO/H_2O_2/Cl^- system, which indicates that MPO inhibitors are more efficient in reducing HClO than HClO scavengers.

Pattison & Davies (2006) has demonstrated that HClO reacts readily with many biological molecules, particularly those with thiols such as GSH and sulfur-containing amino acids such as methionine and cysteine. GSH, methionine, and cysteine showed the highest HClO scavenging efficiency in previous studies (Winterbourn et al., 1985;

Pattison & Davies, 2006) and the reactivities of the three compounds with HClO were similar-at least 100-times more reactive than other amino acids. Given the rapid reaction rates of HClO with biological materials, high doses of conventional antioxidants such as L-ascorbic acid (vitamin C) and thiols are required to effectively protect against direct oxidative damage by HClO (Winterbourn et al., 1985). Other biological ROS such as $ONOO^-$ and $^{\cdot}OH$ may also compete with HClO for antioxidants. In addition, antioxidants such as taurine can react with HClO and generate chloramines (RNHCl) which are reactive oxidants and key intermediates in HClO-mediated damage (Peskin et al., 2001; Anraku et al., 2003). Therefore, inhibiting the generation of HClO may be a better choice than scavenging HClO after its generation, for amelioration of HClO induced biological damage.

3.3.5 Time course of QD fluorescence quenching

The time course of QDs quenching due to PMA stimulation and H_2O_2 addition to the neutrophil-like cells was also investigated. Figure 3.5 shows that the H_2O_2 QD fluorescence quenching reaction went to completion within 10 minutes while PMA stimulation caused a gradual quenching process extending over 30 minutes. The results indicate different mechanisms of HClO generation by H_2O_2 and PMA. The addition of H_2O_2 quenched the QD fluorescence faster than the PMA stimulation because H_2O_2 can be directly used as a substrate by MPO to generate HClO whereas after PMA addition the amount of HClO is limited by the generation of H_2O_2 which

needs activation of NADPH oxidase and superoxide dismutase (SOD) as illustrated by Figure 2.2 (Boersma et al., 2003; Teufelhofer et al., 2003; van der Veen et al., 2009).

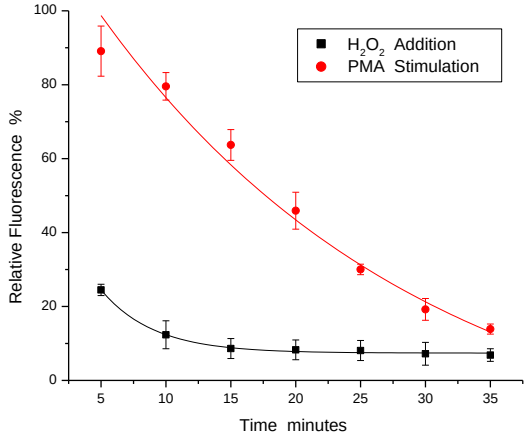

Figure 3.5 The time course curve of QD fluorescence quenching by neutrophil-like cells after PMA stimulation or H_2O_2 addition. The relative fluorescence was calculated as formula: $[(F_p-F_b)/(F_c-F_b)]*100]$, where F_p= QD fluorescence with PMA or H_2O_2 treatment, F_b = background fluorescence without QDs, F_c = QD fluorescence without PMA or H_2O_2 treatment. All three fluorescence parameters were measured every 5 minutes. The error bars represent the standard deviations of four replicated wells (n = 4).

Neutrophil-like cells stimulated by PMA undergo a "respiratory burst", which leads to extracellular release of MPO and HClO (Mancini et al., 2008; Kohnen et al., 2007). Although PMA stimulation is a classic method for HClO generation in neutrophil-like cells, the selectivity of the assay may be compromised by other "respiratory burst" relevant enzyme inhibitors such as NADPH oxidase inhibitor diphenyliodonium (DPI) which also blocks HClO generation, as demonstrated in a previous study (Teufelhofer et al., 2003). To overcome this disadvantage, the cells were directly exposed to H_2O_2 which could be converted to HClO by MPO catalysis. Wagner et al. (2000) reported a fast conversion of H_2O_2 to HClO by HL60 cells within minutes. To avoid inhibition of MPO, the H_2O_2 concentration employed in the assay was kept below 20

μM, as recommended by Kettle et al. (2004). The potency order of HClO scavengers showed a slight difference between the PMA stimulation and H_2O_2 addition methods, which may be due to the different mechanisms of HClO generation by neutrophil-like cells. However, this does not influence the performance of this assay for screening highly efficient MPO inhibitors and HClO scavengers such as resveratrol and thiourea.

Another difference between PMA stimulation and H_2O_2 addition to generate HClO is that PMA caused neutrophil degranulation leading to extracellular MPO and HClO release, whereas the added H_2O_2 is mainly converted by intracellular MPO in HClO which later diffuse outside the cells. The addition of H_2O_2 may therefore be more suitable for evaluation of intracellular MPO inhibitors. Unlike organic fluorescent probes, QDs have poor cell permeability and could not enter the cell in a diffusible way especially in such a short time of 30 minutes. This could provide QDs with another advantage, in that the quenching of QDs fluorescence would not be influenced by the complex intracellular environment containing other interfering peroxidases (Drozdetskaya & Ilin, 1972; Henderson & Chappell, 1993). So there is no need for extraction and purification of MPO from neutrophils or the whole blood cells (Kettle & Winterbourn, 1994), which makes the QDs based microplate assay less time-consuming and laborious compared with previous methods. Meanwhile, although the chlorination activity measured in this assay is considered to be the dominant and specific activity of MPO *in vivo* (Kettle & Winterbourn, 1997;

Furtmuller et al., 2000), the definition of a MPO inhibitor also includes the inhibition of the peroxidation and nitration activities (Malle et al. 2007). Therefore, supplemental assays described previously should be conducted for a comprehensive assessment of the MPO inhibition activity after a lead compound is screened and identified by the assays developed in this study.

3.3.6 DCFH-DA microplate assay

A microplate assay using another ROS fluorescent probe DCFH-DA was conducted to evaluate the tested chemicals in the QD based microplate assay. Table 3.3 shows that only GSH and L-ascorbic acid (320 μM) significantly inhibited the ROS induced fluorescence increase in H_2O_2 and PMA stimulated cells. This result is in stark contrast to the inhibition order of the test chemicals from the QD based microplate assay, which indicated the different selectivity of the two fluorescent probes for ROS generated by the cells. Also, the effect of H_2O_2 and PMA on the DCFH-DA fluorescence in KRPB without cells was investigated and no significant influence was found (Figure 3.6).

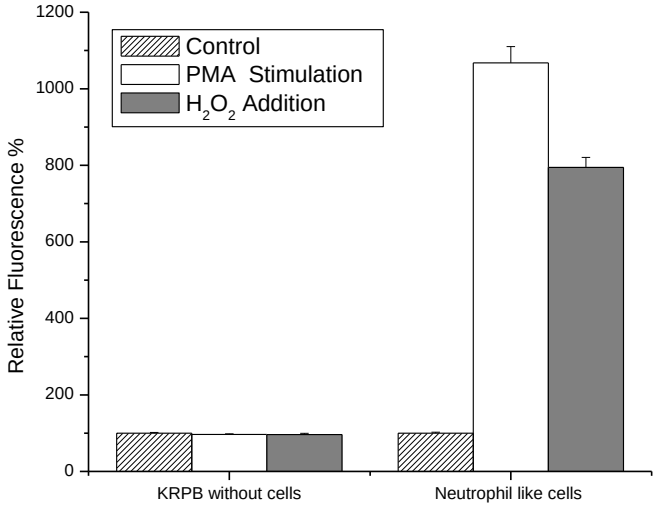

Figure 3.6 The influence of PMA stimulation and H_2O_2 addition on the DCFH-DA fluorescence increase. The PMA or H_2O_2 was incubated with neutrophil-like cells for 30 minutes after the addition of DCFH-DA. The DCFH-DA fluorescence in KRPB or cell suspensions (1×10^6/mL) without PMA and H_2O_2 treatment was taken as 100% of relative fluorescence. The error bars represent the standard deviations of four replicated wells (n = 4).

Table 3.3 Comparison of the potency of MPO inhibitors and HClO scavengers in inhibiting the DCFH-DA fluorescence increase induced by PMA stimulation and H_2O_2 addition

Compounds	PMA stimulation			H_2O_2 addition		
	Inhibition (%) (mean ± S.D.) at 320 μM	Inter-day variation (%) (R.S.D., ,n=3)	Intra-day variation (%) (R.S.D., ,n=4)	Inhibition (%) (mean ± S.D.) at 320 μM	Inter-day variation (%) (R.S.D., ,n=3)	Intra-day variation (%) (R.S.D., ,n=4)
MPO inhibitors						
Resveratrol	-	-	-	-	-	-
ABAH	24.35 ± 3.32	13.63	5.04	-	-	-
Sodium Azide	-	-	-	-	-	-
HClO scavengers						
L-ascorbic Acid	52.29 ± 3.31	6.33	17.25	17.25 ± 7.32	42.43	14.32
GSH	31.74 ± 6.00	18.90	13.27	29.49 ± 0.74	2.51	4.17
Methionine	14.50 ± 7.85	54.14	6.86	17.86 ± 3 .24	18.14	5.84
Taurine	-	-	-	-	-	-
Thiourea	-	-	-	-	-	-

-, No inhibition effect.

DCFH-DA is an organic fluorescent probe widely used for quantification of cellular oxidative stress and assessment of antioxidant effects (Wang et al., 1999; Takamatsu et al., 2003). L-ascorbic acid (Vitamin C) in this assay exhibited a strong antioxidant efficacy, which is consistent with the result of a previous assay based on the same principle (Takamatsu et al., 2003). However, in the same assay, all the MPO inhibitors

showed weak or no inhibitory effects for ROS-induced fluorescence increase, and similar results were observed for methionine and thiourea which are known to be highly efficient HClO scavengers, from both the present and previous studies (Pattison & Davies, 2006; Winterbourn et al., 1985; Wasil et al., 1987). The reason for the contrast between QDs and DCFH-DA based microplate assays may be due to different selectivity of two fluorescent probes for ROS. DCFH-DA is a non-specific ROS probe and its intracellular hydrolysis product 2,7-dichlorofluorescin (DCFH) was reported to have a low reactivity with HClO (Setsukinai et al., 2003). Therefore, ROS other than HClO generated by neutrophil-like cells may be the main contributors of the observed DCFH-DA fluorescence increase which is not significantly influenced by HClO scavengers and MPO inhibitors. From this perspective, when used for the evaluation of antioxidants, the DCFH-DA based microplate assay may lose a group of important substances which can scavenge or remove HClO effectively. In a previous study by Takamatsu et al. (2003), the authors also stated that the cell based microplate assay using DCFH-DA may "overlook" some well known antioxidants such as carotene and vitamin E which are lipophilic compounds largely diffusing into cells and thus cannot scavenge the extracellular ROS effectively. However, in the current study the hydrophilic thiourea and methionine also did not exhibit significant antioxidant activity in the DCFH-DA microplate assay, which indicates that the performance of the assay may be more related to the selectivity of the probe used than the solubility of the compounds tested.

3.3.7 APF microplate assay

APF is a cell permeable probe for selective detection of highly reactive oxygen species (hROS) and exhibits highest reactivity with HClO. Table 3.4 shows the reactivity profile of APF compared with that of DCFH-DA.

Table 3.4 Reactivity Profiles of APF and DCFH-DA

ROS	APF(ex:499 em:515)	DCFH-DA(ex:500 em:520)
Hydroxyl Radical: $^{\cdot}OH$	1200	7400
Peroxynitrite: $ONOO^-$	560	6600
Hypochlorite: HClO	3600	86
Oxygen Radical: $^1O_2$	9	26
Superoxide: $O_2^{\cdot-}$	6	67
Hydrogen Peroxide: H_2O_2	<1	190
Nitric Oxide: NO	<1	150
Alkylperoxyl Radical: $ROO^{\cdot}$	2	710
Autoxidation	<1	2000

(Setsukinai et al., 2003. J. Biol. Chem. 278, 3170-3175.)

The dose response relationships of thiourea and resveratrol were investigated in the APF microplate assay. Compared with QD based assay, a significantly improved sensitivity was observed in the microplate assay using APF (Figure 3.7) which is an organic fluorescent probe detecting both intracellular and extracellular HClO. At the concentration of 1.25 μM, resveratrol and thiourea shared similar inhibition efficiency while at the concentration of 10 μM resveratrol showed a significantly higher inhibition rate than thiourea. The comparable dose response relationships exhibited by the QD and APF microplate assays further confirmed the difference between

resveratrol and thiourea in terms of their HClO-eliminating mechanisms and efficiencies.

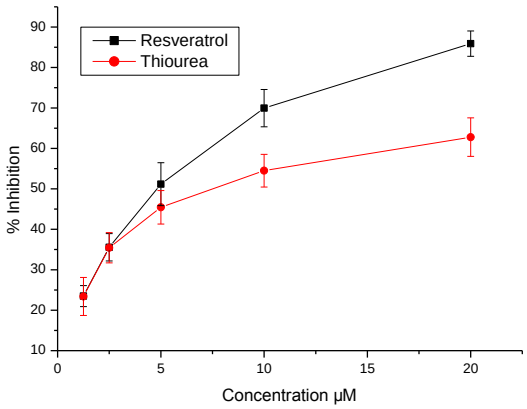

Figure 3.7 The inhibitory effect of resveratrol and thiourea on APF fluorescence increase. Resveratrol and thiourea were incubated with the neutrophil-like cells for 1 h before the addition of APF and PMA. The error bars represent the inter-day variations of three independent assays (n = 3) in which the mean of data was from 4 replicate wells (n = 4).

3.3.8 Resveratrol as a MPO inhibitor

Resveratrol, the most potent MPO inhibitor found in this study, has been reported to significantly decrease HClO production in human and equine neutrophils (Cavallaro et al., 2003; Kohnen et al., 2007). In contrast to synthetic MPO inhibitors such ABAH and NaN_3, resveratrol is a phytoalexin from grape and other plants, implying a great potential of screening and identification of potent MPO inhibitors from natural products. Resveratrol also showed HClO scavenging potency comparable to L-ascorbic acid (Maldonado et al., 2005). However, in this study, resveratrol had

much higher fluorescence quenching inhibition efficiency than L-ascorbic acid, which indicates that resveratrol mainly functions as a MPO inhibitor to reduce the HClO production by neutrophil-like cells. Since a previous study (Kohnen et al., 2007) showed that even a small dose of resveratrol (4.38 nM) attainable by the alimentary route could effectively inhibit HClO generation in human neutrophils, resveratrol could act as a reference compound to evaluate the performance of other peanut stilbenoids as potential MPO inhibitors .

3.4 Conclusion

As a promising selective and sensitive HClO probe in biological systems, QDs-poly-COO^- was successfully applied to the detection of HClO in HL60 microphage-like cells by fluorescent imaging under confocal microscopy, which has the potential for finding out intracellular HClO scavengers and MPO inhibitors. QD based microplate assay was also developed for high throughout screening of HClO scavengers and MPO inhibitors. The QD fluorescence quenching by HClO generated from neutrophil-like cells induced by PMA stimulation or H_2O_2 addition were inhibited by MPO inhibitors and HClO scavengers with different dose response relationships. The MPO inhibitors exhibited a significantly higher efficiency for QD fluorescence quenching inhibition than the HClO scavengers, which indicates more potential of MPO inhibitors as effective HClO removers. Although the HClO generation mechanisms of PMA stimulations and H_2O_2 addition were different, the similar potency orders of HClO scavengers and MPO inhibitors shown by the two

methods indicated the selectivity of the QDs for detection of HClO produced by HL60 cells. The specificity of the QD microplate assay was further confirmed by the performances of the microplate assays using DCFH-DA and APF as probes respectively. In DCFH-DA microplate assay the potent HClO scavenger thiourea and MPO inhibitor resveratrol showed no inhibitory effects at all while in APF microplate assay resveratrol and thiourea displayed different dose response relationships as observed in the QD microplate assay. In both APF and QDs microplate assays, resveratrol showed the highest MPO inhibition efficiency, indicating a potential of exploring peanut stilbenoids as potential effective MPO inhibitors.

Chapter 4 New stilbenoids isolated from fungus-challenged India peanut seeds and their structure elucidations.

4.1Introduciton

Peanut (*Arachis hypogaea*) is a widely consumed crop around the world and has recently attracted much attention because of their health-promoting properties attributed to the inducible phytoalexins that the plants synthesize for self-defense against microbial infections. Fungus-stressed stilbenoid phytoalexins from peanuts are of considerable interest due to their potent bioactivities as antioxidant, anticancer, and anti-inflammatory agents (Lopes et al., 2011). A number of monomeric stilbenoids have been isolated by various research groups from peanut seeds treated with different stress methods as elicitors (Keen & Ingham, 1976; Ingham, 1976; Cooksey et al., 1988; Medina-Bolivar et al., 2007; Sobolev et al., 1995; Sobolev et al., 2006a; Sobolev et al., 2009; Sobolev et al., 2010; Wu et al., 2011). The biosynthetic pathway of stilbenoids suggests that fungus-stressed peanut seeds are capable of producing more complex stilbenoid-derived oligomers (Wu et al., 2011) typically found from other plant sources (Shen et al., 2009). Stilbenoids may possess bioactivities beneficial for human health as natural pharmaceutical ingredients. Resveratrol was reported to possess anti-diabetic activity (Szkudelska et al., 2010), and anti-aging activity via, arguably, activation of Sirtuins (Baur & Sinclair, 2006). The research on the bioactivities of resveratrol and its oligomers has been intensified in recent years and great progress has also been made on the isolation of novel

stilbene oligomers from various plants including *Cyperus rhizome* (coco-grass) (Ito et al., 2012), and *Cenchrus echinatus* L (southern sandspur) (Silva et al., 2012), *Hopea hainanensis* (Polei in Chinese) (Ge et al., 2009). However, prenylated stilbene oligomers from natural sources are rarely reported. Until now, there are only two prenylated stilbene dimers isolated from fungus-stressed peanut seeds by Sobolev et al.(2010).

Peanut seeds are readily available plant materials for obtaining stilbene derivatives via different stress treatment methods. In a previous study by our group (Feng et al., 2007), germinating black soybeans stressed by *Rhizopus oligoporus* (*R. oligoporus*), a popular food fermentation fungus in Southeast Asia, were found to produce health-promoting phytochemicals including glyceollins, oxylipins, and oxooctadecadienoic acids. In this study, the same fungal strain was applied to stress India peanut seeds via a different processing method from the previous study (Feng et al., 2007). The stilbene production profile of fungus-stressed India peanut seeds was analyzed and two new stilbene dimers (arahypin-8 and arahypin-9) with novel construction patterns and one new stilbene derivative (arahypin-10) were successfully isolated **(Figure 4.1**).

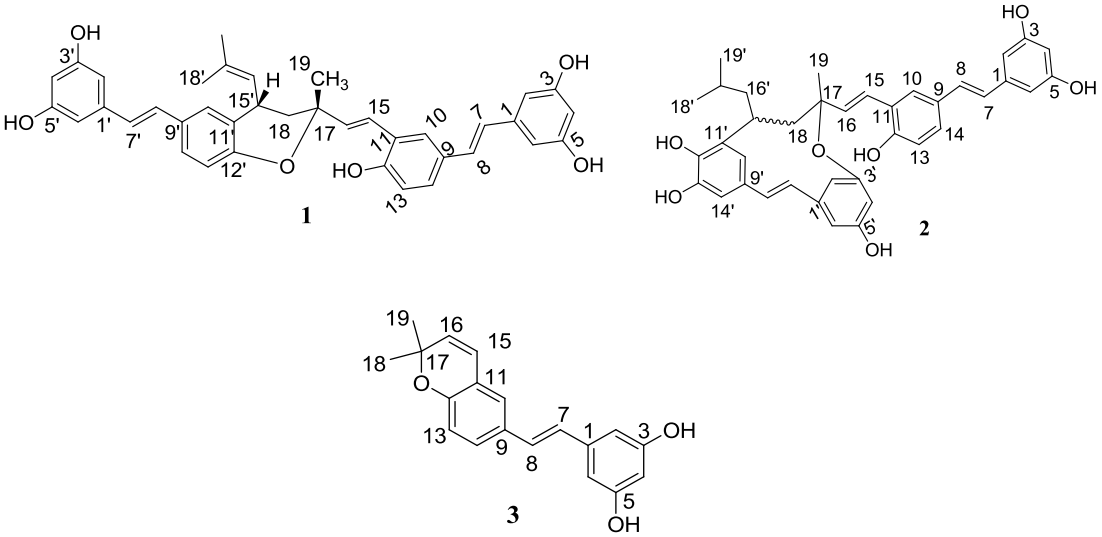

Figure 4.1 The structures of three new stilbenoids arahypin-8 (**1**), arahypin-9 (**2**), and arahypin-10 (**3**) isolated from fungus-stressed India peanut seeds.

4.2 Materials and Methods

4.2.1 Materials

The peanut seeds (Somnath Java 70/80 imported from Gujarat, India) were purchased from Sheng Siong supermarket in Singapaore. Food grade *R. oligosporus* was obtained from PT Aneka Fermentasi Industri (Bandung, Indonesia). To obtain a spore suspension, *R. oligosporus* culture powder (5.0 g) was stirred in 2.0 L sterilized water overnight at the room temperature.

HPLC-grade solvents for preparation of mobile phases were from Tedia Company Inc. (Fairfield, OH). Analytical-grade reagents used for peanut seeds extraction and silica gel chromatography were from Fisher Scientific, UK Limited (Loughborough, U.K.).

The silica gel (0.040-0.063 mm) for column chromatography was purchased from Merck (Darmstadt, Germany).

4.2.2 Instruments

HPLC analysis was performed on a Waters HPLC system (Milford, MA) with an Alliance 2695 separation module and a 2996 photodiode array (PDA) detector. The LC-MS system consisted of HPLC (Ultimate 3000) interfaced to Bruker Amazon X mass spectrometer with an ion trap mass analyzer. HR-MS analysis was carried out on Bruker microOTOFQ II mass spectrometer. Optical rotations were measured on a polAAr 3001 polarimeter with a sodium lamp of wavelength 589 nm and recorded as $[\alpha]_{\lambda}^{T^{\circ}C}$ (c= g/100 mL, solvent). NMR data was recorded in deuterated acetone and $CDCl_3$ with a Bruker Avance 500 (AV500) spectrometer (Karlsruhe, Germany).

4.2.3 Processing of India peanut seeds

The surface of 750 g peanut seeds was sterilized with 70% ethanol for 3 min and then rinsed with distilled water before the seeds were allowed to imbibe distilled water overnight at room temperature. A hand blender was applied to chop the seeds into 3-7 mm pieces which were incubated with 2 L *R. oligoporus* spore suspension at a concentration of 2.5 g/L for 5 min. The peanut pieces were blotted with paper towels, dried by air until leaving no water spots on absorbent paper, and then placed on plastic trays with a thickness less than 1 cm. The trays were kept in the dark at room temperature for 120 hrs. The peanut pieces were stirred everyday and blotted with

paper towels to remove moisture on the surface of peanut pieces and prevent bacterial growth during incubation.

Control peanut pieces without *R. oligoporus* stress were also prepared with the same protocols. To obtain nonviable peanuts as a second control, a portion of the sliced peanut pieces was boiled in distilled water for 3 min and incubated with *R. oligoporus* suspension followed by the identical processing procedures. 20 g of stressed peanuts pieces and two other control samples were ground and extracted with 60 mL of methanol for subsequent HPLC and LC-MS analysis.

4.2.4 HPLC and LC-MS analysis

HPLC analysis was performed on a Waters 2695 system equipped with a PDA detector. The UV detection wavelength was set from 210 to 400 nm. A Waters C_{18} column (5 μm, 4.6 mm×100 mm) was used for separation with the mobile phase of 0.05% acetic acid (A) and acetonitrile (B). The column temperature was 25℃ and the injection volume was 5 μL. The gradients of the eluents were as follows: 0-5 min, isocratic with A 50 % (of total A and B); 5-45 min, A was linearly decreased from 50% to 10%; 45-50 min, A was kept constant at 10%; 50-55 min, A was increased from 10% to 50%; 55-65 min, A remained at 50%. The flow rate was 0.2 mL/min.

The LC conditions for LC-MS analysis were identical to those used for HPLC analysis above. The injection volume was 5 μL of each sample. For ESI-MS, both the

positive and the negative ion modes were applied using ion source voltage of 4.5 kV, a nebulizer pressure of 4 bar, dry gas at a flow rate of 8.0 L/min, and dry temperature set at 220 ℃. The mass spectrum monitored ions in the range *m/z* 70-1200 amu.

4.2.5 Extraction and isolation of new peanut stilbenoids

Stressed peanut pieces (750 g) were extracted with methanol (3.0 L) in a high-speed blender for one minute. The combined extract was filtered and defatted twice with n-hexane (750 mL). Silica gel powder (30 g) and isopropanol (100 mL) were added to the methanol solution and the volatiles were evaporated to give dry powder, which was loaded on top of a chromatographic column (60 mm i.d.) packed with silica gel (suspended in n-hexane) to a height of 170 mm. The column was subsequently eluted with a gradient of n-hexane-acetone (4:1, 3:1, 2:1, 1:1). Each fraction was collected as two 500-mL portions. The silica gel chromatographic method was modified from a reported method (Sobolev et al., 1995). Fractions eluted from the silica column were analyzed by HPLC and LC-ESI-MS. Peaks with different UV absorption spectra or different molecular weights from previous literature records were targeted as potential new stilbene derivatives in peanuts. Fraction eluted with n-hexane-acetone (4:1) containing compound **3** (molecular weight 294) and fraction eluted with n-hexane-acetone (1:1) containing compound **1** (molecular weight 588) and compound **2** (molecular weight 606) were evaporated, dissolved in methanol, and subjected to a final purification using semi-preparative HPLC.

Semi-preparative HPLC separation was conducted in a Waters 717 system with a PDA detector using an YMC-Pack ODS-AM C_{18} (10 × 250 mm, 5 μm) column maintained at room temperature and the injection volume was 250 μL. The mobile phases and gradient programs were the same as conditions in the HPLC analysis above except that the flow rate was set at 3 mL/min. The fractions corresponding to the peaks of the target compounds were repeatedly collected by multi-wavelength UV monitoring. The collected solutions were evaporated to dryness and the purified compounds were redissolved in different solvents for subsequent spectroscopic measurements.

4.2.6 Spectroscopic measurements of new peanut stilbenoids

The identities of the three compounds were further confirmed by HPLC and LC-MS analyses based on their UV spectra and chromatographic behaviour. The molecular formulae of the three new compounds were established by HR-MS analysis. The structures of the three compounds were elucidated by their 1D and 2D NMR spectra.

Arahypin-8 (1): 4 mg; yellow solid; $[\alpha]_D^{23}$ 0 (c 0.4, $CHCl_3$); UV (mobile phase) λ_{max} 222, 314 nm; ^{1}H NMR and ^{13}C NMR data are listed in Table 4.1; HRESIMS, *m/z* 587.2421 $[M-H]^-$, calcd for $C_{38}H_{35}O_6$, 587.2439.

Arahypin-9 (2): 3 mg; yellow solid; $[\alpha]_D^{23}$ 0 (c 0.4, $CHCl_3$); UV (mobile phase) λ_{max} 227, 320 nm; ^{1}H NMR and ^{13}C NMR data are listed in Table 4.1; HRESIMS, *m/z*

605.2548 $[M-H]^-$, calcd for $C_{38}H_{37}O_7$, 605.2545.

Arahypin-10 (3): 4.5 mg; a colorless oil; UV (mobile phase) λ_{max} 230, 275, 323 nm; ^1H NMR and ^{13}C NMR data are listed in Table 4.1; HRESIMS, *m/z* 293.1175 $[M-H]^-$, calcd for $C_{19}H_{17}O_3$, 293.1183.

4.3 Results and discussions

4.3.1 Profiles of stilbenoids productions in stressed, unstressed and nonviable peanut seeds

The peanut seeds were cut into pieces to enlarge the infected surface area where the peanut stilbenoids were found to be most concentrated (Sobolev, 2008). The incubation was conducted in an open instead of a sealed environment because keeping peanut pieces in a dry and ventilatory condition can effectively prevent bacterial growth and enhance biosynthesis of peanut stilbenoids. The identities of known peanut stilbenes were confirmed by characteristic HPLC-UV spectrum and [M+H] values from LC-MS. Four major peaks (**Figure 4.2**) were identified as arachidin-1 (Ara-1, *m/z* 313.2, 340 nm), arachidin-2 (Ara-2, *m/z* 297.2, 308 and 322 nm), arachidin-3 (Ara-3, *m/z* 297.2, 336 nm), and SB-1 (SB-1, *m/z* 345.3, 365 nm), which are mostly reported stilbene compounds isolated from fungus-challenged peanuts by studies before (Sobolev et al., 2006 a; Sobolev et al., 2009; Sobolev et al., 2010; Wu et al., 2011).

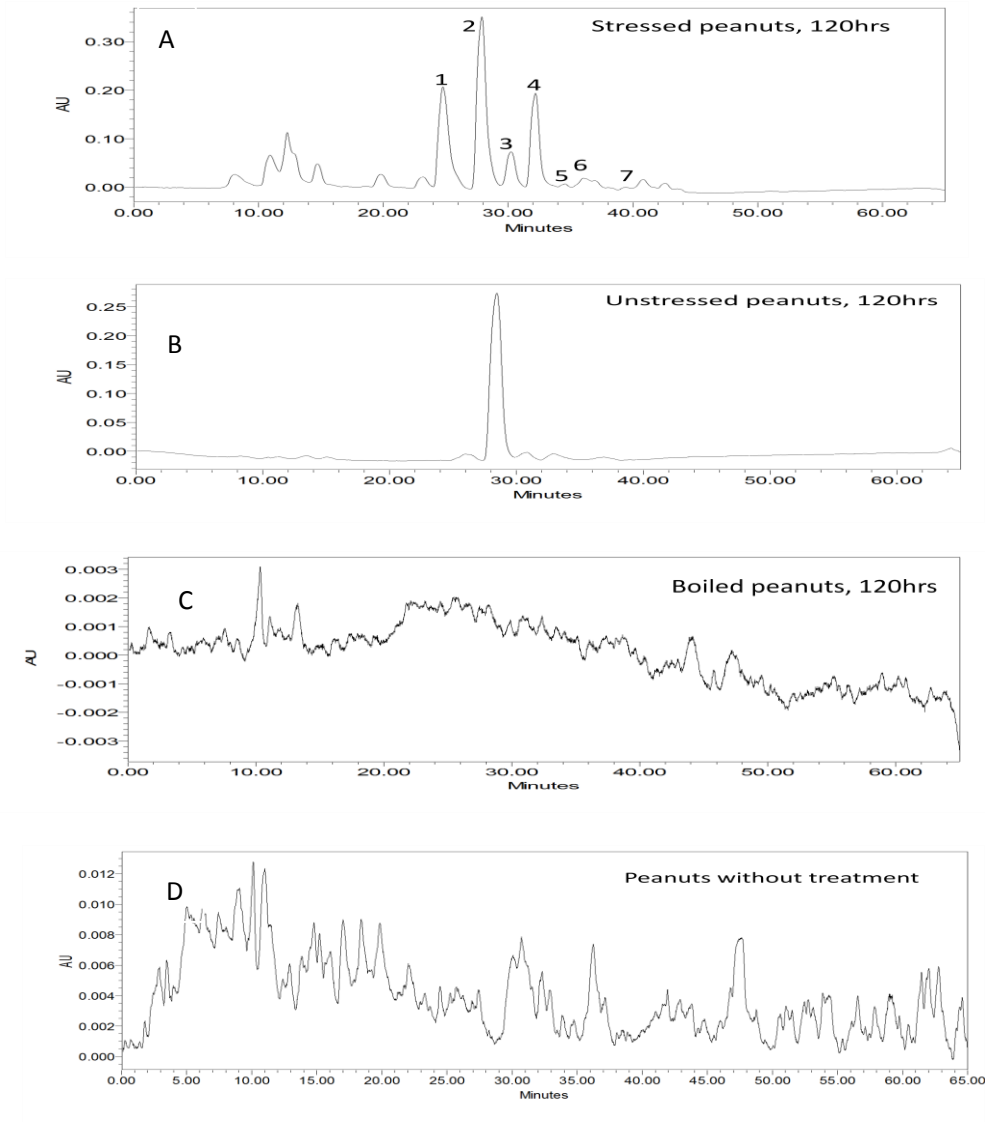

Figure 4.2 Comparative HPLC chromatograms (320 nm) of MeOH extract of (A) fungus-stressed peanut pieces; (B) unstressed peanut pieces; (C) boiled peanut pieces; (D) peanuts without treatments. 1, SB-1 (1); 2, arachidin-1 (2); 3, arachidin-2 (3); 4, arachidin-3 (4); 5, arahypin-8 (5); 6, arahypin-10 (6); 7, arahypin-9 (7)

Viable India peanut pieces under fungus-stressed condition were able to produce a characteristic set of the four prenylated stilbenoids at significant concentrations; whereas no stilbenoids were detected in nonviable control samples and much lower concentrations of stilbenoids were detected in unstressed viable control samples (**Figure 4.2**). It is noticeable that SB-1, a degenerated product of arachidin-1 caused

by fungal enzymes (Sobolev et al., 2006a), was not observed in unstressed viable control samples (**Appendices A.1**), which rules out the possibility of contaminations of peanut pieces by other airborne fungal spores under the experiment conditions.

4.3.2 Targeting new stilbenoids from fungus-challenged India peanut seeds

Upon analysis of HRESIMS (**Appendices A.3)**, compound **3** ($C_{19}H_{18}O_3$) and compound **2** ($C_{38}H_{38}O_7$) were found to have the same molecular formulae as arahypin-5 and arahypin-6 which are monomeric and dimeric stilbenoids isolated from fungus-stressed peanut seeds before (Sobolev et al. 2009; Sobolev et al. 2010). However, the UV spectra (**Figure 4.3**) indicated that **3 (**λ_{max} 230, 275, 323 nm) and **2 (**λ_{max} 227, 320 nm) are isomers of arahypin-5 (λ_{max} 217, 339 nm) and arahypin-6 (λ_{max} 224, 272, 339 nm). Compound **1** ($C_{38}H_{36}O_6$) and compound **2** share a similar UV spectrum, which suggests resemblance of their structural patterns. The three new compounds cannot be found in either nonviable or unstressed viable control samples by LC-MS analysis (**Appendices A.1**), indicating that they are products of stressed peanut seeds in response to the fungal action.

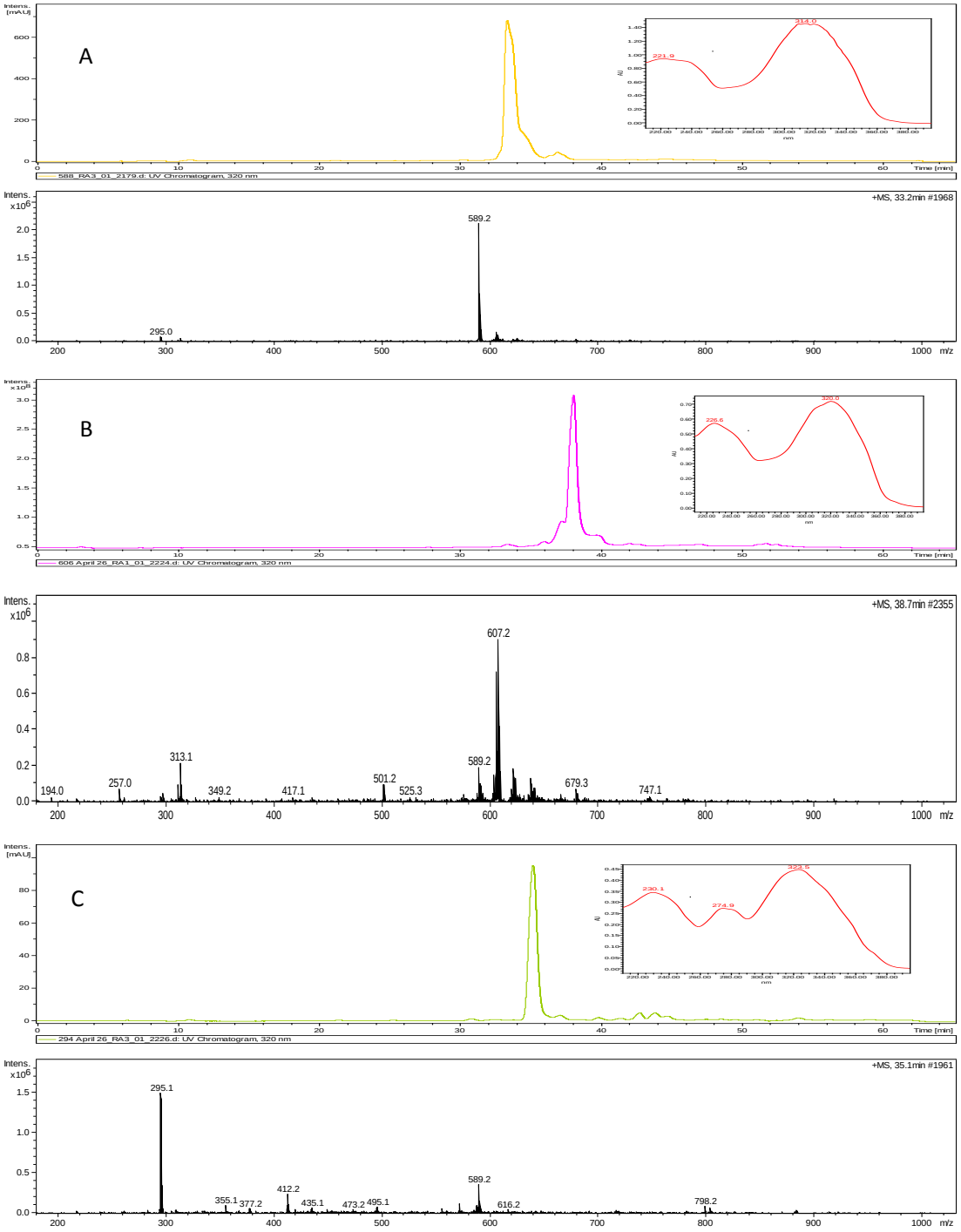

Figure 4.3 LC-MS chromatogram and UV spectra of (A) arahypin-8; (B) arahypin-9; (C) arahypin-10 in mobile phase.

4.3.3 Structural elucidations of the new peanut stilbenoids by NMR analysis.

The proton NMR spectra of compound **1** (arahypin-8) showed that there were only three methyl groups in the compound. To date, all of the reported dimeric stilbenoids have four methyl groups. The HMBC correlations from H-18′ (δ_H 1.83) and H-19′ (δ_H 1.82) to C-16′ (δ_C 129.1) and C-17′ (δ_C 134.6) indicate the presence of two prenyl derived methyl groups. The methyl group at δ_H 1.53 supports that the carbon next to this methyl group is connected with an oxygen. There are two protons at δ_H 6.55 and two protons at δ_H 6.56; four carbons at δ_C 106.3 and four carbons at δ_C 160.3. These data revealed two 3,5-dihydroxyphenyl groups in the molecule. The entire structure of **1** is established by assigning signals from ^{1}H, ^{13}C, COSY, HMQC and HMBC experiments. The NMR data is summarized in Table 4.1.

The HMBC correlations from H-2 (δ_H 6.55) to C-7 (δ_C 127.9), H-8 (δ_H 7.07) to C-1 (δ_C 141.5) combining that coupling constants between H-7 and H-8 is 16.6 Hz, suggest that a *trans* double bond is attached to C-1 of the 3,5-dihydroxyphenyl group. Coupling constant between H-15 (δ_H 7.05) and H-16 (δ_H 6.62) is 16.3 Hz, which supports a *trans* double bond. HMBC correlations from H-15 to C-17 (δ_C 78.1), H-16 to C-18 (δ_C 40.8) and H-19 (δ_H 1.53) to C-17 and C-18 revealed that C-18, which is derived from a methyl group of one of the constituent stilbene monomers, is a methylene unit that links the dimer. The HMBC correlations from H-18 (δ_H 2.09 & 1.78) to C-11′ (δ_C 126.3), C-15′ (δ_C 33.3) and C-16′ (δ_C 129.1) establish connections between the two monomers to give the isolated product (Figure 4.4). In addition, the

relative stereochemistry of compound **1** was measured by NOESY experiment. H-15′ (δ_H 3.90) showed correlation with H-19, which indicated that both of the protons locate at the same side of the six-member ring. The relative stereochemistry of compound **1** was thus established.

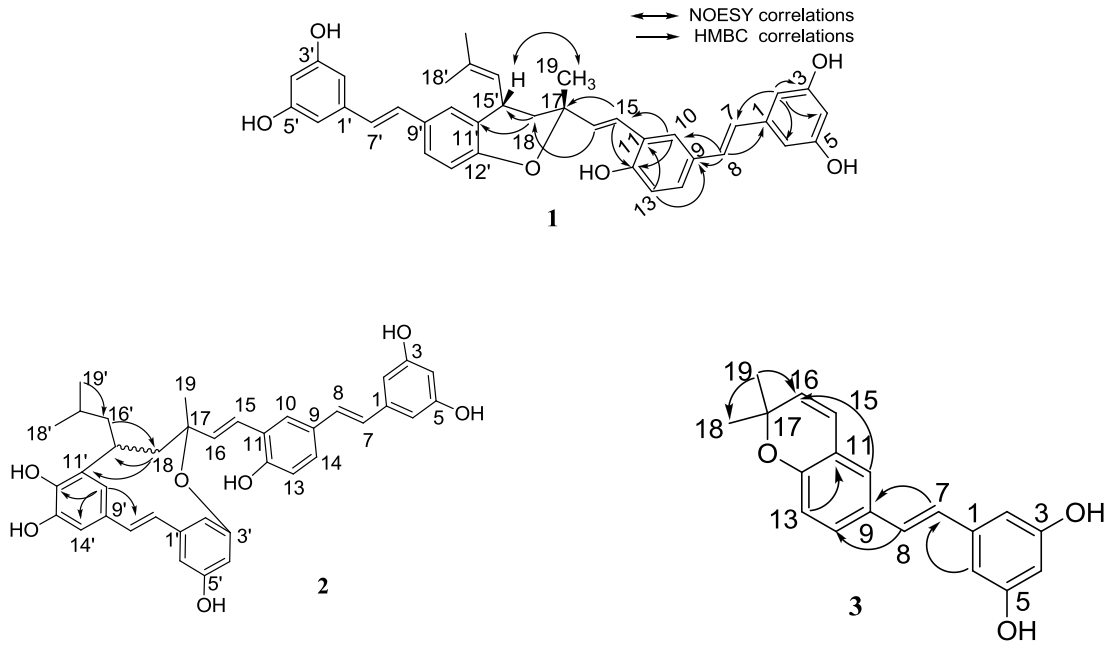

Figure 4.4 HMBC correlations of arahypin-8 (**1**), arahypin-9 (**2**) and arahypin-10 (**3**).

Table 4.1 NMR data of arahypin-8 (**1**)

position	δ_H, (*J* in Hz)	δ_C	HMBC correlations
1		141.5	
2	6.55, d (2.0)	106.3	C-3, C-4, C-6, C-7
3		160.3	
4	6.27, t (2.0)	103.3	C-2, C-3, C-5, C-6
5		160.3	
6	6.55, d (2.0)	106.3	C-2, C-4, C-5, C-7
7	6.97, d (16.6)	127.9	C-1, C-2, C-6, C-8, C-9
8	7.07, d (16.6)	129.9	C-1, C-7, C-9, C-10
9		131.0	
10	7.72, d (2.1)	126.7	C-8, C-11, C-12, C-15
11		125.8	
12		156.2	
13	6.90, d (8.4)	117.6	C-9, C-11, C-12, C-14
14	7.31, dd (8.4, 2.1)	128.3	
15	7.05, d (16.3)	123.8	C-10, C-12, C-16, C-17
16	6.62, d (16.3)	136.9	C-11, C-15, C-18, C-19
17		78.1	
18	a. 2.09, m b. 1.78, m	40.8	C-16, C-17, C-19, C-11′, C-15′, C-16′
19	1.53	25.0	C-16, C-17, C-18
1′		141.5	
2′	6.56, d, 2.0	106.3	C-3′, C-4′, C-6′, C-7′
3′		160.3	
4′	6.27, t, 2.0	103.3	C-2′, C-3′, C-5′, C-6′
5′		160.3	
6′	6.56, d, 2.0	106.3	C-2′, C-4′, C-5′, C-7′
7′	6.85, d, 17.4	127.8	C-1′, C-2′, C-6′, C-8′, C-9′
8′	7.02, d, 17.4	129.7	C-1′, C-7′, C-9′, C-10′
9′		131.1	
10′	7.22, d (2.1)	129.3	C-8′, C-11′, C-12′, C-15′
11′		126.3	
12′		154.2	
13′	6.85, d (8.5)	119.1	C-9′, C-11′, C-12′, C-14′
14′	7.39, dd (8.5, 2.1)	127.9	
15′	3.90, m	33.3	C-18, C-11′, C-12′, C-14′, C-17′
16′	5.20, d, (6.8)	129.1	
17′		134.6	
18′	1.83, s	18.8	C-16′, C-17′, C-19′
19′	1.82, s	26.7	C-16′, C-17′, C-18′

Data (δ in ppm) were recorded in acetone-d_6

The proton NMR spectra of compound **2** (arahypin-9) showed that there were only three methyl groups in the compound. The two methyl resonance doublets at δ_H 0.93 and 0.87 suggest that both groups terminate an aliphatic chain. This is a clear difference between compound **1** and **2**. The methyl group at δ_H 1.54, two protons at δ_H 6.50, two carbons at δ_C 106.3 and two carbons at δ_C 160.2 revealed that the structure of monomer, composed of C-1 to C-19, is not changed. However, it is notable that H-2′ and H-6′ are not equivalent in compound **2**, indicating that 3′-OH or 5′-OH may form ether or ester bond with other carbons. Carbon signals at δ_C 146.7 and 146.8 support a 1,2-dihydroxyphenyl structure originating from the constituent monomer 3′-prenyl-3, 5, 4′,5′ -tetrahydroxystilbene. The entire structure of compound **2** is established by assigning signals from ^{1}H, ^{13}C, COSY, HMQC and HMBC experiments. The HMBC correlations from H-18 (δ_H 2.55 & 1.79) to C-11′ (δ_C 115.8), C-15′ (δ_C 29.1) and C-16′ (δ_C 45.1) combining the HMBC correlations from H-10′ to C-8′ (δ_C 129.4), C-12′ (δ_C 146.8) and C-14′ (δ_C 120.5) establish connections between the two monomers (Figure 4.4). The NMR data is summarized in Table 4.2.

Table 4.2 NMR data of arahypin-9 (**2**)

position	δ_H, (*J* in Hz)	δ_C	HMBC correlations
1		141.5	
2	6.50, d (1.7)	106.3	C-3, C-4, C-6, C-7
3		160.2	
4	6.24, brs	103.3	C-2, C-3, C-5, C-6
5		160.2	
6	6.50, d (1.7)	106.3	C-2, C-4, C-5, C-7
7	6.87, d (16.3)	127.8	C-1, C-2, C-6,C-8, C-9
8	6.97, d (16.3)	129.7	C-1, C-7, C-9, C-10
9		131.5	
10	7.55, brs	126.7	C-8, C-9, C-12, C-15
11		125.5	
12		155.9	
13	6.85, d (8.4)	117.5	C-9, C-11, C-12, C-14
14	7.28, brd (8.4)	127.9	
15	6.90, d (16.4)	125.1	C-10, C-12, C-17
16	6.47, d (16.4)	135.3	C-11, C-17, C-18, C-19
17		78.4	
18	a. 2.55, dd (14.0, 7.5) b. 1.79, m	41.3	C-16, C-17, C-19, C-11′, C-15′, C-16′
19	1.54	30.1	C-16, C-17, C-18
1′		138.2	
2′	6.53, brs	107.1	C-3′, C-4′, C-6′, C-7′
3′		157.8	
4′	6.83, m	116.9	C-2′, C-6′
5′		157.4	
6′	6.60, brs	108.5	C-2′, C-4′, C-5′, C-7′
7′	6.80, d, 16.0	127.4	C-1′, C-2′, C-6′, C-9′
8′	6.91, d, 16.0	129.4	C-1′, C-9′, C-10′, C-14′
9′		130.8	
10′	7.05, brs	114.5	C-8′, C-12′, C-14′
11′		115.8	
12′		146.8	
13′		146.7	
14′	6.89, m	120.5	C-8′, C-10′, C-12′
15′	3.07, m	29.1	
16′	2.35, m 1.23, m	45.1	C-18, C-11′, C-15′, C-17′, C-18′, C-19′
17′	1.90, m	27.1	
18′	0.93, d (6.5)	22.3	C-16′, C-17′, C-19′
19′	0.87, d (6.5)	25.3	C-16′, C-17′, C-18′

Data (δ in ppm) were recorded in acetone-d_6

The UV spectrum of compound **3** (arahypin-10) is similar to that of its dimethyl ether analogue, lonchocarpene, previously isolated from the roots of *Lonchocarpus nicou* (Kaouadji et al., 1986). The two oxygenated carbons C-17 (δ_C 76.6) and C-12 (δ_C 152.9) combined with HMBC correlations from H-10 (δ_H 7.10) and H-18/19 (δ_H 1.44) to C-16 (δ_C 122.2) suggest the presence of a cyclized prenyl group linked to a benzene ring. The HMBC experiments also revealed correlations from H-6 (δ_H 6.53) to C-7 (δ_C 125.8) and H-7 (δ_H 6.79) to C-9 (δ_C 129.8) , which is suggestive of the presence of an olefinic double bond in the stilbene skeleton. Combining with other data in **Table 4.3**, the structure of compound **3** was established as shown in **Figure 4.4**

Table 4.3 NMR data of arahypin-10 (**3**)

position	δ_H, (*J* in Hz)	δ_C	HMBC correaltions
1		140.4	
2	6.53, bs	105.9	C-4, C-7
3		157.0	
4	6.25, bs	102.0	
5		157.0	
6	6.53, bs	105.9	C-4, C-7
7	6.79, d (16.0)	125.8	C-2, C-6, C-9
8	6.93, d (16.0)	129.1	C-1, C-10, C-14
9		129.8	
10	7.10, bs	124.4	C-8, C-16
11		121.3	
12		152.9	
13	6.77, d (8.4)	116.6	C-11, C-12
14	7.22, bd (8.4)	127.6	
15	5.63, d (9.8)	131.1	C-16, C-17
16	6.33, d (9.8)	122.2	C-10, C-11, C-12
17		76.6	
18 & 19	1.44	28.1	C-16, C-17, C-18/19

Data (δ in ppm) were recorded in $CDCl_3$

4.3.4 Proposed formation mechanisms of the new peanut stilbenoids

Arahypin-10 may be formed from cyclization reaction of its diene precursor trans-3′-isopentadienyl-3, 5, 4′-trihydroxystilbene (IPD, Cooksey et al., 1988). Based on a similar mechanism, arahypin-5 previously discovered by Sobolev et al. (2009) may be a cyclized product of arachidin-3 as well (Figure 4.5). IPD may also be the precursor of arahypin-8 which was formed through a coupling reaction as illustrated in Figure 4.6. The heterodimer structure of arahypin-9 formed through coupling between IPD and 3′-prenyl-3, 5, 4′, 5′ -tetrahydroxystilbene suggests some multiple step transformation. A previous study (Sobolev et al., 2010) demonstrated that the abundant source of arachidin-1 and arachidin-3 can also form dimers through oxidative coupling in fungus-stressed peanut seeds. The selective utilization of IPD to form compound **1** and **2** in this study indicates the selectivity of reactants. Both compound **1** and **2** have chiral carbons but exhibit no optical activity, which suggests that these dimers are racemic mixtures (1:1) and the catalyzed mechanism of their formation is in need of further investigation. Stilbene dimers and oligomers isolated so far typically connect through the stilbene olefinic and aromatic carbon and the phenolic groups (Shen et al., 2009). Connection through prenyl groups has not been reported in previous literature of dimeric and oligomeric stilbenes.

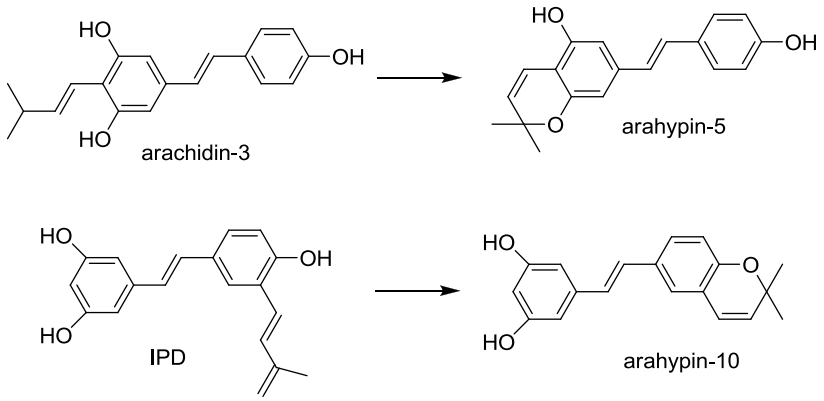

Figure 4.5 The cyclized reactions of arachidin-3 and IPD to form arahypin-5 and arahypin-10 (**3**) .

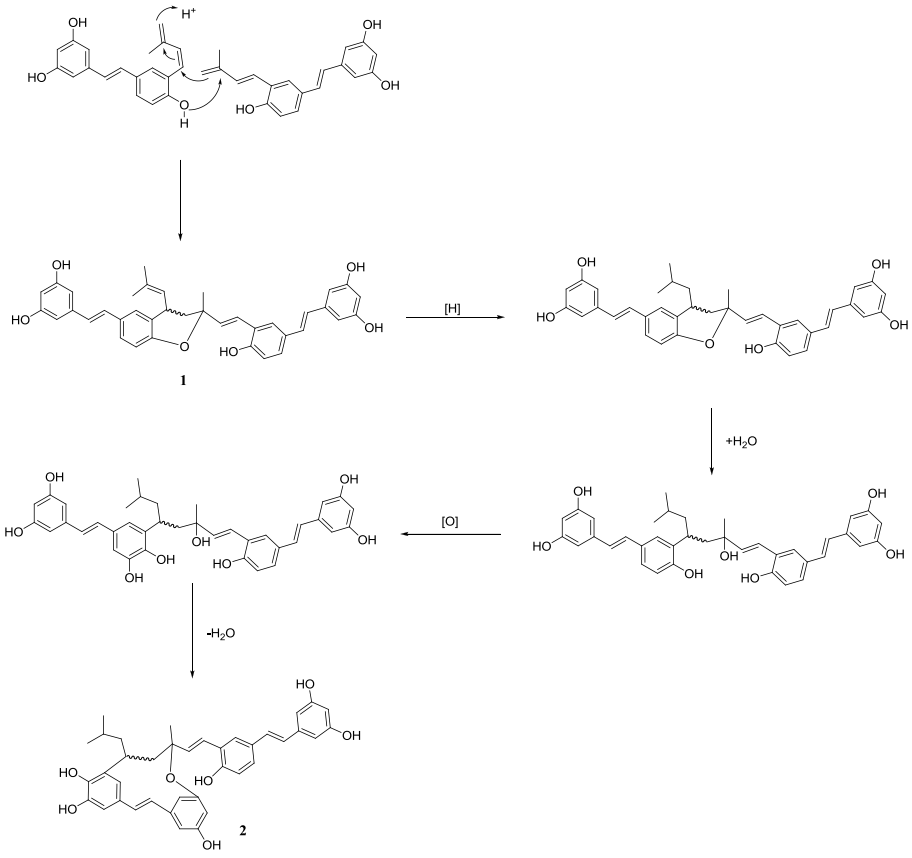

Figure 4.6 Plausible coupling formation routes to arahypin-8 (**1**) and arahypin-9 (**2**) from prenylated monomeric stilbenoids.

4.4 Conclusion

In summary, a new processing method for eliciting stilbenoid production in fungus-challenged peanut seeds was established. It was demonstrated that the wounded India peanut seeds stressed by a *R. oligoporus* strain were able to produce an array of stilbenoids at significant concentrations compared with viable unstressed control samples, whereas no stilbenoids could be detected in nonviable control samples. Two new stilbene dimers arahypin-8 (**1**) and arahypin-9 (**2**) and one monomeric stilbene derivative arahypin-10 (**3**) were isolated for the first time from fungus-stressed India peanut seeds. The structures of the three new compounds were elucidated by HRESIMS, UV, 1D and 2D NMR spectroscopy and the mechanisms of their formation were also proposed.

Chapter 5 New stilbenoids isolated from fungus-challenged black skin peanut seeds and their structure elucidations.

5.1 Introduction

Although peanut seeds of different cultivars were found to produce the same characteristic set of prenylated stilbene compounds including arachidin-1, arachidin-3, IPD, and SB-1 in response to fungal infection (Sobolev et al., 1995; Sobolev et al., 2006a; Sobolev et al., 2009; Sobolev et al., 2010), the genetic diversity of peanut cultivars (Knauft & Gorbet, 1989) indicated that their stilbene production profiles may not be uniform. This supposition was confirmed by a previous study (Wu et al., 2011), in which the three types of peanut seeds germinating under fungal stress showed slightly different stilbenoid phytoalexin and polyphenolic antioxidant profiles. Therefore, combinations of new fungal species and different peanut types may have a potential to produce stilbenes of novel structures.

Until now, *Aspergillus* species is the main microbe used to challenge a few types of peanut seeds to produce stilbene phytoalexins (Sobolev et al., 1995; Sobolev et al., 2006a; Sobolev et al., 2009; Sobolev et al., 2010). Compared with the above mentioned stilbene phytoalexins, other peanut stilbenoids in minor amounts are rarely reported except for a few studies in which arahypins and two stilbene dimers were isolated from peanut seeds challenged by *Aspergillus* strains reported by Sobolev et al.

(2009; 2010). In chapter 4, a fungal strain, *R. oligoporus*, a starter for tempeh fermentation, was applied to challenge wounded Indian peanut seeds, from which two new dimeric stilbenoids arachidin-8, arachidin-9, and one new monomeric stilbenoid arachidin-10 (**Figure 4.1**) were isolated.

In this chapter, the same fungal strain was used to challenge black skin peanut seeds, a Chinese specialty peanut type, to produce novel stilbenoids that we were able to isolate and characterize. Two new stilbene dimers arahypin-11 (**1**), arahypin-12 (**2**) and one new stilbene derivative MIP (**3**) (**Figure 5.1**) together with three known peanut stilbenoids arachidin-1, arachidin-3, and SB-1 were isolated from fungus-stressed black skin peanut seeds. At the same time, a dynamic analysis of stilbenoid production by fungus stressed black skin peanut seeds was carried out to validate the optimal incubation time applied.

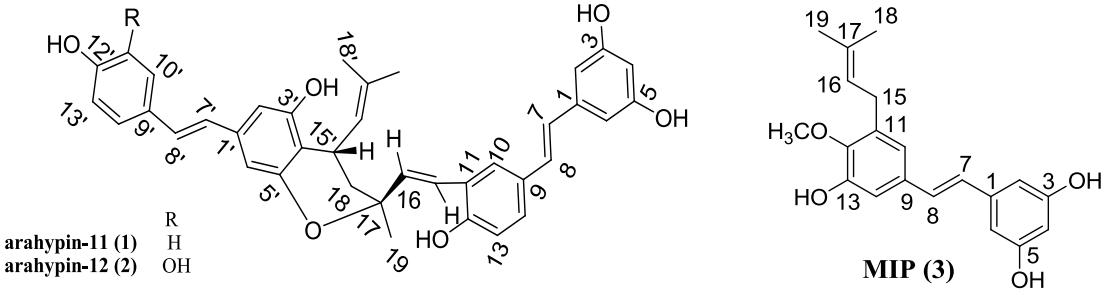

Figure 5.1 The structures of new stilbenoids isolated from black skin peanut seeds: arahypin-11(**1**); arahypin-12 (**2**); MIP (**3**).

5.2 Materials and methods

5.2.1 Materials

Black skin peanut seeds were purchased from Beyond Organic food store (Beijing, China) and produced from Jianping in Liaoning province in China. For other chemicals and reagents, please refer to section 4.2.1.

5.2.2 Instruments

For detailed information about instruments, please refer to section 4.2.2

5.2.3 Processing of black skin peanut seeds

Black skin peanut seeds (1.2 kg) were surface-sterilized with 70% ethanol for 3 min before imbibing distilled water overnight at room temperature. The peanut seeds were then processed according to the procedures described in section 4.2.3.

5.2.4 Dynamic analysis of peanut stilbenoids production by HPLC and LC-MS

Stilbenoid production was determined in 20 g peanut pieces after 0, 24, 48, 72, and 96 hrs of incubation with *R. oligoporus* according to the identical processing method. The fungal stressed peanuts pieces were ground and extracted with 60 mL of methanol for subsequent HPLC and LC-MS analyses according to the conditions

described in section 4.2.4.

5.2.5 Extraction and isolation of new peanut stilbenoids

Stressed peanut pieces were extracted with 4.0 L methanol by shaking overnight. The combined extract was filtered and concentrated to 1.2 L, which was defatted with 400 mL n-hexane three times. Silica gel powder (50 g) and isopropanol (150 mL) were added to the methanol solution and the mixture was evaporated until a free-flowing yellow power appeared. The silica power with peanut extract was applied to a chromatographic column (60 mm i.d.) packed with silica gel (suspended in n-hexane) to a height of 200 mm. The column was sequentially eluted with a gradient of n-hexane-acetone (4:1, 3:1, 2:1, 1:1, 1:2), acetone, acetone-methanol (1:1), methanol. Each fraction was collected as two 600 mL portions. The method of silica gel chromatography was modified from a previous method reported by Sobolev et al. (Sobolev et al. 1995).

Peaks with novel molecular weights were targeted as new stilbenoids in peanuts. Fraction eluted with n-hexane-acetone (2:1) containing compound **3** (molecular weight 326) and fraction eluted with n-hexane-acetone (1:1) containing compound **1** (molecular weight 588), fraction eluted with n-hexane-acetone (1:2) compound **2** (molecular weight 604) were evaporated, dissolved in methanol, and subjected to a final purification using semi-preparative HPLC according to the conditions described in section 4.2.5.

5.2.6 Spectroscopic measurements of new peanut stilbenoids

The spectral parameters of the three new isolated compounds were determined as described in the section 4.2.6.

Arahypin-11 (1): 3.0 mg; yellow solid; $[\alpha]_D^{23}$ 0 (c 0.4, $CHCl_3$); UV λ_{max} 221, 312 nm; ^1H NMR and ^{13}C NMR data are listed in **Table 5.1** ; HRESIMS, *m/z* 587.2447 $[M-H]^-$, calcd for $C_{38}H_{35}O_6$, 587. 2439.

Arahypin-12 (2): 5.0 mg; yellow brown solid; $[\alpha]_D^{23}$ 0 (c 0.4, $CHCl_3$); UV λ_{max} 225, 320 nm; ^1H NMR and ^{13}C NMR data are listed in **Table 5.1**; HRESIMS, *m/z* 603.2399 $[M-H]^-$, calcd for $C_{38}H_{35}O_7$, 603.2388.

3,5,3′-trihydroxy-4′-methoxy-5′-isopentenylstilbene (**MIP, 3) :** 5.5 mg; pale yellow solid; UV λ_{max} 223, 309 nm; ^1H NMR and ^{13}C NMR data are listed in **Table 5.2**; HRESIMS, m/z 325.1452 $[M-H]^-$, calcd for $C_{20}H_{21}O_4$, 325.1445.

5.3 Results and discussion

5.3.1 Dynamics of stilbenoid production in fungal-stressed black skin peanut seeds

R. oligosporus was chosen as the elicitor to produce stilbenoids in black skin peanut seeds because it was highly efficient in eliciting the phytoalexin production in

soybeans and peanut seeds demonstrated by previous studies (Feng et al., 2007, Feng et al., 2008, Wu et al., 2011). Dynamic changes of stilbenoid production after *R. oligosporus* inoculation were studied by HPLC and LC-MS analyses of the methanol extracts of the peanut pieces collected every 24 hours. The three main peaks of black peanut methanol extract were assigned as SB-1 (*m/z* 345.1, 360 nm), arachidin-1 (*m/z* 313.1, 340 nm), and arachidin-3 (*m/z* 297.1, 336 nm) according to their characteristic UV spectra and molecular weights. **Figure 5.2** illustrates that from 0 to 72 hrs, the stilbenoid production profile changed dramatically and the concentrations of SB-1 (**1**), arachidin-1 (**2**), and arachidin-3 (**3**) increased significantly. From 72 to 120 hrs, the profiles of the three major stilbenoids basically stabilized while there was a gradual increase in the concentrations of the minor stilbene components.

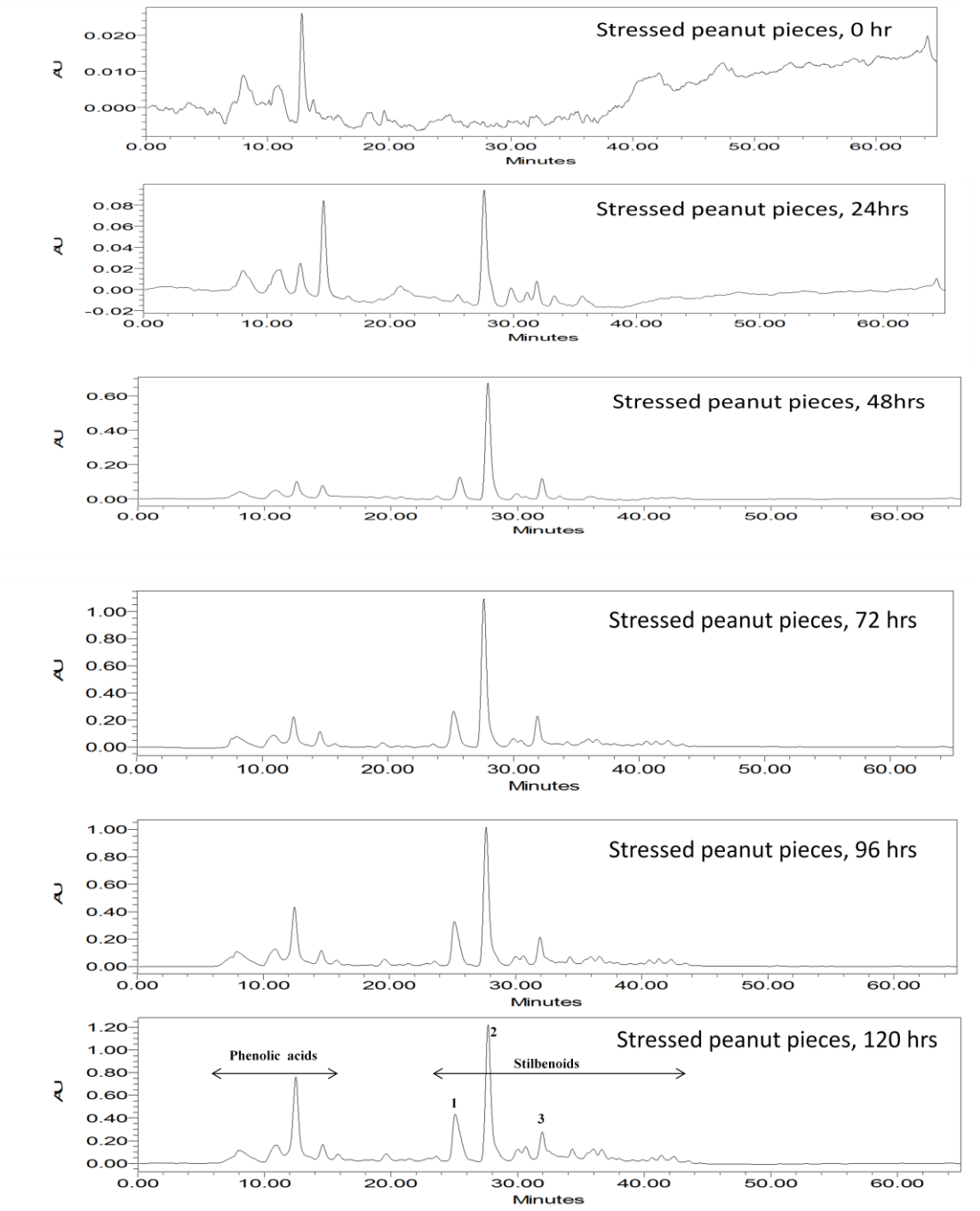

Figure 5.2 The dynamic change of stilbenoid production in 20 g fungus-stressed peanut seeds over 120 hrs. Peak identities: 1, SB-1; 2, arachidin-1; 3, arachidin-3 .

The dynamic changes of SB-1, arachidin-1, and arachidin-3 in black skin peanut seeds challenged by *R. oligosporus* were also quantified (Figure 5.3) and compared with the dynamics of the stilbenoid production (Figure 5.4) in Georgia Green peanut seeds

challenged by *Aspergillus flavus* (Sobolev et al., 2006a). Although the total contents of the stilbenoid phytoalexins were similar in the two different fungus-stressed peanut cultivars, different patterns of their production were observed in the two studies. In the study of Sobolev et al. (2006a), resveratrol was the dominant stilbene between 24 and 48 hrs of incubation while the accumulation of SB-1 exceeded accumulation of other stilbene phytoalexins after 72 hrs. However, in this study the concentration of arachidin-1 was higher than the concentrations of other stilbene phytoalexins including SB-1 throughout the incubation and only a very low concentration of resveratrol was detected. Since resveratrol was the simplest peanut stilbenes serving as a building block for other peanut stilbenoids and SB-1 was the product of fungal enzymatic detoxification of arachidin-1, it is reasonable to speculate that the distinct stilbene production patterns in the two studies could be attributed to the different stilbene metabolic rates of the fungal species and the different stilbene synthase activities of specific peanut cultivars in response to fungal infection.

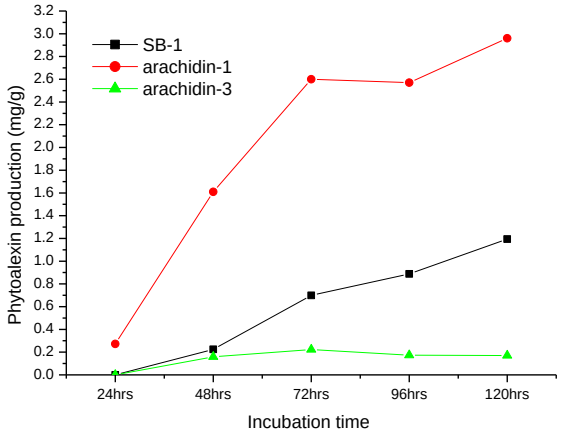

Figure 5.3 Dynamics of the three major prenylated stilbene phytoalexins in black skin peanut seeds challenged by *R. oligosporus*

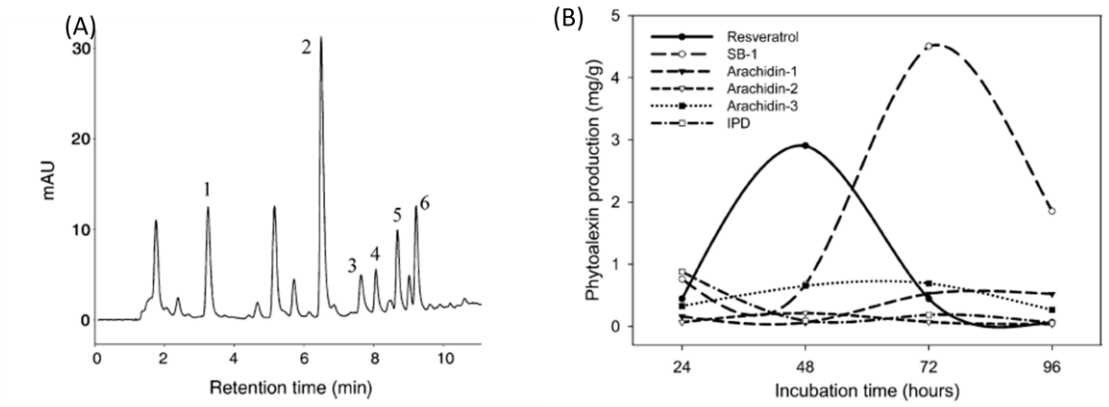

Figure 5.4 (A) HPLC (at 317 nm) of methanol extract of Georgia Green peanut seeds after incubation with *A. flavus* for 48 hrs. Peaks: 1, trans-resveratrol; 2, SB-1; 3, arachidin-1; 4, arachidin-2; 5 arachidin-3; 6, IPD. (B). Dynamics of stilbene phytoalexins production by Georgia Green peanut kernels challenged by *A. flavus.* (Sobolev et al., 2006a. J. Agric. Food Chem. 54, 2111–2115.)

5.3.2 Isolation of new and known stilbenoids from fungus-stressed peanut seeds.

SB-1 (33 mg), arachidin-1 (30 mg), and arachidin-3 (8.5 mg) were isolated from different eluting fractions using semi-preparative HPLC and their structures were further confirmed according to 1-D NMR spectral data reported previously (Chang et al., 2006; Sobolev et al., 2006a). The three new stilbenoids arahypin-11, arahypin-12,

and MIP were identified because their UV spectra and molecular weights (Figure 5.5) were different from those of known stilbenoids from stressed peanut seeds. Arahypin-11 ($C_{38}H_{36}O_6$) and arahypin-8 are isomers with similar UV spectra but exhibit significantly different chromatographic behaviour under the same gradient elution conditions. Figure 5.6 show the HPLC chromatograms of the 4.0 L black peanut methanol extract and the six purified compounds at a concentration of 0.2 mM.

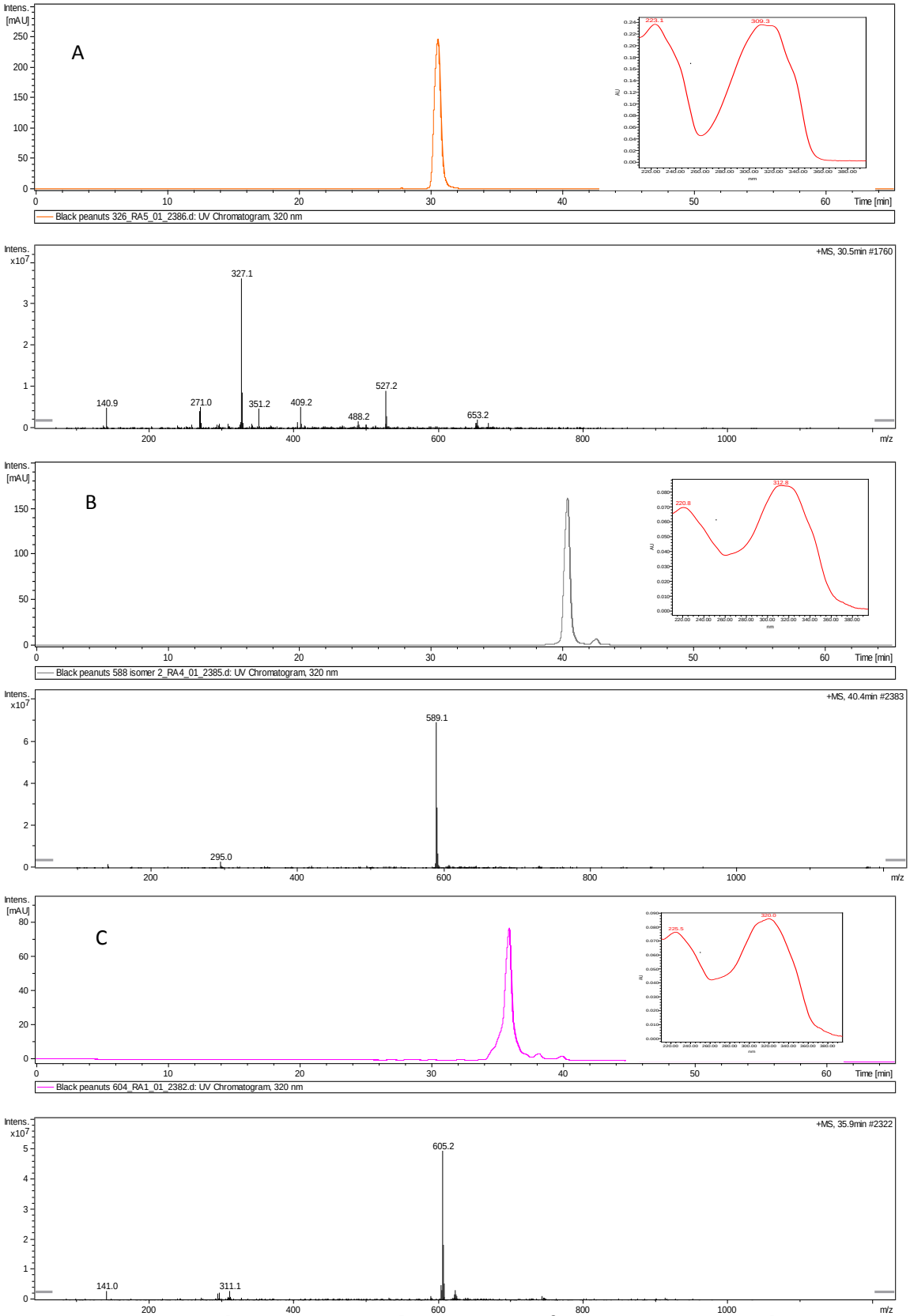

Figure 5.5 LC-MS chromatogram and UV spectra of (A) MIP (**3**); (B) arahypin-11(**1**); (C) arahypin-12 (**2**)

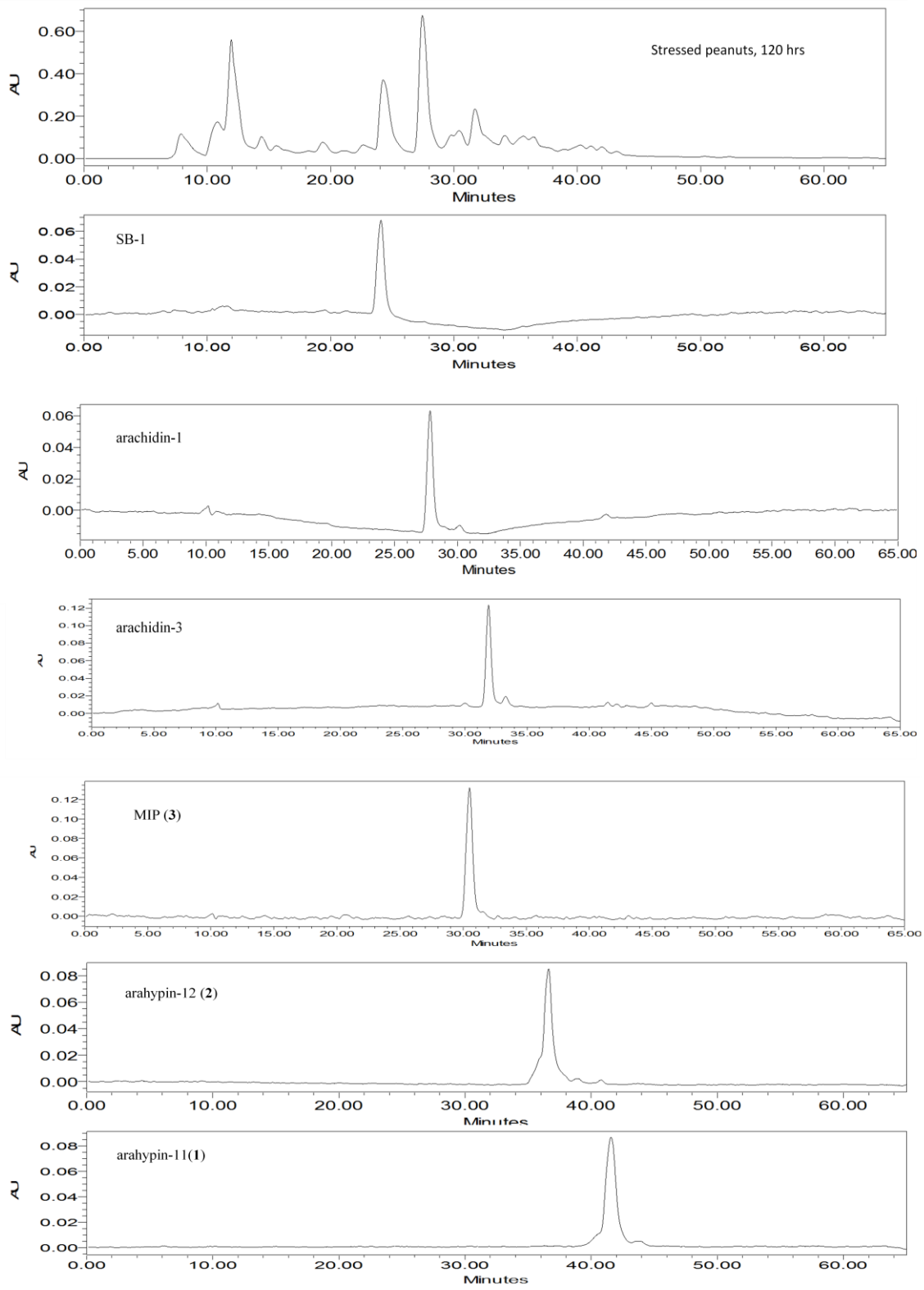

Figure 5.6 HPLC chromatograms (320 nm) of methanol extract of fungus-stressed black skin peanut seeds and six purified compounds at the concentration of 0.2 mM.

5.3.3 Structural elucidation of the new stilbenes

The NMR proton spectra of compound **1** (arahypin-11) are similar to that of arahypin-8 which has three methyl groups. The HMBC correlations from H-18′ (δ_H 1.82) and H-19′ (δ_H 1.76) to C-16′ (δ_C 129.6) and C-17′ (δ_C 134.3) indicate the presence of two prenyl derived methyl groups. However, the two protons at δ_H 7.43 and two protons at δ_H 6.84 suggest the existence of a 1,4-disubstituted benzene ring. Therefore, **1** is formed by two different monomers. The entire structure of **1** is established by assigning signals from ^{1}H, ^{13}C, COSY, HMQC and HMBC experiments. The NMR data is summarized in Table 5.1.

The HMBC correlations from H-11′&13′ (δ_H 6.84) to C-9′ (δ_C 130.8), C-12′ (δ_C 158.8), C-14′(δ_C 129.4) combining that HMBC correlations from H-8′ (δ_H 6.98) to C-10′ (δ_C 129.4) and H-6′ (δ_H 6.64) to C-4′ (δ_C 113.0), C-5′ (δ_C 157.0), and C-7′ (δ_C 127.2) revealed the skeleton of one unreported monomer. The connection of the two monomers was established through the HMBC from H-15′ (δ_H 3.80) to C-18 (δ_C 41.3), C-3′ (δ_C 158.1), C-4′ and C-5′. In addition, the relative stereochemistry of arahypin-11 was measured by NOESY experiment. There are no correlations between H-15′ and H-19 (δ_H 1.53), which was found in arahypin-8. Instead, there are correlations between H-15′ and H-16 (δ_H 6.52), which proved that the H-15′ and H-19 are on the different side of the six-member ring. The relative stereochemistry of compound **1** was established as shown in Figure 5.7.

Table 5.1 NMR data of arahypin-11 (**1**) and arahypin-12 (**2**)

position	arahypin-11			arahypin-12		
	δ_H, (*J* in Hz)	δ_C	HMBC correlations	δ_H, (*J* in Hz)	δ_C	HMBC correlations
1		141.5			141.5	
2	6.51, d (2.2)	106.3	C-3, C-4, C-6, C-7	6.50, d (2.2)	106.3	C-3, C-4, C-6, C-7
3		160.3			160.3	
4	6.25, t (2.2)	103.4	C-2, C-3, C-5, C-6	6.24, t (2.2)	103.3	C-2, C-3, C-5, C-6
5		160.3			160.3	
6	6.51, d (2.2)	106.3	C-2, C-4, C-5, C-7	6.50, d (2.2)	106.3	C-2, C-4, C-5, C-7
7	6.86, d (16.2)	127.8	C-1, C-2, C-6, C-8, C-9	6.86, d (16.4)	127.8	C-1, C-2, C-6, C-8, C-9
8	7.03, d (16.2)	129.7	C-1, C-7, C-9, C-10	6.97, d (16.4)	129.7	C-1, C-7, C-9, C-10
9		130.8			130.8	
10	7.58, d (2.0)	126.9	C-8, C-11, C-12, C-15	7.58, d (2.2)	126.9	C-8, C-11, C-12, C-15
11		125.6			125.6	
12		155.9			156.0	
13	6.83, d (8.4)	117.1	C-9, C-11, C-12, C-14	6.83, d (8.2)	117.5	C-9, C-11, C-12, C-14
14	7.28, dd (8.4, 2.0)	128.0		7.28, dd (8.2, 2.2)	128.0	
15	6.90, d (16.0)	125.4	C-10, C-12, C-16, C-17	6.89, d (16.4)	125.4	C-10, C-12, C-16, C-17
16	6.52, d (16.0)	134.7	C-11, C-15, C-18, C-19	6.52, d (16.4)	134.7	C-11, C-15, C-18, C-19
17		78.1			78.1	
18	a. 2.28, (13.7, 6.8) b. 1.75, m	41.3	C-16, C-17, C-19, C-4', C-15', C-16'	a. 2.27, (13.7, 6.7) b. 1.73, m	41.3	C-16, C-17, C-19, C-11', C-15', C-16'
19	1.53	30.0	C-16, C-17, C-18	1.52, S	30.0	C-16, C-17, C-18
1'		125.6			139.0	
2'	6.52, d, 1.8	107.1	C-3', C-4', C-6', C-7'	6.50, d, 1.8	107.1	C-3', C-4', C-6', C-7'
3'		158.1			158.1	
4'		113.0			113.0	
5'		157.0			157.0	
6'	6.64, d, 1.8	108.2	C-2', C-4', C-5', C-7'	6.62, d, 1.8	108.2	C-2', C-4', C-5', C-7'
7'	6.86, d, 16.4	127.2	C-1', C-2', C-6', C-8', C-9'	6.81, d, 16.4	127.3	C-1', C-2', C-6', C-8', C-9'
8'	6.98, d, 16.4	129.4	C-1', C-7', C-9', C-10'	6.96, d, 16.4	129.7	C-1', C-7', C-9', C-10'
9'		130.8			131.3	
10'	7.43, d (8.7)	129.4	C-12', C-14'	7.08, d (1.8)	114.4	C-8', C-11', C-12', C-14'
11'	6.84, d (8.7)	117.1	C-9', C-12', C-13', C-14'		146.8	
12'		158.8			146.9	
13'	6.84, d (8.7)	117.1	C-9', C-11', C-12', C-14'	6.80, d (8.1)	116.9	C-9', C-11', C-12', C-14'
14'	7.43, d (8.7)	129.4	C-10', C-12'	6.91, dd (8.1, 1.8)	120.6	
15'	3.80, m	31.0	C-18, C-3', C-4', C-5', C-16', C-17'	3.79, m	30.8	C-18, C-3', C-4', C-5', C-16', C-17'
16'	5.21, d, (9.2)	129.6		5.20, d, (9.3)	129.6	C-4', C-19'
17'		134.3			134.2	
18'	1.82, s	18.8	C-16', C-17', C-19'	1.81, s	18.7	C-16', C-17', C-19'
19'	1.76, s	26.6	C-16', C-17', C-18'	1.76, s	26.6	C-16', C-17', C-18'

Data (δ in ppm) were Recorded in acetone-d_6

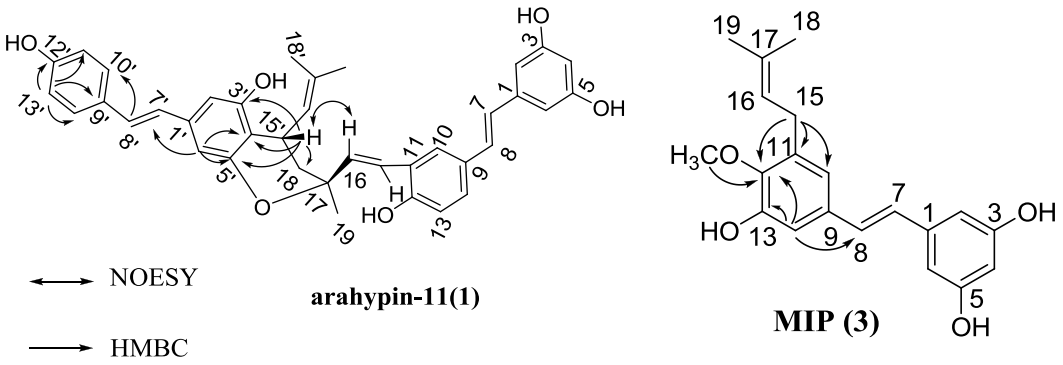

Figure 5.7 Selected HMBC correlations of arahypin-11(**1**) and MIP(**3**)

The proton spectra of compound **2** (arahypin-12) are quite similar to the spectra of compound **1** except the disappearance of the four proton signals which represent the 1,4-disubstituted benzene ring. In addition, the ^{13}C spectra showed two carbons at δ_C 146.8 and δ_C 146.9, indicating two adjacent phenol carbons. Therefore, it was supposed that C-11′ was oxygenated and this hypothesis was confirmed by HMBC correlations from H-10′ (δ_H 7.08) and H-13′(δ_H 6.80) to C-11′ (δ_C 146.8) and C-12′ (δ_C 146.9). The entire structure of compound **2** was established by assigning signals from ^1H, ^{13}C, COSY, HMQC and HMBC experiments. The NMR data is summarized in Table 5.1.

The structure of compound **3** (MIP) was established by analysis of its 1D and 2D NMR data summarized in Table 5.2. The HMBC correlations from H-15 (δ_H 3.36) to C-10 (δ_C 120.3), C-11 (δ_C 136.4), C-12 (δ_C 146.8), C-16 (δ_C 124.3), and C-17(δ_C 132.7) suggest the presence of a methylene group in the isopentenyl moiety connected with a benzene ring. The methoxy group (δ_H 3.80, δ_C 61.0) showed correlation with

C-12, indicating it is a substituent on the benzene ring as well. The HMBC experiments also revealed correlations from H-14 (δ_H 6.99) to C-8 (δ_C 129.3), C-12 and C-13 (δ_C 151.2), which is indicative of the presence of an olefinic double bond in the stilbene skeleton. Combining with other data in Table 3, the structure of compound 3 was established as shown in Figure 5.7.

Table 5.2 NMR data of MIP (**3**)

position	δ_H, (*J* in Hz)	δ_C	HMBC correaltions
1		140.7	
2	6.56, d (2.1)	106.1	C-3, C-4, C-6, C-7
3		159.8	
4	6.30, t (2.1)	103.1	C-2, C-3, C-5, C-6
5		159.8	
6	6.56, d (2.1)	106.1	C-2, C-3, C-4, C-7
7	6.90, d (16.7)	128.8	C-1, C-2, C-6, C-8, C-9
8	6.97, d (16.7)	129.3	C-1, C-7, C-9, C-10, C-14
9		134.6	
10	6.88, d (2.1)	120.3	C-8, C-9, C-11, C-12, C-14, C-15
11		136.3	
12		146.8	
13		151.2	
14	6.99, d (2.1)	112.9	C-8, C-10, C-12, C-13
15	3.36, d (7.3)	29.4	C-10, C-11, C-12, C-16, C-17
16	5.32, t (7.3)	124.3	C-18, C-19
17		132.7	
18	1.77, bs	18.1	C-16, C-17, C-19
19	1.75, bs	26.0	C-16, C-17, C-18
OMe	3.80, s	61.0	C-12

Data (δ in ppm) were Recorded in acetone-d_6

5.3.4 Proposed formation mechanisms of the new peanut stilbenoids

MIP was supposed to be the methylated product of 3′-isopentenyl-3, 5, 4′, 5′ -tetrahydroxystilbene since in the previous study (Sobolev et al., 2006b), mucilagin A

(Figure 5.8), a methylated product of arachidin-3, was also identified as in the peanut root mucilage by combined HPLC-PAD and LC-MS^n analysis. This discovery further confirmed the natural methylation products of prenylated stilbenoids in peanuts. In addition, the dihydro derivative of MIP (3) was firstly isolated from *Glycyrrhiza glabra* (Biondi et al., 2003), the content of which (yield 0.35%, fresh wt) was much higher than MIP (3) in stressed peanuts. Given the fact that the concentrations of the prenylated stilbenoids were low in fungus-stressed peanut seeds, chemical synthesis study will be needed for efficient production of these compounds and some researchers have made achievements in this direction (Park et al., 2011).

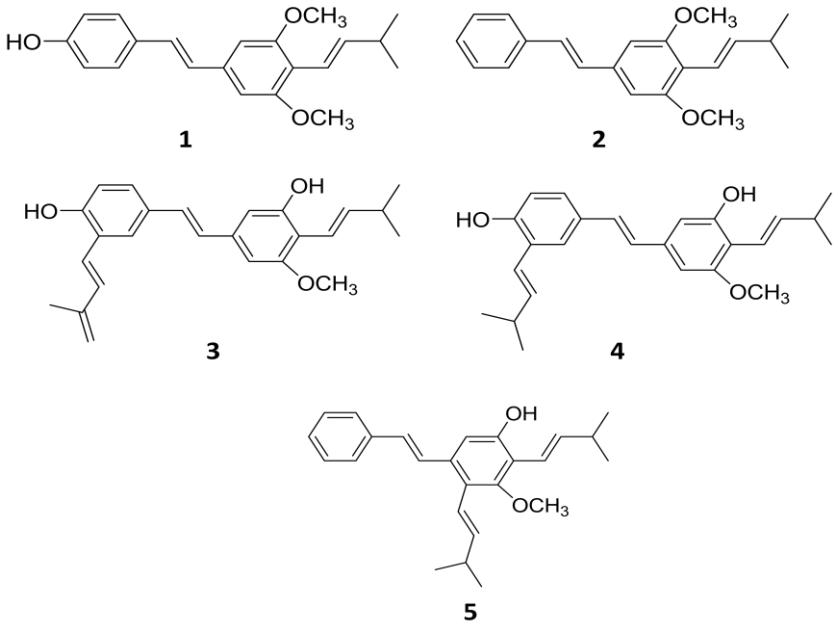

Figure 5.8 Proposed structures of methylated stilbenoids detected in peanut mucilage extract by LC-MS^n. The concentration of mucilagin A (**1**) in the mucilage was 250 μg/g, while the total concentration of the other stilbenoids (**2**-**5**) was 130 μg/g.

It is also noticeable that the stereochemistry of arahypin-11 (**1**) and arahypin-12 (**2**) was different than that of arahypin-8 and all the three compounds have chiral carbons

but show no optical rotation activity. However, this does not exclude the possibility that these stilbene dimers were formed through an enzymatic reaction. In a recent study by Wan et al. (2011), the authors showed that *Momordica charantia* peroxidase (MCP) could also catalyze the coupling reaction to produce piceatannol dimers as racemic mixtures in a non stereo-selective way. A radical reaction mechanism was supposed to be involved in the dimerization of piceatannol catalyzed by MCP (Figure 5.9). Although there is a lack of evidence on whether a similar catalyzed mechanism also plays a critical role in the production of the four new arahypin dimers in fungus-stressed peanut seeds, finding out the potential synthase responsible for dimerization of stilbenes in the fungus-stressed peanut seeds may have important implications for improving the yields of peanut oligomeric stilbenes.

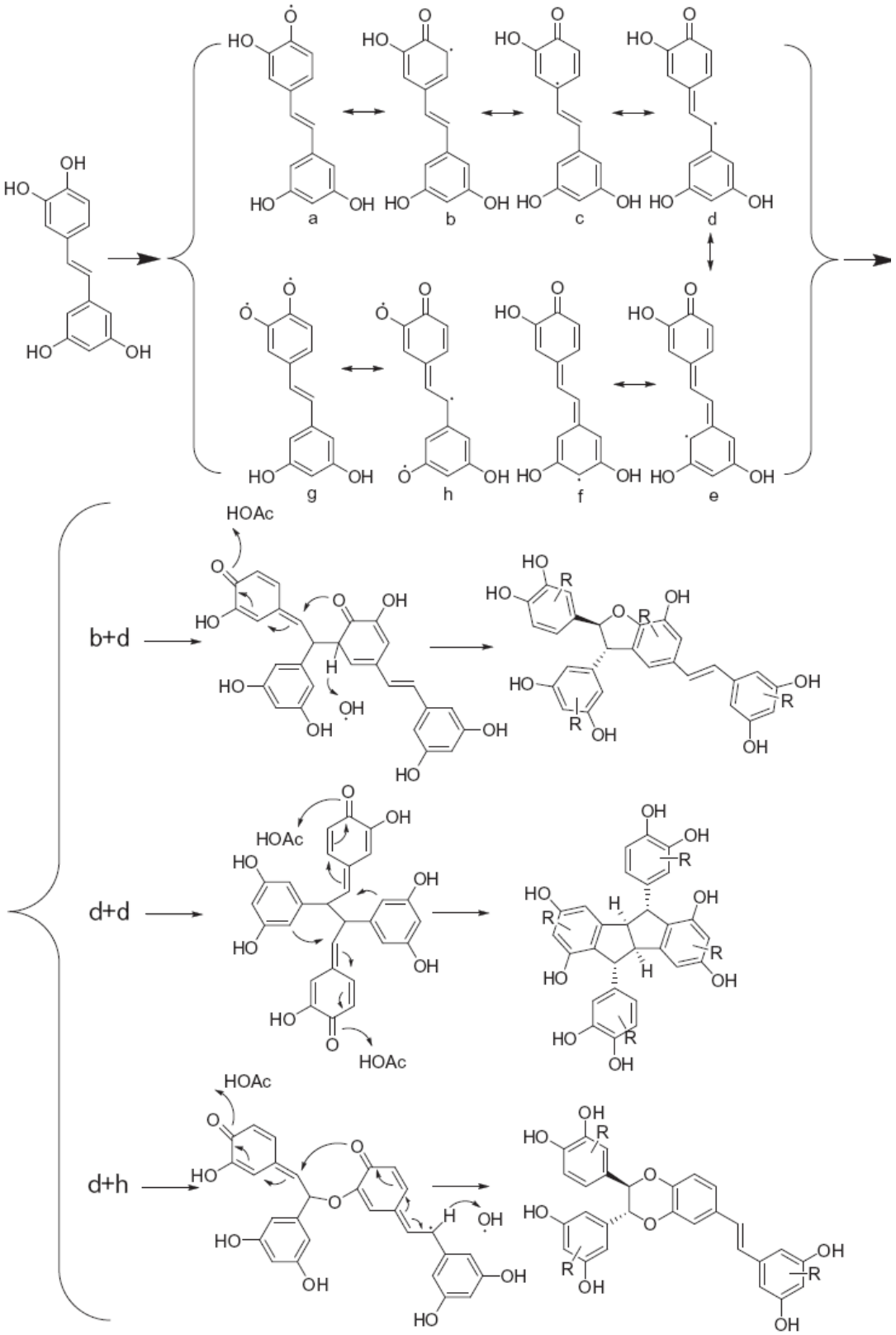

Figure 5.9 proposed mechanism of dimerization of piceatannol by MCP (Wan et al., 2011. Bioorgan. Med. Chem. *19*, 5085-5092.)

5.4 Conclusion

A fungal strain *R. oligoporus* was applied to elicit stilbenoid production in Chinese black skin peanut seeds. The dynamics of stilbenoid production in the fungus-stressed black skin peanut seeds were investigated and compared with the dynamic profile of peanut stilbenoid production reported previously by other researchers. Two new stilbene dimers (arahypin-11 and arahypin-12) and one monomeric stilbene derivative MIP were isolated for the first time from fungus-stressed black skin peanut seeds. The structures of the three new compounds were elucidated by HRESIMS, UV, 1D and 2D NMR spectroscopy. Until now, the construction pattern of arahypin-11 and arahypin-12 was specific for peanut seeds challenged by *R. oligoporus* because stilbene dimers arahypin-8 and arahypin-9 connected through prenyl groups were only reported in chapter 4. The skeletons of the four stilbene dimers cannot be categorized into any of 29 known construction patterns of stilbene oligomers, indicating unknown biological potential of the molecules to be explored.

Chapter 6 Evaluation of biological activity of peanut stilbenoids

6.1 Introduction

Stilbene derivatives from peanuts (*Arachis hypogaea*) have attracted considerable interest of different research groups around the world due to the diverse range of health-promoting properties they tend to display such as anti-inflammatory, antioxidant, anticancer activities and possible therapeutic values for chronic diseases (Lopes et al., 2011). In chapters 4 & 5, six new stilbenoids (arahypin-8, arahypin-9, arahypin-10, arahypin-11, arahypin-12, MIP) and three known stilbenoids (SB-1, arachidin-1, arachidin-3) were isolated from fungus-stressed peanut seeds. In this chapter, the biological activities of the nine isolated peanut stilbenoids plus resveratrol as a reference control were evaluated in a broad spectrum of bioassays to determine their antioxidant, anti-diabetic, anti-obesity, and cytotoxic effects in mammalian cells.

It was demonstrated that resveratrol was a highly efficient MPO inhibitor in both QDs and APF microplate assays as described in chapter 3. Although peanut stilbenoids such as arachidin-1 and piceatannol were reported to be effective antioxidant and anti-inflammatory agents (Chang et al., 2006; Djoko et al., 2007), there are no reports on the MPO inhibitory activity of peanut prenylated stilbenoids which bear a close structural relationship with resveratrol. Therefore, in this study the antioxidant activity of the isolated peanut stilbenoids were tested in APF/HPF microplate assays to determine their inhibitory effects on highly reactive oxidative species (hROS) generation by MPO in HL60 differentiated cells.

Although numerous studies reported the anti-diabetic effects of natural stilbenes based on different action mechanisms (Shen et al., 2009), the potential utility of natural stilbenes for reversing fat-induced insulin resistance in type 2 diabetes is still rarely reported. As for the studies on the anti-diabetic peanut stilbenoids, only resveratrol and piceatannol were reported to promote glucose uptake in L6 myocytes through stimulation of glucose transporter 4 (GLUT4) and decrease blood glucose levels in type 2 diabetic animal models (Breen et al., 2008; Minakawa et al., 2012). Hence, in order to fully explore the therapeutic potential of natural stilbenes to ameliorate insulin resistance in type 2 diabetes, the insulin sensitizing activity of the nine isolated peanut stilbenoids was examined in a fluorescent glucose uptake microplate assay using differentiated 3T3-L1adipocytes.

Since recent studies revealed the anti-obesity effect of some natural stilbenes such as piceatannol and Vitisin A which could inhibit adipocyte differentiation (Kwon et al., 2012; Kim et al., 2008c), it also indicates the potential adipogenesis inhibitory activity of peanut stilbenoids. However, little is known about the effects of peanut prenylated stilbenoids on the lipid metabolism in 3T3-L1 adipocytes. In the present study, the adipogenesis inhibitory activity of the nine peanut prenylated stilbenoids together with resveratrol was determined by 3T3-L1 adipocyte differentiation assay. At the same time, the cytotoxicity of these compounds in 3T3-L1 preadipocytes was evaluated in a MTT assay.

6.2 Materials and methods

6.2.1 Chemicals and reagents.

Phorbol 12-myristate 13-acetate (PMA, 99%), resveratrol (99%), thiazolyl blue tetrazolium bromide (MTT), Oil Red O,3-isobutyl-1-methyl-xanthine (IBMX) and dexamethasone (DEX) were purchased from Sigma Chemical Co. (St. Louis, MO, USA). Fluorescence hypochlorite detection kit composed by aminophenyl fluorescein (APF, 5mM solution in DMF) and hydroxyphenyl fluorescein (HPF, 5mM solution in DMF) was purchased from Cell Technology, Inc. Arachidin-1, arachidin-3, SB-1, arahypin-8, arahypin-9, arahypin-10, arahypin-11, arahypin-12 and MIP were isolated from fungus-stressed peanut seeds as described previously. PMA (1 mg/ml), the nine isolated peanut stilbenoids and resveratrol (10 mM) were dissolved in ethanol as stock solutions. Krebs-Ringers phosphate buffer (KRPB; 114 mM NaCl, 4.6 mM KCl, 2.4 mM $MgSO_4$, 1.0 mM $CaCl_2$, 15 mM NaH_2PO_4, 15 mM Na_2HPO_4, pH 7.4) was used for dilution of the above stock solutions for the subsequent HL60 cell based analyses. 2-(*N*-(7-nitrobenz-2-oxa-1,3-diazol-4-yl)amino)-2-deoxyglucose (2-NBDG) was obtained from Invitrogen Inc. (Carlsbad, CA, USA). Recombinant human insulin from yeast was purchased from Roche Applied Science (Indianapolis, IN, USA) and rosiglitazone was obtained from Cayman Chemical Company (Ann Arbor, MI, USA). Other chemicals were of analytical grade unless otherwise specified.

6.2.2 Cell cultures

The culture method of HL60 cells was described in section 3.2.2.

3T3-L1 preadipocytes (5 passages) were kindly provided by Professor Benny Tan Kwon Huat from the Department of Pharmacology, National University of Singapore. The cells were grown in Dubecco's modified Eagle's medium (DMEM) (Gibco BRL, NY, U.S.A) containing 10% fetal bovine serum (FBS) (Gibco BRL, NY, USA), antibiotics (100 U/ml penicillin and 100 μg/ml streptomycin (Gibco BRL, NY, USA) at 37 ℃ under a humidified 5% CO_2 atmosphere.

6.2.3 MPO inhibition assay

HL60 cells were differentiated into neutrophil-like cells which were applied to 96-well plate assay as described in section 3.2.5. PMA (2 μg/mL) was used to stimulate the generation of MPO-derived hROS detected by fluorescent probes APF and HPF with an excitation wavelength at 485 nm and emission at 530 nm. The MPO inhibition rates of peanut stilbenoids were calculated according to the method described in section 3.2.6.

6.2.4 3T3-L1 adipocyte differentiation and glucose uptake assay

3T3-L1 preadipocytes were seeded in 48-well culture plates at a density of 5 $\times 10^4$/well and maintained for two additional days until confluence. For adipocyte

differentiation, cells were incubated in differentiation medium containing 0.5 mM IBMX, 10 μg/mL insulin, and 0.25 μM DEX in DMEM supplemented with 10% FBS for two days. The cell culture medium was then changed to DMEM containing 10 μg/mL insulin and 10% FBS. After another two days, the medium was replaced again with DMEM containing 10% FBS. 6-8 days after the initiation of differentiation, fully differentiated adipocytes were incubated with 1 μM DEX for 24hrs and used for glucose uptake assay. Various concentrations of the tested stilbenoids were incubated with the fully differentiated adipocytes for two days. Before assay, cell culture media were discarded and incubated with 500 μL serum-free, low glucose DMEM (1.0 g/L glucose, Invitrogen, OR, USA) for 2 hrs. The cells were then incubated in 75 μL of low glucose DMEM with 100 nM insulin for 10 min at 37 ℃. Glucose uptake assay was initiated by the addition of 75 μL of low glucose DMEM containing 500 μM 2-NBDG, after 30 min, the supernatant was removed. Plates were washed with ice-cold PBS three times to terminate the reactions. Cells were lysed by freeze-thaw and fluorescence of 2-NBDG was measured using fluorescence spectrophotometer (excitation wavelength at 480 nm, emission wavelength at 530 nm).

6.2.5 3T3-L1 adipogenesis inhibition assay

In adipogenesis study, 3T3-L1 preadipocytes were seeded in 96-well plate at a density of 1×10^4/well and maintained for 2 additional days until confluence (designated as day 0). For adipocyte differentiation, the cells were incubated in a differentiation

medium (10% FBS/DMEM containing 0.5 mM IBMX, 10 μg/mL insulin, and 0.25 μM DEX) for 2 days. The medium was then changed to 10% FBS/DMEM containing 10 μg/mL insulin. After another two days, the medium was replaced with 10% FBS/DMEM and the cell continued to differentiate until day six. Test stilbenoids were administered during the differentiation process and on day six the cells were subjected to Oil Red O staining to quantify intracellular lipid content as described previously (Kwon et al., 2012; Kim et al., 2008c). Briefly, the cells were fixed for 1 h at room temperature with 10% formalin in PBS, washed three times with PBS, and then stained for 1 h with filtered Oil Red O (0.5% in 60% isopropanol/40% PBS). After washed three times with distilled water, the stained lipid droplets were dissolved in isopropanol and quantified by measuring the absorbance at 510 nm.

6.2.6 Cell viability Assay

The cells were treated with the tested stilbenoids at indicated concentrations in differentiation medium for 48 hrs. Then the cells were incubated with MTT solution (0.5 mg/mL) for 3 hrs at 37 ℃ and the supernatant was replaced by DMSO to dissolve the violet precipitate formazan. The absorbance was measured at 490 nm on a microplate reader.

6.3 Results and discussion

6.3.1 MPO inhibition activity of peanut stilbenoids

APF and HPF are selective for detection of highly reactive oxygen species (hROS) including $^{\bullet}OH$, $ONOO^-$ and HClO (Table 6.1), which can be defined as ROS with oxidizing power sufficient to directly hydroxate aromatic rings. HPF/APF in combination can be used to differentiate HClO from other hROS (Setsukinai et al., 2003). Compared with other ROS such as H_2O_2, $O_2^{\cdot -}$ and NO, hROS are more aggressive and able to oxidize additional classes of molecules. For example, $^{\bullet}OH$ has been shown to directly peroxidize lipids (Warner et al., 2004), participate in apoptosis (Ren et al., 2001; Santos et al., 2008) and cause severe damage to DNA (Wiseman and Halliwell, 1996). Similarly, $ONOO^-$ can alter many critical cellular molecules and induce apoptosis (Taylor et al., 2007; Natal et al., 2008). More importantly, it has been proven that MPO also catalyzed the formation of $^{\bullet}OH$ and $ONOO^-$ during the respiratory burst in neutrophils (Fujimoto et al., 1993; Burner et al., 2000). In chapter 3, resveratrol was shown to be an efficient MPO inhibitor with the highest HClO eliminating potency among the tested chemicals in the QD microplate assay. Therefore, in the current APF/HPF microplate assay, resveratrol was taken as the reference compound for evaluating the inhibitory activity of the isolated peanut stilbenoids on the generation of hROS by MPO in HL60 neutrophil-like cells upon stimulation by PMA.

Table 6.1 Reactivity Profiles of APF and HPF

ROS	APF(ex:490 em:515)	HPF(ex:490 em:515)
Hydroxyl Radical: $^{\cdot}OH$	1200	730
Peroxynitrite: $ONOO^-$	560	120
Hypochlorite: HClO	3600	6
Oxygen Radical: $^1O_2$	9	5
Superoxide: $O_2^{\cdot-}$	6	8
Hydrogen Peroxide: H_2O_2	<1	2
Nitric Oxide: NO	<1	6
Alkylperoxyl Radical: $ROO^{\cdot}$	2	17
Autoxidation	<1	1

(Setsukinai et al., 2003. J. Biol. Chem. 278, 3170-3175.)

Figure 6.1 shows that all the tested peanut stilbenoids possessed MPO inhibition activity with different potency. Compared with resveratrol, only arachidin-1 exhibited significantly higher MPO inhibition potency in both APF/HPF microplate assays. In the anti-inflammatory assay using DCFH-DA for detecting ROS generation by PMA stimulated HL60 cells (Sobolev et al., 2011), arachidin-1, arachidin-3, SB-1 and resveratrol demonstrated strong antioxidant effect comparable to that of Trolox. The current assay further supplements antioxidant and anti-inflammatory profiles of peanut stilbenoids as DCFH-DA is not a selective probe for detecting cellular hROS generation compared with APF and HPF (Choung et al., 2009). Since arachidin-1 is a major stilbene component with a high production yield in the fungus-stressed peanut seeds, it is of great interest to explore the potential of this novel MPO inhibitor as an alternative to resveratrol. However, more detailed studies on the MPO inhibition mechanism of arachidin-1 such as its MPO putative binding site and its effect on the

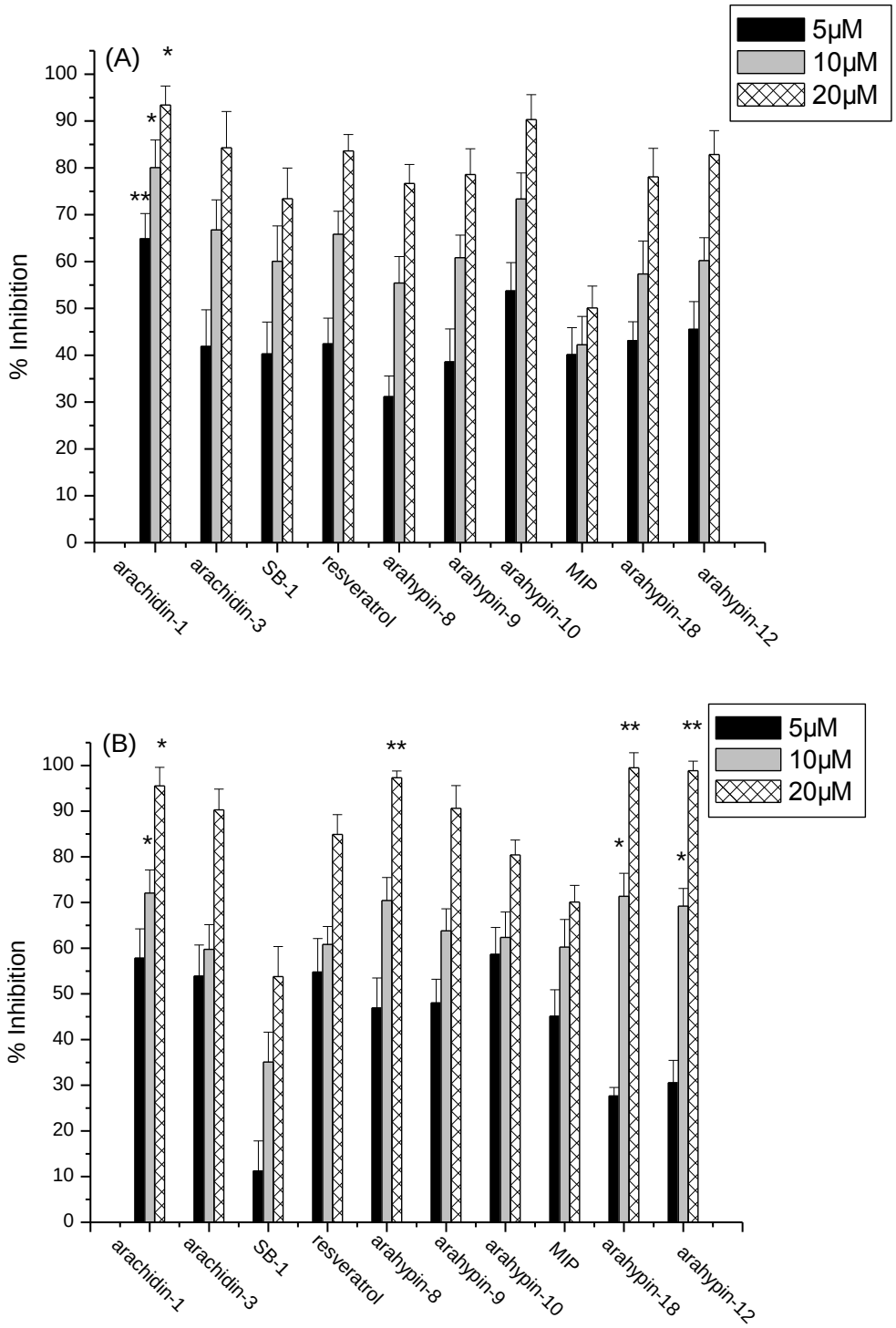

Figure 6.1 The inhibitory effects of the nine isolated peanut stilbenoids and resveratrol on PMA-stimulated hROS generation by MPO in differentiated HL60 cells detected by APF (A) and HPF (B). Error bars represent standard deviations, n = 4. *P < 0.05, **P < 0.01 when compared with resveratrol treatment groups at corresponding concentrations.

MPO chlorination and peroxidase activities would be essential for developing arachidin-1 as a pharmaceutical ingredient for reducing MPO-derived hROS associated with cellular damage .

6.3.2 The glucose uptake stimulatory activity of peanut stilbenoids

The effect of the nine isolated peanut stilbenoids plus resveratrol on insulin-stimulated glucose uptake in differentiated 3T3-L1 was examined compared with the positive control Rosiglitazone which is an anti-diabetic drug working as insulin sensitizer. As shown in Figure 6.2, arahypin-8, arahypin-9, arahypin-10, significantly increased insulin-stimulated glucose uptake in differentiated 3T3-L1 adipocytes at a concentration of 10 μM compared with insulin control groups. These results indicate that the three new peanut stilbenoids were able to ameliorate insulin resistance *in vitro* and thus may be potential insulin sensitizers.

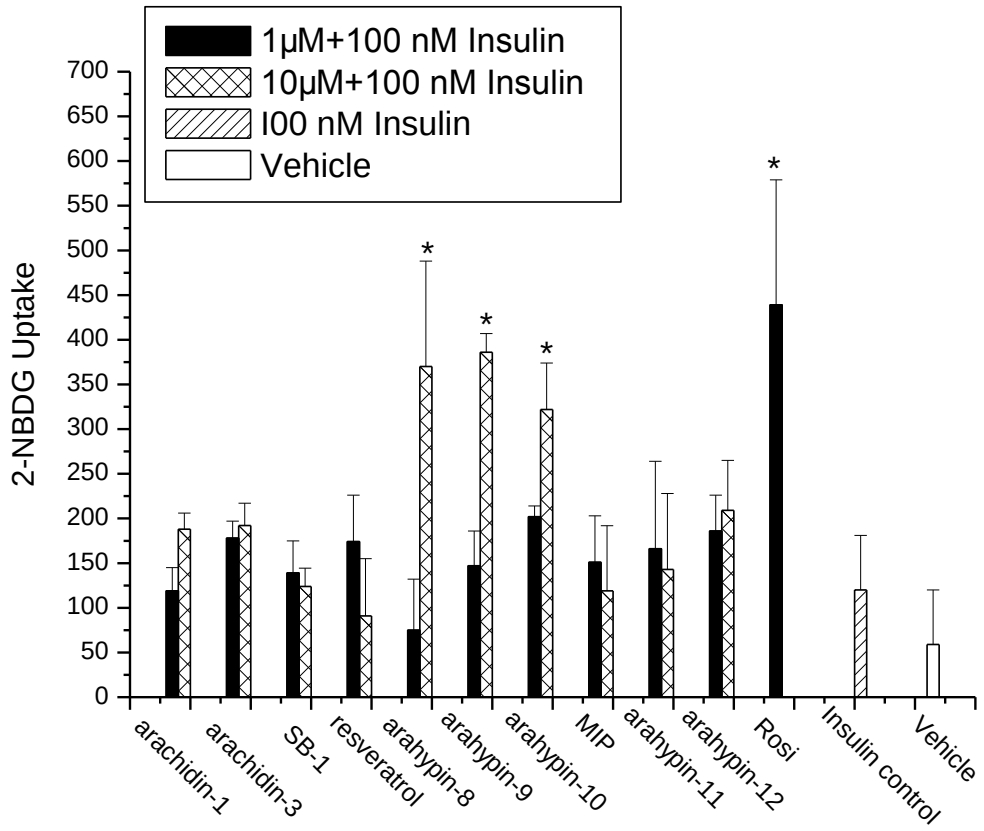

Figure 6.2. Effect of the nine isolated peanut stilbenoids and resveratrol on insulin-stimulated glucose uptake in differentiated 3T3-L1 adipocytes. The glucose uptake effect of 1 μM rosiglitazone (Rosi) with insulin (100 nM) stimulation served as a positive control. Error bars represent standard deviations, n = 4. *P < 0.05, **P < 0.01 when compared with the insulin control group (100 nM).

2-NBDG is a novel fluorescence glucose analog which had been widely used for measuring glucose uptake in non-mammalian and mammalian cells in recent years (Loaiza et al., 2003; Porras et al., 2004; Zou et al., 2005; Yamada et al., 2007; Hassanein et al., 2010). It was proven that 2-NBDG was transported intracellularly by the same glucose transporters (GLUTs) as glucose. 2-NBDG uptake could be inhibited by D-glucose based on a competition mechanism and by GLUTs inhibitors such as cytochalasin B and phloretin in mammalian cells (Demartino & McGuire,

1988; Yoshioka et al., 1996; Lloyd et al., 1999; Gaudreault et al., 2008; Hassanein et al; 2010). Although resveratrol and piceatannol were reported to promote glucose uptake in L6 myocytes through activation of GLUT4, their prenylated analogs arachidin-3 and arachidin-1 did not exhibit a significant glucose uptake stimulatory effect in differentiated 3T3-L1 adipocytes (Figure 6.3). In addition, the performance of resveratrol in this assay was consistent with a previous finding that resveratrol inhibited insulin-dependent changes in glucose uptake in differentiated 3T3-L1 adipocytes accompanied by a decreased GLUT4 protein level (Floyd et al., 2008).

6.3.3 The adipogenesis inhibitory activity of peanut stilbenoids

The effect of the nine isolated peanut stilbenoids plus resveratrol on adipogenesis was evaluated. Quantitative analysis of intracellular lipids by Oil Red O staining (Figure 6.3) showed that only arachidin-1 displayed dose-dependent inhibition of adipogenesis in 3T3-L1 cells. The lipid accumulation level of 3T3-L1 adipocytes treated with 5 and 10 μM arachidin-1 was reduced to 73% and 57%, respectively, of that of control adipocytes (Diff.). Arachidin-1 was a prenylated analog of piceatannol and the latter was reported recently to be a potent inhibitor for adipogenesis in 3T3-L1 cells (Kwon et al., 2012). Compared with resveratrol and arachidin-3, arachidin-1 possesses an extra hydroxyl group at the 3′ position which may enhance its anti-adipogenic activity. More studies on the molecular action mechanism of arachidin-1 in 3T3-L1 cells are needed to elucidate the relationship between the structure and biological effect of the compound.

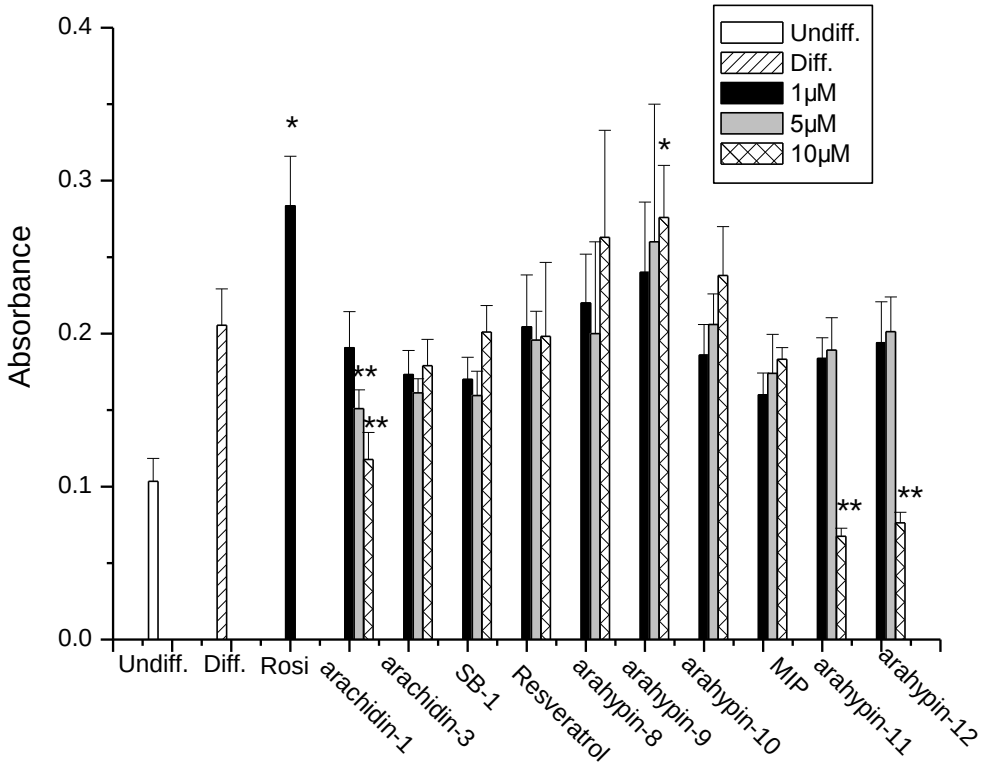

Figure 6.3 Effect of the nine isolated peanut stilbenoids and resveratrol on the 3T3-L1 adipocyte differentiation. Undifferentiated preadipocytes (Undiff.), differentiated adipocytes (Diff.), and adipocytes treated with stilbenes were subjected to Oil Red O staining. Rosiglitazone (Rosi) was taken as a positive control for promoting adipogenesis. Error bars represent standard deviations, n = 4. *P < 0.05, **P < 0.01when compared with differentiation group (Diff.).

On the other hand, the insulin sensitizer arahypin-9 in the glucose uptake assay was found to significantly enhance adipocyte differentiation in 3T3-L1 cells. Although the adipogenesis promoting effect of the other two insulin sensitizers arahypin-8 and arahypin-10 was not as significant as that of arahypin-9 and Rosiglitazone, the result indicates that the three arahypin compounds may be PPARγ agonists as Rosiglitazone which enhances insulin dependent glucose uptake and stimulates adipocyte differentiation by upregulating transcriptional activity of PPARγ (Nugent et al., 2001).

The cellular action mechanism of these potential anti-diabetic peanut stilbenoids warrants further investigation.

6.3.4 The cytotoxicity of peanut stilbenoids

The MTT assay result (Figure 6.4) showed that arachidin-1 inhibited adipogenesis without cytotoxic effect on the viability of the differentiating preadipocytes. Since arahypin-11 and arahypin-12 displayed dose-dependent cytotoxicity in MTT assay, further investigation would be focused on their anti-cancer activities in different cell lines. Interestingly, the two dimers arahypin-8 and arahypin-9 did not show cytotoxic effect on 3T3-L1 preadipocytes at the same concentration range. Although arahypin-8, arahypin-9, arahypin-11 and arahypin-12 share the same construction pattern, the difference in their monomeric units and relative stereo configurations may explain why these compounds exhibited different cytotoxicity in 3T3-L1 cells.

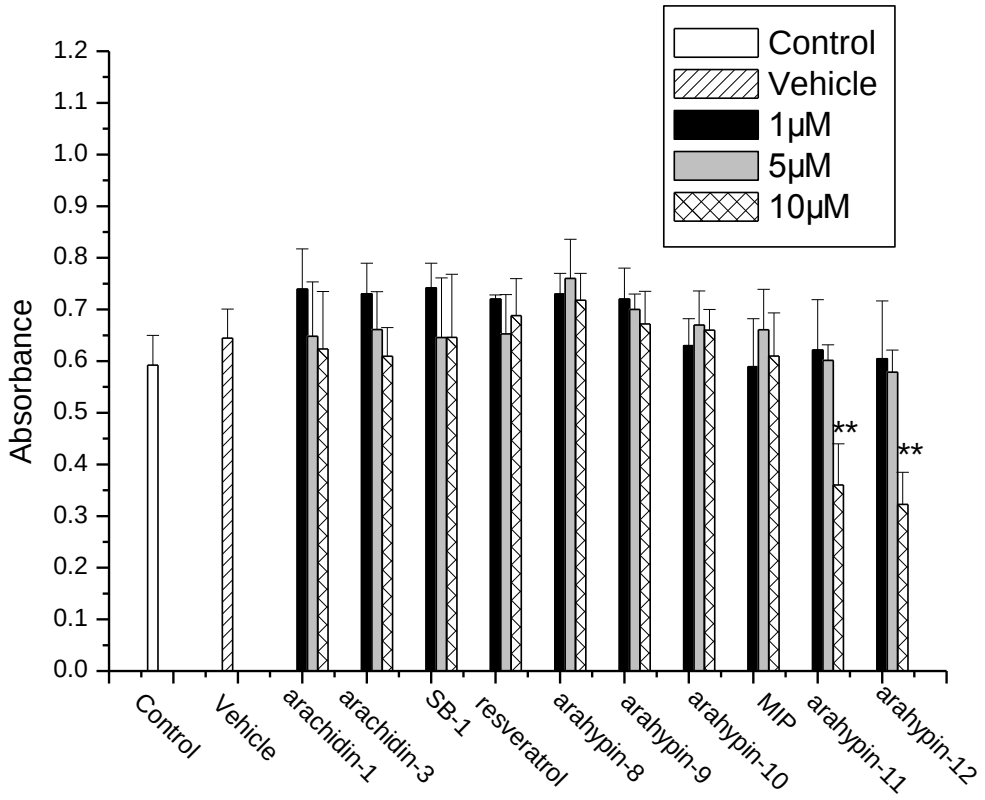

Figure 6.4 The viability of 3T3-L1 pre-adipocytes treated with peanut stilbenes in the differentiation medium for 48 hrs assessed by MTT assay. Error bars represent standard deviations, n = 4. *P < 0.05, **P < 0.01 when compared with control group treated with the differentiation medium alone.

6.4 Conclusion

The biological activities of new and known peanut stilbenoids were explored in a series of cell based microplate assays. The known monomeric stilbenoid arachidin-1 exhibited highest activity in both antioxidant and adipogenesis inhibition assay among all the tested peanut stilbenoids. Despite sharing similar construction patterns, the four new dimeric stilbenoids displayed significantly different bioactivities in the bioassays employed. The new dimers arahypin-8 and arahypin-9 isolated from India peanut

seeds were found to be insulin sensitizers in the glucose uptake assay while the other two dimers arahypin-11 and arahypin-12 from Chinese black skin peanut seeds exerted significant cytotoxicity in the MTT assay. These preliminary results indicates that the number and positions of hydroxyl groups, stereo configurations tend to be crucial factors in determining biological activities of individual peanut monomeric and dimeric stilbenoids. The diverse range of bioactivities displayed by the nine isolated stilbenoids revealed the potential of fungus-stressed peanut seeds as a new source of natural pharmaceutical ingredients.

Chapter 7 General conclusions and future work

7.1 General conclusions

In the quantum dots (QDs) based assay, resveratrol showed the highest hypochlorous acid (HClO) elimination potency compared with other efficient myeloperoxidase (MPO) inhibitors and HClO scavengers. Therefore, resveratrol was taken as a reference control for evaluating MPO inhibition efficiency of other isolated peanut stilbenoids.

The fungal strain *Rhizopus oligoporus* was applied to challenge two different varieties of peanut seeds to elicit the production of stilbene phytoalexins. Six new stilbenoids were identified and isolated according to their chromatographic behaviour, molecular weights, and UV spectra which were different from those of known peanut stilbenoids. The structures of the six new stilbenoids were elucidated by NMR analysis and a novel construction pattern of stilbene dimers was discovered. The dynamic profiles of stilbenoid production in fungus-stressed peanut seeds were also investigated and it was found that both fungal species and peanut varieties play important roles in the structural diversification of prenylated stilbenoids.

Finally, a systematic study of the biological activity of new and known peanut stilbenoids was carried out in a series of cell based assays. Prenylated peanut

stilbenoid arachidin-1 displayed significantly higher MPO inhibition and anti-adipogenic activities than resveratrol. Despite close structural similarities, the four stilbene dimers exhibited different potencies in the insulin sensitizing and cytotoxic assays. In summary, the results of the present research revealed the diverse biological activity of peanut stilbenoids which need further investigations on structure activity relationship and chemopreventive applications.

7.2 Suggestions for future work

This research on the discovery and biological evaluations of new stilbenoids from fungus-stressed peanut seeds shows a great promise for developing the peanut prenylated stilbenoids as health promoting products. However, more research work needs to be done before the peanut stilbenoids can appear as pharmaceutical ingredients in the market.

Investigation on the molecular action mechanism of peanut prenylated stilbenoids and their therapeutic potential in animal models should be carried out. Since peroxisome proliferator-activated receptors (PPARs, namely PPARα, PPARδ, and PPARγ) play essential roles in regulating lipid metabolism as well as glucose homeostasis and thus becoming drug targets in treating type 2 diabetes and obesity (Kersten et al., 2000), the effect of peanut prenylated stilbenoids on the expression level of PPARs in

adipocytes should be further investigated. Also, PPARs are ligand-activated transcription factors (Staels and Fruchart, 2005) and therefore PPARs ligand binding assay should be conducted to find out those peanut stilbenoids as potent PPARs ligands (agonists). The result of the binding assay would provide valuable guidance on the structure-activity relationship study for screening of efficient anti-diabetic and anti-obesity stilbenoids.

Verification of peanut stilbenoids' therapeutic potential through *In vivo* studies is another interesting area to be explored. Up to date, there are still no reports on the peanut prenylated stilbenoids applied in animal model experiments because the peanut prenylated stilbenoids are not commercially available yet. Although it was shown that the peanut stilbenoid arachidin-1 had strong MPO and adipogenesis inhibition activities, the *in-vitro* experiment did not take into consideration factors such as potential toxicity, ability to act in gastrointestinal tract, bioavailability and metabolic rates which may limit the *in vivo* use of arachidin-1 through oral route administration. Hence, animal dietary intervention experiments can provide solid evidences for comprehensively evaluating chemopreventive and therapeutic effects of the bioactive peanut stilbenoids.

Finally, from a practical viewpoint, peanut prenylated stilbenoids should be produced from a lab-preparation scale to a commercial scale. Total chemical synthesis of peanut prenylated stilbenoids may be a solution but the costly multiple step reactions and

synthetic chemical background significantly limit its application in the consumer market. Theoretically, there is a great potential for the improvement of stilbenoid productivity by peanut seeds as the natural bioreactor. How to enhance the biosynthesis of peanut prenylated stilbenoids is a challenge but promising task and three proposals were forwarded to achieve that goal. The first proposal is to increase the input of peanut prenylated stilbenoid biosynthesis precursors, which is supported by a very recent study by Russian scientists (Kizselv et al., 2013) who found that the increased stilbene precursor phenylalanine could significantly upregulate the gene expression of phenylalanine ammonialase (PAL) as well as stilbene synthase (SS) and enhance the production of resveratrol by 8.5 times in *Vitis amurensis* Rupr. cell culture system. The second proposal is to apply different fungal strains to find out the most efficient elicitor for peanut stilbenoids production. A previous study (Feng et al., 2007) showed the different efficiency of fungal strains on inducing phytoalexin production by germinated black soybean, which indicates the potential of finding more efficient fungal elicitors for peanut stilbenoid production. In addition, new fungal elicitors can increase the chance for discovering new bioactive stilbenoids as demonstrated by the finding that the four new arahypin dimers possessing novel skeletons were specific for *R. oligosporus*. The third proposal is to develop transgenic peanut species overexpressing stilbene synthase through plant metabolic engineering, which has provided a method to improve not only polyphenol composition but also its levels (Giovinazzo et al., 2012). Promising results have been obtained with SS-encoding genes in transgenic plants either to improve the resistance of plant or the

nutritional value. It is noticeable that there is still no report on the peanut stilbene synthase transgenic research. Given the fact that no cheap and efficient industrial production of resveratrol and prenylated stilbenoids has been developed up to date, it was predicted that transgenic peanut butter with high levels of prenylated stilbenoid may appear as a novel functional food in the future. However, all the above hypotheses and proposals must be based on the condition that the biosynthetic mechanism of prenylated stilbenoids in the fungus-peanut seeds interaction system is fully clarified, which still needs a great deal of research work.

Reference

Abbott, J.A., Medina-Bolivar, F., Martin, E.M., Engelberth, A.S., Villagarcia, H., Clausen, E.C., Carrier, D.J., 2010. Purification of resveratrol, arachidin-1, and arachidin-3 from hairy root cultures of peanut (*Arachis hypogaea*) and determination of their antioxidant activity and cytotoxicity. Biotechnol. Prog. 26, 1344–1351.

Ackerma, J.J., Duerre, J.A., 1989. Long-term culturing of TPA-induced differentiated HL-60 cells results in increased levels of lytic enzymes. Exp. Cell Res. 183, 353-360.

Aggarwal, B.B., Bhardwaj, A., Aggarwal, R. S., Seeram, N. P., Shishodia, S., Takada, Y., 2004. Role of resveratrol in prevention and therapy of cancer: preclinical and clinical studies. Anticancer Res. 24, 2783–2840.

Aguamah, G.A., Langcake, P., Leworthy, D.P., Page, J.A., Pryce, R.J., Strange, R.N., 1981. Two novel stilbene phytoalexins from *Arachis hypogaea*. Phytochemistry. 20,1381–1383.

Amri, A., Chaumeil, J.C., Sfar, S., Charrueau, C., 2012. Administration of resveratrol: What formulation solutions to bioavailability limitations? J. Control Release 158, 182 - 193

Anraku, M., Kragh-Hansen, U., Kawai, K., Maruyama, T., Yamasaki,Y., Takakura,Y., Otagiri, M., 2003. Validation of the chloramine-T induced oxidation of human serum albumin as a model for oxidative damage in vivo. Pharm. Res. 20, 684-692.

Athar, M., Back, J.H., Tang, X., Kim, K.H., Kopelovich, L., Bickers, D.R., Kim, A.L., 2007. Resveratrol: a review of preclinical studies for human cancer prevention. Toxicol. Appl. Pharmacol. 224, 274-283.

Baur, J.A., Sinclair, D.A., 2006. Therapeutic potential of resveratrol: the in vivo evidence. Nat. Rev. Drug Discov. 5, 493-506.

Biondi, D.M., Rocco, C., Ruberto, G., 2003. New dihydrostilbene derivatives from the leaves of *Glycyrrhiza glabra* and evaluation of their antioxidant activity. *J. Nat. Prod. 66,* 447-480.

Boersma, B.J., D'Alessandro, T., Benton, M.R., Kirk, M., Wilson, L.S., Prasain, J., Botting, N.P., Barnes, S., Darley-Usmar, V.M., Patel, R.P., 2003. Neutrophil myeloperoxidase chlorinates and nitrates soy isoflavones and enhances their antioxidant properties. Free Radic. Biol. Med. 35,1417-1430.

Bradamante, S., Barenghi, L., Villa, A., 2004. Cardiovascular protective effects of resveratrol. Cardiovasc. Drug Rev. 22, 169-188.

Brasnyo, P., Molnar, G.A., Mohas, M., Marko, L., Laczy, B., Cseh, J., Mikolas, E., Szijarto, I.A., Merei, A., Halmai, R., Meszaros, L.G., Sumegi, B., Wittmann, I., 2011. Resveratrol improves insulin sensitivity, reduces oxidative stress and activates the Akt pathway in type 2 diabetic patients. Br. J. Nutri. 106, 383-389.

Breen, D.M., Sanli, T., Giacca, A., Tsiani, E., 2008. Stimulation of muscle cell glucose uptake by resveratrol through sirtuins and AMPK. Biochem. Biophys. Res. Commun. 374, 117–122.

Brents, L.K., Medina-Bolivar, F., Seely, K.A., Nair, V., Bratton, S.M., Nopo-Olazabal, L., Patel, R.Y., Liu, H., Doerksen, R.J., Prather, P.L., Radominska-Pandya, A., 2012. Natural prenylated resveratrol analogs arachidin-1 and -3 demonstrate improved glucuronidation profiles and have affinity for cannabinoid receptors. Xenobiotica 42, 139–156.

Burner, U., Furtmuller, P.G., Kettle, A.J., Koppenol, W.H., Obinger, C., 2000. Mechanism of reaction of myeloperoxidase with nitrite. J. Biol. Chem. 275,

20597–20601.

Cai, H., Sale, S., Britton, R.G., Brown, K., Steward, W.P., Gescher, A.J., 2011. Pharmacokinetics in mice and metabolism in murine and human liver fractions of the putative cancer chemopreventive agents 3,4,5,5,7- pentamethoxyflavone and tricin (4,5,7-trihydroxy-3,5-dimethoxyflavone). Cancer Chemother. Pharmacol. 67, 255–263.

Cassidy, A., Hanley, B., Lamuela Raventos, R.M., 2000. Isoflavones, lignans, and stilbenes-origins, metabolism and potential importance to human health. J. Sci. Food Agric. 80, 1044-1062.

Cavallaro, A., Ainis, T., Bottari, C., Fimiani, V., 2003. Effect of resveratrol on some activities of isolated and in whole blood human neutrophils. Physiol. Res. 52, 555–562.

Chan, W.C., Nie, S., 1998. Quantum dot bioconjugates for ultrasensitive nonisotopic detection. Science 281, 2016-2018.

Chang, J.C., Lai, Y.H., Djoko, B., Wu, P.L., Liu, C.D., Liu, Y.W., Chiou, R.Y.Y., 2006. Biosynthesis enhancement and antioxidant and anti-inflammatory activities of peanut

(*Arachis hypogaea* L) arachidin-1, arachidin-3, and isopentadienyl resveratrol. J. Agric. Food Chem. 54, 10281-10287.

Chapple, I.L.C., 1997. Reactive oxygen species and antioxidants in inflammatory diseases. J. Clin. Periodontol. 24, 287–296.

Chen, R.S., Wu, P.L., Chiou, R.Y.Y., 2002. Peanut roots as a source of resveratrol. J. Agric. Food Chem. 50, 1665–1667.

Chen, S., Lu, J.X., Sun, C.D., Ma, H.M., 2010. A highly specific ferrocene-based fluorescent probe for hypochlorous acid and its application to cell imaging. Analyst 135,577-582.

Chen, W.P., Chi, T.C., Chuang, L.M., Su, M.J., 2007. Resveratrol enhances insulin secretion by blocking K_{ATP} and K_V channels of beta cells. Eur. J. Pharmacol. 568, 269–277.

Chen, X.Q., Wang, X.C., Wang, S.J., Shi, W., Wang, K., Ma, H.M., 2008. A highly selective and sensitive fluorescence probe for the hypochlorite anion. Chem-Eur. J. 14, 4719-4724**.**

Chong, J.L., Poutaraud, A., Hugueney, P., 2009. Metabolism and roles of stilbenes in

plants. Plant Sci. 177, 143-155.

Choung, Y.H., Taura, A., Pak, K., Choi, S.J., Masuda, M., Ryan, A.F., 2009. Generation of highly-reactive oxygen species is closely related to hair cell damage in rat organ of corti treated with gentamicin. Neuroscience 161, 214-226.

Cooksey, C.J., Garratt, P.J., Richards, S.E., Strange, R.N., 1988. A dienyl stilbene phytoalexin from *Arachis hypogaea*. Phytochemistry 27, 1015–1016.

D'Archivio, M., Filesi, C., Benedetto, R.D., Gargiulo, R., Giovannini, C., Masella, R., 2007. Polyphenols, dietary sources and bioavailability. Ann. Ist Super. Sanita 43, 348-61.

Das, M., Das, D.K., 2010. Resveratrol and cardiovascular health. Mol. Aspects Med. 31, 503–512.

Day, A.J., DuPont, M.S., Ridley, S., Rhodes, M., Rhodes, M.J.C., Morgan, M.R.A., Williamson, G., 1998. Deglycosylation of flavonoid and isoflavonoid glycosides by human small intestine and liver [beta]-glucosidase activity. FEBS Lett. 436, 71-75.

Demartino, N.G., McGuire, J.M., 1988. The multicatalytic proteinase: a high-Mr endopeptidase. Biochem. J. Lett. 255,750–751.

Djoko, B., Chiou, R.Y.Y., Shee, J.J., Liu, Y.W., 2007. Characterization of immunological activities of peanut stilbenoids, arachidin-1, piceatannol, and resveratrol on lipopolysaccharide-induced inflammation of RAW 264.7 macrophages. J. Agric. Food. Chem. 55, 2376–2383.

Drozdetskaya, E.P., Ilin, K.G., 1972. Polarographic determination of hypochlorite. Zh. Anal. Khim, 27, 200-202.

Feng, S.B., Saw, C.L., Lee, Y.K., Huang, D.J., 2007. Fungal-stressed germination of black soybeans leads to generation of oxooctadecadienoic acids in addition to glyceollins. J. Agric. Food. Chem. 55, 8589-8595.

Feng, S.B., Saw, C.L., Lee, Y.K., Huang, D.J., 2008. Novel process of fermenting black soybean [Glycine max (L.) Merrill] yogurt with dramatically reduced flatulence-causing oligosaccharides but enriched soy phytoalexins. J. Agric. Food. Chem. 56, 10078-10084.

Floyd, Z., Wang, Z., Kilroy, G., Cefalu, W., 2008. Modulation of peroxisome proliferator-activated receptor gamma stability and transcriptional activity in adipocytes by resveratrol. Metabolism 57, S32-S38.

Fujimoto, S., Kawakami, N., Ohara, N., 1993. Formation of hydroxyl radical by the

myeloperoxidase NADH system. Biol. Pharm. Bull. 16, 525-528.

Furtmuller, P.G., Burner, U., Regelsberger, G., Obinger, C., 2000. Spectral and kinetic studies on the formation of eosinophil peroxidase compound I and its reaction with halides and thiocyanate. Biochemistry 39,15578–15584.

Gaudreault, N., Scriven, D.R., Laher, L., Moore, E.D., 2008. Subcellular characterization of glucose uptake in coronary endothelial cells. Microvasc. Res.75,73–82.

Ge, H. M., Yang, W. H., Zhang, J., Tan, R. X., 2009. Antioxidant oligostilbenoids from the stem wood of *Hopea hainanensis.* J. Agric. Food Chem. 57, 5756-5761.

Ghanim, H., Sia, C.L., Korzeniewski, K., Lohano, T., Abuaysheh, S., Marumganti, A., Chaudhuri, A., Dandona, P., 2011. A resveratrol and polyphenol preparation suppresses oxidative and inflammatory stress response to a high-fat, high-carbohydrate meal. J. Clin. Endocrinol. Metab. 96, 1409-1414.

Giovinazzo, G., Ingrosso, I., Paradiso, A., De Gara, L., Santino, A., 2012. Resveratrol biosynthesis: Plant metabolic engineering for nutritional improvement of food. Plant Foods Hum. Nutr. 67,191–199.

Halliwell, B., Zhao, K., Whiteman, M., 2000. The gastrointestinal tract: a major site of antioxidant action? Free Radic. Res. 33, 819-30.

Harikumar, K.B., Aggarwal, B.B., 2008. Resveratrol: a multitargeted agent for age-associated chronic diseases. Cell Cycle 7, 1020–1035

Hassanein, M., Weidow, B., Koehler, E., Bakane, N., Garbett, S., Shyr, Y., Quaranta, V., 2010. Development of high-throughput quantitative assays for glucose uptake in cancer cell lines. Mol. Imaging Biol. 13, 840-852.

Hay, K.X., Waisundara, V.Y., Zong, Y., Han, M.Y., Huang, D.J., 2007. CdSe nanocrystals as hydroperoxide scavengers: A new approach to highly sensitive quantification of lipid hydroperoxides.Small 3, 290–293.

Henderson, L.M., Chappell, J.B., 1993. Dihydrorhodamine 123: a fluorescent probe for superoxide generation? Eur. J. Biochem. 217, 973–980.

Hoshino, J., Park E.J., Kondratyuk T.P., Marler L., Pezzuto J.M., van Breemen R.B., Mo S., Li Y., Cushman M., 2010. Selective synthesis and biological evaluation of sulfate-conjugated resveratrol metabolites. J. Med. Chem. 53,5033‐5043.

Huang, C.P., Au, L.C., Chiou, R.Y.Y., Chung, P.C., Chen, S.Y., Tang, W.C., Chang,

C.L., Fang, W.H., Lin, S.B., 2010. Arachidin-1, a peanut stilbenoid, induces programmed cell death in human leukemia HL-60 cells. J. Agric. Food Chem. 58, 12123–12129.

Hung, H.Y., Qian, K., Morris-Natschke, S.L., Hsu, C.S., Lee, K.H., 2012. Recent discovery of plant-derived anti-diabetic natural products. Nat. Prod. Rep. 29, 580-606.

Ingham, J. L., 1976. 3,5,4′-Trihydroxystilbene as a phytoalexin from groundnuts (*Arachis hypogaea*). Phytochemistry 15, 1791–1793.

Ito, T., Akao, Y., Yi, H., Ohguchi, K., Matsumoto, K., Tanaka, T., Iinuma, M., Nozawa, Y., 2003. Antitumor effect of resveratrol oligomers against human cancer cell lines and the molecular mechanisms of apoptosis induced by vaticanol C. Carsinogenesis 24,1489–1497.

Ito, T., Endo, H., Oyama, M., Iinuma, M., 2012. Novel isolation of stilbenoids with enantiomeric and meso forms from a cyperus rhizome. Phytochem. Let. 5, 267-270.

Jerlich, A., Fritz, G., Kharrazi, H., Hammel, M., Tschabuschnig, S., Glatter, O., Schaur, R.J., 2000. Comparison of HClO traps with myeloperoxidase inhibitors in prevention of low density lipoprotein oxidation. Biochim. Biophys. Acta 1481, 109–118.

Jiang, H., Ju, H.X., 2007. Electrochemiluminescence sensors for scavengers of hydroxyl radical based on its annihilation in CdSe quantum dots film/peroxide system. Anal. Chem. 79, 6690-6696.

Kaouadji, M., Agban, A., Mariotte, A.M., 1986. Lonchocarpene, a stilbene, and lonchocarpusone, an isoflavane-2 new pyranopolyphenols from Lonchocarpus nicou roots. J.Nat.Prod. 49, 281-285.

Keen, N.T., Ingham, J.L., 1976. New stilbene phytoalexins from American cultivars of *Arachis hypogaea*. Phytochemistry 15, 1794 –1795.

Kennedy, D.O., Wightman, E.L., Reay, J.L., Lietz, G., Okello, E.J., Wilde, A., Haskell, C.F., 2010. Effects of resveratrol on cerebral blood flow variables and cognitive performance in humans: a double-blind, placebo-controlled, crossover investigation. Am. J. Clin. Nutr. 91, 1590-1597.

Kersten, S., Desvergne, B., Wahli, W., 2000. Roles of PPARs in health and disease. Nature 405, 421-424.

Kettle, A.J., Winterbourn, C.C., 1994. Assays for the chlorination activity of myeloperoxidase. Methods Enzymol. 233, 502– 512.

Kettle, A.J., Winterbourn, C.C., 1997. Myeloperoxidase: a key regulator of neutrophil oxidant production. Redox Rep. 3, 3 – 15.

Kettle, A.J., Chan, T., Osberg, I., Senthilmohan, R., Chapman, A.L.P., Mocatta, T.J., Wagener, J.S., 2004. Myeloperoxidase and protein oxidation in the airways of young children with cystic fibrosis. Am. J. Respir. Crit. Care. Med. 170, 1317-1323.

Kim, J.S., Lee, S.Y., Park, S.U., 2008a. Resveratrol production in hairy root culture of peanut, *Arachis hypogaea L.* transformed with different *Agrobacterium rhizogenes* strains. Afr. J. Biotechnol. 7, 3788–3790.

Kim, Y.H., Kwon, H.S., Kim, D.H., Cho, H.J., Lee, H.S., Jun, J.G., Park, J.H., Kim, J.K., 2008b. Piceatannol, a stilbene present in grapes, attenuates dextran sulfate sodium-induced colitis. Int. Immunopharmacol. 8, 1695–1702.

Kim, S.H., Park, H.S., Lee, M.S., Cho, Y.J., Kim, Y.S., Hwang, J.T., Sung, M.J., Kim, M.S., Kwon, D.Y., 2008c. Vitisin A inhibits adipocyte differentiation through cell cycle arrest in 3T3-L1cells. Biochem. Biophys. Res. Commun. 372, 108–113.

Kizselv, K.V., Shumakova, O.A., Manyakhin, A.Y., 2013. Effect of plant precursors on the biosynthesis of resveratrol in *Vitis amurensis* rupr. cell cultures. Appl. Biochem. Micro. 49, 53-58.

Klebanoff, S.J., 1999. Myeloperoxidase. Proc. Assoc. Amer. Phys.111,383-389.

Knauft, D.A., Gorbet, D.W., 1989. Genetic diversity among peanut cultivars. Crop Sci. 29,1417–1422.

Kohnen, S., Franck, T., Van Antwerpen, P., Zouaoui Boudjeltia, K., Mouithys-Mickalad, A., Deby, C., Moguilevsky, N., Deby-Dupont, G., Lamy, M., Serteyn, D., 2007. Resveratrol inhibits the activity of equine neutrophil myeloperoxidase by a direct interaction with the enzyme. *J. Agric. Food Chem.* 55, 8080–8087.

Ku, K.L., Chang, P.S., Cheng, Y.C., Lien, C.Y., 2005. Production of stilbenoids from the callus of *Arachis hypogaea:* a novel source of the anticancer compound piceatannol. J. Agric. Food Chem. 53, 3877–3881.

Kwon, J.Y., Seo, S.G., Heo, Y.S., Yue, S., Cheng, J.X., Lee, K.W., 2012. Piceatannol, natural polyphenolic stilbene, inhibits adipogenesis via modulation of mitotic clonal expansion and insulin receptor-dependent insulin signaling in early phase of differentiation. J. Biol. Chem. 287, 11566-11578.

Lam, S.H., Chen, J.M., Kang, C.J., Chen, C.H., Lee, S.S., 2008. α-glucosidase inhibitors from the seeds of *Syagrus romanzoffiana*. Phytochemistry 69,1173–1178.

Lappano, R., Rosano, C., Madeo, A., Albanito, L., Plastina, P., Gabriele, B., Forti, L., Stivala, L.A., Iacopetta, D., Dolce, V., Ando, S., Pezzi, V., Maggiolini, M., 2009. Structure-activity relationships of resveratrol and derivatives in breast cancer cells. Mol. Nutr. Food Res. 53, 845–858.

Li, D.W., Qin, L.X., Li, Y., Nia, R.P., Long, Y.T., Chen, H.Y., 2011. CdSe/ZnS quantum dot-Cytochrome c bioconjugates for selective intracellular $O^{2\cdot-}$ sensing. Chem. Commun. 47, 8539-8541.

Li, J.J., Zhu, J.J., 2013. Quantum dots for fluorescent biosensing and bio-imaing applications. Analyst 138, 2506-2515.

Lin, W.Y., Long, L.L., Chen, B.B., Tan, W., 2009. A ratiometric fluorescent probe for hypochlorite based on a deoximation reaction. Chem. Eur. J. 15, 2305-2309.

Lloyd, P.G., Hardin, C.D., Sturek, M., 1999. Examining glucose transport in single vascular smooth muscle cells with a fluorescent glucose analog. Physiol. Res. 48, 401–410.

Loaiza, A., Porras, O.H., Barros, L.F., 2003. Glutamate triggers rapid glucose transport stimulation in astrocytes as evidenced by real-time confocal microscopy. J. Neurosci. 23, 7337–7342.

Lopes, R.M., Agostini-Costa, T.D., Gimenes, M.A., Silveira, D., 2011. Chemical composition and biological activities of arachis species. J. Agric. Food Chem. 59, 4321-4330.

Macickova, T., Pecivova, J., Harmatha, J., Svitekova, K., Nosal, R., 2012. Effect of stilbene derivative on superoxide generation and enzyme release from human neutrophils *in vitro*. Interdiscip. Toxicol. 5, 71–75.

Maldonado, P.D., Rivero-Cruz, I., Mata, R., Pedraza-Chaverr ́ı J., 2005. Antioxidant activity of A-type proanthocyanidins from *Geranium niveum* (*Geraniaceae*). J. Agric. Food Chem. 53,1996-2001

Malle, E., Buch, T.,Grone, H.J., 2003. Myeloperoxidase in kidney disease. Kidney Int. 64,1956-1967.

Malle, E., Furtmuller, P.G., Sattler, W., Obinger, C., 2007. Myeloperoxidase: a target for new drug development? Br. J. Pharmacol. 152,838–854.

Mancini, M.C., Kairdolf, B.A., Smith, A.M., Nie, S., 2008. Oxidative quenching and degradation of polymer-encapsulated quantum dots: new insights into the long-term fate and toxicity of nanocrystals in vivo. J. Am. Chem. Soc.130, 10836-10837.

Matsuoka, A., Takeshita, K., Furuta, A., Ozaki, M., Fukuhara, K., Miyata, N., 2002. The 4′-hydroxy group is responsible for the in vitro cytogenetic activity of resveratrol. Mutat. Res. 521, 29–35.

Medina-Bolivar, F., Condori, J., Rimando, A.M., Hubstenberger, J., Shelton, K., O'Keefe, S.F., Bennett, S., Dolan, M.C., 2007. Production and secretion of resveratrol in hairy root cultures of peanut. Phytochemistry 68, 1992–2003.

Milne, J.C., Lambert, P.D., Schenk, S., Carney, D.P., Smith, J.J., Gagne, D.J., Jin, L., Boss, O., Perni, R.B., Vu, C.B., Bemis, J.E., Xie, R., Disch, J.S., Ng, P.Y., Nunes, J.J., Lynch, A.V., Yang, H., Galonek, H., Israelian, K., Choy, W., Iffland, A., Lavu, S., Medvedik, O., Sinclair, D.A., Olefsky, J.M., Jirousek, M.R., Elliott P.J., Westphal, C.H., 2007. Small molecule activators of SIRT1 as therapeutics for the treatment of type 2 diabetes. Nature 450,712-716.

Minakawa, M., Miura, Y., Yagasaki, K., 2012. Piceatannol, a resveratrol derivative, promotes glucose uptake through glucose transporter 4 translocation to plasma membrane in L6 myocytes and suppresses blood glucose levels in type 2 diabetic

model db/db mice. Biochem. Biophys. Res. Commun. 422, 469-475.

Na, M., Hoang, D.M., Njamen, D., Mbafor, J.T., Fomum, Z.T., Thuong, P.T., Ahn, J.S., Oh, W.K., 2007. Inhibitory effect of 2-arylbenzofurans from *Erythrina addisoniae* on protein tyrosine phosphatase-1B. Bioorg. Med. Chem. Lett. 17, 3868-3871.

Natal, C., Modol, T., Osés-Prieto, J.A., López-Moratalla, N., Iraburu, M.J., López-Zabalza, M.J., 2008. Specific protein nitration in nitric oxide-induced apoptosis of human monocytes. Apoptosis 13,1356–1367.

Neves, A.R., Lucio, M., Lima, J.L., Reis, S., 2012. Resveratrol in medicinal chemistry: a critical review of its pharmacokinetics, drug-delivery, and membrane interactions. Curr. Med. Chem. 19, 1663-1681.

Nugent, C., Prins, J.B., Whitehead, J.P., Savage, D., Wentworth, J.M., Chatterjee, V.K., Rahilly, S., 2001. Potentiation of glucose uptake in 3T3-L1 adipocytes by PPARγ agonists is maintained in cells expressing a PPARγ dominant-negative mutant: evidence for selectivity in the downstream responses to PPARγ activation. Mol. Endocrinol. 15,1729-1738.

Park, B.H., Lee, H.J., Lee, Y.R., 2011. Total synthesis of Chiricanine A, arahypin-1,

trans-arachidin-2, trans-arachidin-3, and arahypin-5 from peanut seeds. J. Nat. Prod. 74, 644-649.

Pattison, D.I., Davies, M.J., 2006. Reactions of myeloperoxidase-derived oxidants with biological substrates: Gaining chemical insight into human inflammatory diseases. Curr. Med. Chem. 13, 3271 – 3290.

Peskin, A.V., Winterbourn, C.C., 2001. Kinetics of the reactions of hypochlorous acid and amino acid chloramines with thiols, methionine, and ascorbate. Free Radic. Biol. Med. 30, 572–579.

Pont, V., Pezet, R., 1990. Relation between the chemical structure and the biological activity of hydroxystilbenes against *Botrytis cinerea*. J. Phytopathol. 130, 1–8.

Porras, O.H., Loaiza, A., Barros, L.F., 2004. Glutamate mediates acute glucose transport inhibition in hippocampal neurons. J. Neurosci. 24, 9669–9673.

Ren, J.G., Xia, H.L., Just, T., Dai, Y.R., 2001. Hydroxyl radical-induced apoptosis in human tumor cells is associated with telomere shortening but not telomerase inhibition and caspase activation. FEBS Lett. 488, 123–132.

Reuter, S., Gupta, S.C., Chaturvedi, M.M., Aggarwal, B.B., 2010. Oxidative stress,

inflammation, and cancer: how are they linked? Free Radic. Biol. Med. 49, 1603-1616.

Riviere, C., Pawlus, A.D., Merillon, J.M., 2012. Natural stilbenoids: distribution in the plant kingdom and chemotaxonomic interest in Vitaceae. Nat. Prod. Rep. 29, 1317-1333.

Rovera, G., Santoli, D., and Damsky, C., 1979. Human promyelocytic leukemia cells in culture differentiate into macrophage-like cells when treated with a phorbol diester. Proc. Natl. Acad. Sci. 76, 2779-2784.

Sanders, T.H., McMichael, R.W., Hendrix, K.W., 2000. Occurrence of resveratrol in edible peanuts. J. Agric. Food Chem. 48, 1243–1246.

Santos, N.A., Bezerra, C.S., Martins, N.M., Curti, C., Bianchi, M.L,, Santos, A.C. 2008. Hydroxyl radical scavenger ameliorates cisplatin-induced nephrotoxicity by preventing oxidative stress, redox state unbalance, impairment of energetic metabolism and apoptosis in rat kidney mitochondria. Cancer Chemother. Pharmacol. 61,145–155.

Schultz, T.P., Cheng, Q., Boldin, W.D., Hubbard, T.F., Jin, L., Fisher, T.H., Nicholas,

D.D., 1991. Comparison of the fungicidal activities of (E)-4-hydroxylated stilbenes and related bibenzyls. Phytochemistry 30, 2939–2945.

Schultz, T.P., Boldin, W.D., Fisher, T.H., Nicholas, D.D., McMurtrey, K.D., Pobanz, K., 1992. Structure-fungicidal properties of some 3- and 4-hydroxylated stilbenes and bibenzyl analogues. Phytochemistry 31, 3801–3806.

Schultz, T.P., Nicholas, D.D., Fisher, T.H., 1997. Quantitative structure-activity relationships of stilbenes and related derivatives against wood-destroying fungi. Recent Res. Dev. Agric. Food Chem.1, 289–299.

Setsukinai, K., Urano, Y., Kakinuma, K., Majima, H.J., Nagano, T., 2003. Development of novel fluorescence probes that can reliably detect reactive oxygen species and distinguish specific species. J. Biol. Chem. 278, 3170–3175.

Shen, T., Wang, X.N., Lou, H.X., 2009. Natural stilbenes: an overview. Natural Prod. Rep. 26, 916–935.

Shi, J., Li, Q.Q., Zhang, X., Peng, M., Qin, J.G., Li, Z., 2010. Simple triphenylamine-based luminophore as a hypochlorite chemosensor. Sensor Actuat. B-Chem. 145, 583-587.

Silva, A. A., Haraguchi, S. K., Cellet, T. S. P., Schuquel, I. T. A., Sarragiotto, M. H., Vidotti, G. J., de Melo, J. O., Bersani-Amado, C. A., Zanoli, K., Nakamura, C.V., 2012. Resveratrol-derived stilbenoids and biological activity evaluation of seed extracts of Cenchrus echinatus L. Natural Product Research 26, 865-868.

Sobolev, V.S., Cole, R.J., Dorner, J.W., Yagen, B., 1995. Isolation, purification, and liquid chromatographic determination of stilbene phytoalexins in peanuts. J. AOAC Int. 78, 1177–1182.

Sobolev, V.S., Deyrup, S.T., Gloer, J.B., 2006a. New peanut (*Arachis hypogaea*) phytoalexin with prenylated benzenoid and but-2-enolide moieties. J. Agric. Food Chem. 54, 2111–2115.

Sobolev, V.S., Potter, T.L., Horn, B.W., 2006b. Prenylated stilbenes from peanut root mucilage. Phytochem. Anal. 17, 312-322.

Sobolev, V.S., Guo, B.Z., Holbrook, C.C., Lynch, R.E., 2007. Interrelationship of phytoalexin production and disease resistance in selected peanut genotypes. J. Agric. Food Chem. 55, 2195–2200.

Sobolev, V.S., 2008. Localized production of phytoalexins by peanut (*Arachis hypogaea*) kernels in response to invasion by *Aspergillus* species. J. Agric. Food

Chem. 56, 1949–1954.

Sobolev, V.S., Neff, S.A., Gloer, J.B., 2009. New stilbenoids from peanut (*Arachis hypogaea*) seeds challenged by an *Aspergillus caelatus* strain. J. Agric. Food Chem. 57, 62–68.

Sobolev, V.S., Neff, S.A., Gloer, J.B., 2010. New dimeric stilbenoids from fungal-challenged peanut (*Arachis hypogaea*) seeds. J. Agric. Food Chem. 58, 875–881.

Sobolev, V.S., Khan, S.I., Tabanca, N., Wedge, D.E., Manly, S.P., Cutler, S.J., Coy, M.R., Becnel, J.J., Neff, S.A., Gloer, J.B., 2011. Biological activity of peanut (*Arachis hypogaea*) phytoalexins and selected natural and synthetic stilbenoids. J. Agric. Food Chem. 59, 1673–1682.

Staels, B., Fruchart, J.C., 2005. Therapeutic roles of peroxisome proliferator-activated receptor agonist. Diabetes 54, 2460–2470.

Sun, A.Y., Simonyi, A., Sun, G.Y., 2002. The ‘‘French Paradox’’ and beyond: neuroprotective effects of polyphenols. Free Radic. Biol. Med. 32, 314–318.

Szekeres, T., Saiko, P., Fritzer-Szekeres, M., Djavan, B., Jäger, W., 2011.

Chemopreventive effects of resveratrol and resveratrol derivatives. Ann. NY. Acad. Sci. 1215, 89 – 95.

Szkudelska, K., Szkudelski, T., 2010. Resveratrol, obesity, and diabetes. Eur. J. Pharmacol. 635, 1-8.

Takamatsu, S., Galal, A.M., Ross, S.A., Ferreira, D., ElSohly, M.A., Ibrahim, A.S. EI-Feraly, F.S., 2003. Antioxidant effect of flavanoids on DCF production in HL-60 cells. Phytother. Res. 17, 963-966.

Taylor, E.L., Li, J.T., Tupper, J.C., Rossi, A.G., Winn, R.K., Harlan, J.M., 2007. GEA 3162, a peroxynitrite donor, induces Bcl-2-sensitive, p53-independent apoptosis in murine bone marrow cells. Biochem. Pharmacol. 74,1039–1049.

Teufelhofer, O., Weiss, R.M., Parzefall, W., Schulte-Hermann, R., Micksche, M., Berger, W., Elbling, L., 2003. Promyelocytic HL60 cells express NADPH oxidase and are excellent targets in a rapid spectrophotometric microplate assay for extracellular superoxide. Toxicol. Sci. 76, 376–383.

Thomas, E.L., Grisham, M.B., Jefferson, M.M., 1986. Preparation and characterization of chloramines. Methods Enzymol. 132, 569–585.

Tokusoglu, O., Unal, M.K., Yemis, F., 2005. Determination of the phytoalexin resveratrol (3,5,40-trihydroxystilbene) in peanuts and pistachios by high-performance liquid chromatographic diode array (HPLC-DAD) and gas chromatography-mass spectrometry (GCMS). J. Agric. Food Chem. 53, 5003–5009.

van der Veen, B.S., de Winther, M.P.J., Heeringa, P., 2009. Myeloperoxidase: molecular mechanisms of action and their relevance to human health and disease. Antioxid. Redox Signal 11, 2899-2937.

Vermaak, I., Viljoen, A.M., Hamman, J.H., 2011. Natural products in anti-obesity therapy. Nat. Prod. Rep. 28, 1493-1533.

Wagner, B.A., Buettner, G.R., Oberley, L.W., Darby, C.J., Burns, P.C., 2000. Myeloperoxidase is involved in H_2O_2-induced apoptosis of HL-60 human leukemia cells. J. Biol. Chem. 275, 22461-22469.

Walle, T., Hsieh, F., DeLegge, M.H., Oatis, J.E.Jr., Walle, U.K., 2004. High absorption but very low bioavailibity of oral resveratrol in humans. Drug Metab. Dispos. 32, 1377-1382.

Wan, X., Wang, X.B., Yang, M.H., Wang, J.S., Kong, L.Y., 2011. Dimerization of piceatannol by *Momordica charantia* peroxidase and α-glucosidase inhibitory activity of the biotransformation products. Bioorgan. Med. Chem. 19, 5085-5092.

Wang, H., Joseph, J.A., 1999. Quantifying cellular oxidative stress by dichlorofluorescein assay using microplate reader. Free Radic. Biol. Med. 27, 612–616.

Wang, S.H., Han, M.Y., Huang, D.J., 2009. Nitric Oxide Switches on the Photoluminescence of Molecularly Engineered Quantum Dots. J. Am. Chem. Soc. 131, 11692-11694.

Warner, D.S., Sheng, H., Batinic ́-Haberle, I., 2004. Oxidants, antioxidants and the ischemic brain. J. Exp. Biol. 207, 3221–3231.

Wasil, M., Halliwell, B., Grootveld, M., Moorhouse, C. P., Hutchison, D. C., Baum, H., 1987.The specificity of thiourea, dimethylthiourea and dimethyl sulphoxide as scavengers of hydroxyl radicals. Their protection of alpha 1-antiproteinase against inactivation by hypochlorous acid. Biochem. J. 243,867–870.

Weiss, S.J., Klein, R., Slivka, A., Wei, M., 1982. Chlorination of taurine by human neutrophils. Evidence for hypochlorous acid generation. J. Clin. Invest. 70, 598–607.

Winnik, F.M., Maysinger, D., 2013. Quantum dot cytotoxicity and ways to reduce it. Accounts Chem. Res. 46, 672-680.

Wenzel, E., Somoza, V., 2005. Metabolism and bioavailability of *trans*-resveratrol. Mol. Nutr. Food Res. 49, 472-481.

Winterbourn, C.C., 1985. Comparative reactivities of various biological compounds with myeloperoxidase-hydrogen peroxide-chloride, and similarity of the oxidant to hypochlorite. Biochim. Biophys. Acta 840, 204–210.

Wiseman, H., Halliwell, B., 1996. Damage to DNA by reactive oxygen and nitrogen species role in inflammatory disease and progression to cancer. Biochem. J. 313,17–29.

Wu, Z.Y., Song, L.X., Huang, D.J., 2011. Food grade fungal stress on germinating peanut seeds induced phytoalexins and enhanced polyphenolic antioxidants. J. Agric. Food Chem. 59, 5993-6003.

Yamada, K., Saito, M., Matsuoka, H., Inagaki, N., 2007. A real-time method of imaging glucose uptake in single, living mammalian cells. Nat. Protoc. 2, 753–762.

Yang, Y.K., Cho, H.J., Lee, J., Shin, I., Tae, J., 2009. A Rhodamine-hydroxamic

acid-based fluorescent probe for hypochlorous acid and its applications to biological imagings. Org. Lett.11,859–861.

Yoshioka, K., Saito, M., Oh, K.B., Nemoto, Y., Matsuoka, H., Natsume, M., Abe, H., 1996. Intracellular fate of 2-NBDG, a fluorescent probe for glucose uptake activity, in *Escherichia coli* cells. Biosci. Biotechnol. Biochem. 60, 1899–1901.

Zhang, M., Chen, M., Zhang, H.Q., Sun, S., Xia, B., Wu, F.H., 2009. In vivo hypoglycemic effects of phenolics from the root bark of *Morus alba*. Fitoterapia 80, 475–477.

Zhang, Y., He, J., Wang, P.N., Chen, J.Y., Lu, Z.J., Lu, D.R., Guo, J., Wang, C.C., Yang, W.L., 2006. Time-dependent photoluminescence blue shift of the quantum dots in living cells: effect of oxidation by singlet oxygen. J. Am. Chem. Soc. 128, 13396–13401.

Zou, C.,Wang, Y., Shen, Z., 2005. 2-NBDG as a fluorescent indicator for direct glucose uptake measurement. J. Biochem. Biophys. Methods 64, 207–215.

List of Publications and Presentations

1. Liu, Z.W., Wu, J.E., Huang, D.J., 2013. New arahypins isolated from fungal-challenged peanut seeds and their glucose uptake-stimulatory activity in 3T3-L1 adipocytes. Phytochem. Lett. 6, 123-127.

2. Liu, Z.W., Wu, J.E., Huang, D.J., 2013. New stilbenoids isolated from fungus-challenged black skin peanut seeds and their adipogenesis inhibitory activity in 3T3-L1 cells. J. Agric. Food Chem. 61, 4155-4161.

3. Yan, Y., Wang, S.H., Liu, Z.W., Wang, H.Y., Huang, D.J., 2010. The CdSe-ZnS Quantum Dots for selective and sensitive detection and quantification of hypochlorite. Anal. Chem. 82, 9775-9978.

4. Liu, Z.W., Yan, Y., Wang, S.H., Ong, W.Y., Huang, D.J., 2013. Assaying myeloperoxidase inhibitors and hypochlorous acid scavengers in HL60 cell line using quantum dots as the luminescent probe. Am. J. Biomed. Sci. 5, 140-153.

5. Liu, Z.W., Wu, Z.Y., Wu, J.E., Huang, D.J., 2012. Stilbene derivatives from the fungi-stressed peanut seeds and their bioactivities in 3T3-L1 adipocytes. Poster presentation at the 16th IUFoST World Congress of Food Science and Technology held in Foz do Iguacu, Parana State, Brazil on August 5-9, 2012.

Appendices

A.1 LC-MS chromatogram of (A) fungi stressed India peanut pieces (B) unstressed India peanut pieces (C) India peanut pieces without treatments.

A.2 LC-MS chromatogram and UV spectra of (A) SB-1; (B) arachidin-1; (C) arachidin-3 in mobile phase.

A.3 HR-MS of (A) arahypin-8; (B) arahypin-9; (C) arahypin-10; (D) MIP; (E) arahypin-11; (F) arahypin-12.

A.4 1D and 2D NMR data of (A) arahypin-8

A.5 1D and 2D NMR data of (B) arahypin-9

A.6 1D and 2D NMR data of (C) arahypin-10

A.7 1D and 2D NMR data of (D) MIP

A.8 1D and 2D NMR data of (E) arahypin-11

A.9 1D and 2D NMR data of (E) arahypin-12

A.1 LC-MS chromatogram of (A) fungi stressed India peanut pieces (B) unstressed India peanut pieces (C) India peanut pieces without treatments.

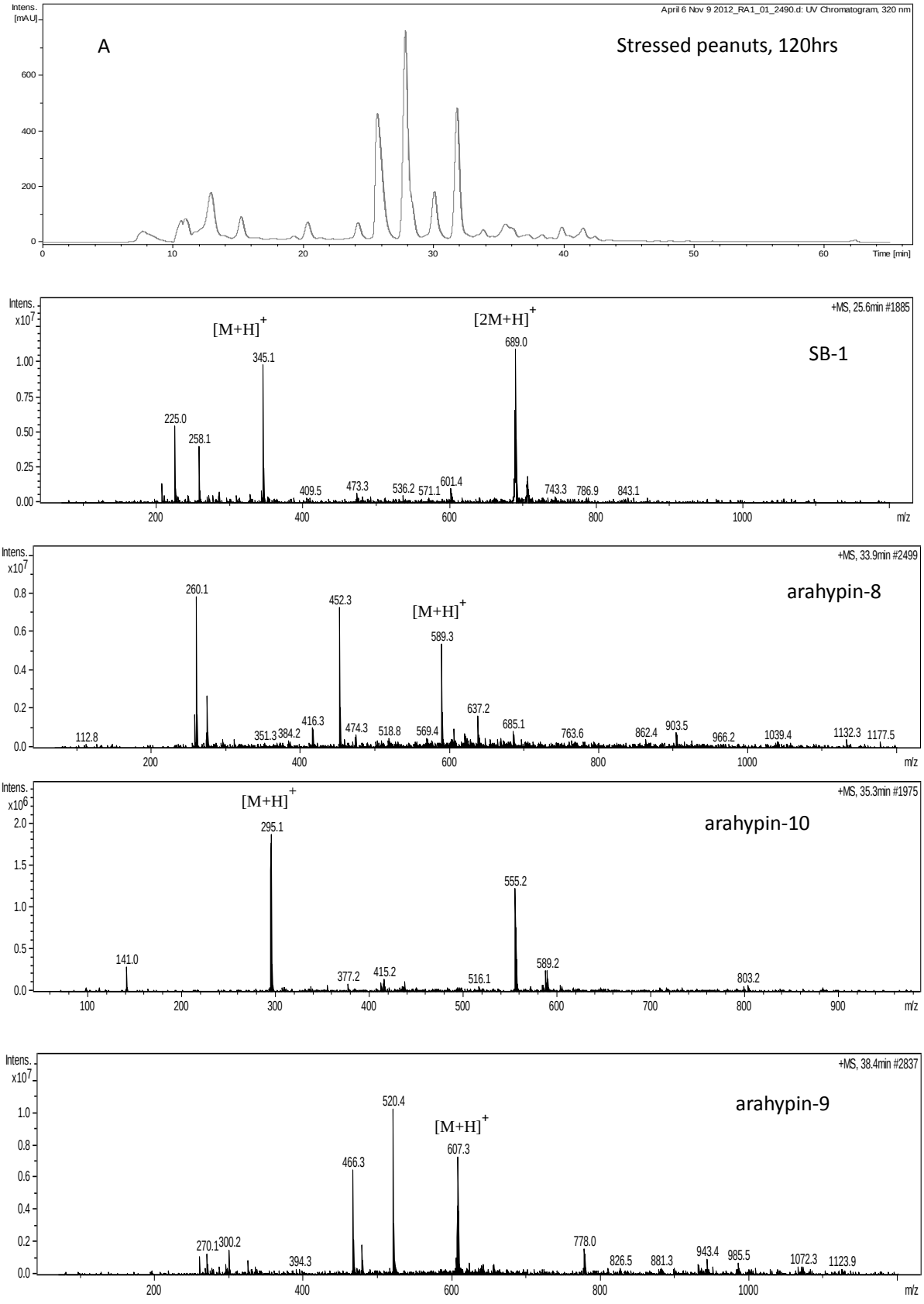

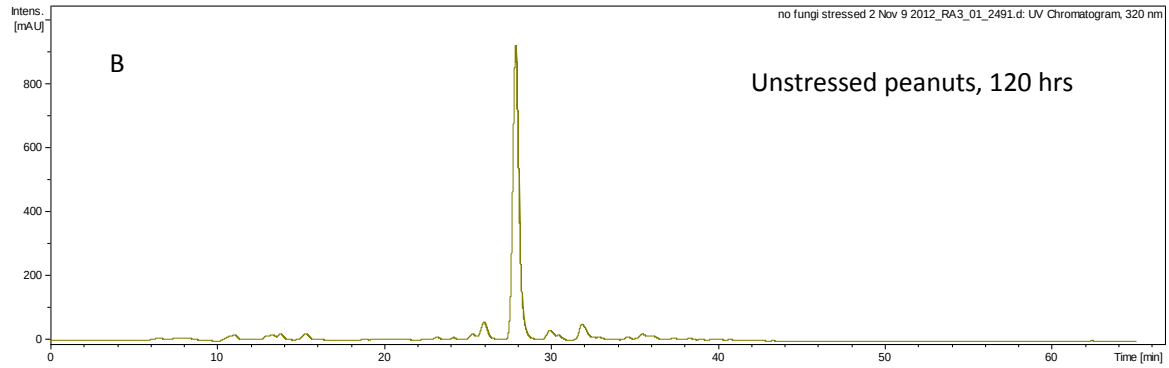
B
Unstressed peanuts, 120 hrs
no fungi stressed 2 Nov 9 2012_RA3_01_2491.d: UV Chromatogram, 320 nm
Intens. [mAU]
Time [min]

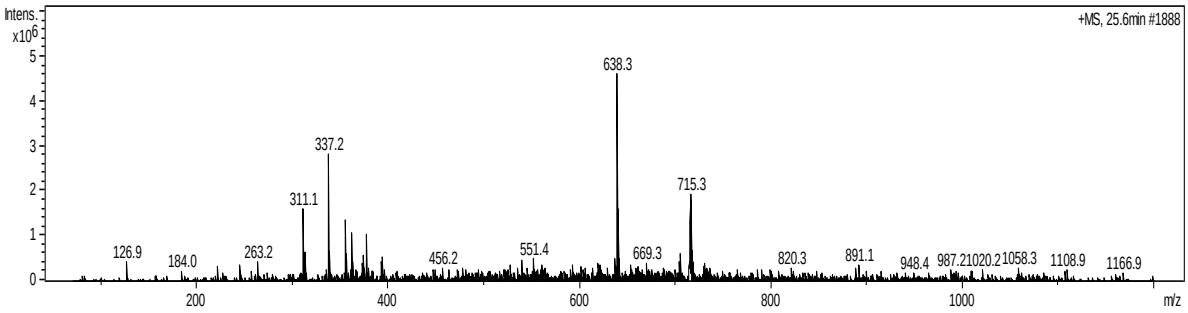
+MS, 25.6min #1888
Intens. x10^6
638.3
337.2
311.1
715.3
126.9
184.0
263.2
456.2
551.4
669.3
820.3
891.1
948.4
987.2
1020.2
1058.3
1108.9
1166.9
m/z

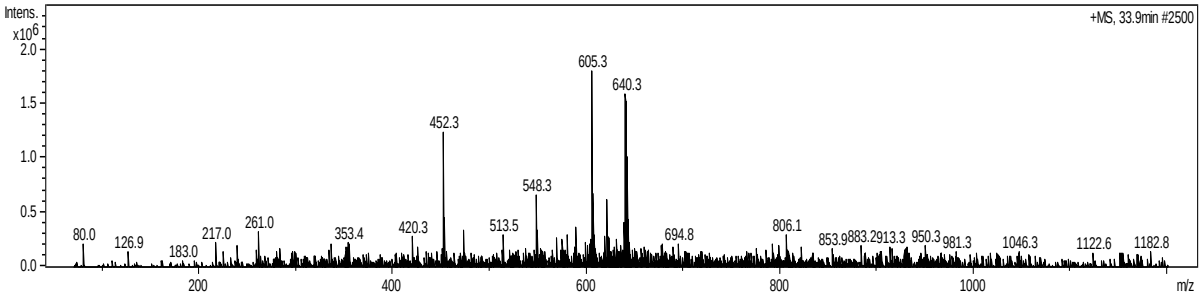
+MS, 33.9min #2500
Intens. x10^6
605.3
640.3
452.3
548.3
80.0
126.9
183.0
217.0
261.0
353.4
420.3
513.5
694.8
806.1
853.9
883.2
913.3
950.3
981.3
1046.3
1122.6
1182.8
m/z

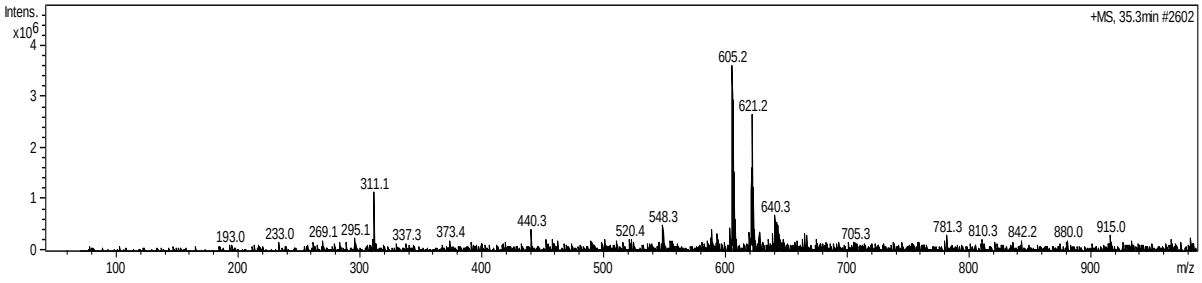
+MS, 35.3min #2602
Intens. x10^6
605.2
621.2
311.1
640.3
193.0
233.0
269.1
295.1
337.3
373.4
440.3
520.4
548.3
705.3
781.3
810.3
842.2
880.0
915.0
m/z

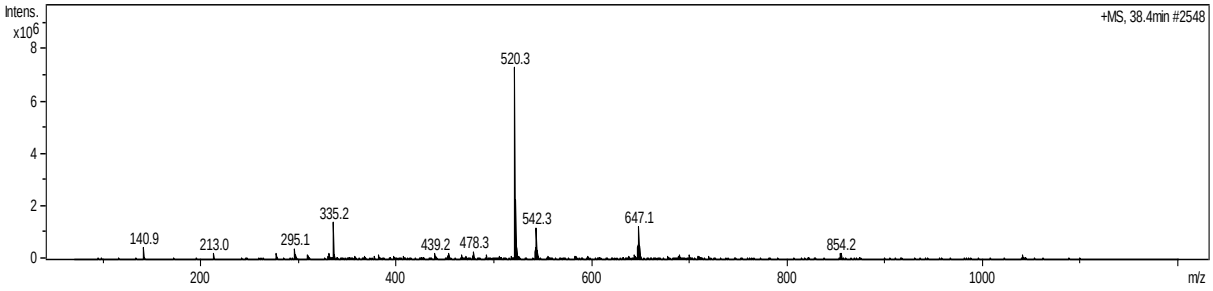
+MS, 38.4min #2548
Intens. x10^6
520.3
335.2
542.3
647.1
140.9
213.0
295.1
439.2
478.3
854.2
m/z

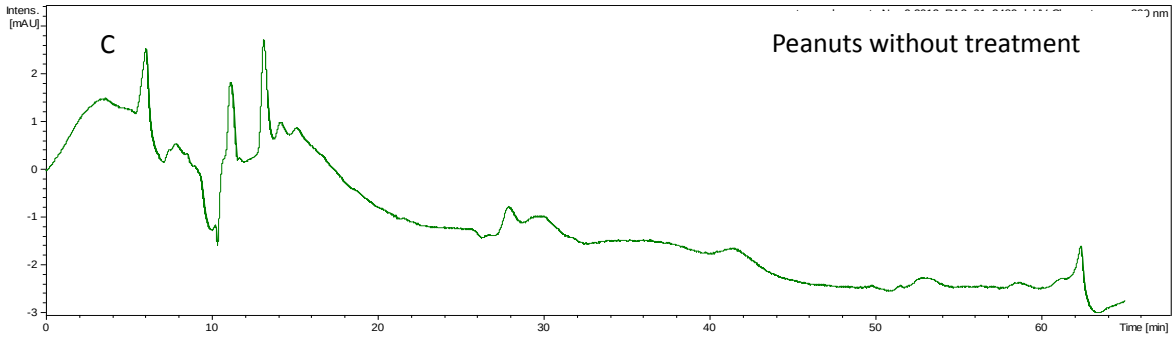
C
Peanuts without treatment
Intens.
[mAU]
Time [min]

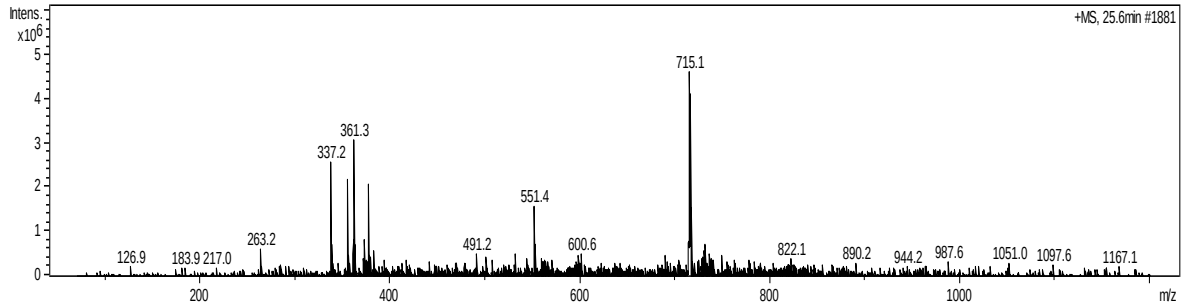
+MS, 25.6min #1881
Intens.
x10^6
715.1
361.3
337.2
551.4
263.2
491.2
600.6
822.1
890.2
944.2
987.6
1051.0
1097.6
1167.1
126.9
183.9
217.0
m/z

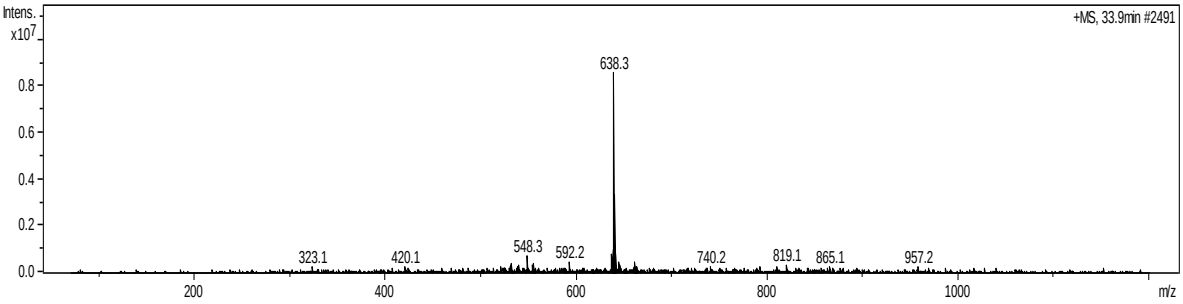
+MS, 33.9min #2491
Intens.
x10^7
638.3
323.1
420.1
548.3
592.2
740.2
819.1
865.1
957.2
m/z

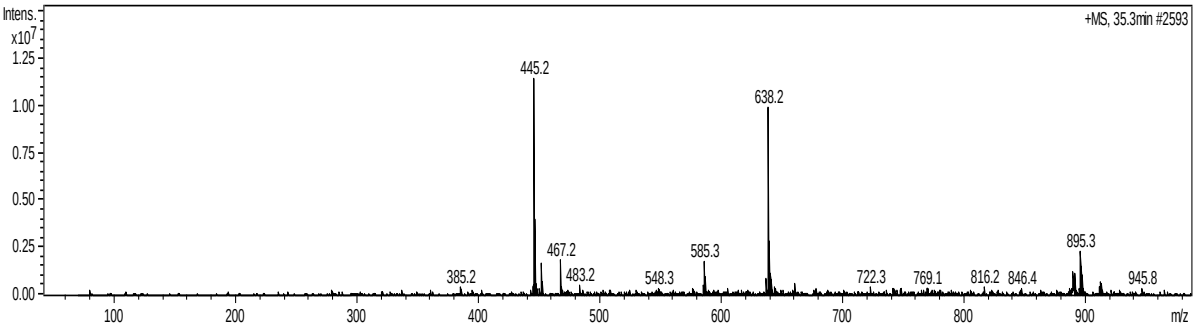
+MS, 35.3min #2593
Intens.
x10^7
445.2
638.2
467.2
585.3
895.3
385.2
483.2
548.3
722.3
769.1
816.2
846.4
945.8
m/z

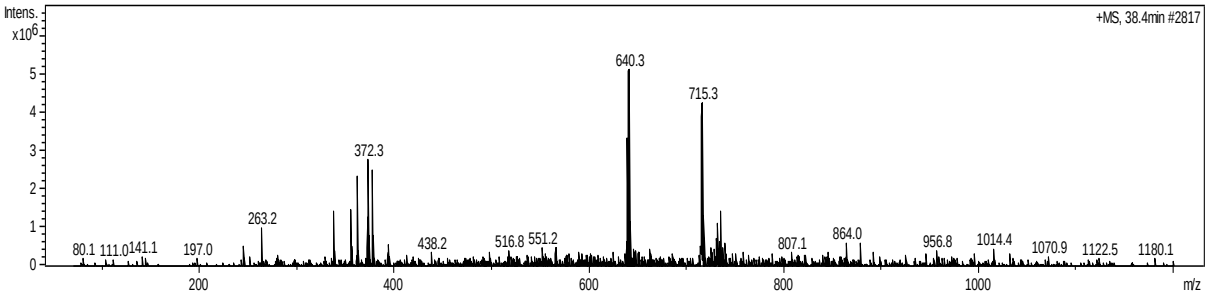
+MS, 38.4min #2817
Intens.
x10^6
640.3
715.3
372.3
263.2
80.1
111.0
141.1
197.0
438.2
516.8
551.2
807.1
864.0
956.8
1014.4
1070.9
1122.5
1180.1
m/z

A.2 LC-MS chromatogram and UV spectra of (A) SB-1; (B) arachidin-1; (C) arachidin-3 in mobile phase.

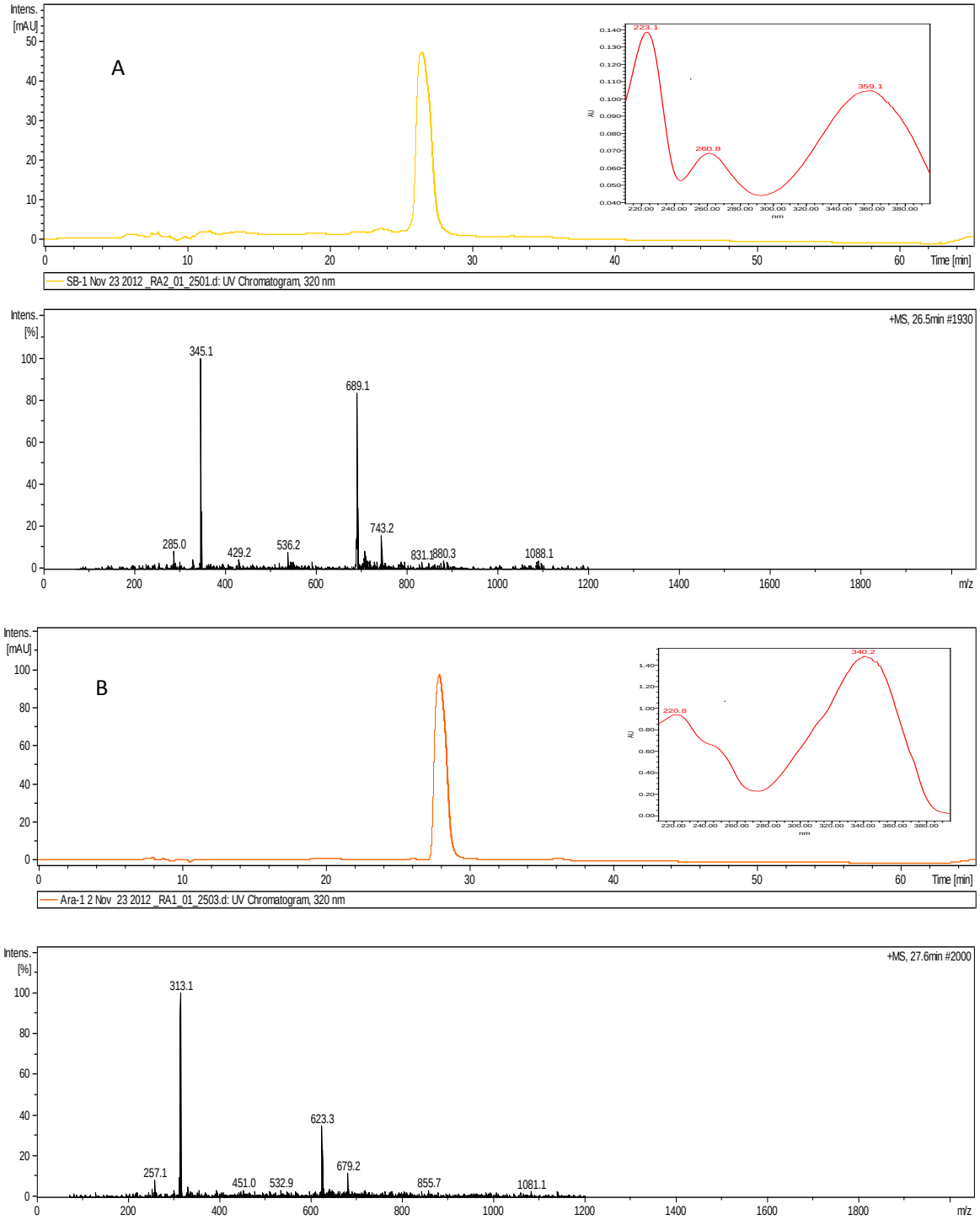

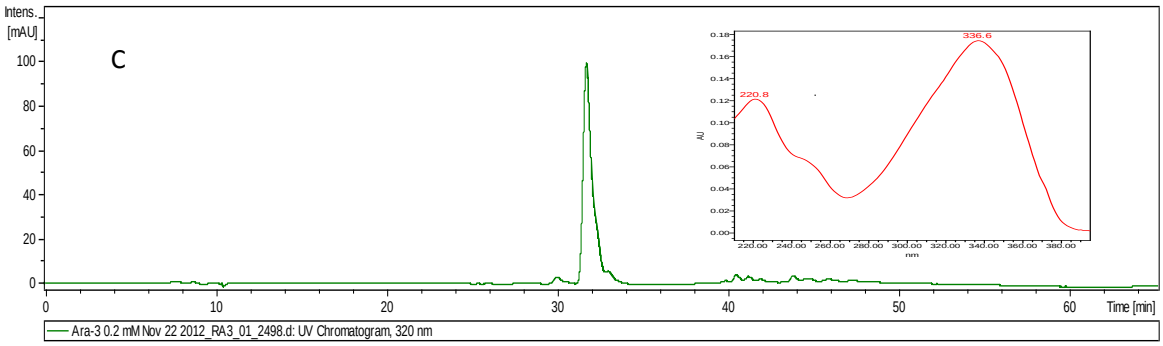
Intens.
[mAU]
C
220.8
336.6
AU
nm
Time [min]
Ara-3 0.2 mM Nov 22 2012_RA3_01_2498.d: UV Chromatogram, 320 nm

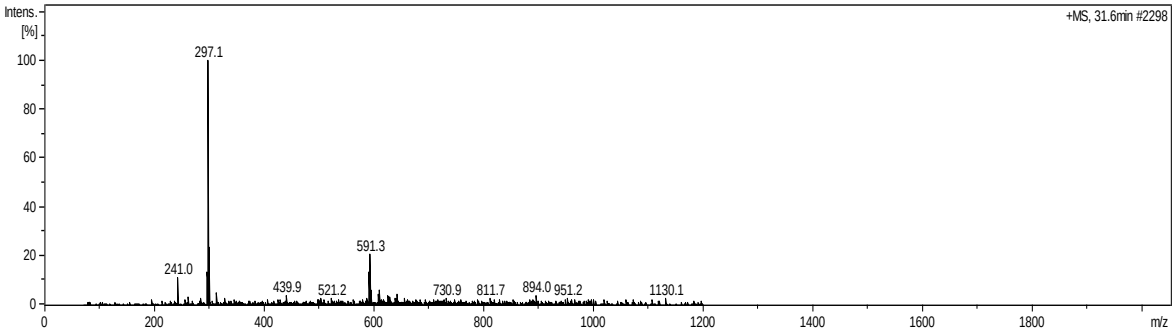
Intens.
[%]
+MS, 31.6min #2298
297.1
241.0
439.9
521.2
591.3
730.9
811.7
894.0
951.2
1130.1
m/z

A.3 HR-MS of (A) arahypin-8; (B) arahypin-9; (C) arahypin-10; (D) arahypin-11; (E) arahypin-12 (F) MIP.

(A) arahypin-8

Mass Spectrum SmartFormula Report

Analysis Info

Analysis Name	D:\Data\Chemistry\2011 Sample\nov2011_sample\587.d	Acquisition Date	11/14/2011 3:13:20 PM
Method	tune_low_neg_200ul.m	Operator	default user
Sample Name	587	Instrument / Ser#	micrOTOF-Q II 10269
Comment	A/P Huang D J		

Acquisition Parameter

Source Type	ESI	Ion Polarity	Negative	Set Nebulizer	2.0 Bar
Focus	Not active	Set Capillary	3500 V	Set Dry Heater	200 °C
Scan Begin	50 m/z	Set End Plate Offset	-500 V	Set Dry Gas	6.0 l/min
Scan End	1100 m/z	Set Collision Cell RF	120.0 Vpp	Set Divert Valve	Waste

Meas. m/z	#	Formula	Score	m/z	err [mDa]	err [ppm]	mSigma	rdb	e¯ Conf	N-Rule
587.2421	1	C 38 H 35 O 6	100.00	587.2439	1.8	3.1	8.8	21.5	even	ok

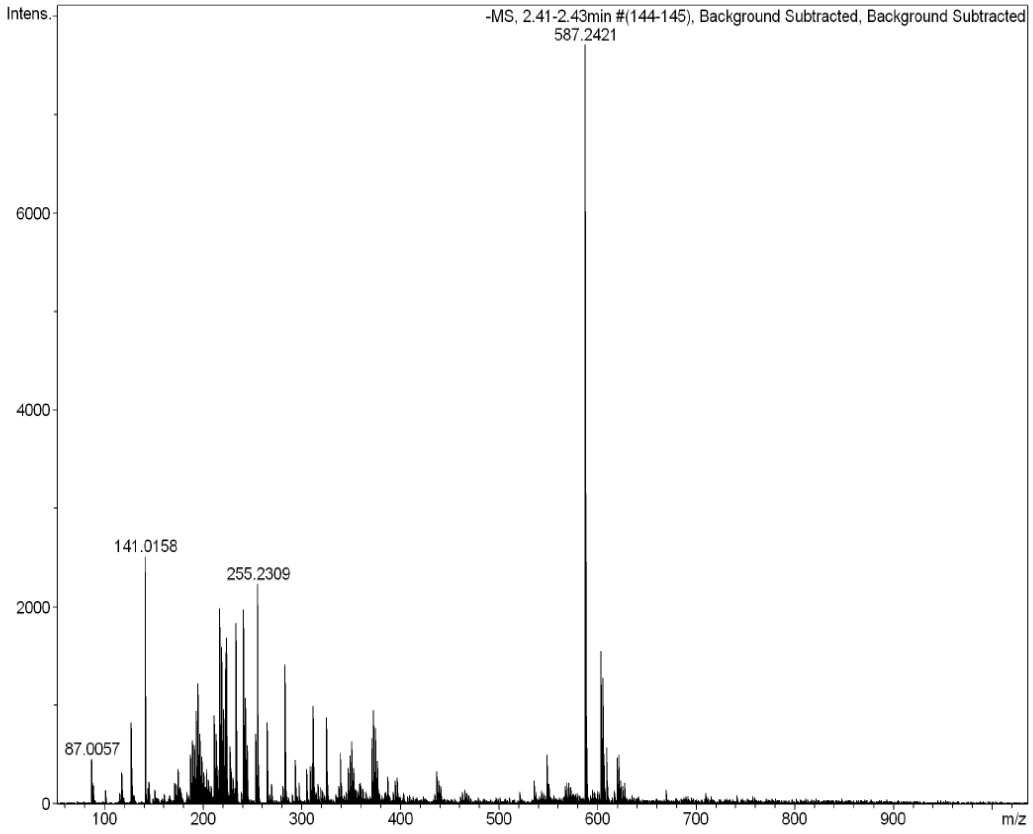

Bruker Compass DataAnalysis 4.0 printed: 11/14/2011 3:21:58 PM Page 1 of 1

(B) arahypin-9

Mass Spectrum SmartFormula Report

Analysis Info

Analysis Name	D:\Data\Chemistry\2011 Sample\nov2011_sample\605.d	Acquisition Date	11/14/2011 3:31:05 PM
Method	tune_low_neg_200ul.m	Operator	default user
Sample Name	605	Instrument / Ser#	micrOTOF-Q II 10269
Comment	A/P Huang D J		

Acquisition Parameter

Source Type	ESI	Ion Polarity	Negative	Set Nebulizer	2.0 Bar
Focus	Not active	Set Capillary	3500 V	Set Dry Heater	200 °C
Scan Begin	50 m/z	Set End Plate Offset	-500 V	Set Dry Gas	6.0 l/min
Scan End	1100 m/z	Set Collision Cell RF	120.0 Vpp	Set Divert Valve	Waste

Meas. m/z	#	Formula	m/z	err [ppm]	rdb	e¯ Conf	z
605.2548	1	C 38 H 37 O 7	605.2545	-0.6	20.5	even	1-

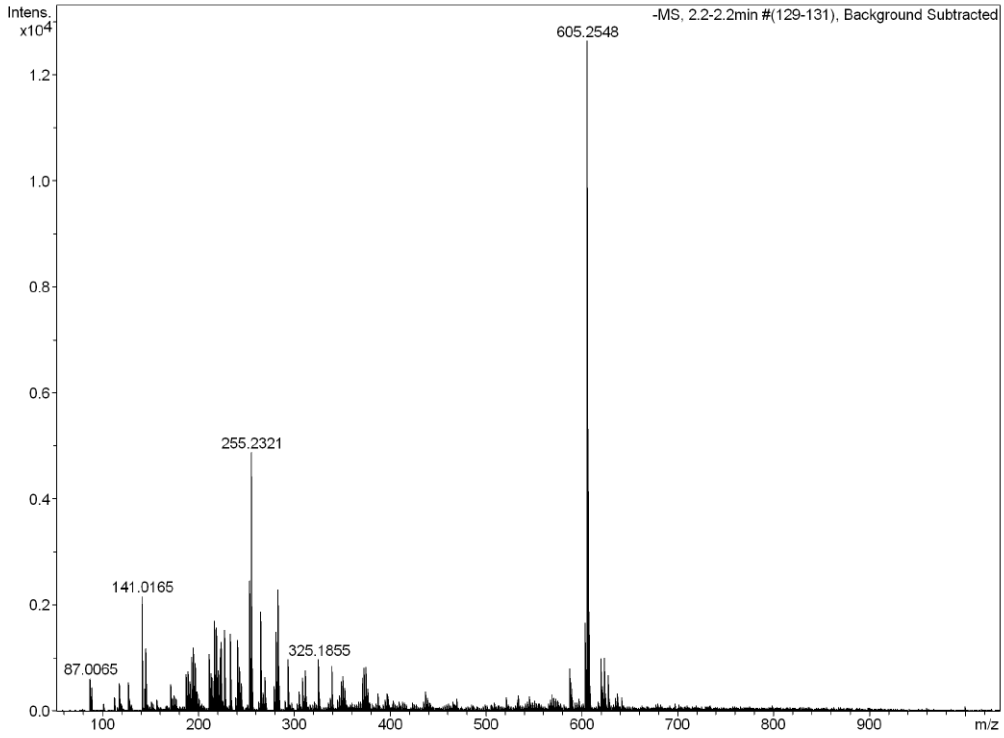

Bruker Compass DataAnalysis 4.0 printed: 11/14/2011 3:35:15 PM Page 1 of 1

(C) arahypin-10

Mass Spectrum SmartFormula Report

Analysis Info

Analysis Name	D:\Data\Chemistry\2011 Sample\aug2011_Sample\293-msms-3.d	Acquisition Date	8/19/2011 9:26:08 AM
Method	tune_low_neg_200ul.m	Operator	default user
Sample Name	293	Instrument / Ser#	micrOTOF-Q II 10269
Comment	A/P HUANG D J		

Acquisition Parameter

Source Type	ESI	Ion Polarity	Negative	Set Nebulizer	2.0 Bar
Focus	Not active	Set Capillary	3500 V	Set Dry Heater	200 °C
Scan Begin	50 m/z	Set End Plate Offset	-500 V	Set Dry Gas	6.0 l/min
Scan End	1000 m/z	Set Collision Cell RF	120.0 Vpp	Set Divert Valve	Waste

Meas. m/z	#	Formula	m/z	err [ppm]	rdb	e¯ Conf	z
293.1175	1	C 19 H 17 O 3	293.1183	2.6	11.5	even	1-

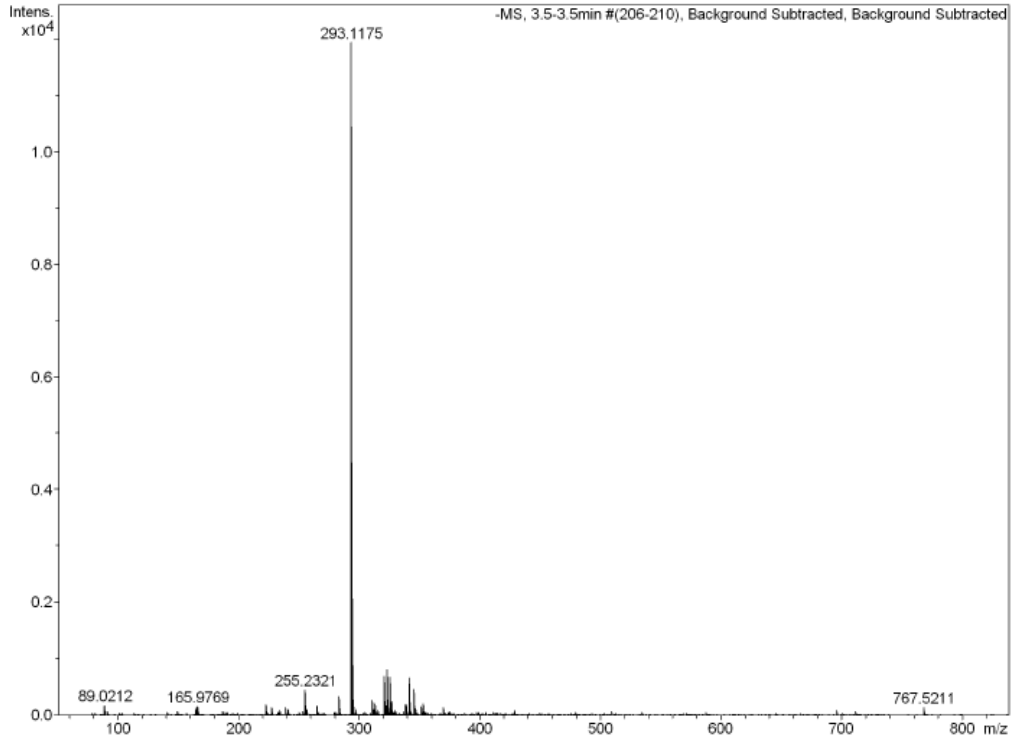

Bruker Compass DataAnalysis 4.0 printed: 8/19/2011 10:28:27 AM Page 1 of 1

(D) arahypin-11

Mass Spectrum SmartFormula Report

Analysis Info

Analysis Name	D:\Data\Chemistry\2012 Sample\Jul 2012\LZW-4.d	Acquisition Date	7/3/2012 5:30:11 PM
Method	tune_low_neg_200ul.m	Operator	default user
Sample Name	LZW-4	Instrument / Ser#	micrOTOF-Q II 10269
Comment	A/P HUANG DEJIAN		

Acquisition Parameter

Source Type	ESI	Ion Polarity	Negative	Set Nebulizer	2.0 Bar
Focus	Not active	Set Capillary	3500 V	Set Dry Heater	250 °C
Scan Begin	50 m/z	Set End Plate Offset	-500 V	Set Dry Gas	6.0 l/min
Scan End	1000 m/z	Set Collision Cell RF	120.0 Vpp	Set Divert Valve	Waste

Meas. m/z	#	Formula	m/z	err [ppm]	rdb	e¯ Conf	z
587.2447	1	C 38 H 35 O 6	587.2439	-1.4	21.5	even	1-

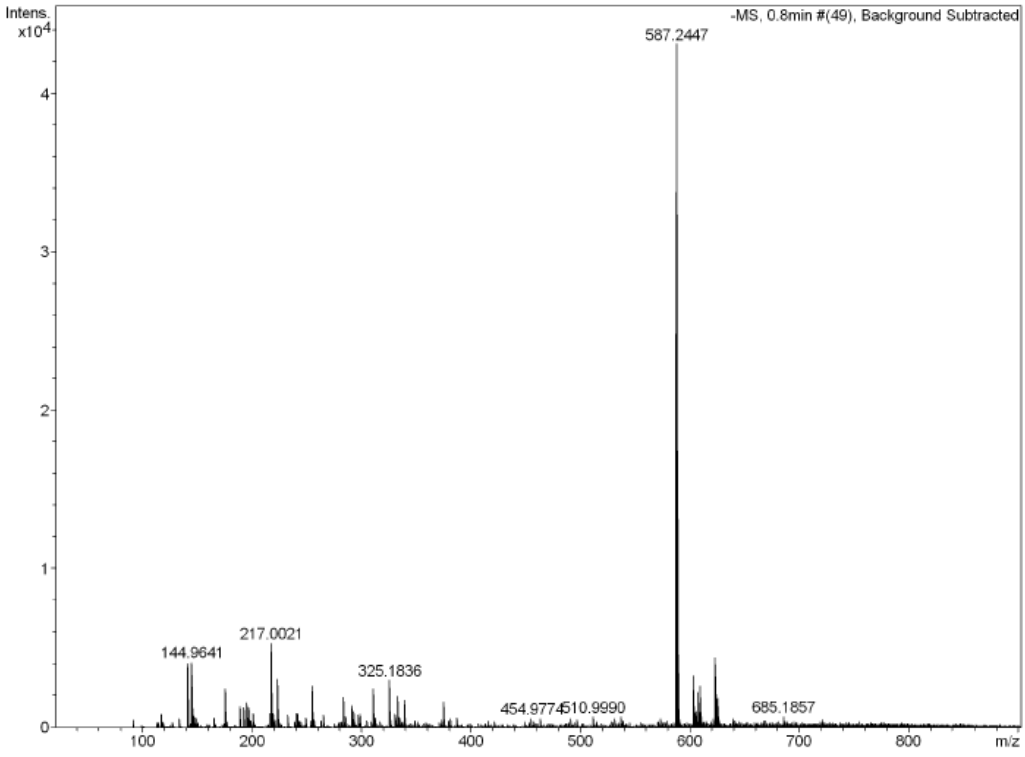

Bruker Compass DataAnalysis 4.0 printed: 7/4/2012 11:01:33 AM Page 1 of 1

(E) arahypin-12

Mass Spectrum SmartFormula Report

Analysis Info

Analysis Name	D:\Data\Chemistry\2012 Sample\Oct 2012\604.d	Acquisition Date	10/10/2012 4:03:19 PM
Method	tune_low_neg_200ul.m	Operator	default user
Sample Name	604	Instrument / Ser#	micrOTOF-Q II 10269
Comment	A/P HUANG D J		

Acquisition Parameter

Source Type	ESI	Ion Polarity	Negative	Set Nebulizer	2.0 Bar
Focus	Not active	Set Capillary	3500 V	Set Dry Heater	250 °C
Scan Begin	50 m/z	Set End Plate Offset	-500 V	Set Dry Gas	5.0 l/min
Scan End	1000 m/z	Set Collision Cell RF	120.0 Vpp	Set Divert Valve	Waste

Meas. m/z	#	Formula	m/z	err [ppm]	rdb	e¯ Conf	z
603.2399	1	C 38 H 35 O 7	603.2388	-1.7	21.5	even	1-

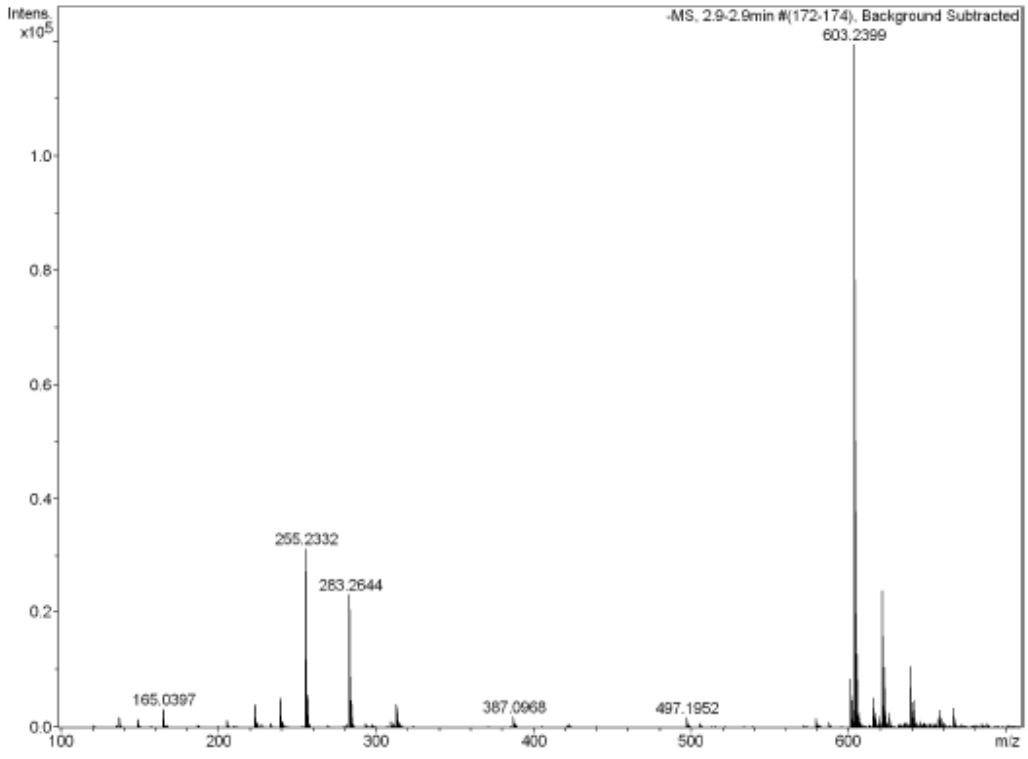

(F) MIP

Mass Spectrum SmartFormula Report

Analysis Info

Analysis Name	D:\Data\Chemistry\2012 Sample\Jul 2012\LZW-5.d	Acquisition Date	7/3/2012 5:33:47 PM
Method	tune_low_neg_200ul.m	Operator	default user
Sample Name	LZW-5	Instrument / Ser#	micrOTOF-Q II 10269
Comment	A/P HUANG DEJIAN		

Acquisition Parameter

Source Type	ESI	Ion Polarity	Negative	Set Nebulizer	2.0 Bar
Focus	Not active	Set Capillary	3500 V	Set Dry Heater	250 °C
Scan Begin	50 m/z	Set End Plate Offset	-500 V	Set Dry Gas	6.0 l/min
Scan End	1000 m/z	Set Collision Cell RF	120.0 Vpp	Set Divert Valve	Waste

Meas. m/z	#	Formula	m/z	err [ppm]	rdb	e¯ Conf	z
325.1452	1	C 20 H 21 O 4	325.1445	-2.1	10.5	even	1-

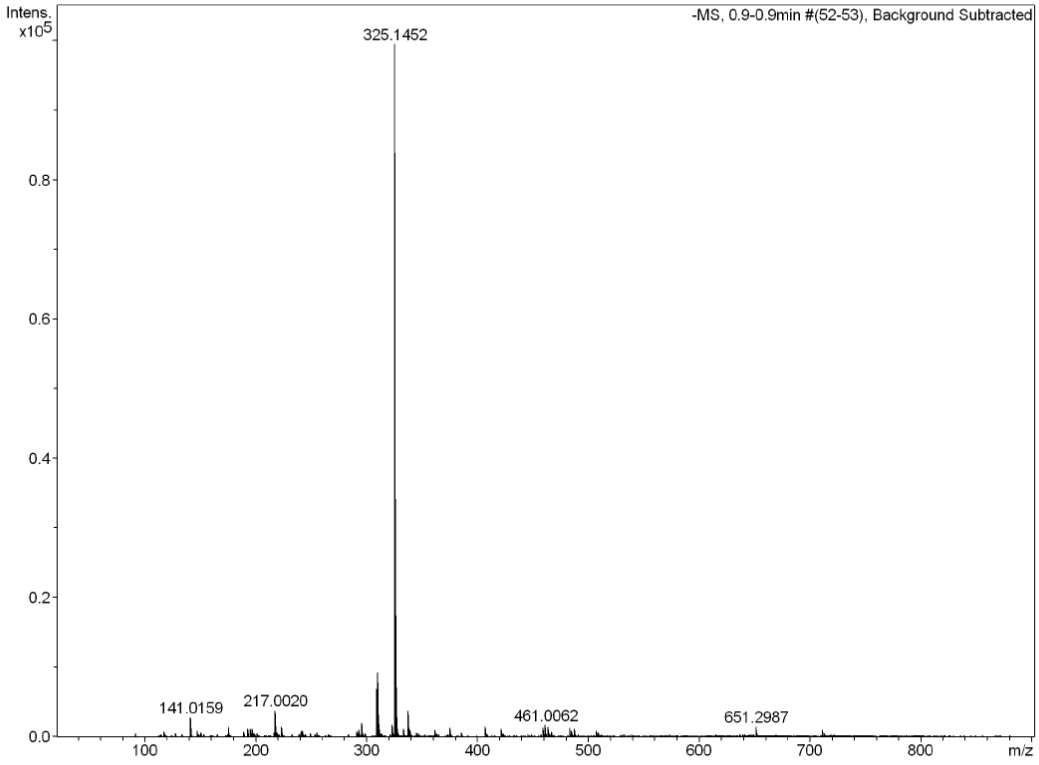

A.4 1D and 2D NMR data of (A) arahypin-8

^{1}H NMR spectrum of arahypin-8

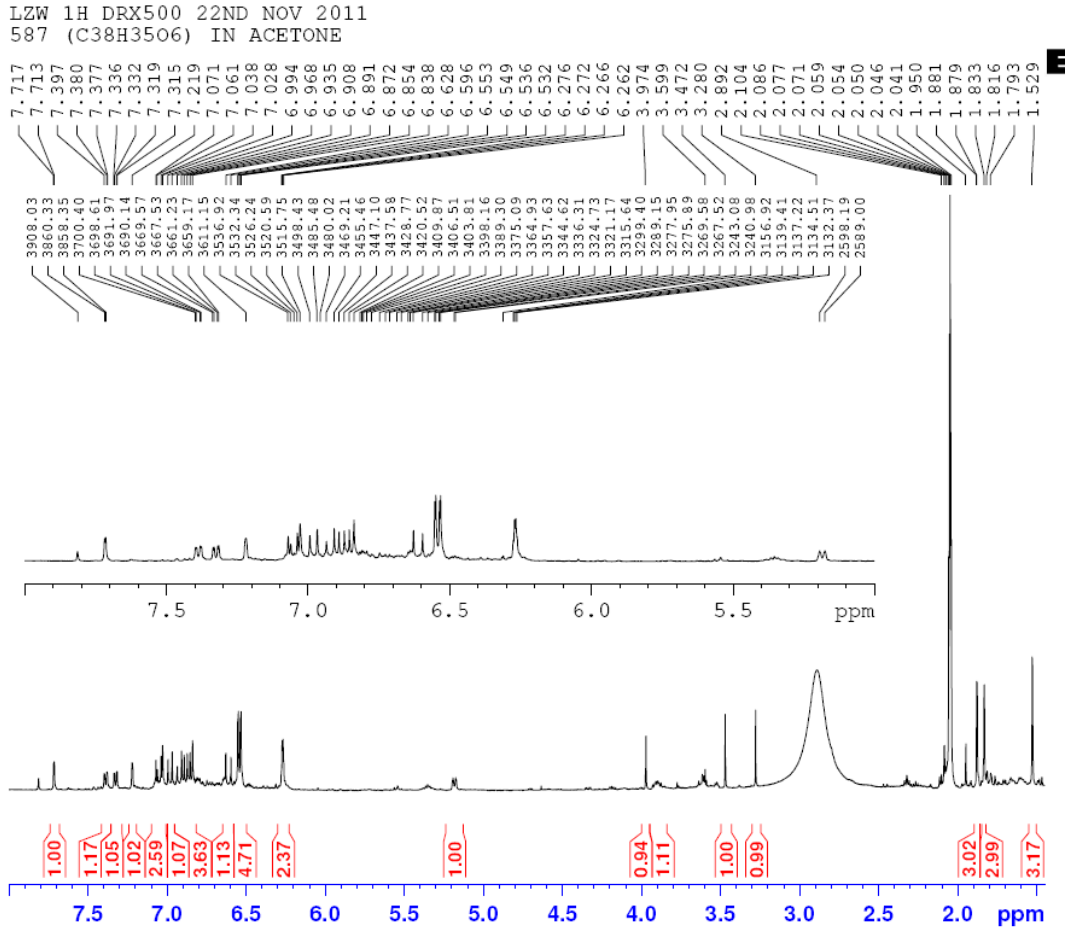

^{13}C NMR spectrum of arahypin-8

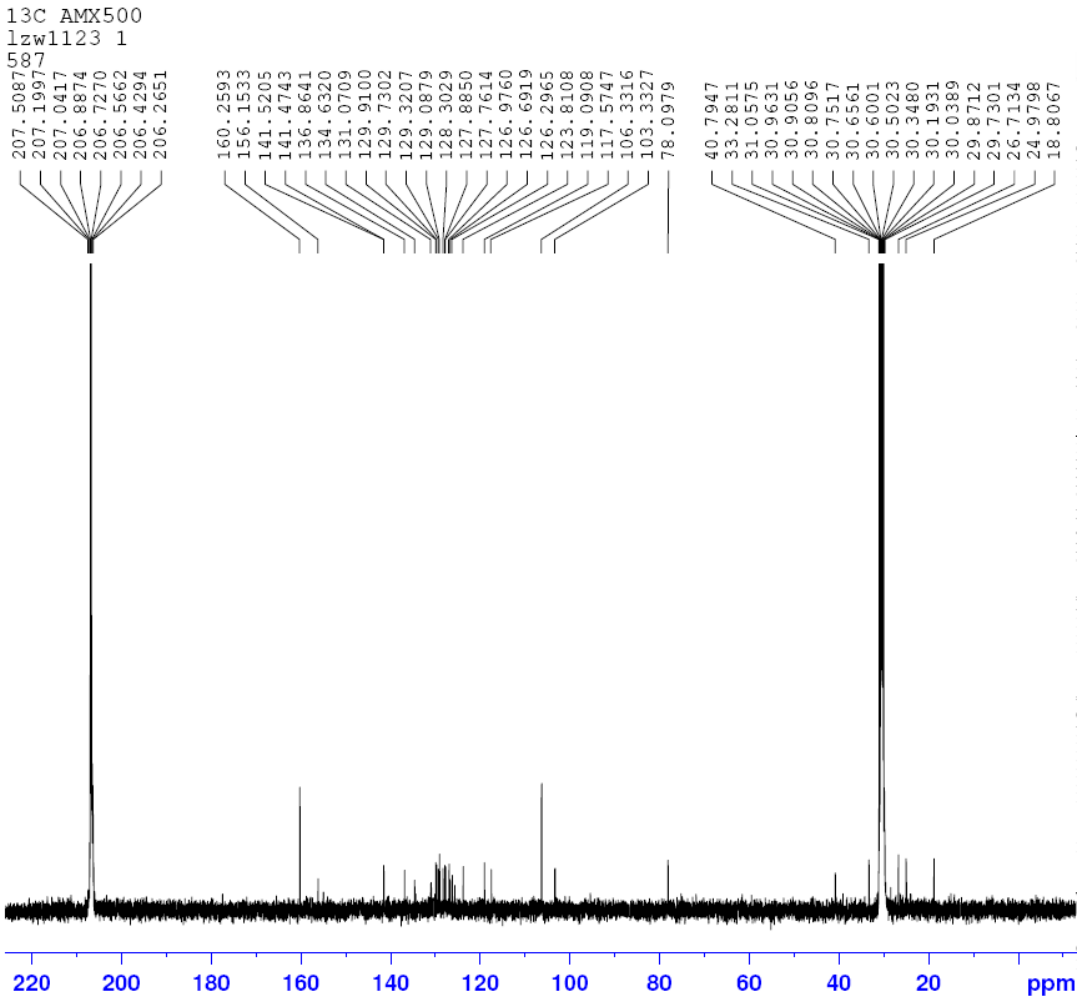

DEPT 135 spectrum of arahypin-8

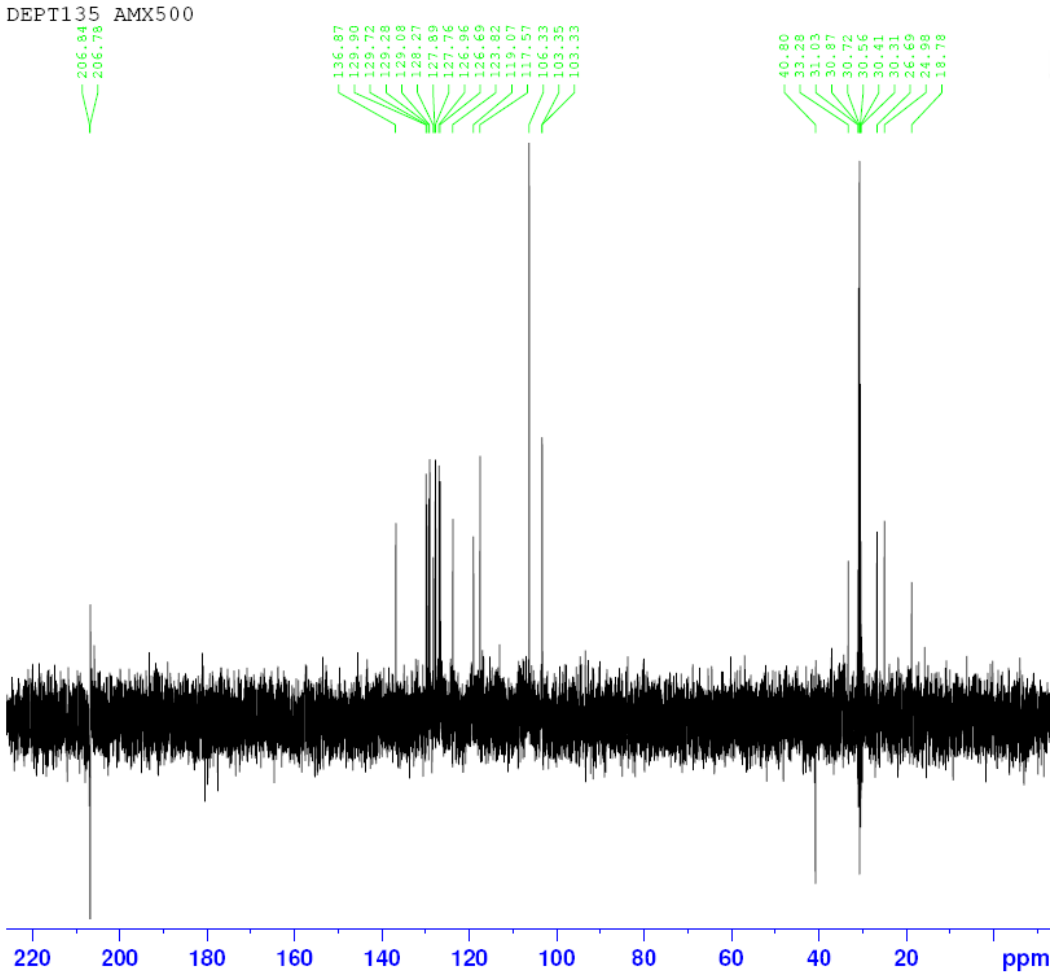

COSY spectrum of arahypin-8

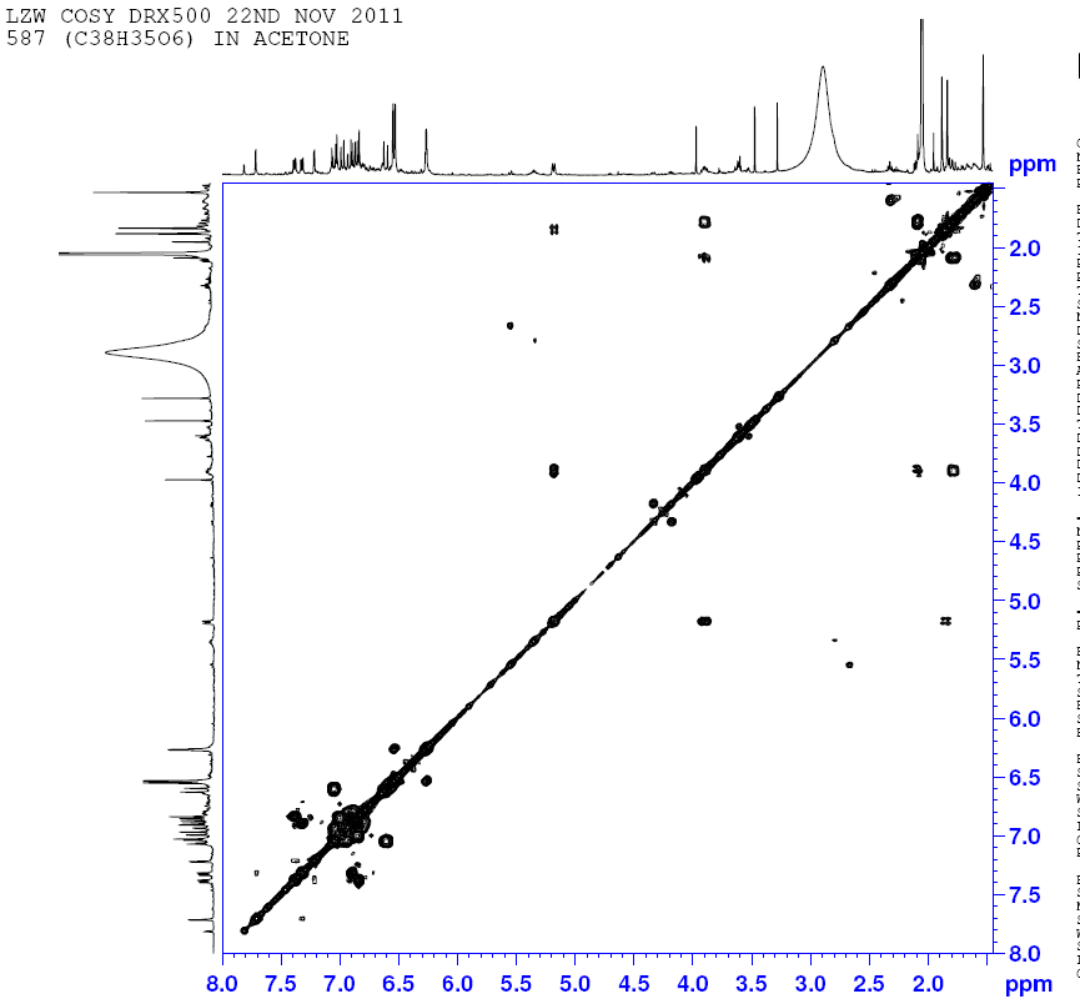

HMBC spectrum of arahypin-8

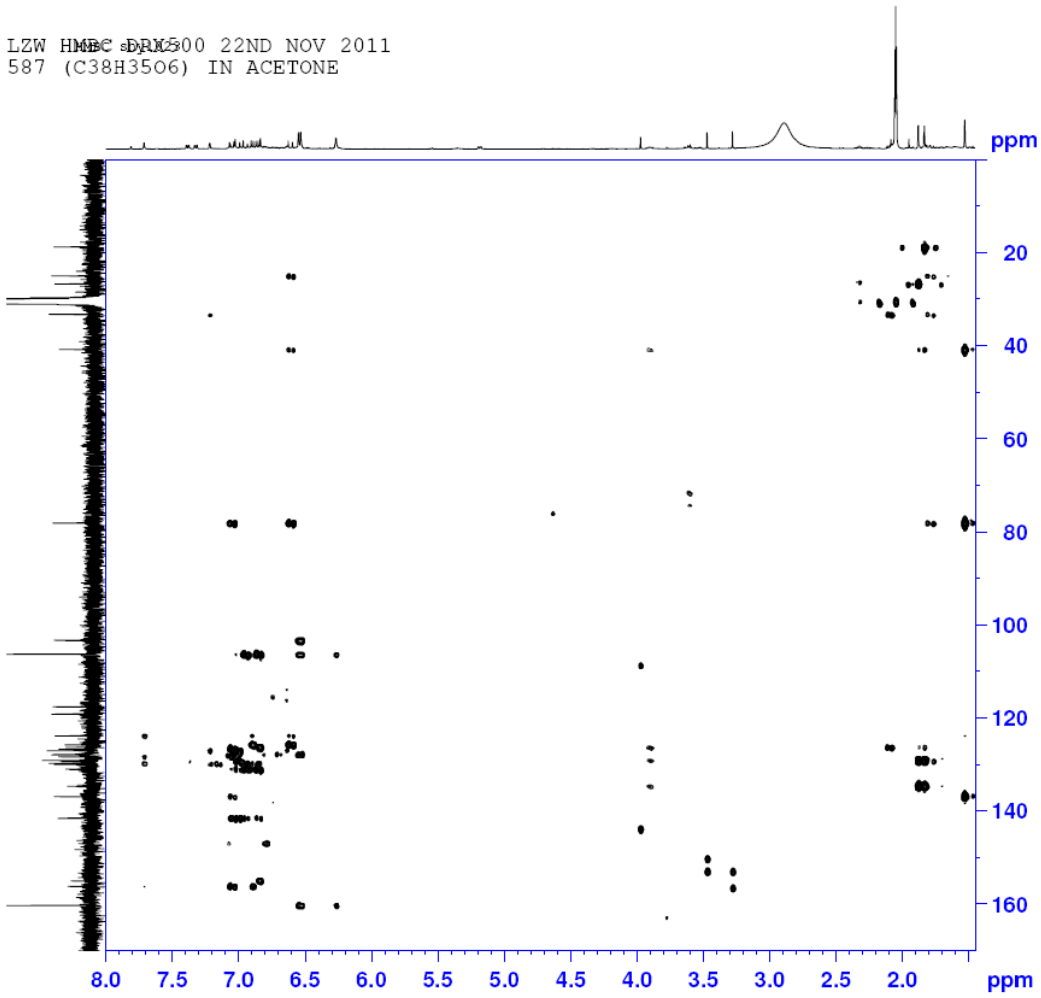

A portion of HMBC spectrum of arahypin-8

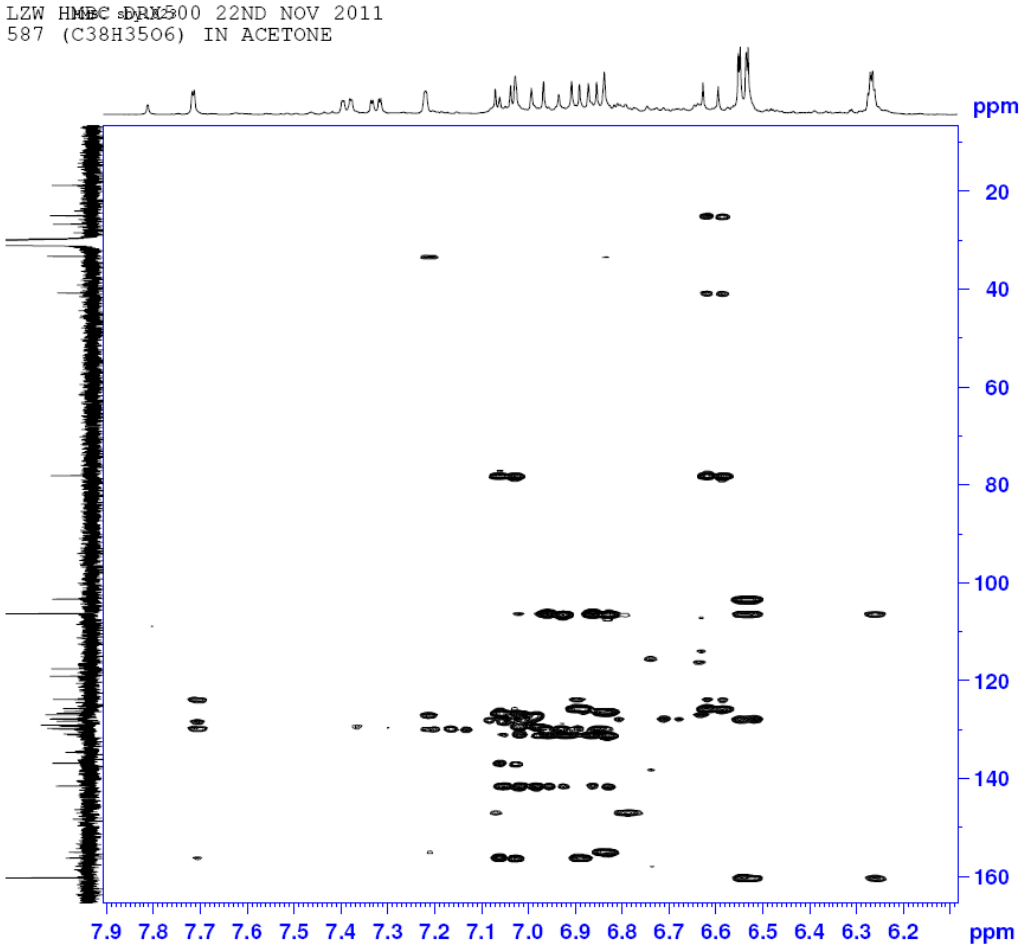

A portion of HMBC spectrum of arahypin-8

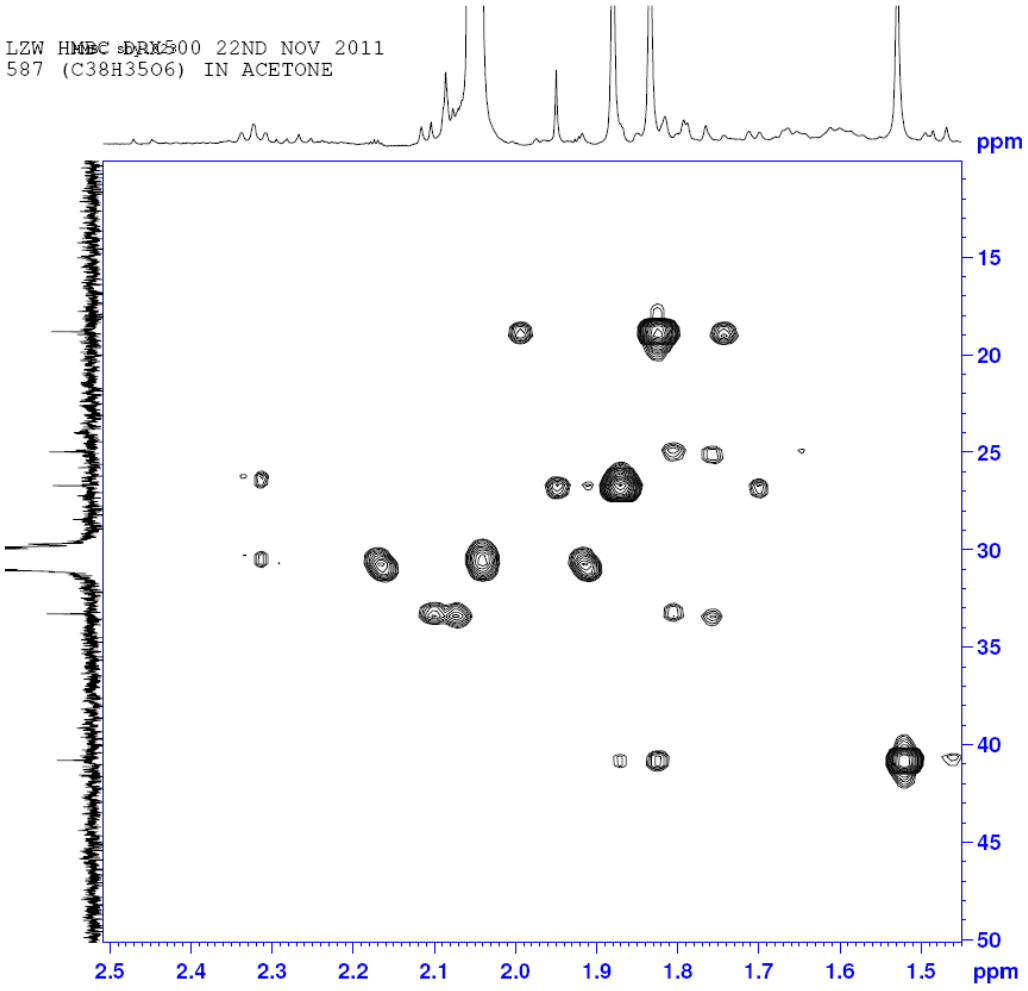

A portion of HMBC spectrum of arahypin-8

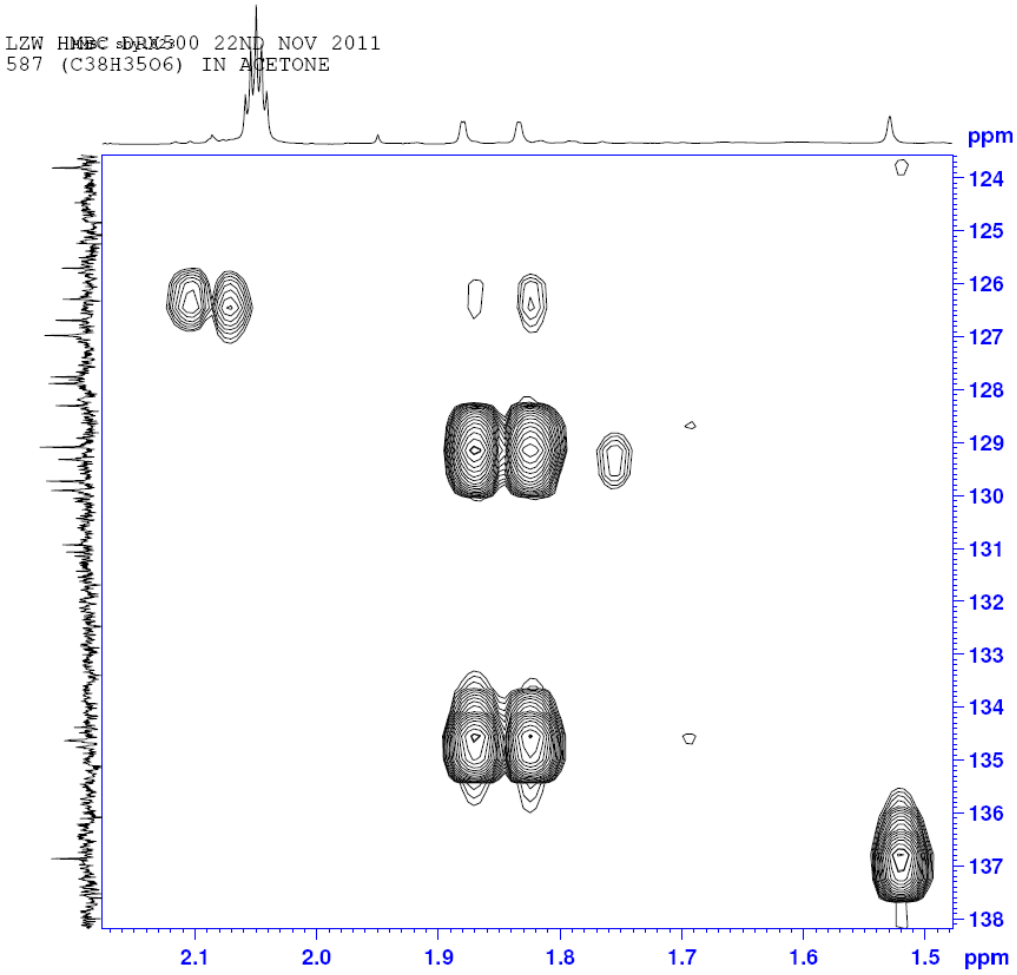

HMQC spectrum of arahypin-8

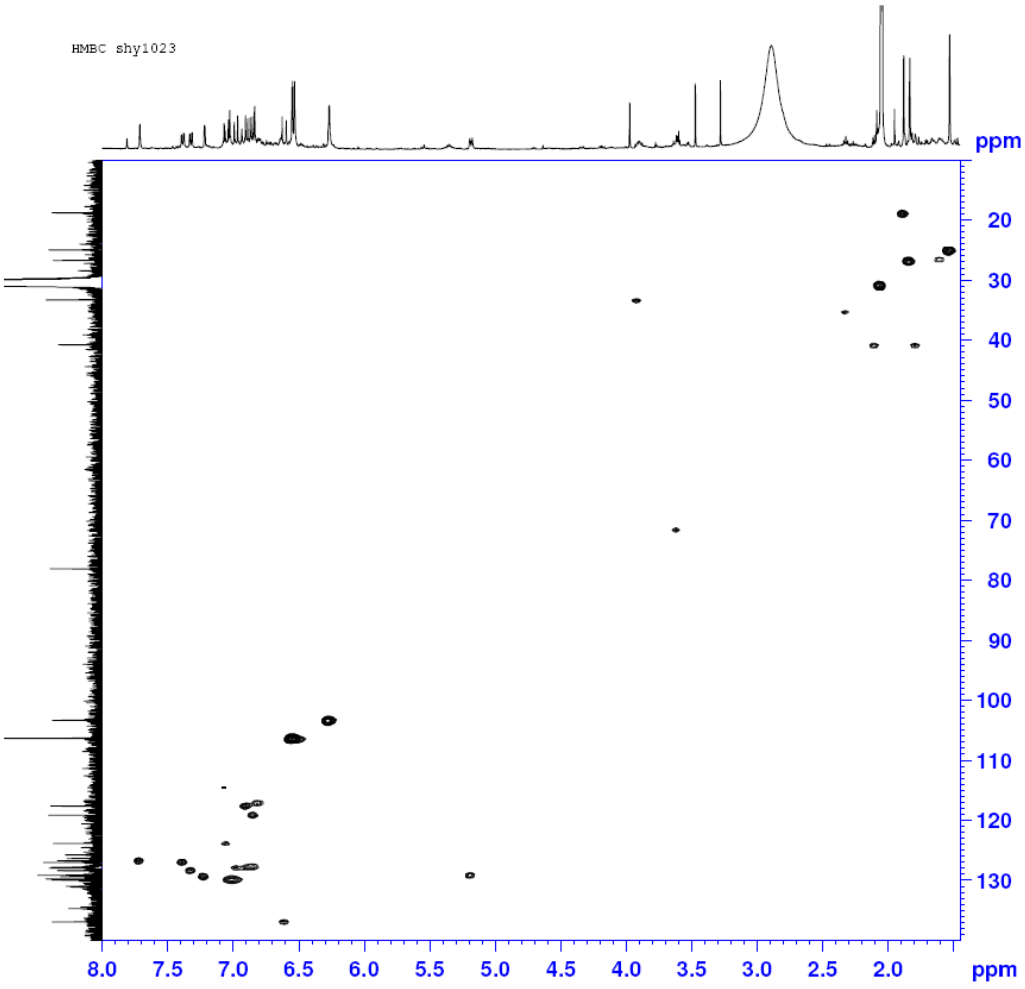

A portion of HMQC spectrum of arahypin-8

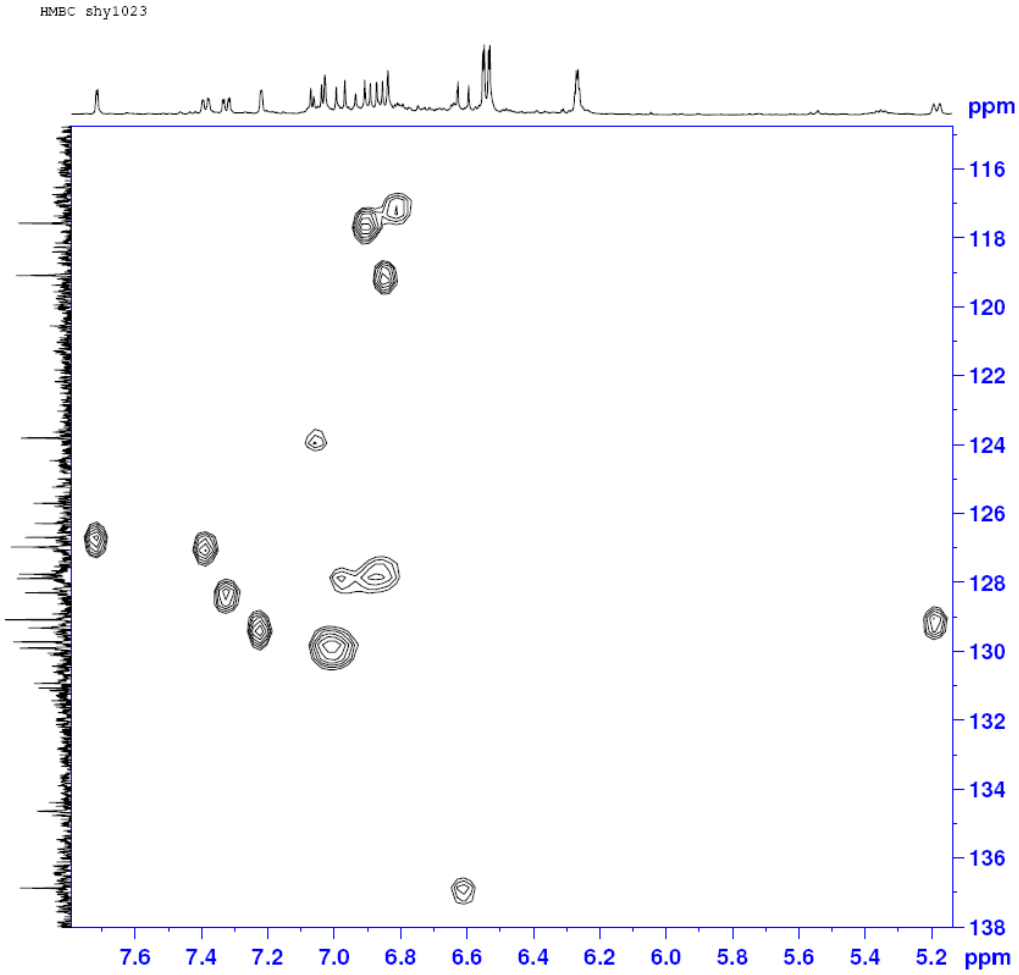

A portion of HMQC spectrum of arahypin-8

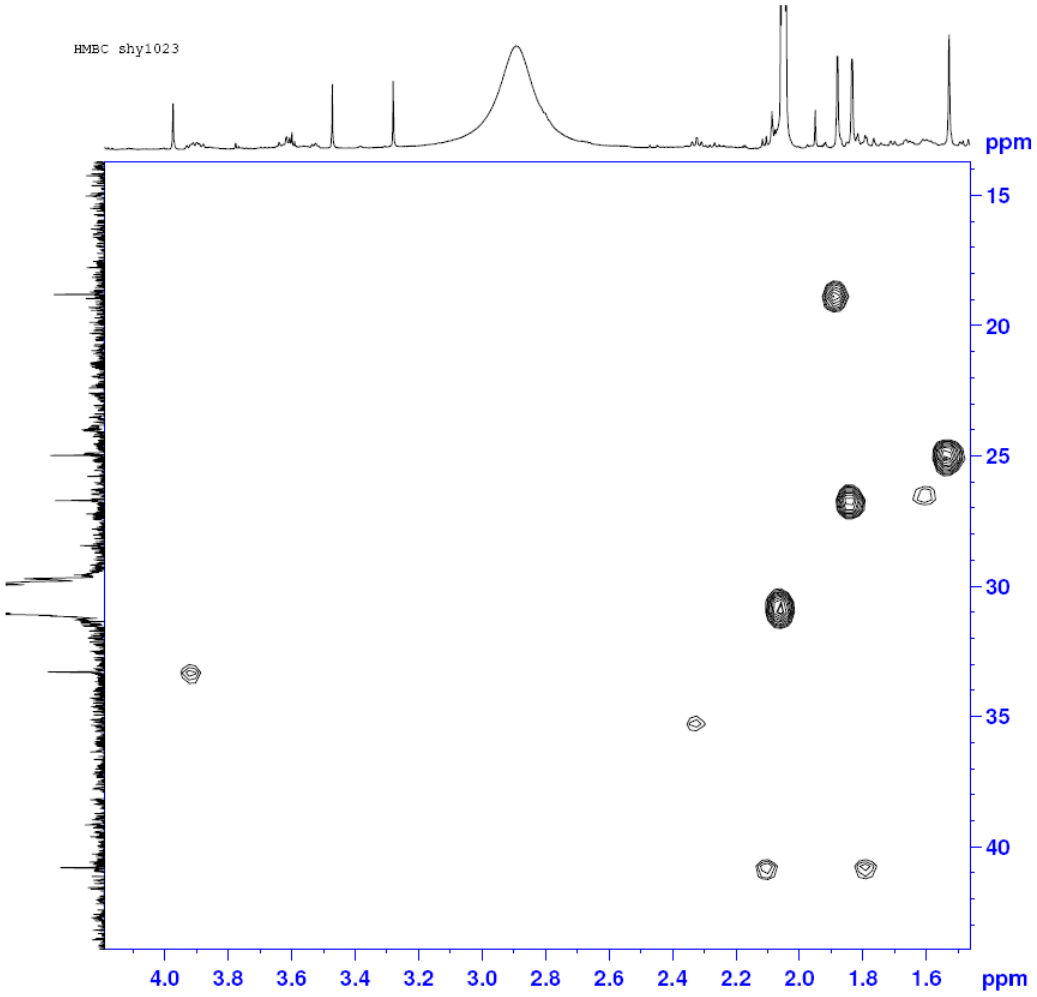

NOSEY spectrum of arahypin-8

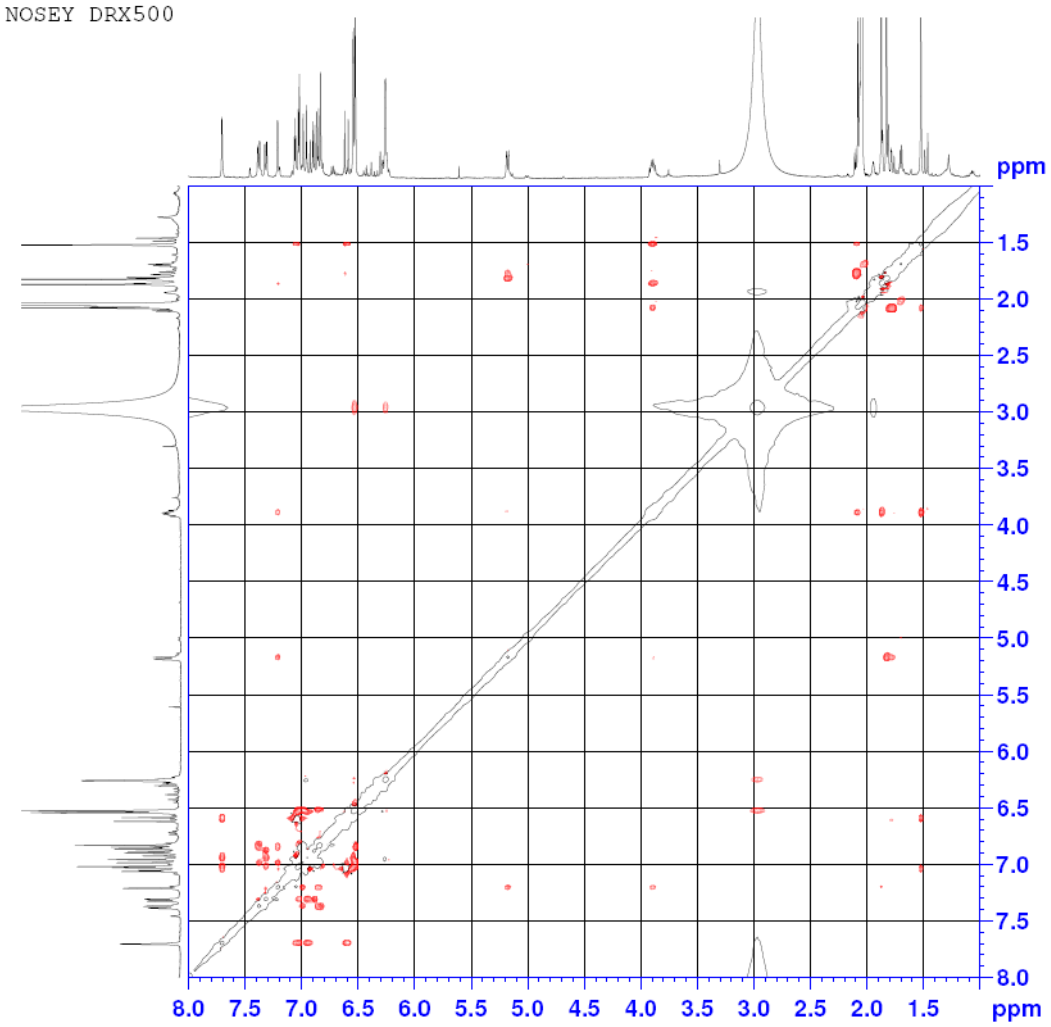

A portion of NOSEY spectrum of arahypin-8

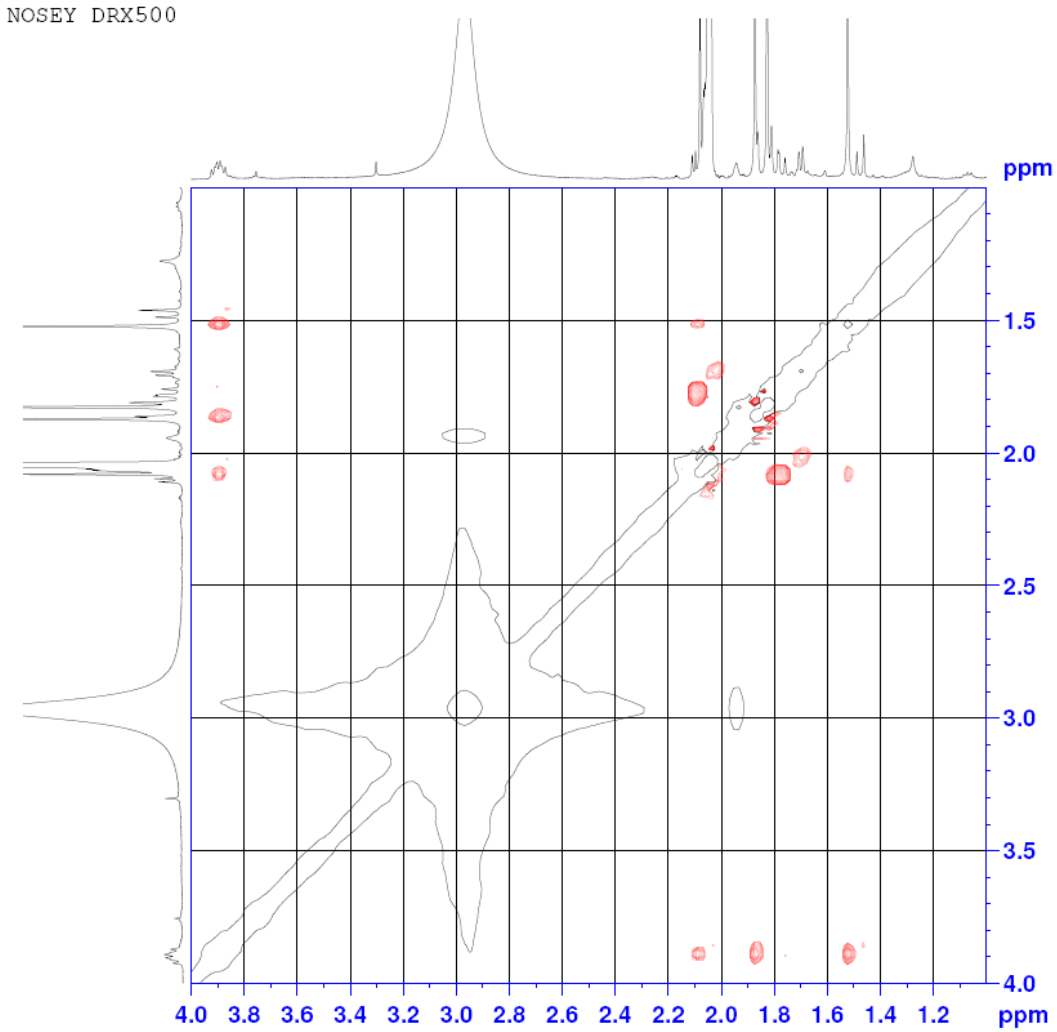

A.5 1D and 2D NMR data of (B) arahypin-9

^{1}H NMR spectrum of arahypin-9

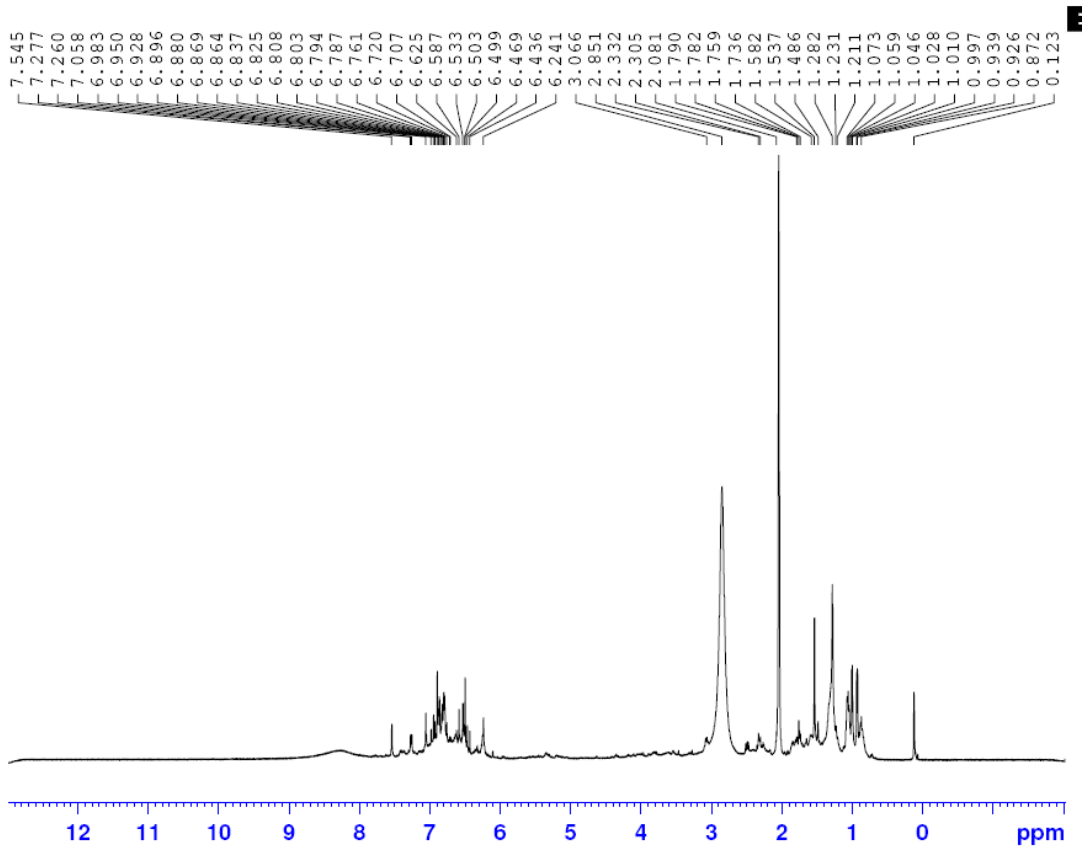

^{13}C NMR spectrum of arahypin-9

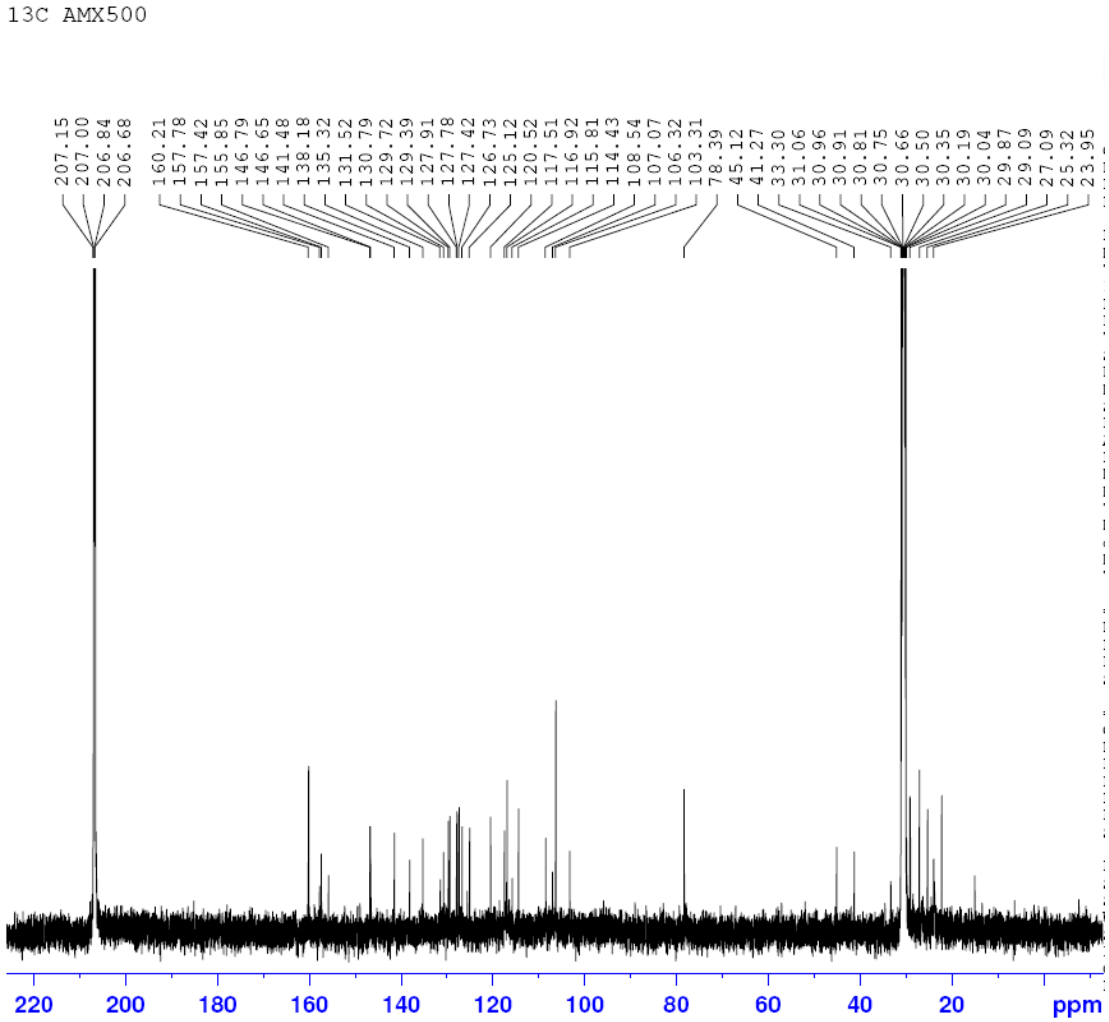

DEPT 135 spectrum of arahypin-9

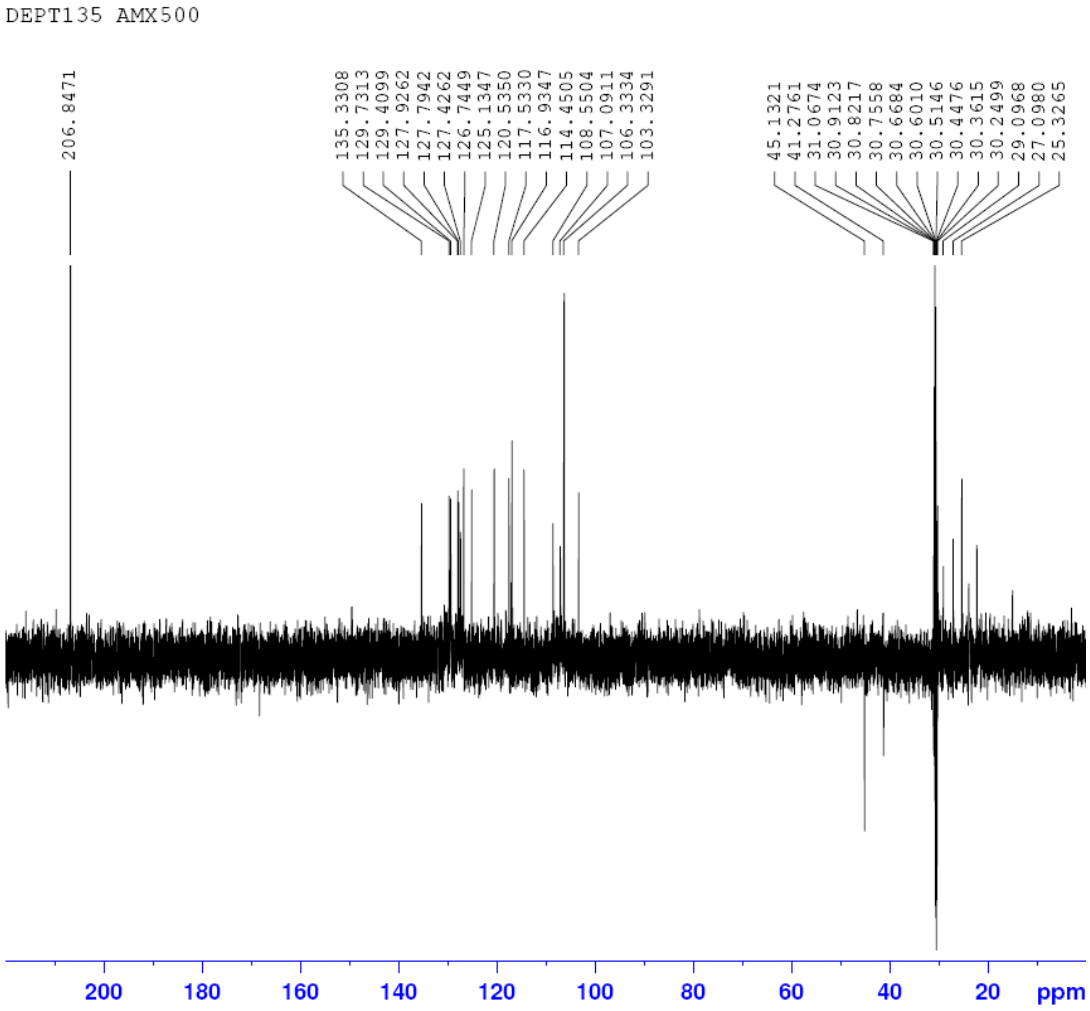

COSY spectrum of arahypin-9

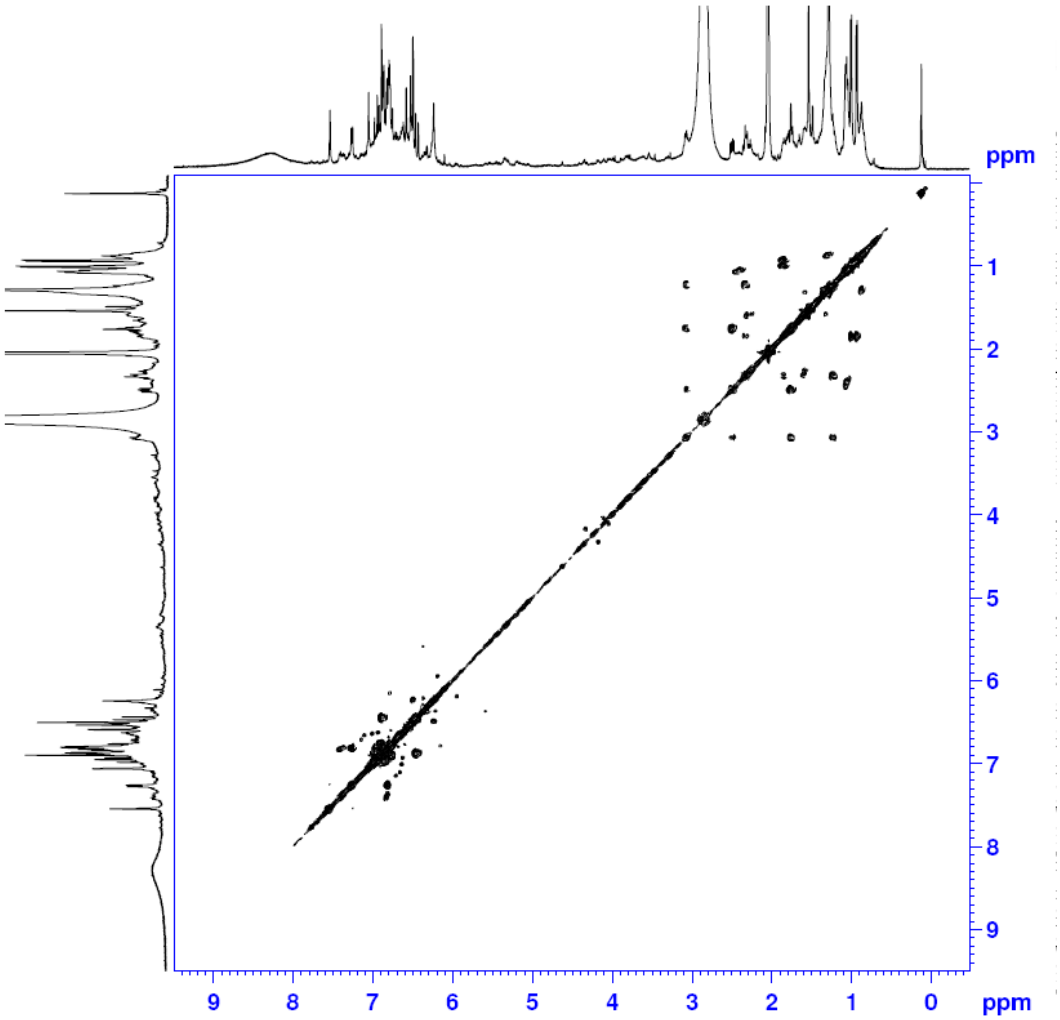

HMBC spectrum of arahypin-9

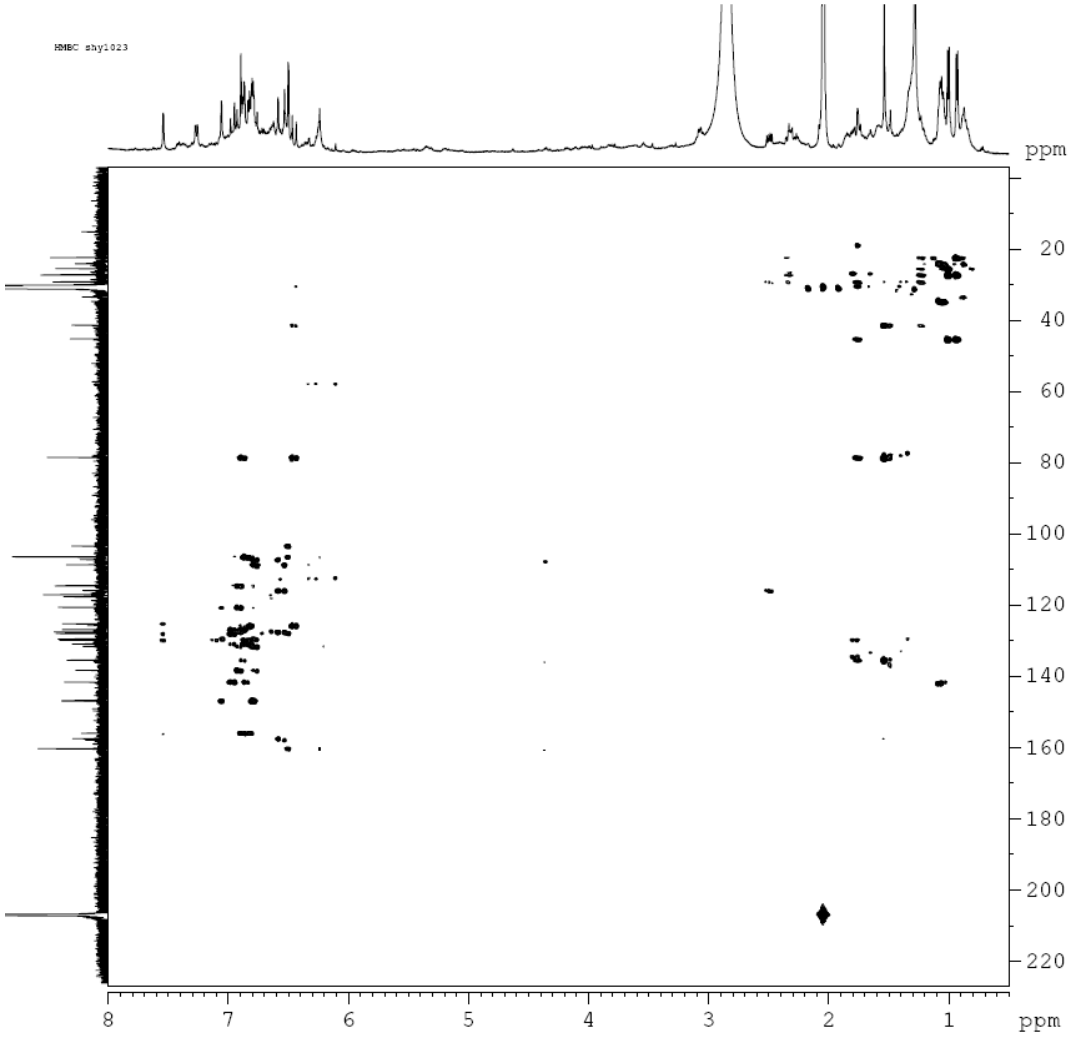

A portion of HMBC spectrum of arahypin-9

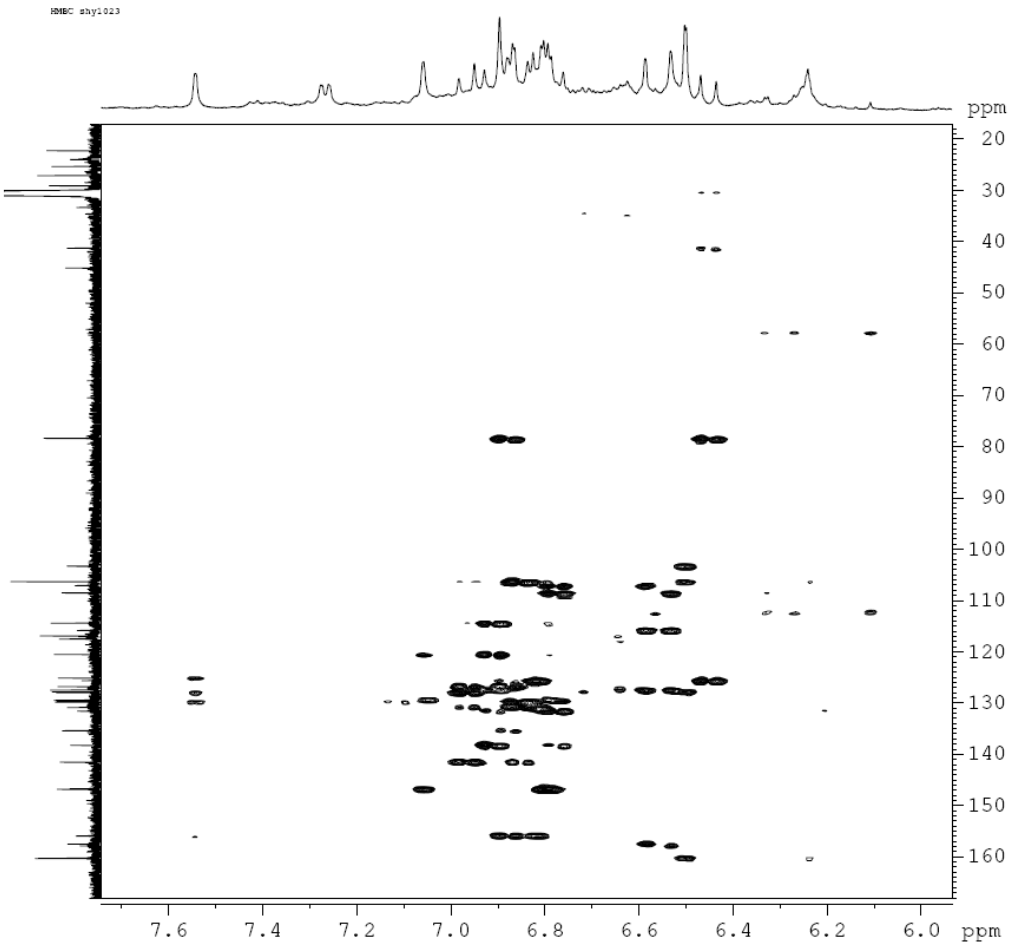

A portion of HMBC spectrum of arahypin-9

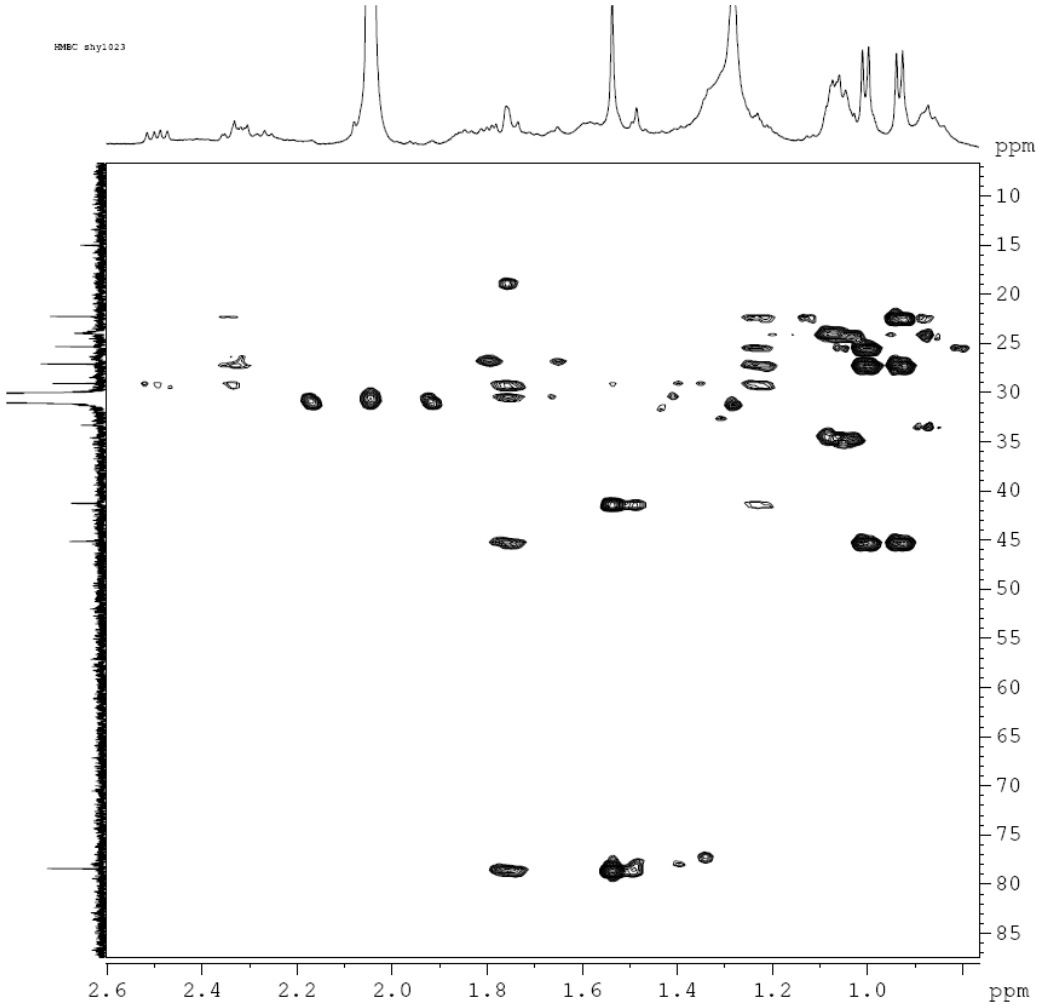

A portion of HMBC spectrum of arahypin-9

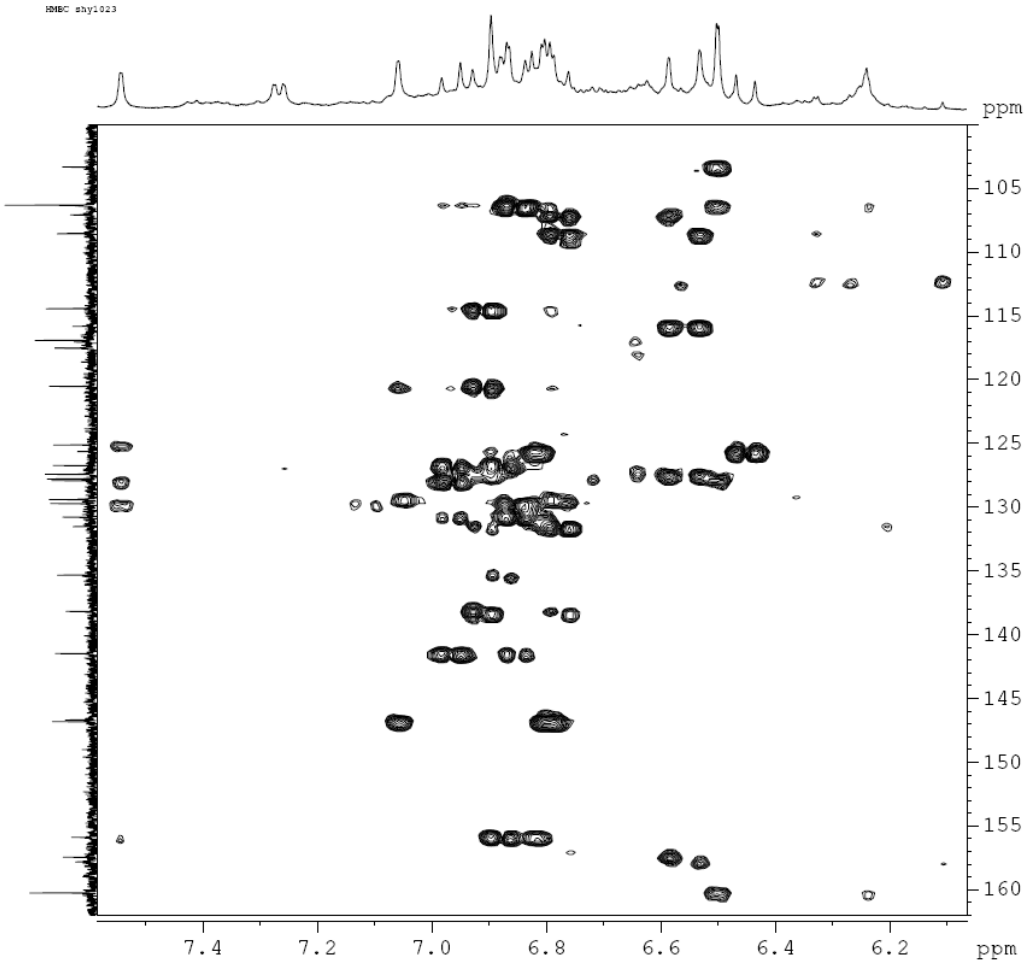

HMQC spectrum of arahypin-9

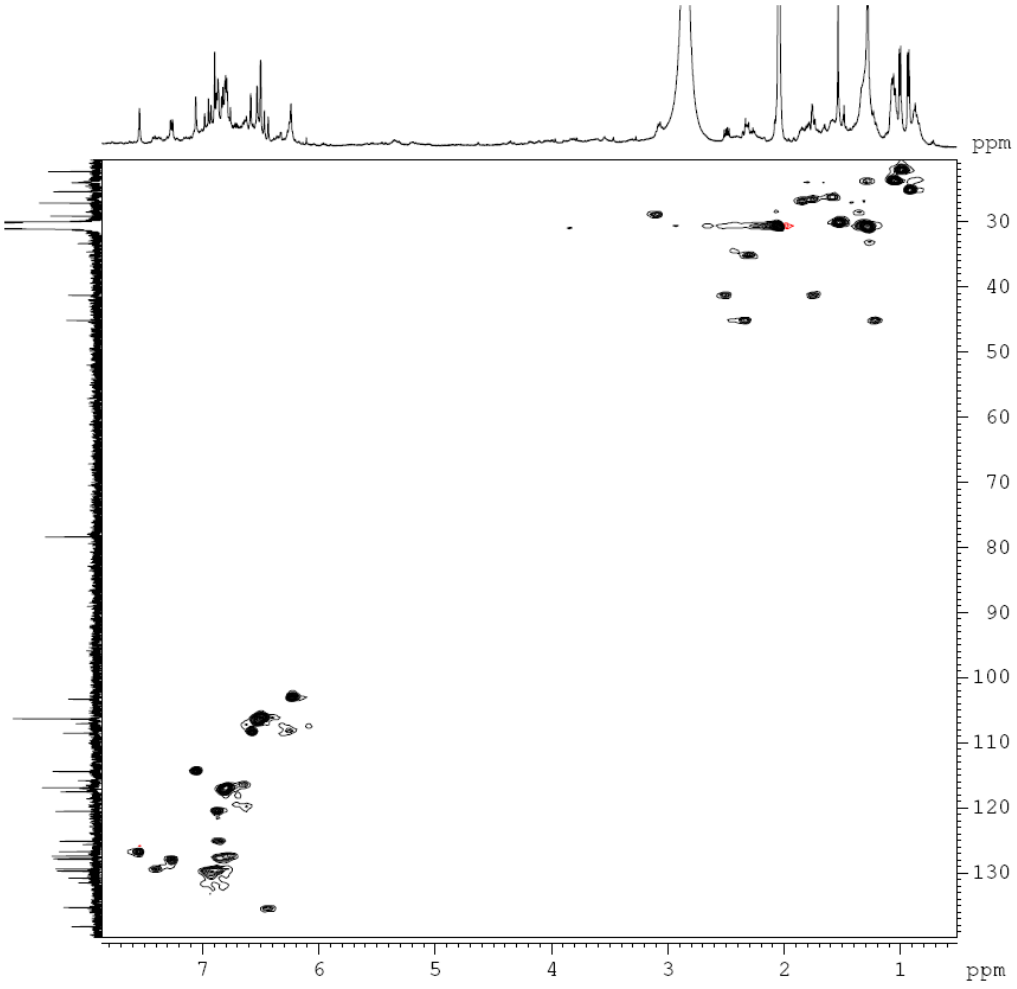

A portion of HMQC spectrum of arahypin-9

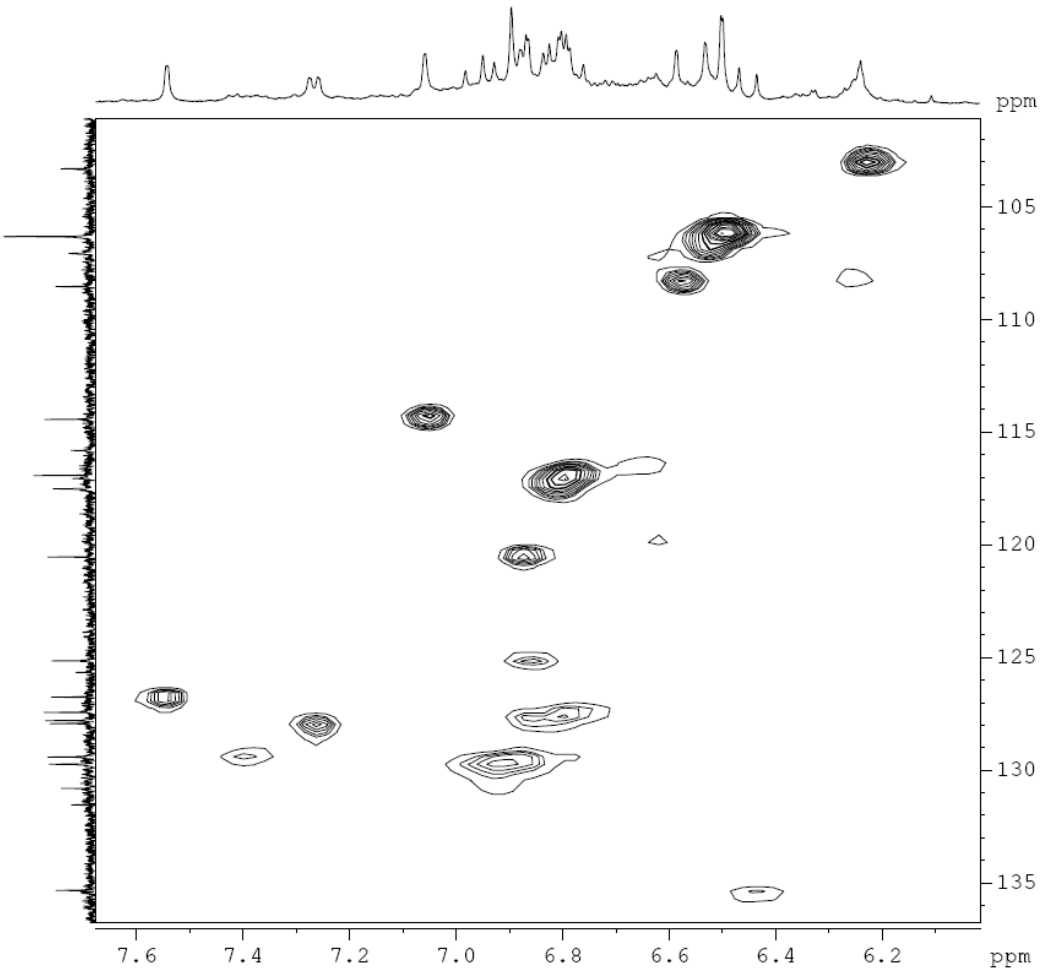

A portion of HMQC spectrum of arahypin-9

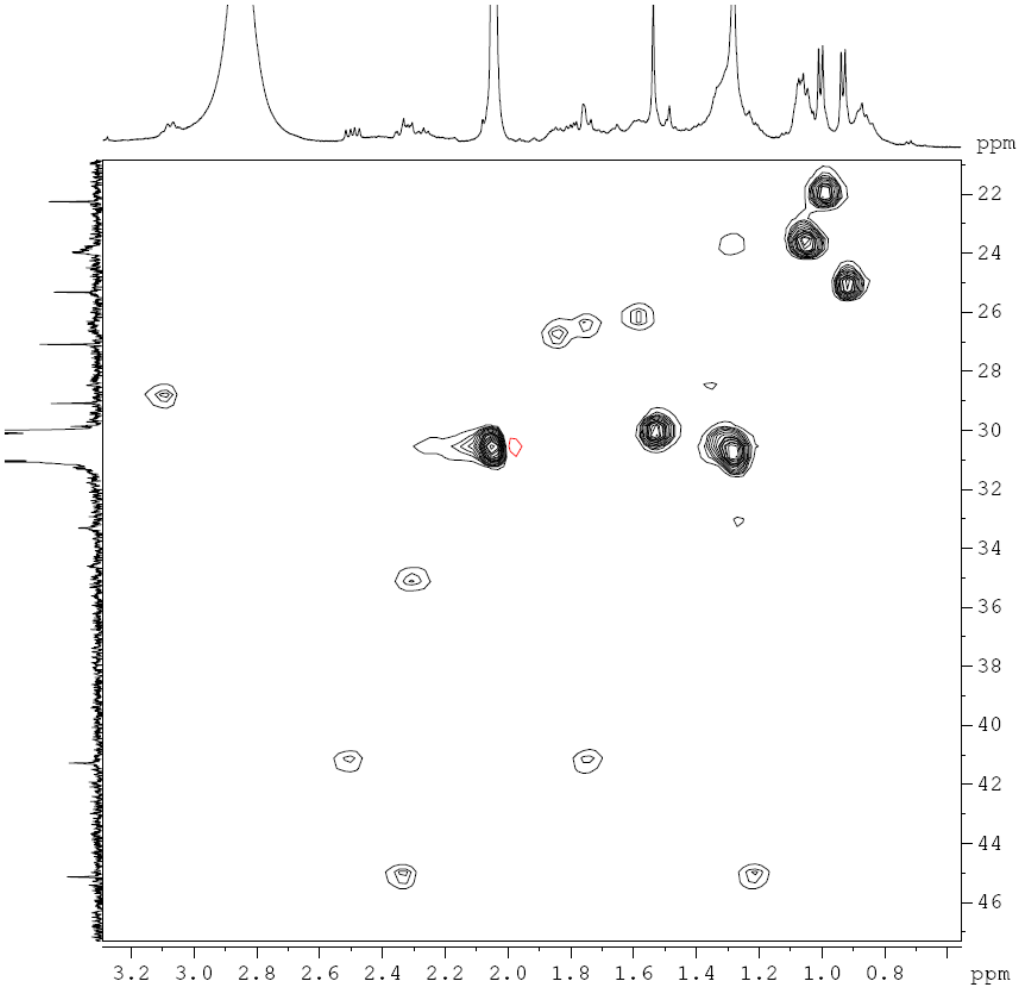

A.6 1D and 2D NMR data of (C) arahypin-10

^{1}H NMR spectrum of arahypin-10

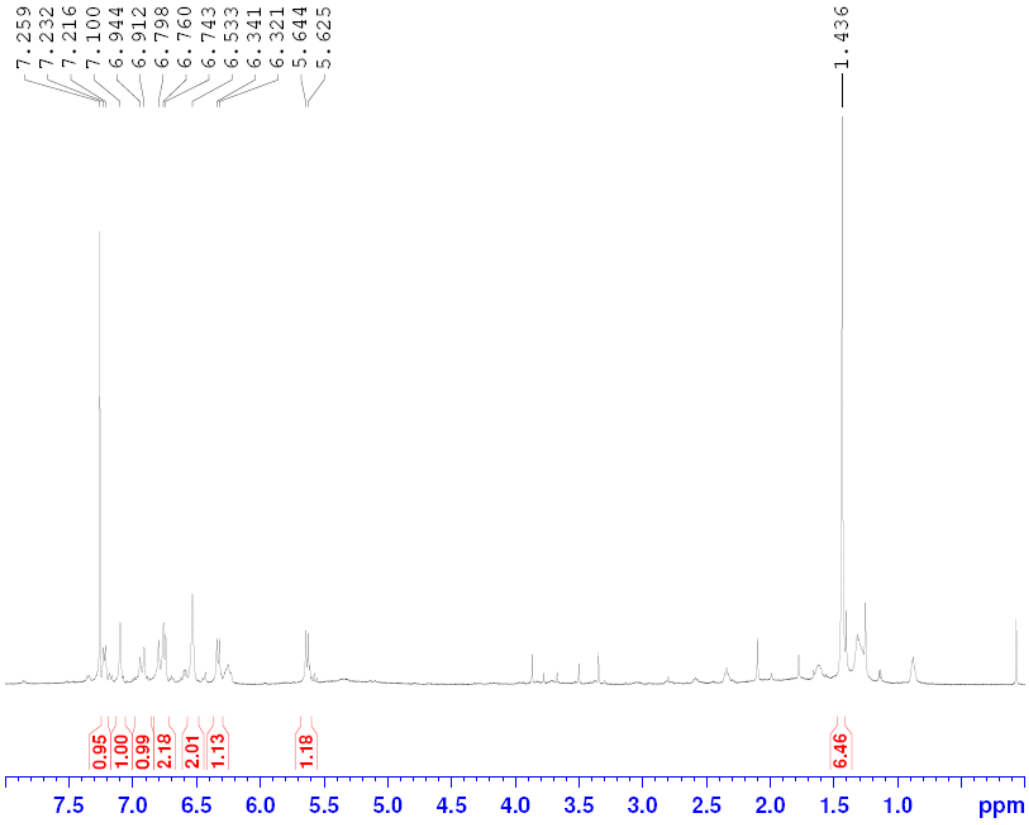

^{13}C NMR spectrum of arahypin-10

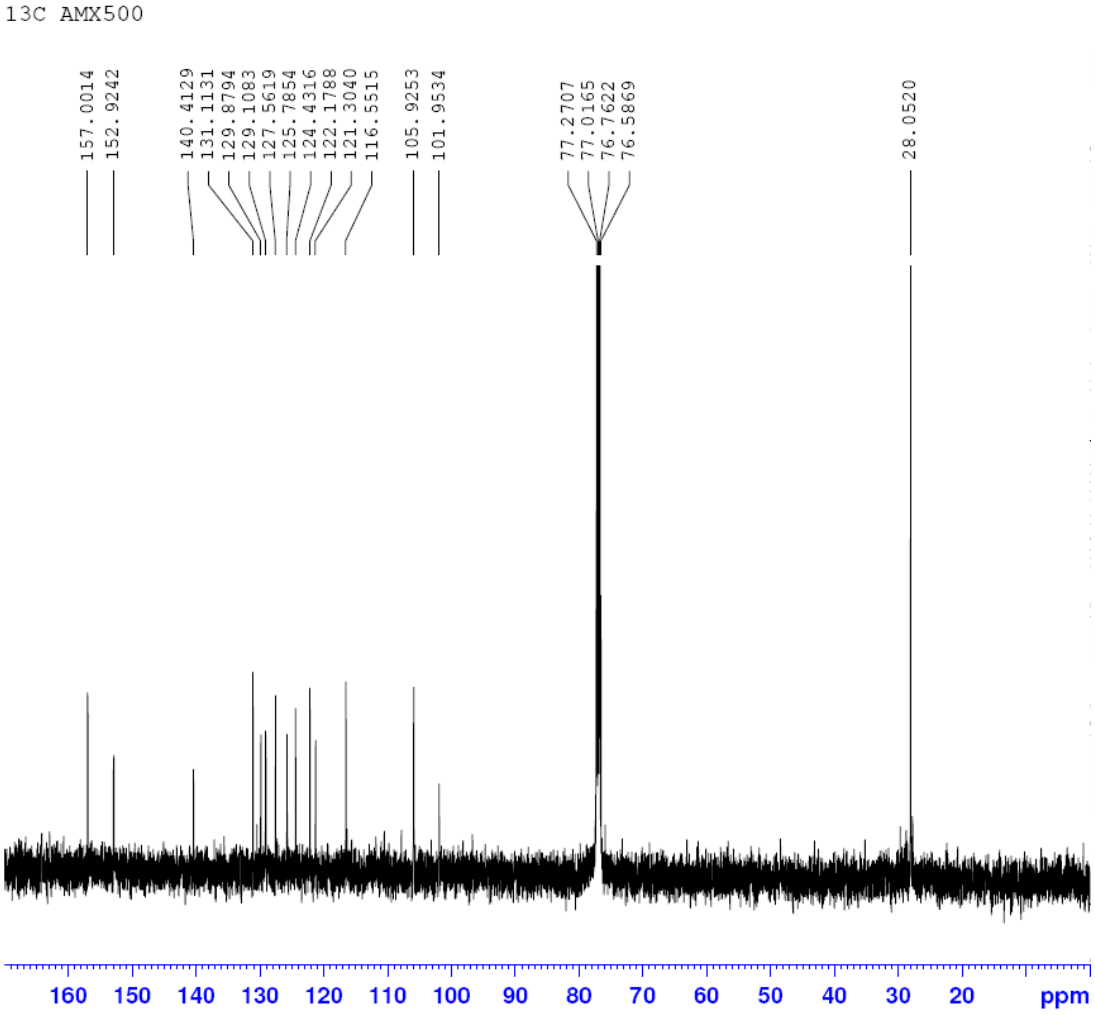

COSY spectrum of arahypin-10

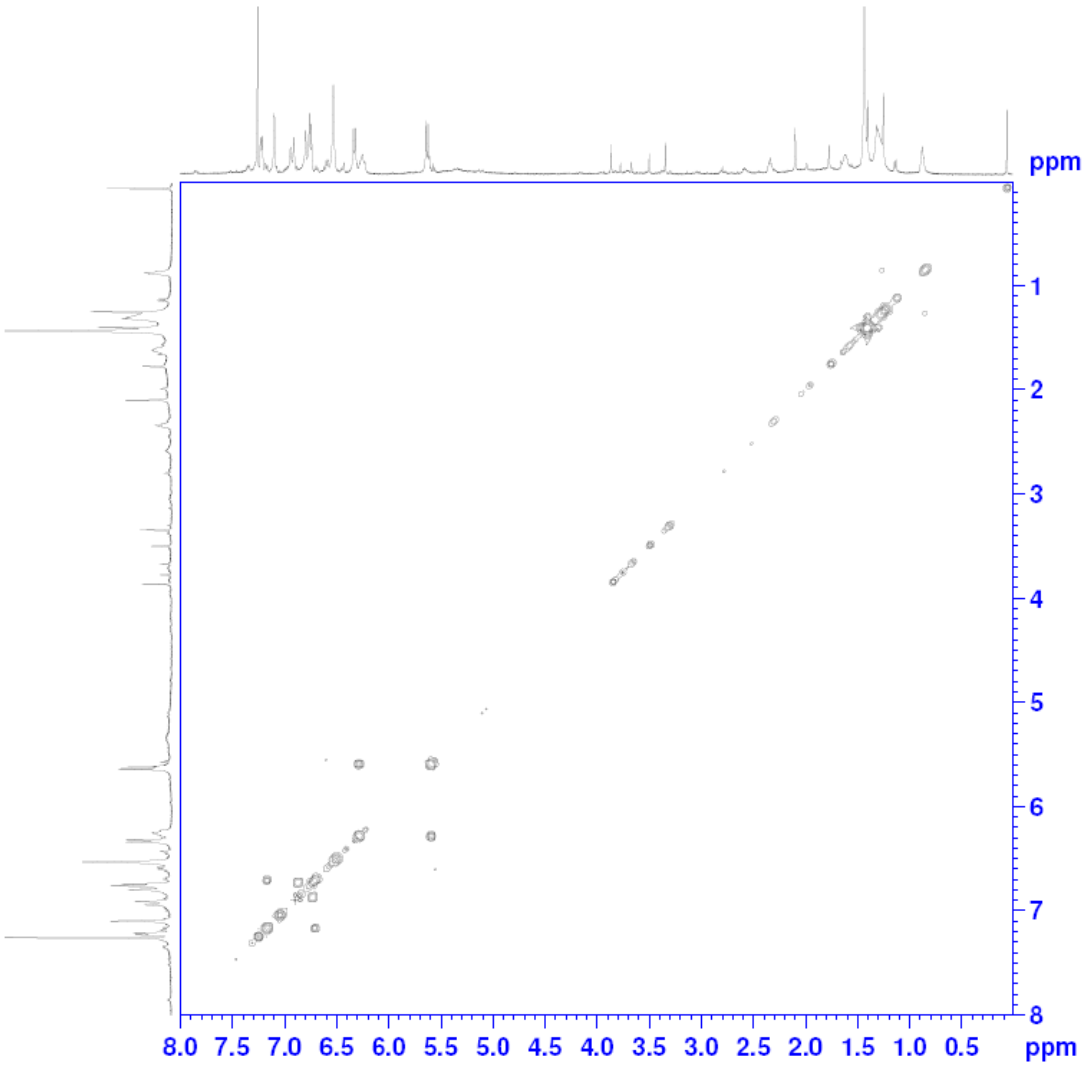

HMBC spectrum of arahypin-10

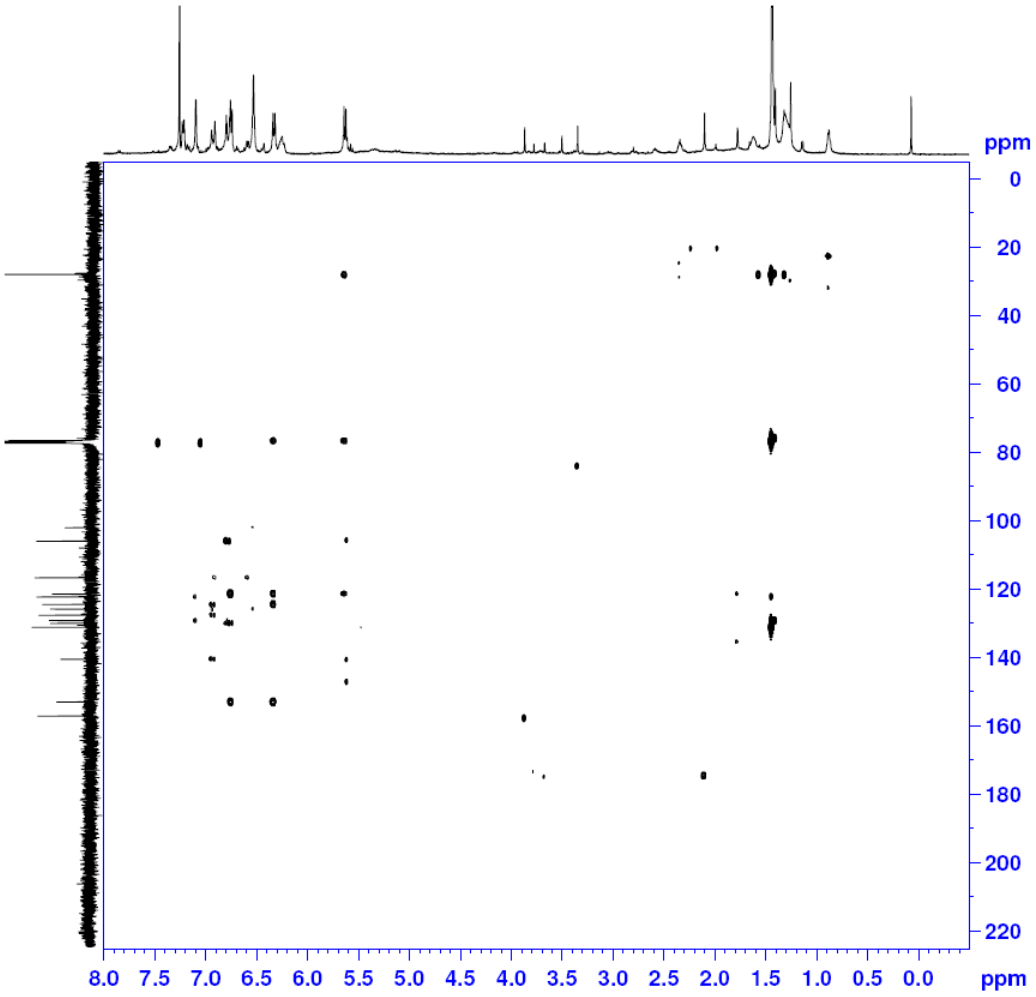

A portion of HMBC spectrum of arahypin-10

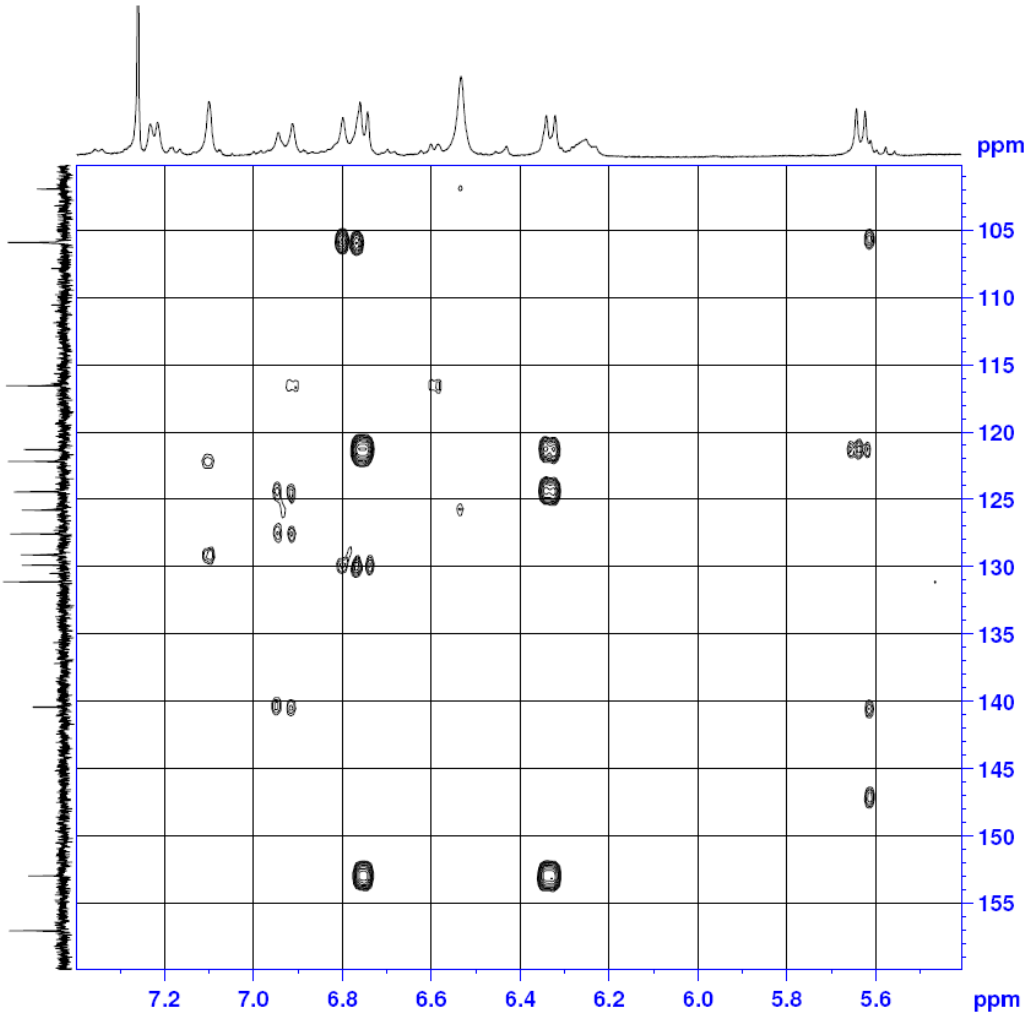

HMQC spectrum of arahypin-10

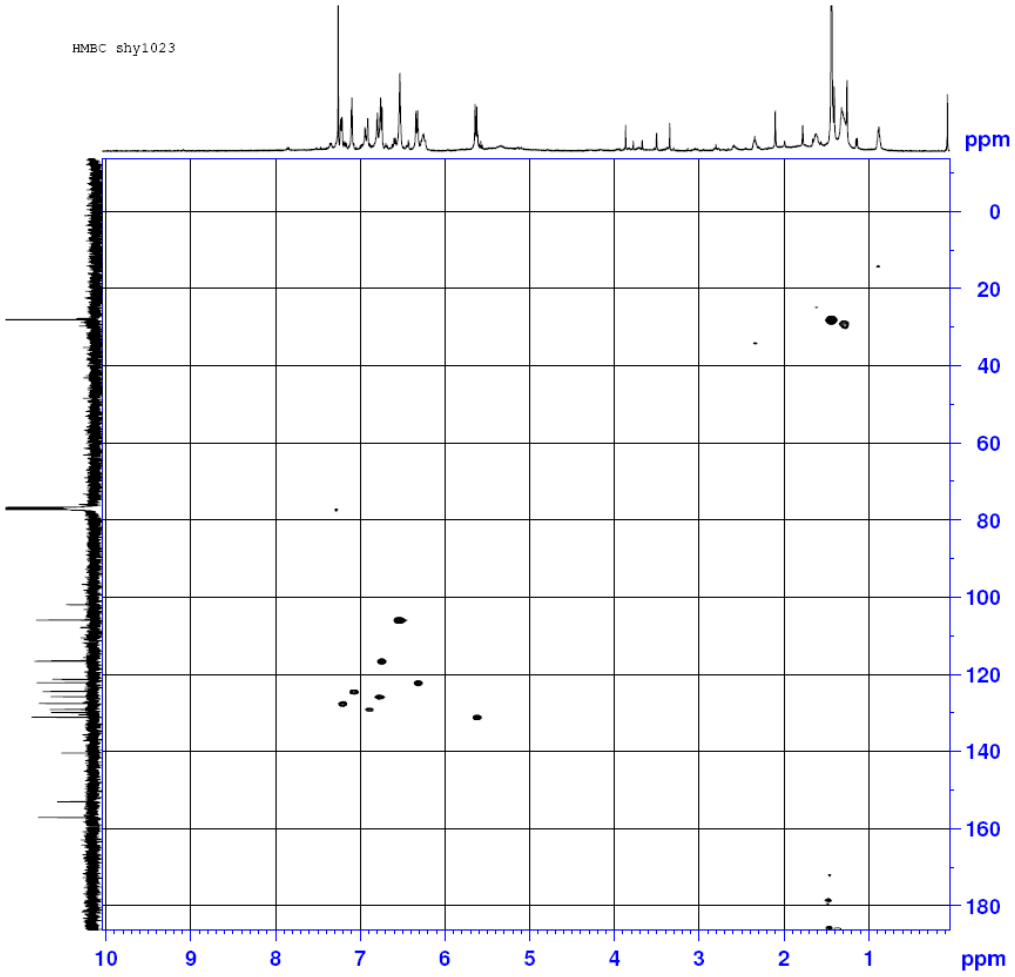

A portion of HMQC spectrum of arahypin-10

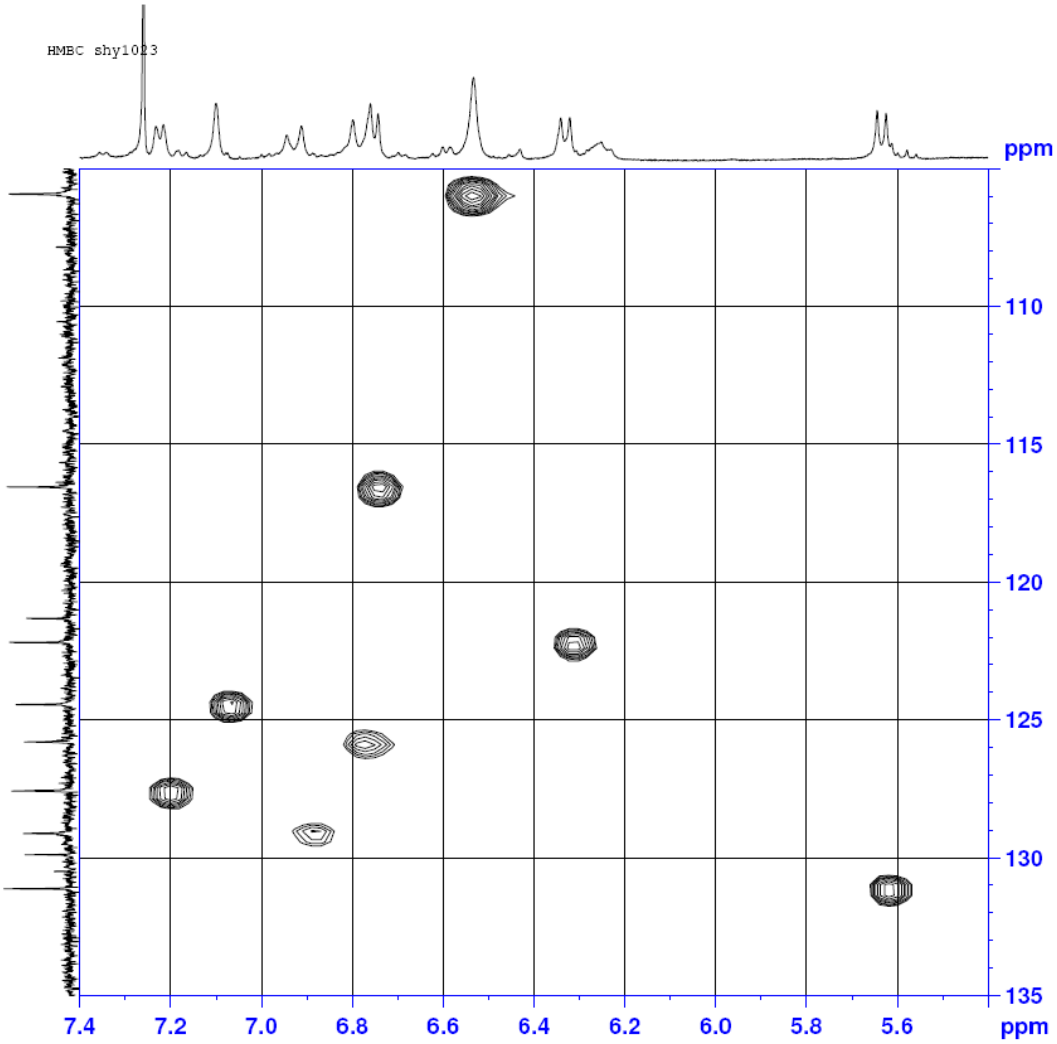

A.7 1D and 2D NMR data of (D) arahypin-11

^{1}H NMR spectrum of arahypin-11

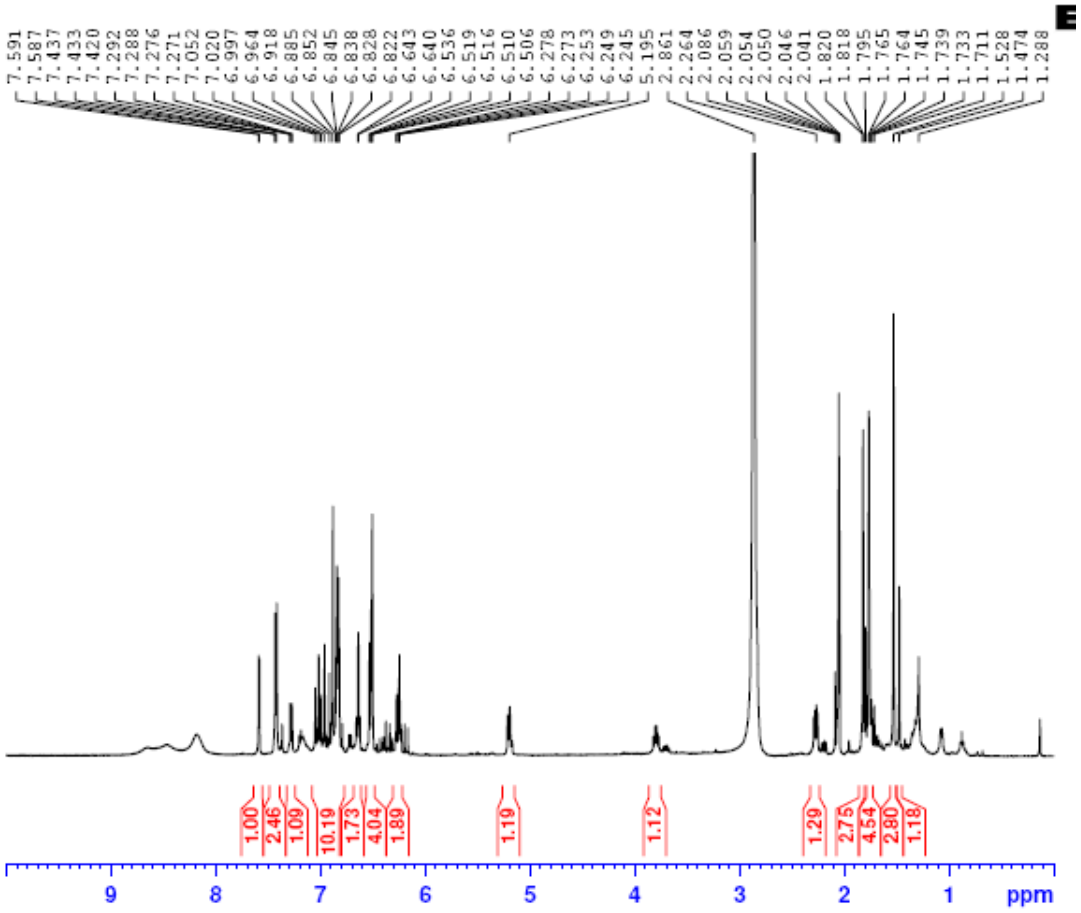

^{13}C NMR spectrum of arahypin-11

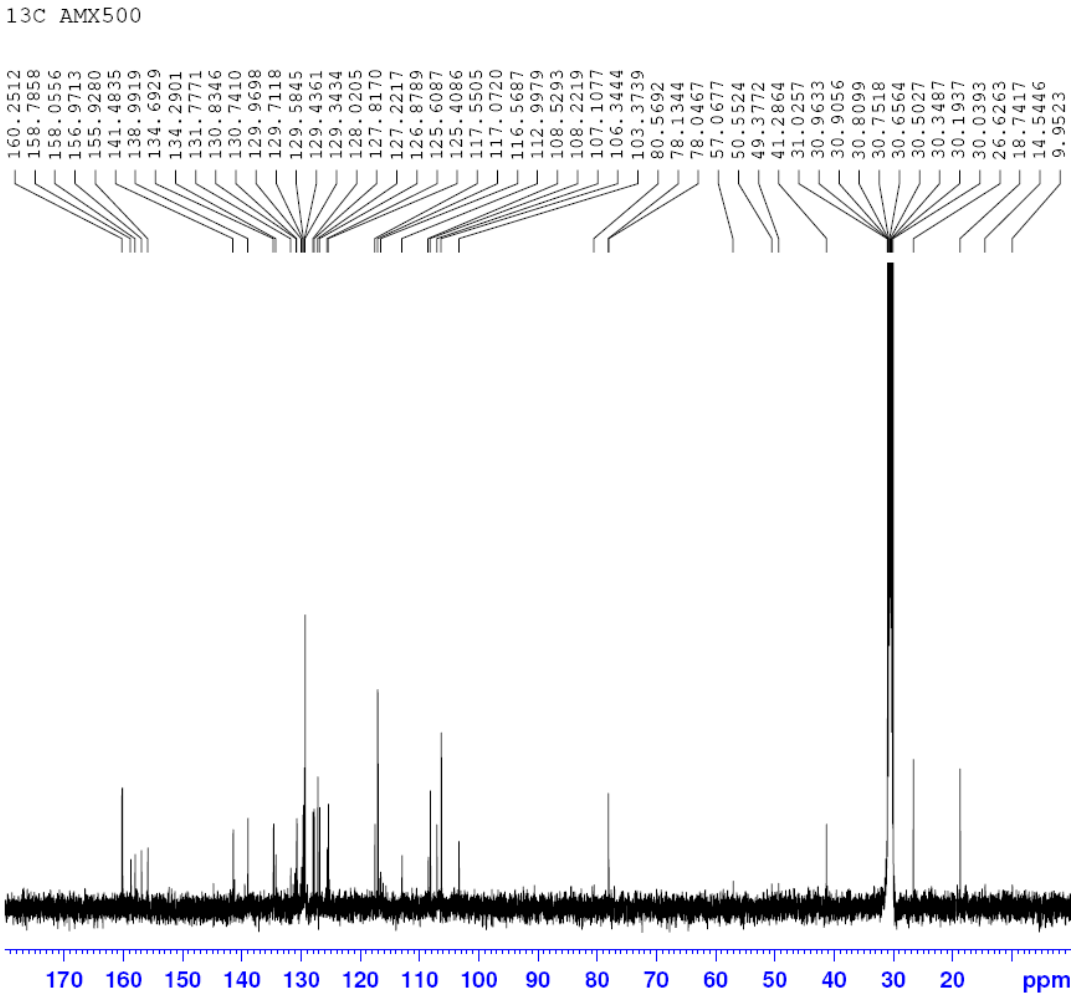

COSY spectrum of arahypin-11

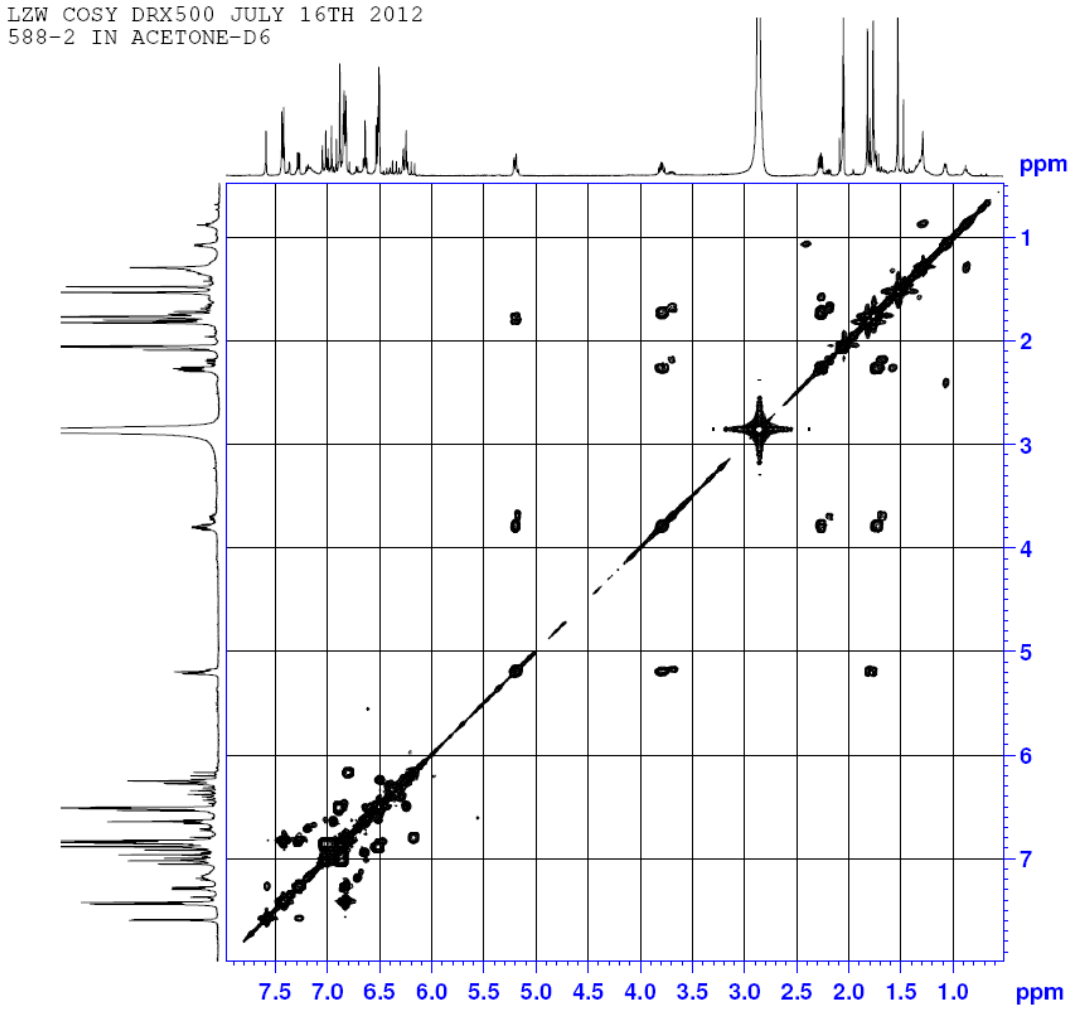

DEPT135 spectrum of arahypin-11

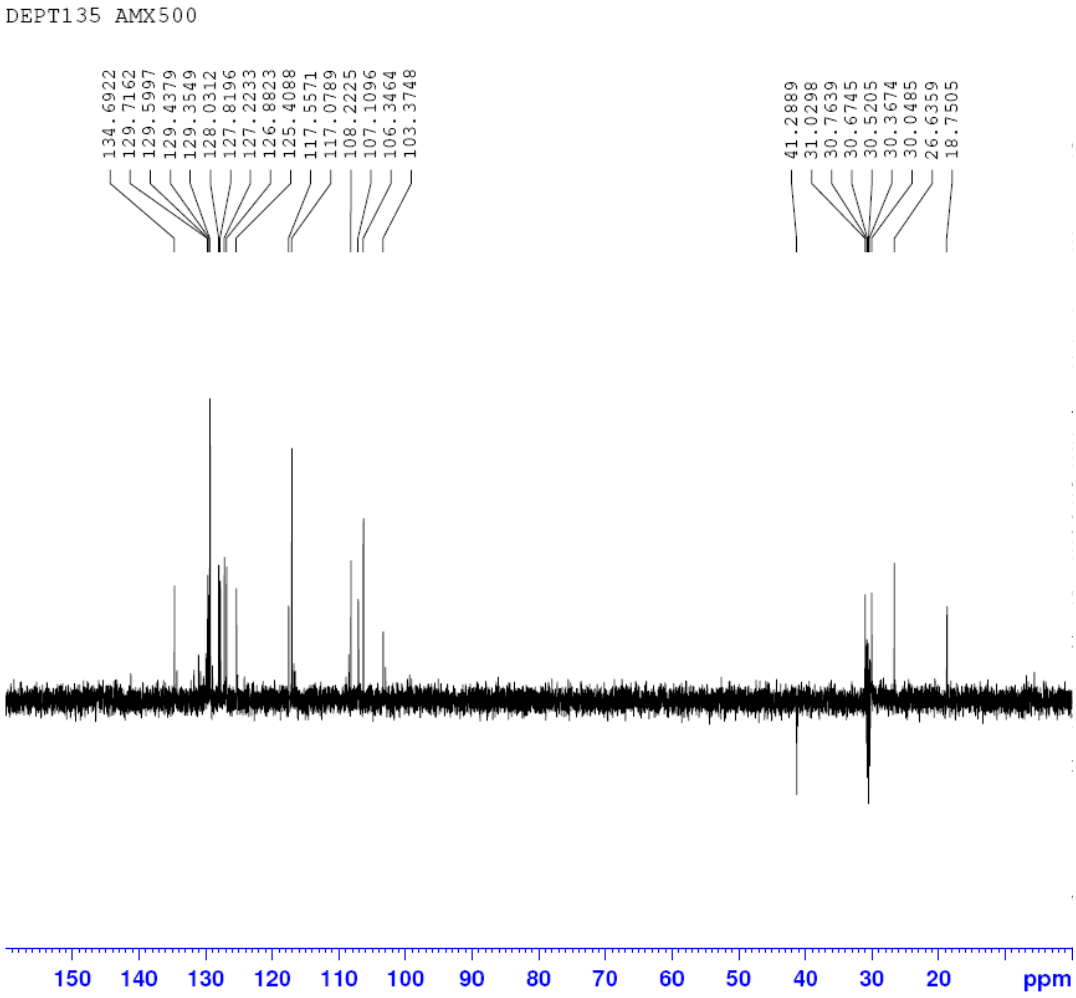

HMBC spectrum of arahypin-11

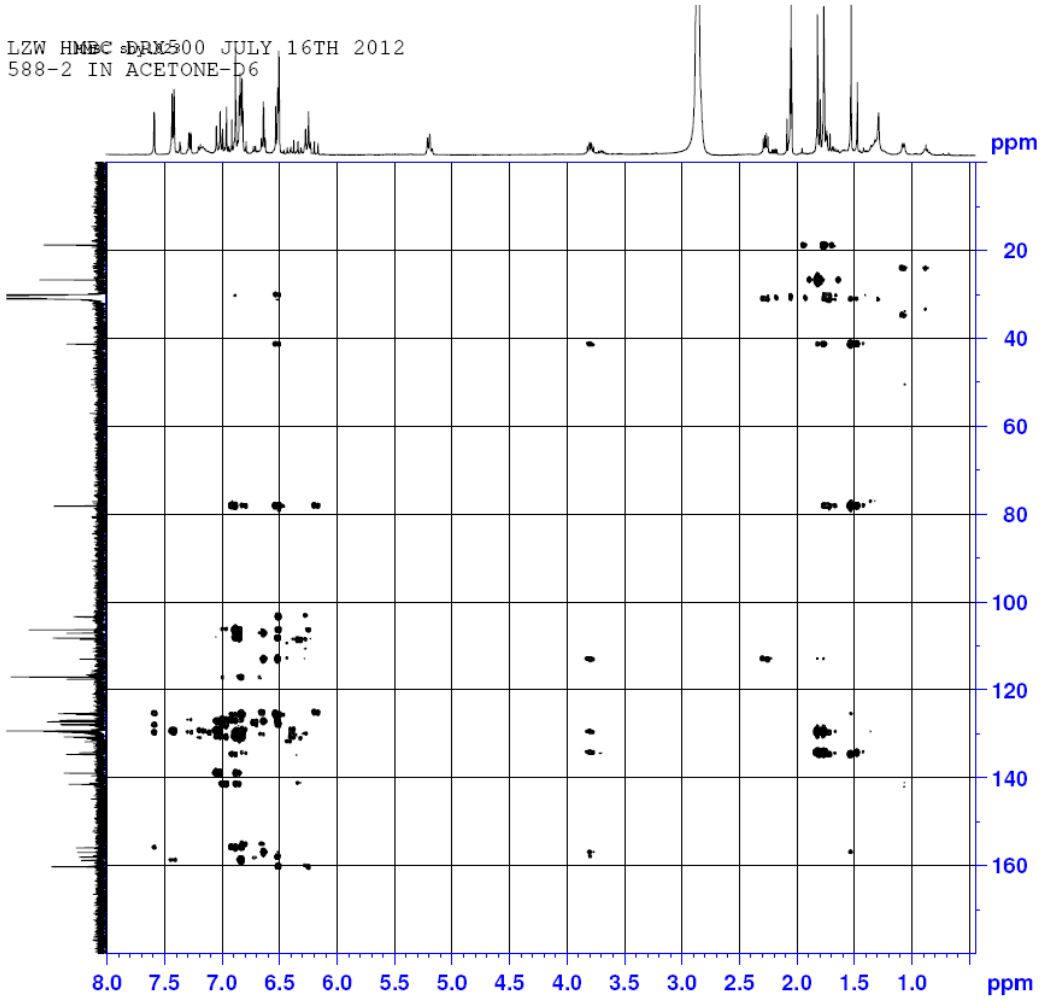

A portion of HMBC spectrum of arahypin-11

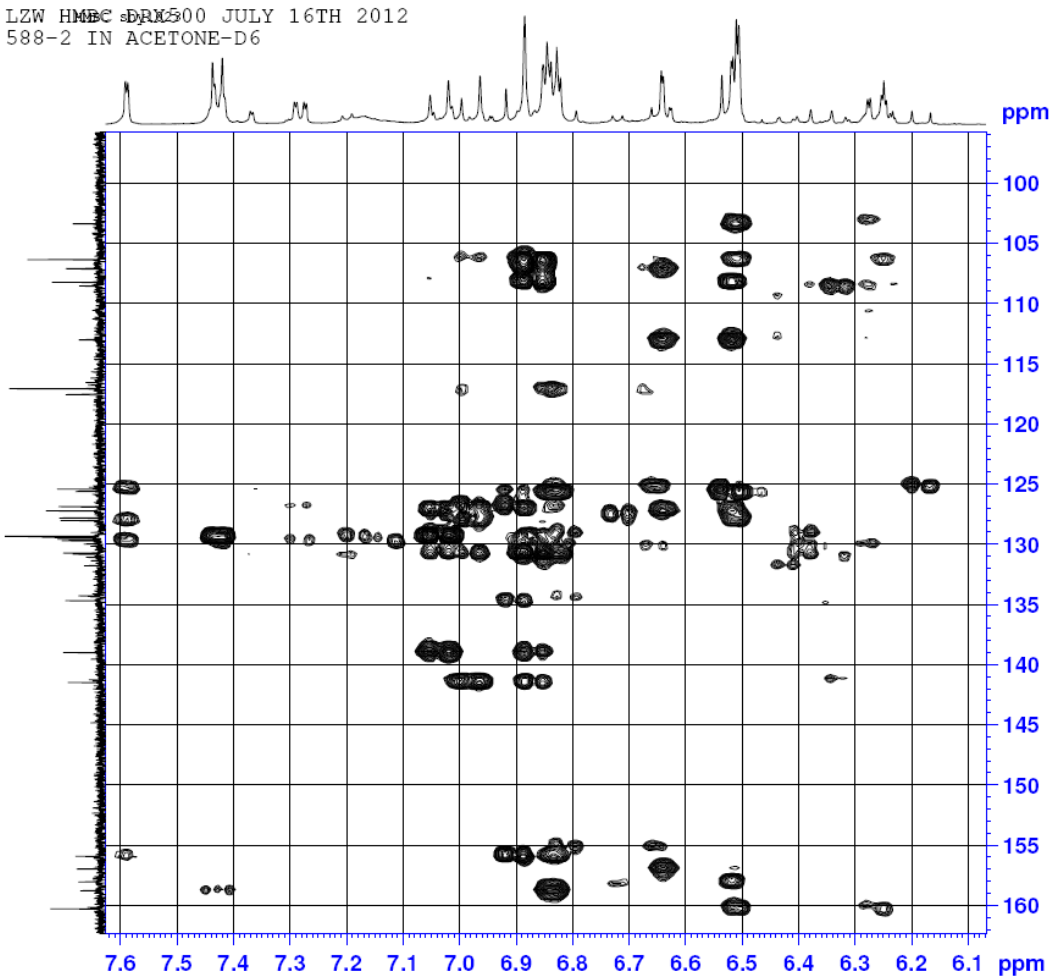

A portion of HMBC spectrum of arahypin-11

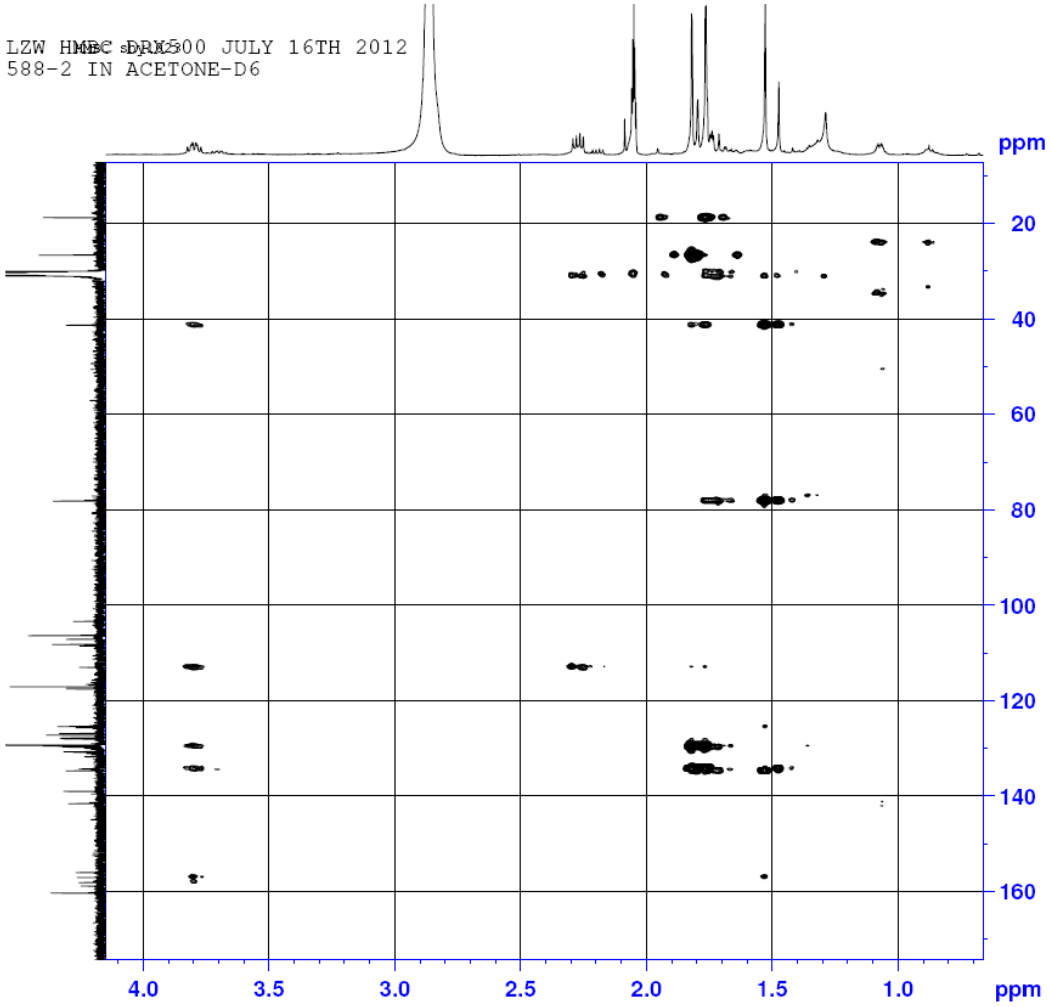

A portion of HMBC spectrum of arahypin-11

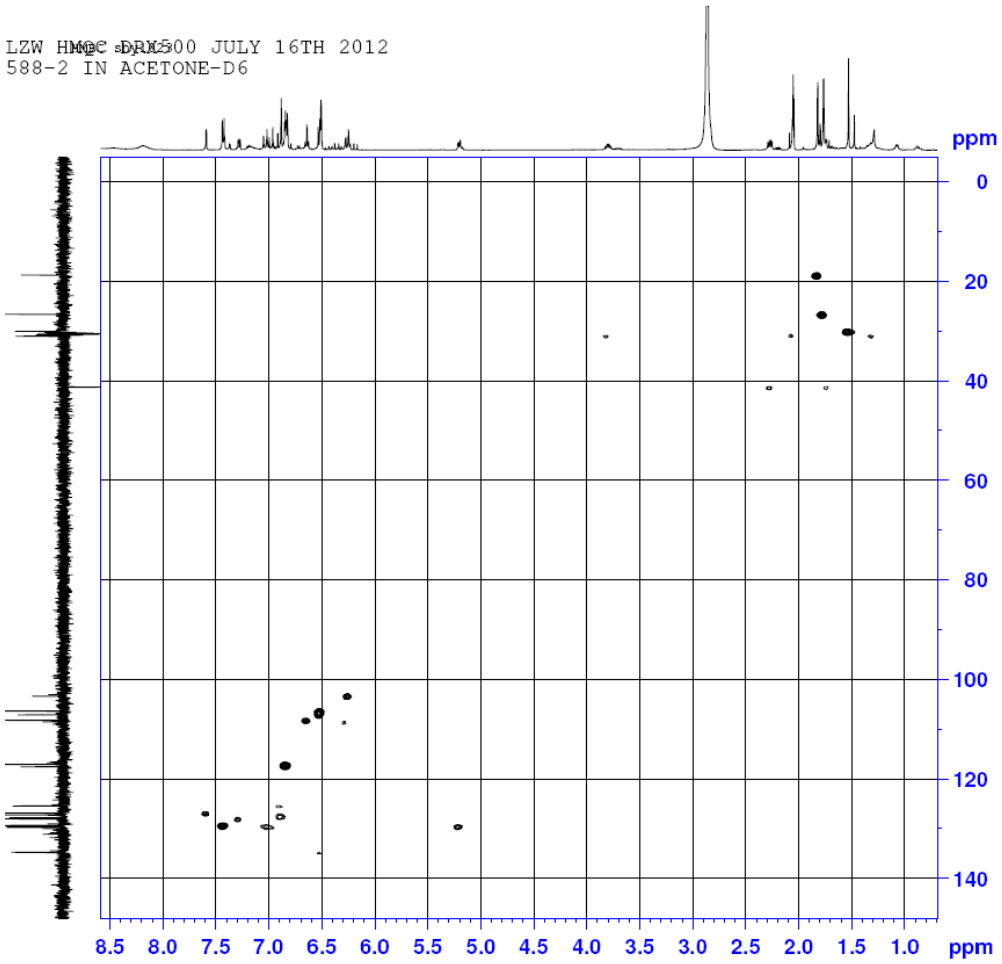

HMQC spectrum of arahypin-11

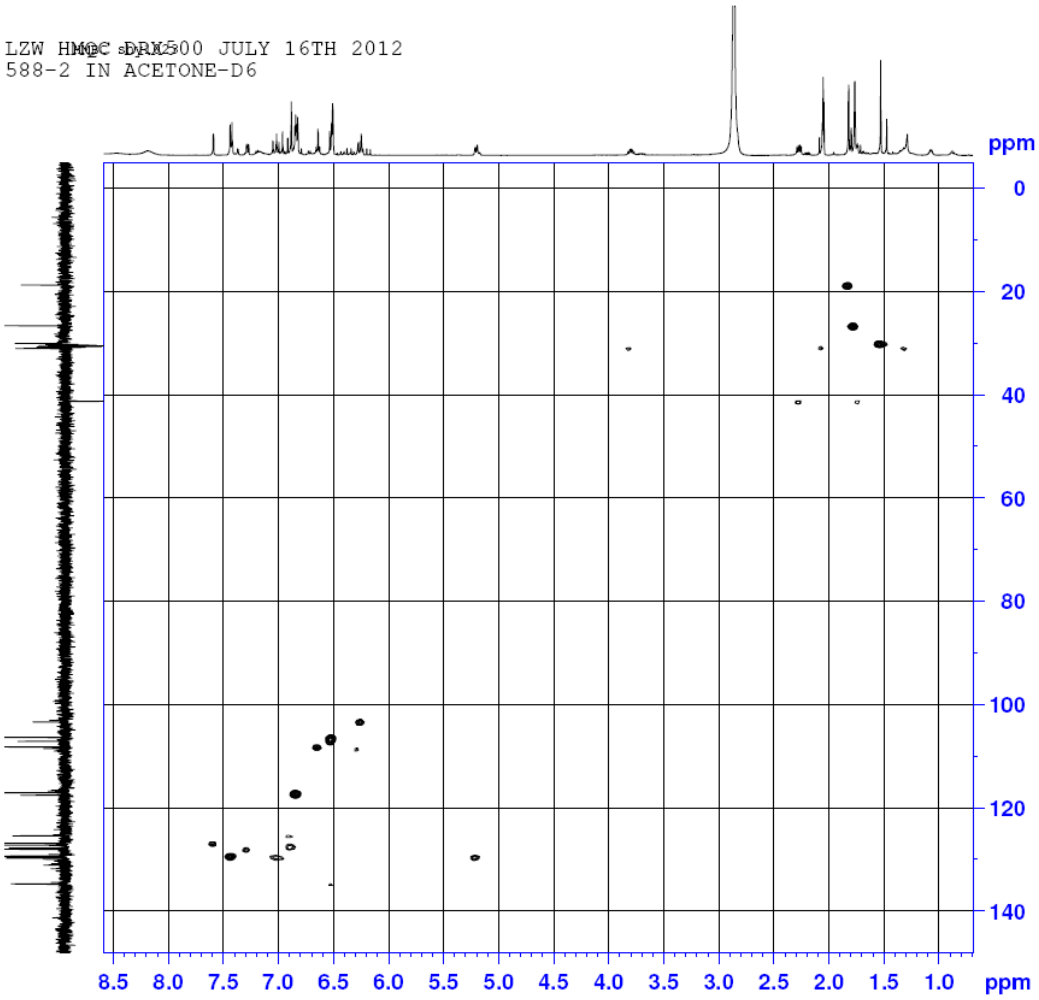

NOESY spectrum of arahypin-11

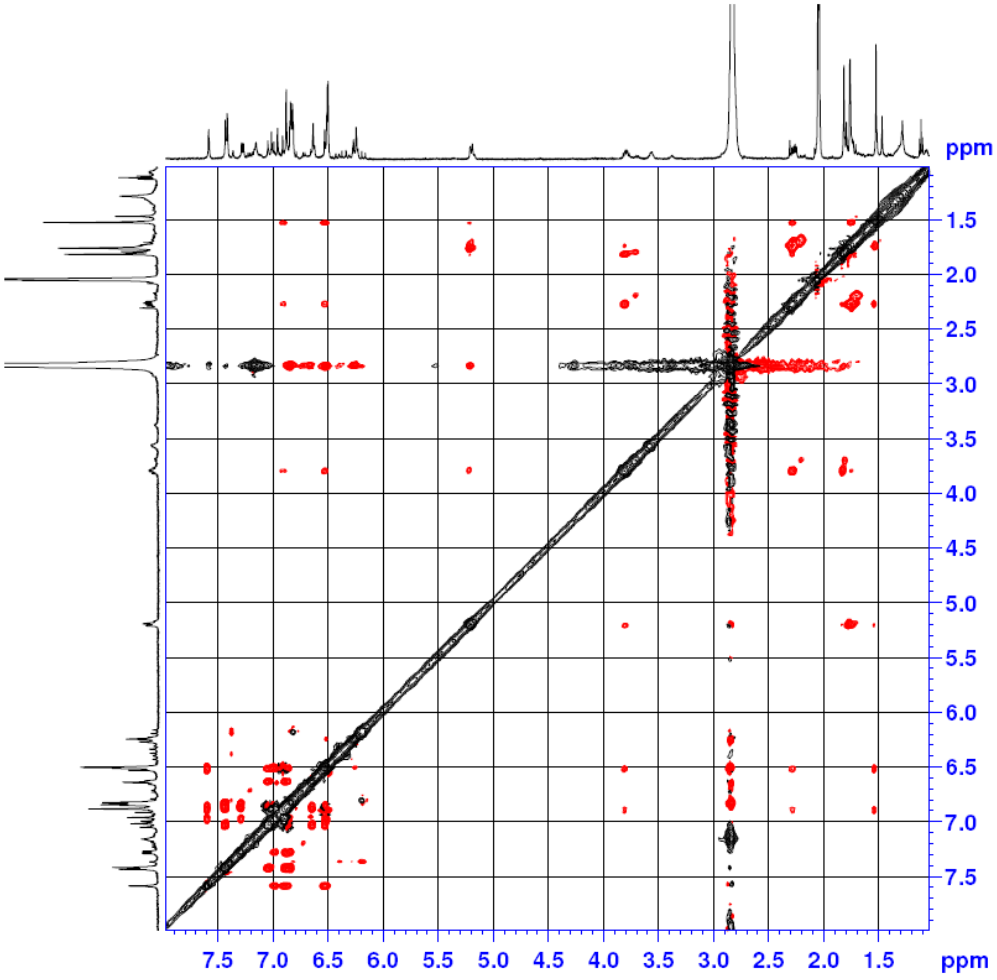

A.8 1D and 2D NMR data of (E) arahypin-12

^{1}H NMR spectrum of arahypin-12

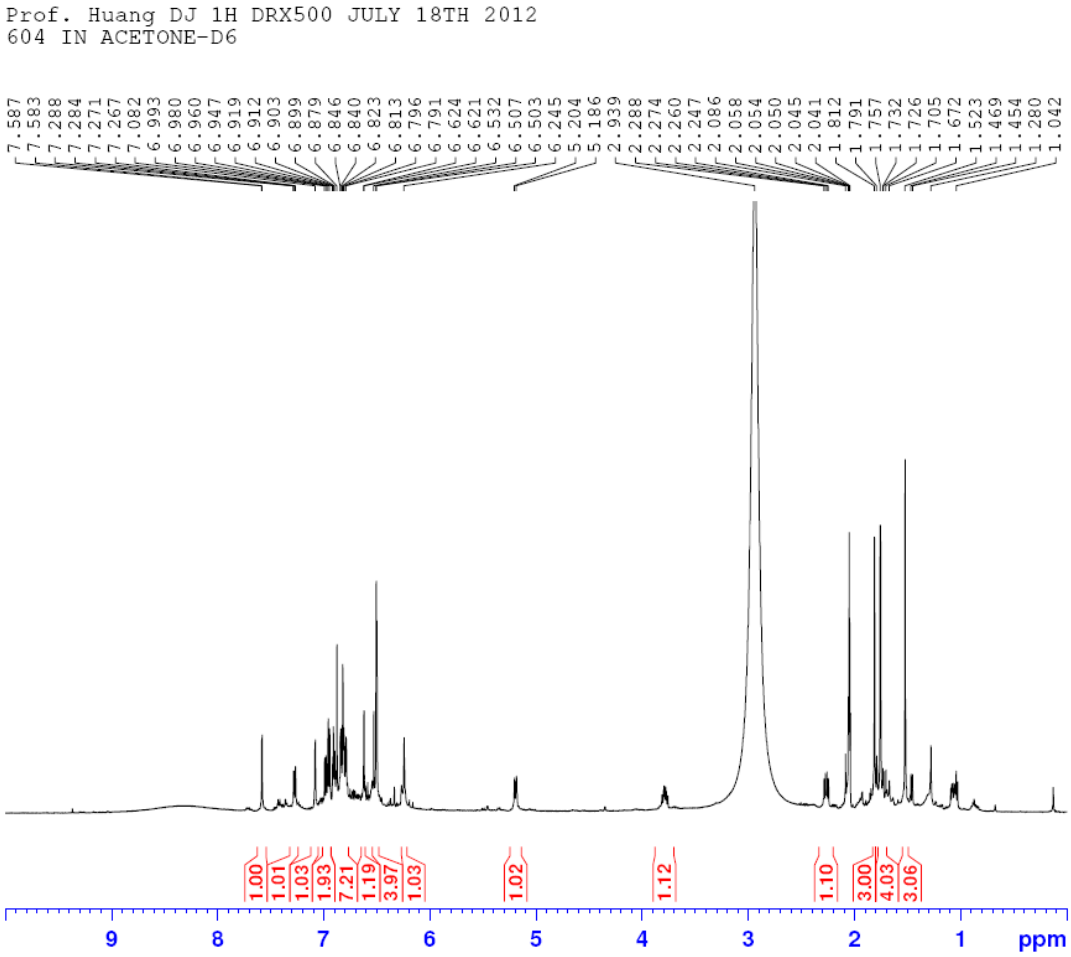

^{13}C NMR spectrum of arahypin-12

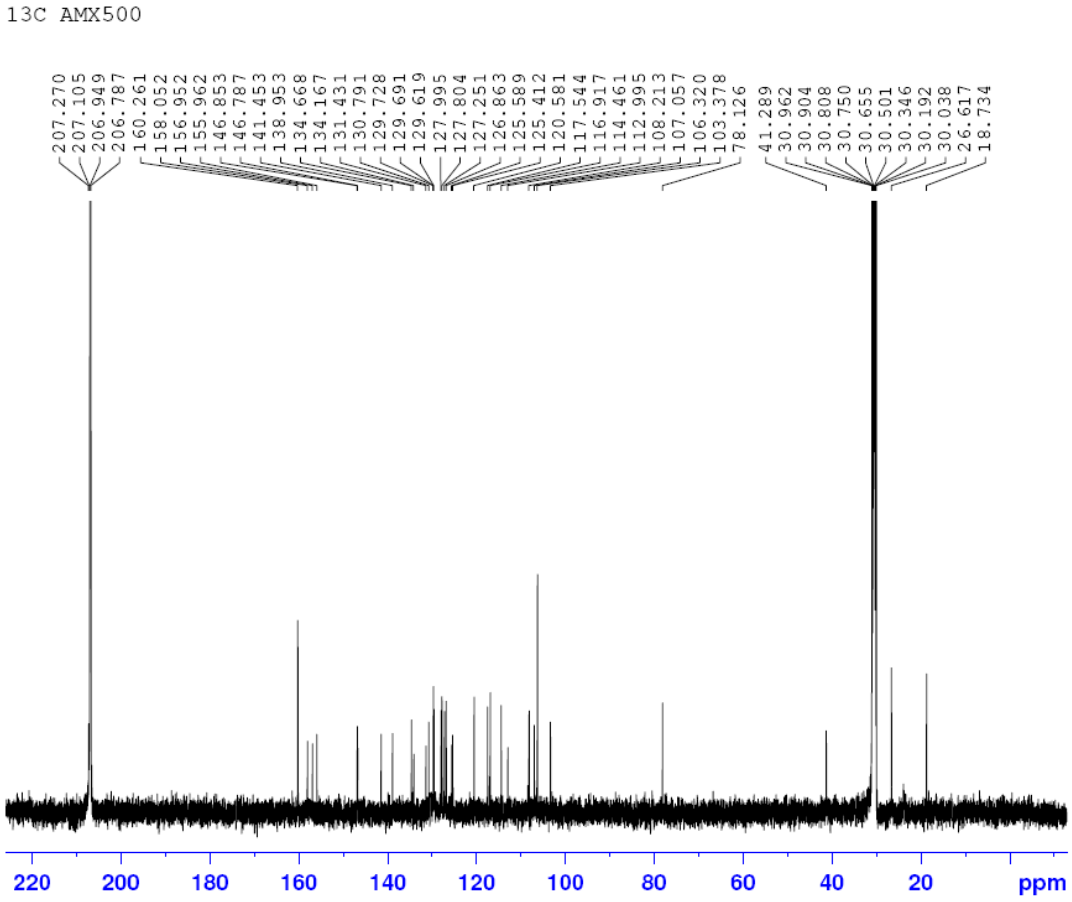

DEPT 135 spectrum of arahypin-12

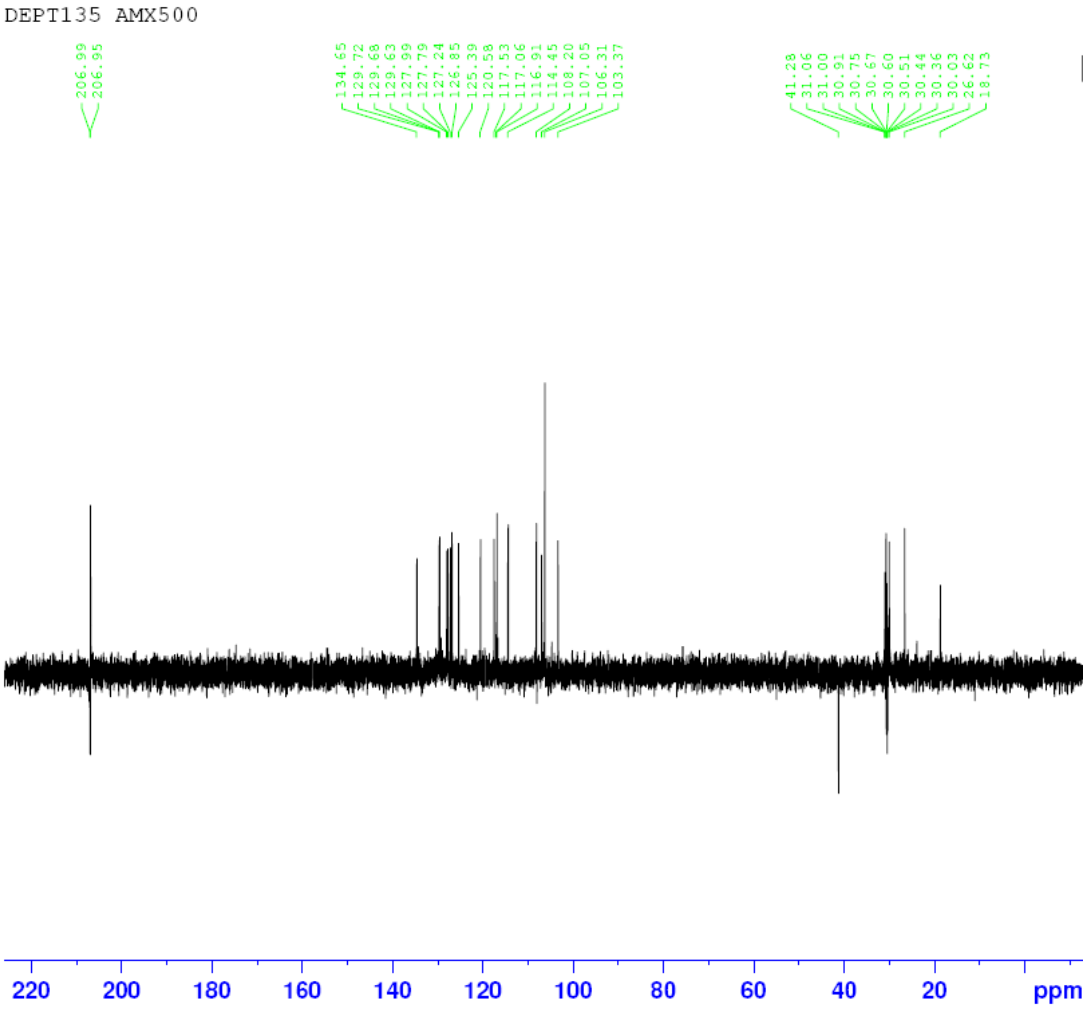

COSY spectrum of arahypin-12

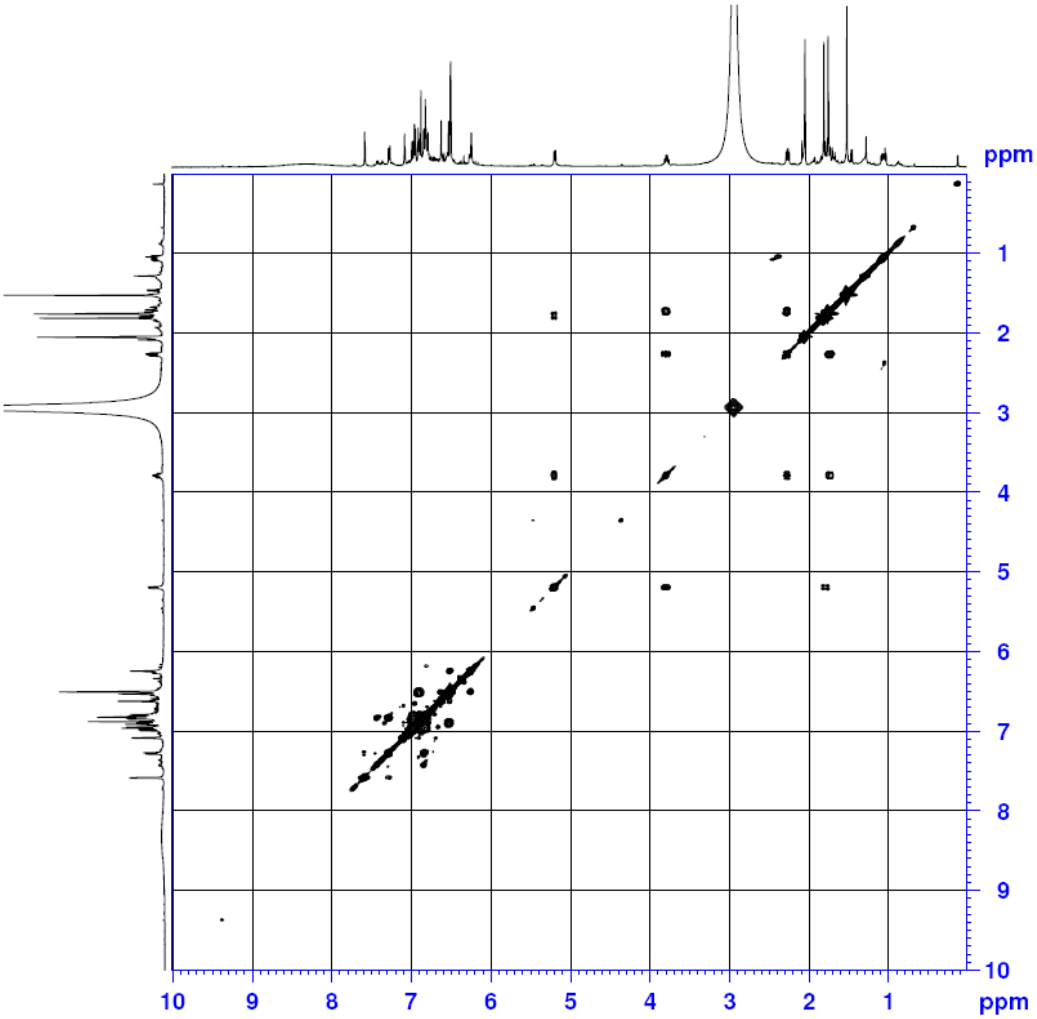

HMBC spectrum of arahypin-12

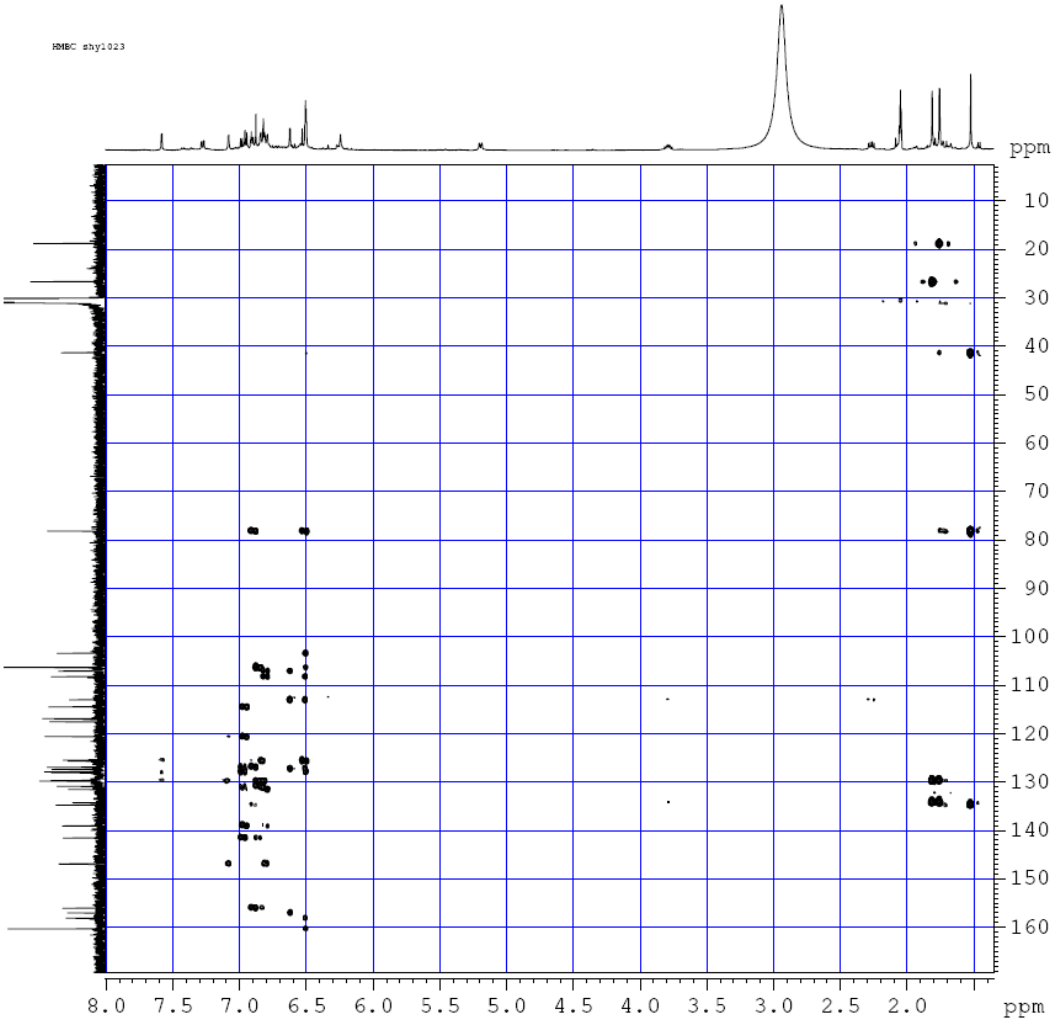

A portion of HMBC spectrum of arahypin-12

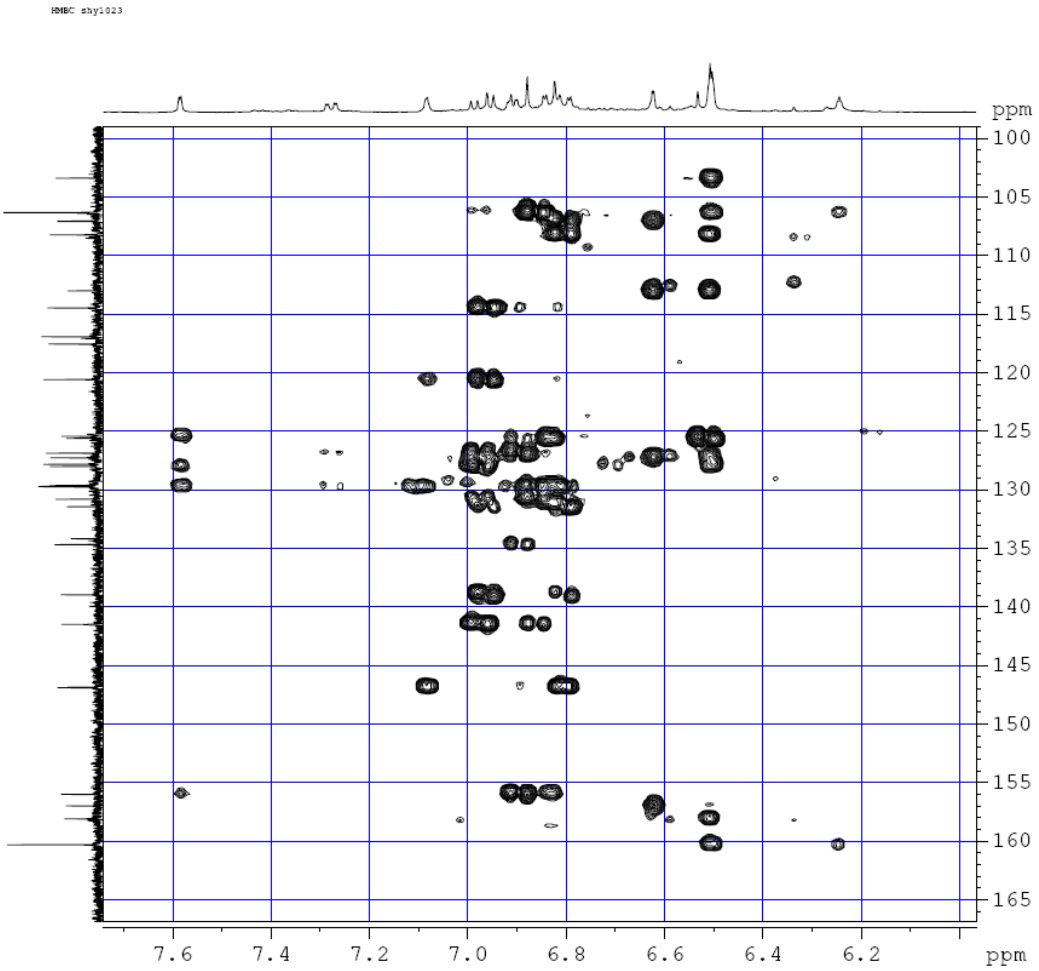

A portion of HMBC spectrum of arahypin-12

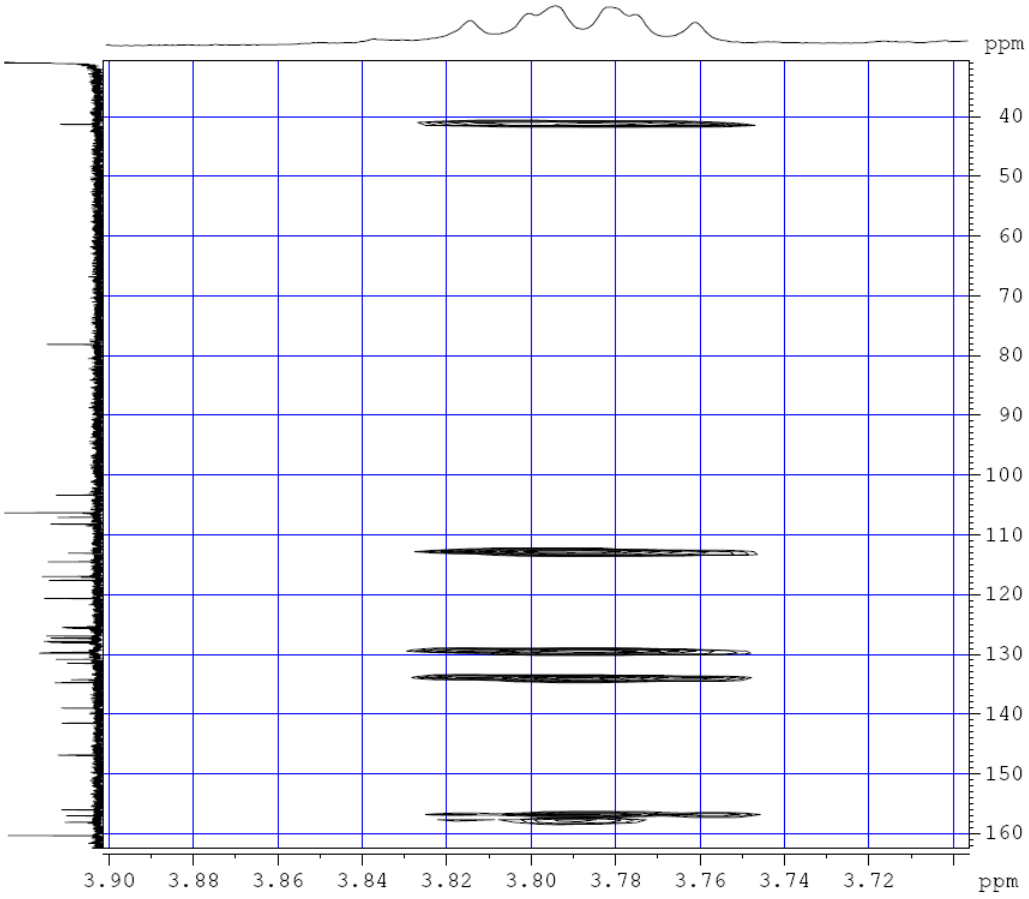

HMQC spectrum of arahypin-12

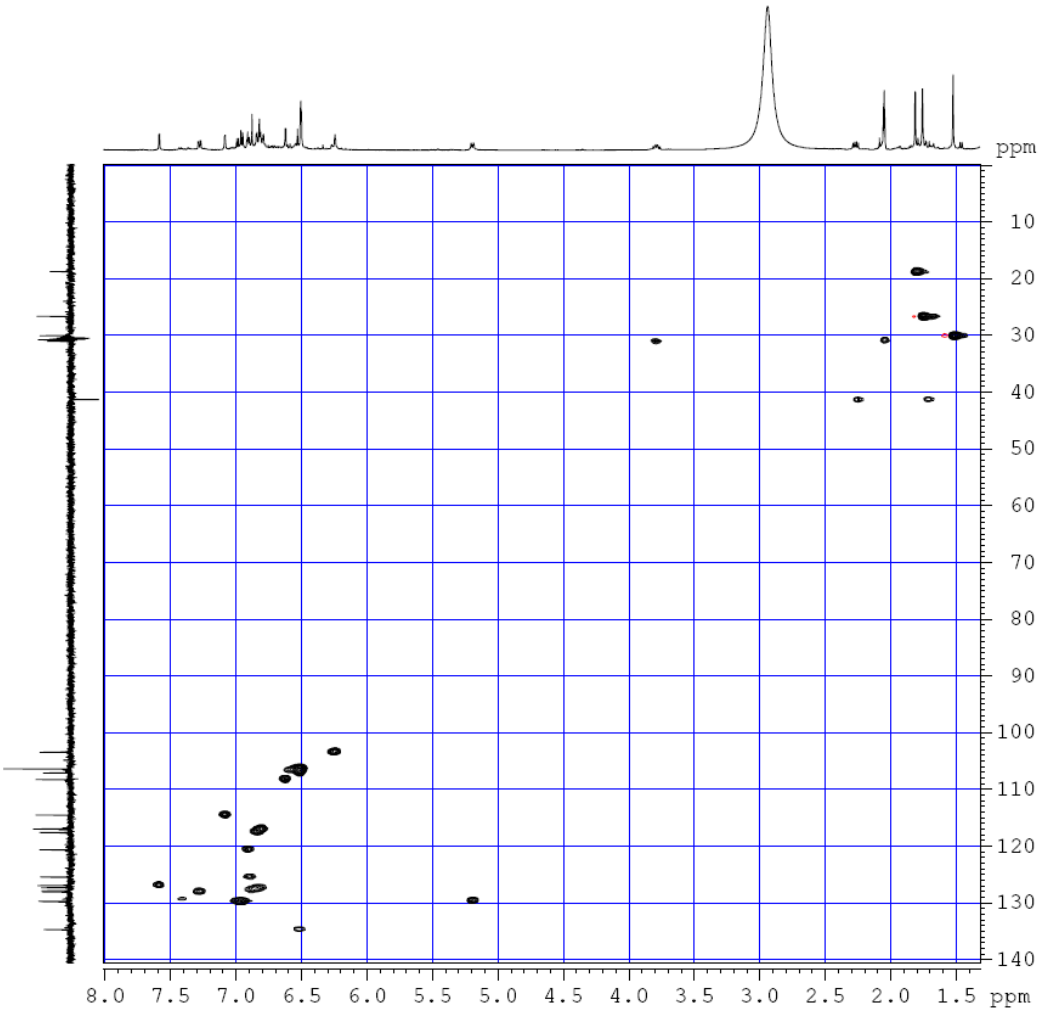

NOESY spectrum of arahypin-12

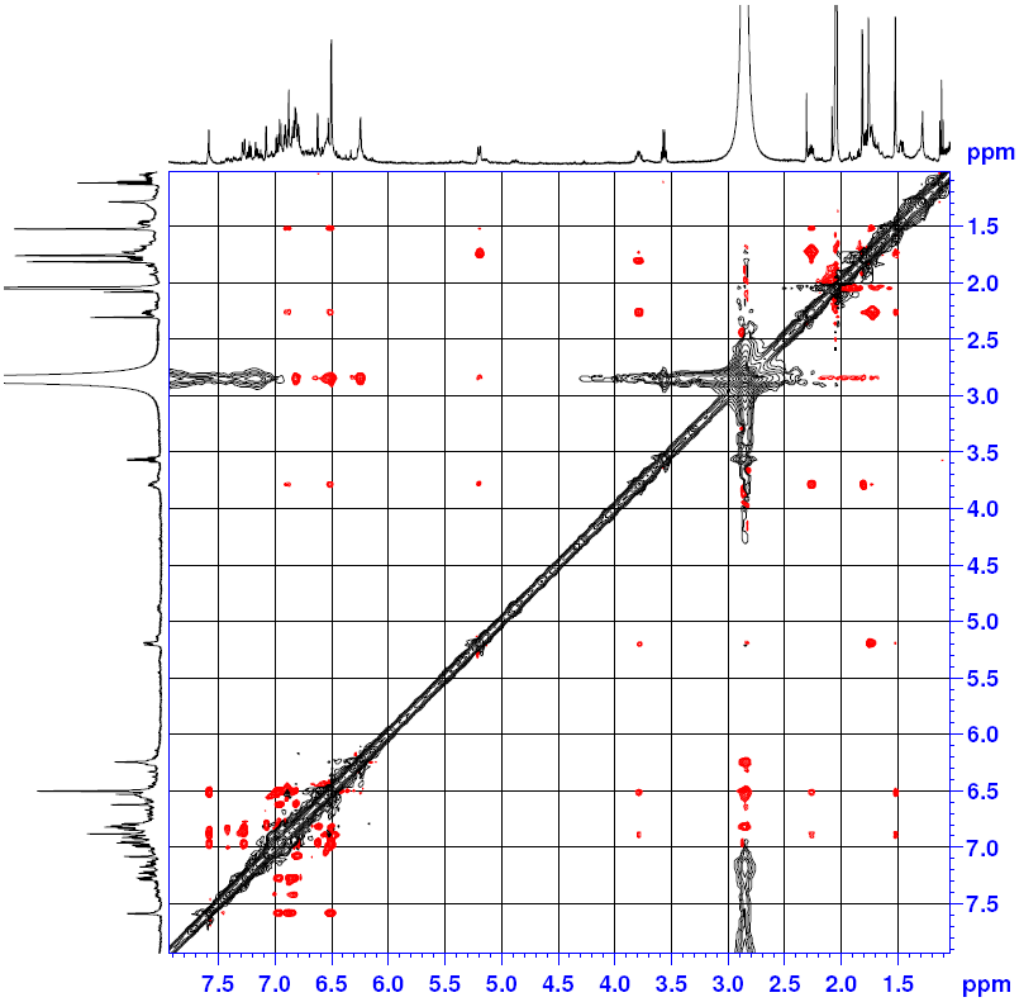

A.9 1D and 2D NMR data of (F) MIP

^{1}H NMR spectrum of MIP

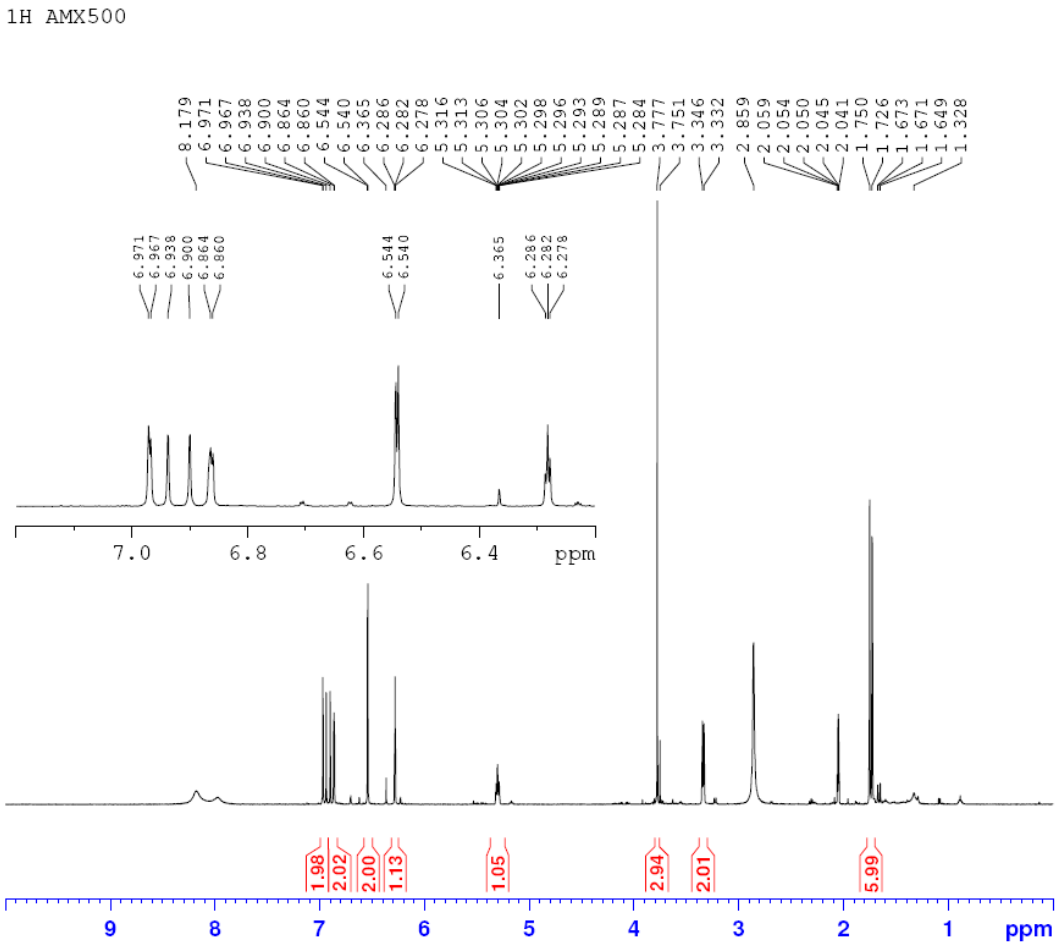

^{13}C NMR spectrum of MIP

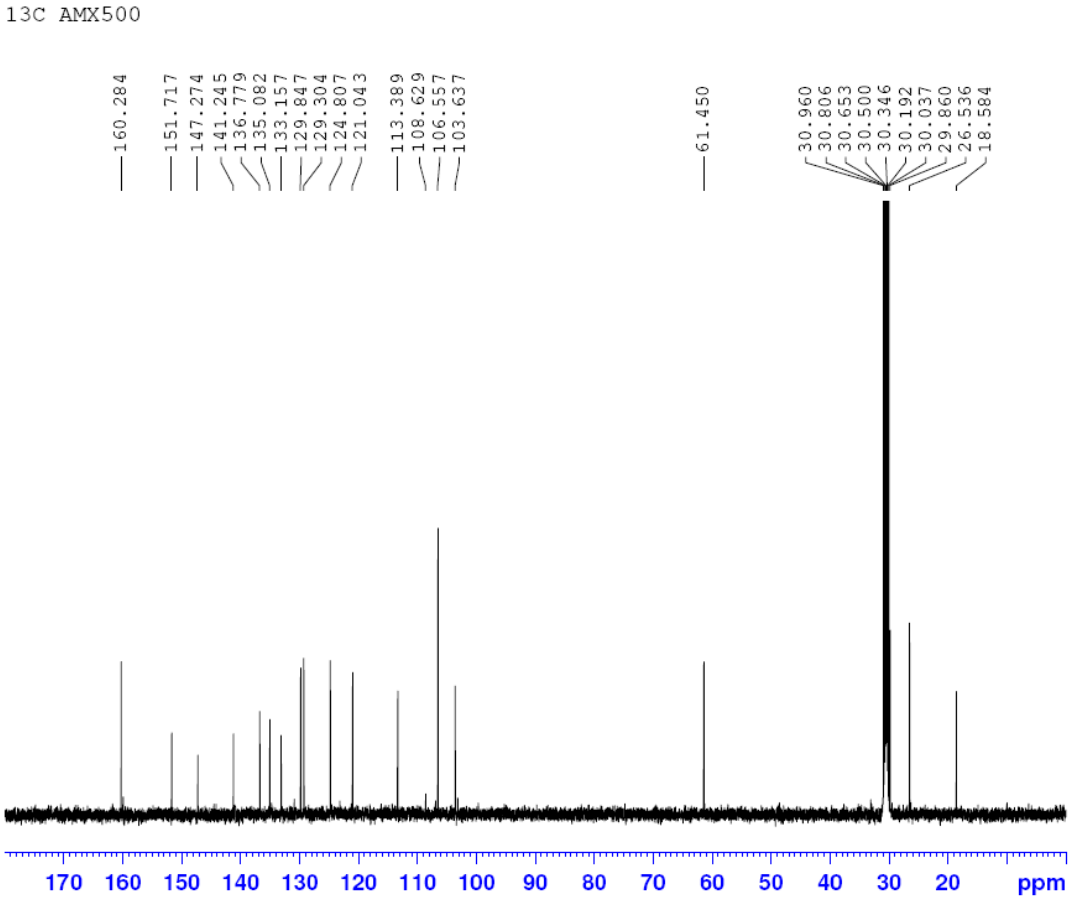

DEPT 135 spectrum of MIP

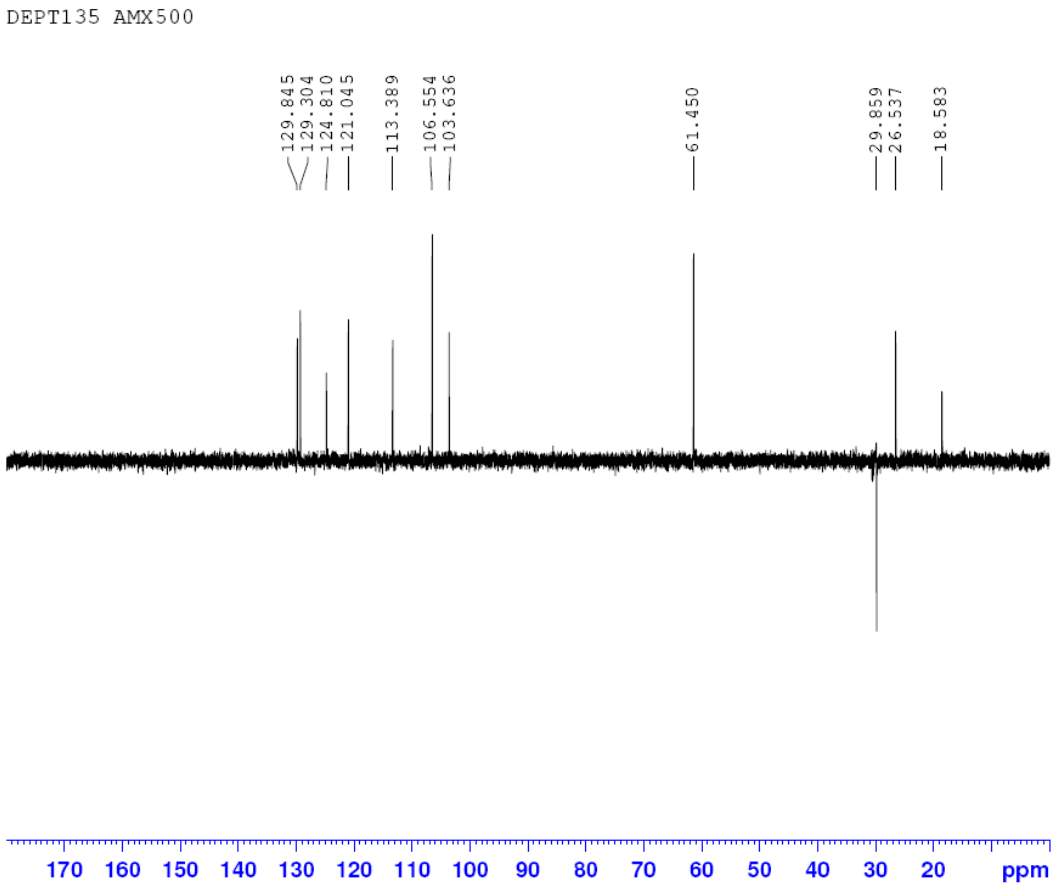

COSY spectrum of MIP

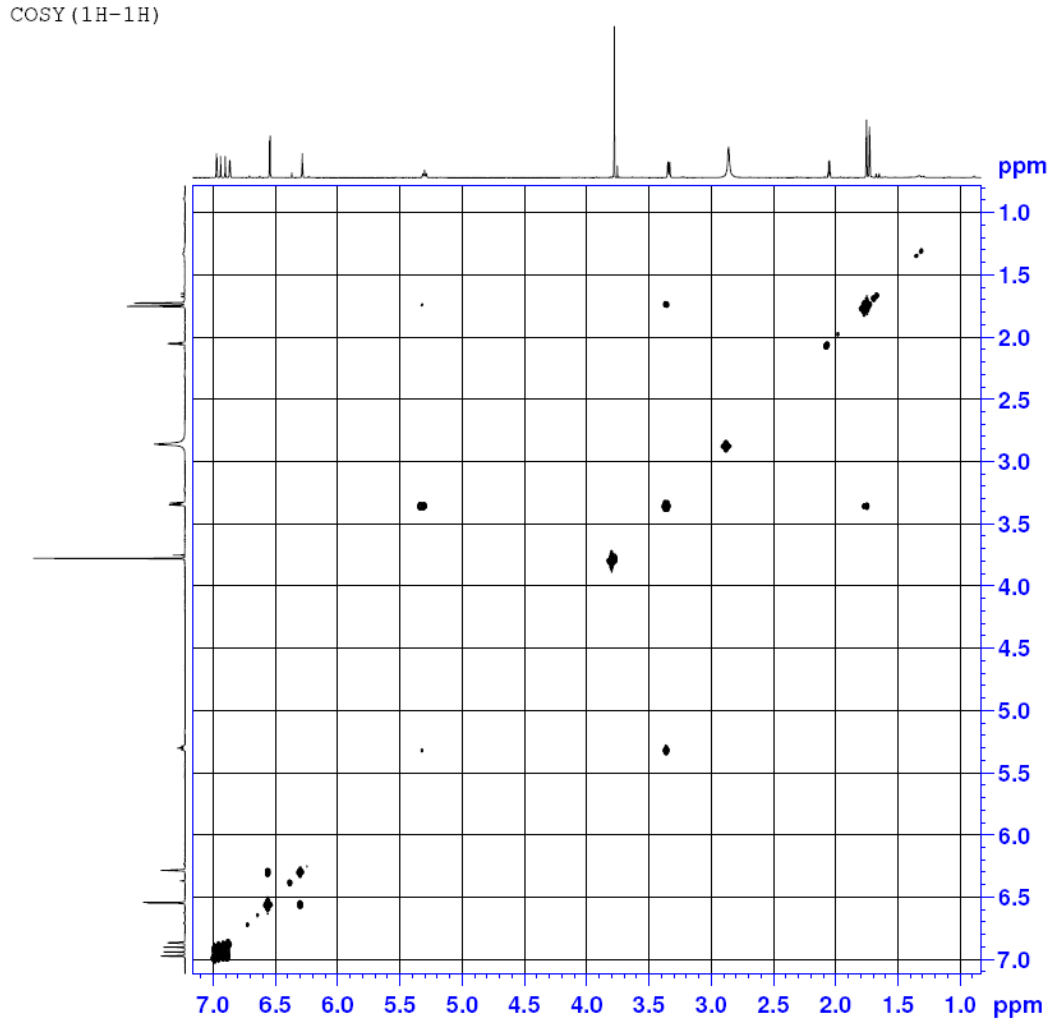

HMBC spectrum of MIP

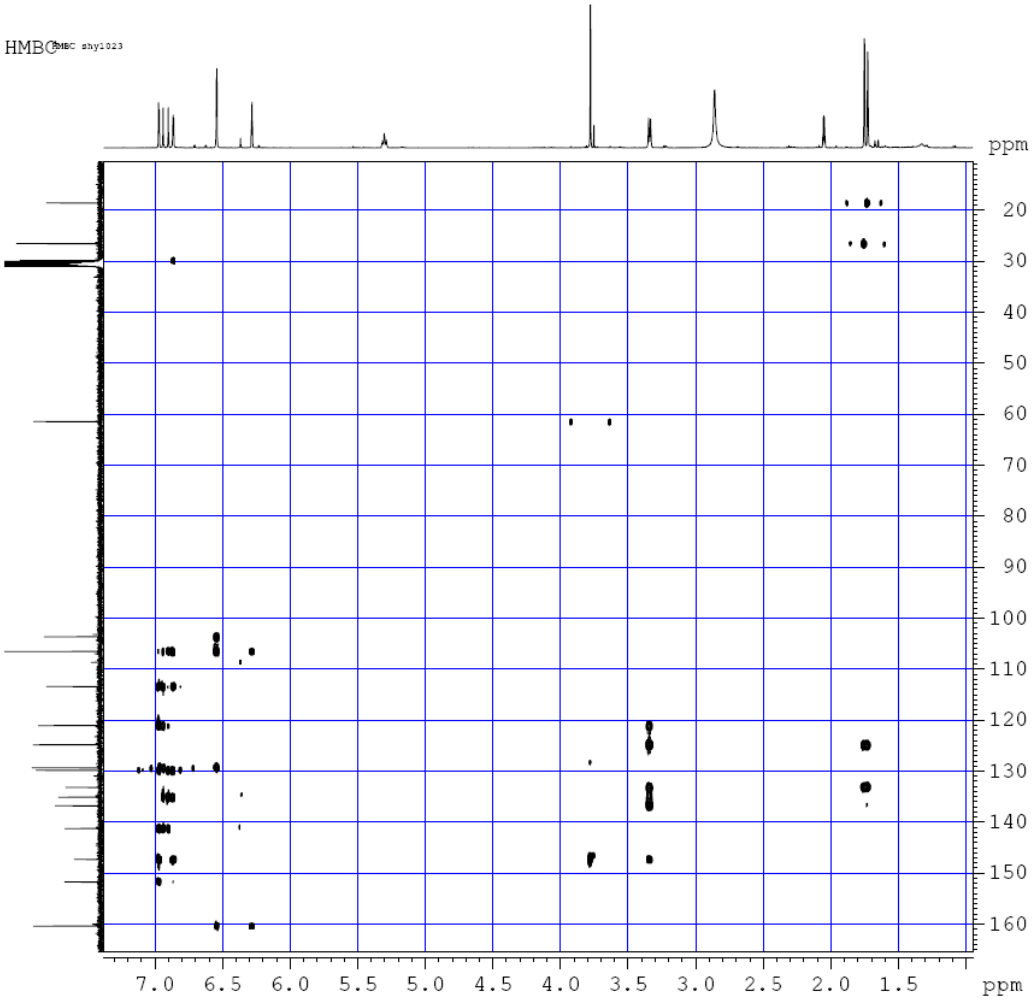

A portion of HMBC spectrum of MIP

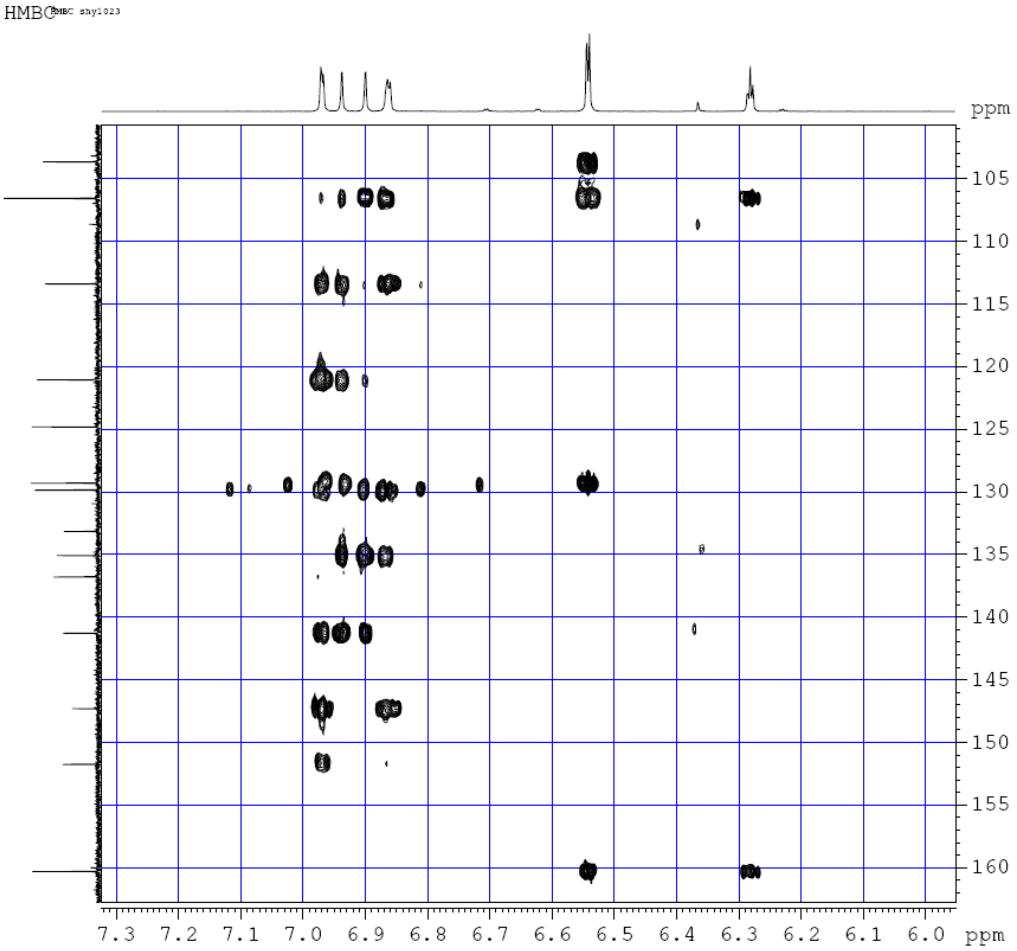

HMQC spectrum of MIP

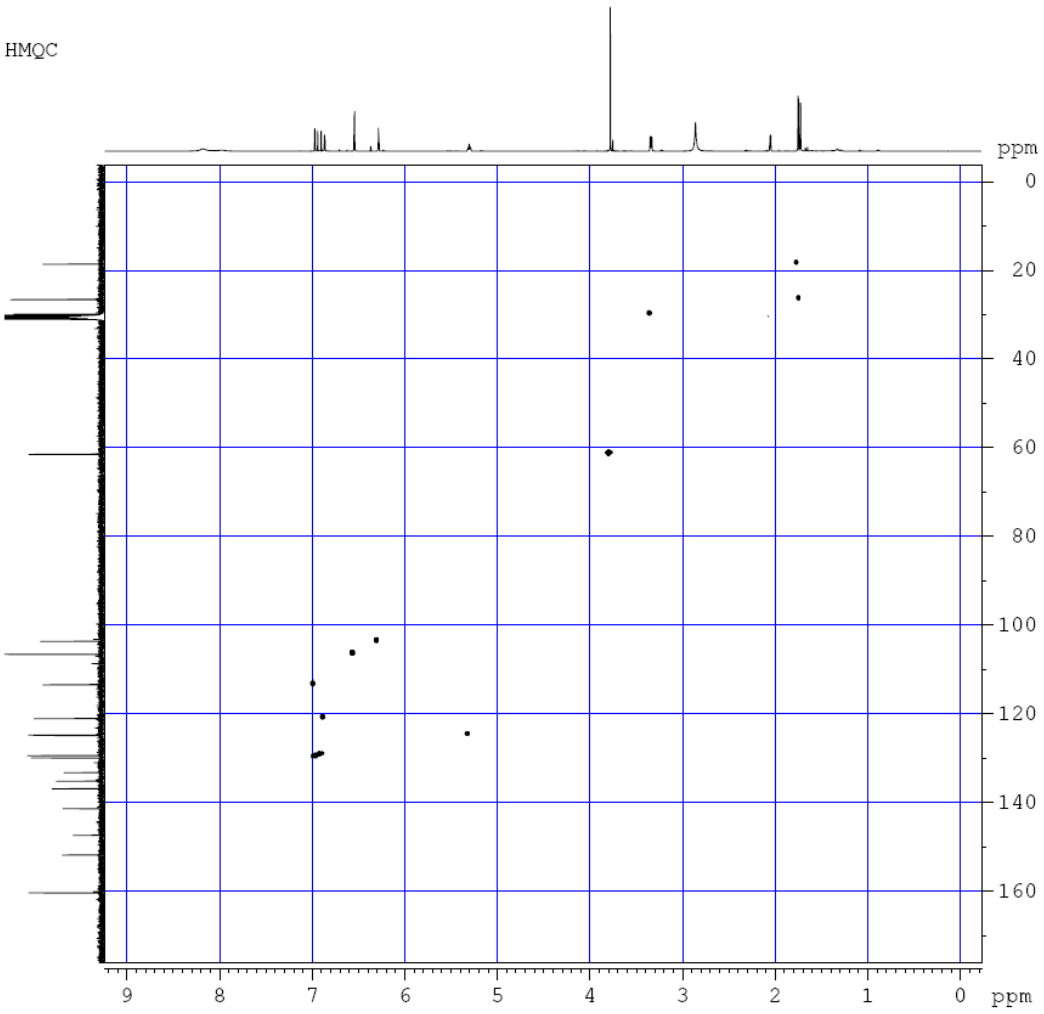

A portion of HMQC spectrum of MIP